

EXTREME MEDICINE

SCIENTIFIC AND PRACTICAL REVIEWED JOURNAL OF FMBA OF RUSSIA

EDITOR-IN-CHIEF Veronika Skvortsova, DSc, professor, RAS corresponding member

DEPUTY EDITOR-IN-CHIEF Igor Berzin, DSc, professor; Daria Kryuchko, DSc

EDITORS Vsevolod Belousov, DSc, professor, RAS corresponding member; Anton Keskinov, PhD

TRANSLATORS Nadezda Tikhomirova, Vyacheslav Vityuk

DESIGN AND LAYOUT Marina Doronina

EDITORIAL BOARD

Agapov VK, DSc, professor (Moscow, Russia)
Bogomolov AV, DSc, professor (Moscow, Russia)
Boyko AN, DSc, professor (Moscow, Russia)
Borisevich IV, DSc, professor (Moscow, Russia)
Bushmanov AY, DSc, professor (Moscow, Russia)
Valenta R, PhD, professor (Moscow, Russia)
Daikhes NA, member of RAS, DSc, professor (Moscow, Russia)
Dudarenko SV, DSc (Saint-Petersburg, Russia)
Ilyin LA, member of RAS, DSc, professor (Moscow, Russia)
Lobzin YV, member of RAS, DSc, professor (Saint-Petersburg, Russia)
Nikiforov VV, DSc, professor (Moscow, Russia)

Olesova VN, DSc, professor (Moscow, Russia)
Petrov RV, member of RAS, DSc, professor (Moscow, Russia)
Sadilov AS, DSc, professor (Saint-Petersburg, Russia)
Rembovsky VR, DSc, professor (Saint-Petersburg, Russia)
Samoilov AS, member of RAS, DSc, professor (Moscow, Russia)
Sergienko VI, member of RAS, DSc, professor (Moscow, Russia)
Sidorceovich SV, DSc (Moscow, Russia)
Troitsky AV, DSc, professor (Moscow, Russia)
Ushakov IB, member of RAS, DSc, professor (Moscow, Russia)
Khaitov MR, member of RAS, DSc, professor (Moscow, Russia)
Yudin SM, DSc, professor (Moscow, Russia)

ADVISORY BOARD

Akleev AV, DSc, professor (Chelyabinsk, Russia)
Arakelov SA, PhD, professor (Saint-Petersburg, Russia)
Baklaushev VP, DSc, professor (Moscow, Russia)
Degteva MO, PhD (Chelyabinsk, Russia)
Efimenko NV, DSc, professor (Pyatigorsk, Russia)
Kazakevich EV, DSc, professor (Arkhangelsk, Russia)
Katuntsev VP, DSc, professor (Moscow, Russia)
Klimanov VA, DSc, professor (Moscow, Russia)
Klinov DV, PhD (Moscow, Russia)
Koshurnikova NA, DSc, professor (Ozersk, Russia)
Minnullin IP, DSc, professor (Saint-Petersburg, Russia)

Mosyagin IG, DSc, professor (Saint-Petersburg, Russia)
Panasenko OM, DSc, member of RAS, professor (Moscow, Russia)
Rogozhnikov VA, DSc, (Moscow, Russia)
Romanov SA, PhD (Ozersk, Russia)
Sotnichenko SA, DSc (Vladivostok, Russia)
Suranova TG, PhD, docent (Moscow, Russia)
Takhauov RM, DSc, professor (Seversk, Russia)
Shandala NK, DSc, professor (Moscow, Russia)
Shinkarev SM, DSc (Moscow, Russia)
Shipulin GA, PhD (Moscow, Russia)
Yakovleva TV, DSc (Moscow, Russia)

SUBMISSION editor@fmba.press

CORRESPONDENCE editor@fmba.press

COLLABORATION manager@fmba.press

ADDRESS Volokolamskoe shosse, 30, str. 1, Moscow, 123182, Russia

Indexed in Scopus in 2022

Indexed in RSCI. IF 2018: 0,570

Listed in HAC 31.01.2020 (№ 1292)

Open access to archive

Scopus®

НАУЧНАЯ ЭЛЕКТРОННАЯ
БИБЛИОТЕКА
LIBRARY.RU



ВЫСШАЯ
АТТЕСТАЦИОННАЯ
КОМИССИЯ (ВАК)

CYBERLENINKA

Issue DOI: 10.47183/mes.2022-02

The mass media registration certificate № 25124 issued on July 27, 2006

Founder and publisher: Federal medical-biological agency fmba.gov.ru

The journal is distributed under the terms of Creative Commons Attribution 4.0 International License www.creativecommons.org



Approved for print 30.06.2022
Circulation: 500 copies. Printed by Print.Formula
www.print-formula.ru

МЕДИЦИНА ЭКСТРЕМАЛЬНЫХ СИТУАЦИЙ

НАУЧНО-ПРАКТИЧЕСКИЙ РЕЦЕНЗИРУЕМЫЙ ЖУРНАЛ ФМБА РОССИИ

ГЛАВНЫЙ РЕДАКТОР Вероника Скворцова, д. м. н., профессор, член-корр. РАН

ЗАМЕСТИТЕЛИ ГЛАВНОГО РЕДАКТОРА Игорь Берзин, д. м. н., профессор; Дарья Крючко, д. м. н., доцент

НАУЧНЫЕ РЕДАКТОРЫ Всеволод Белоусов, д. м. н., профессор, член-корр. РАН; Антон Кескинов, к. м. н.

ПЕРЕВОДЧИКИ Надежда Тихомирова, Вячеслав Витюк

ДИЗАЙН И ВЕРСТКА Марины Дорониной

РЕДАКЦИОННАЯ КОЛЛЕГИЯ

В. К. Агапов, д. м. н., профессор (Москва, Россия)

А. В. Богомолов, д. т. н., профессор (Москва, Россия)

А. Н. Бойко, д. м. н., профессор (Москва, Россия)

И. В. Борисевич, д. м. н., профессор (Москва, Россия)

А. Ю. Бушманов, д. м. н., профессор (Москва, Россия)

Р. Валента, д. м. н., профессор (Москва, Россия)

Н. А. Дайхес, д. м. н., профессор, член-корр. РАН (Москва, Россия)

С. В. Дударенко, д. м. н., доцент (Санкт-Петербург, Россия)

Л. А. Ильин, д. м. н., профессор, академик РАН (Москва, Россия)

Ю. В. Лобзин, д. м. н., профессор, академик РАН (Санкт-Петербург, Россия)

В. В. Никифоров, д. м. н., профессор (Москва, Россия)

В. Н. Олесова, д. м. н., профессор (Москва, Россия)

Р. В. Петров, д. м. н., профессор, академик РАН (Москва, Россия)

А. С. Радилов, д. м. н., профессор (Санкт-Петербург, Россия)

В. Р. Рембовский, д. м. н., профессор (Санкт-Петербург, Россия)

А. С. Самойлов, д. м. н., профессор, член-корр. РАН (Москва, Россия)

В. И. Сергиенко, д. м. н., профессор, член-корр. РАН (Москва, Россия)

С. В. Сидоркевич, д. м. н. (Москва, Россия)

А. В. Троицкий, д. м. н., профессор (Москва, Россия)

И. Б. Ушаков, д. м. н., профессор, академик РАН (Москва, Россия)

М. Р. Хаитов, д. м. н., профессор, член-корр. РАН (Москва, Россия)

С. М. Юдин, д. м. н., профессор (Москва, Россия)

РЕДАКЦИОННЫЙ СОВЕТ

А. В. Аклеев, д. м. н., профессор (Челябинск, Россия)

С. А. Араkelов, к. б. н., профессор (Санкт-Петербург, Россия)

В. П. Баклаушев, д. м. н., профессор (Москва, Россия)

М. О. Дегтева, к. т. н. (Челябинск, Россия)

Н. В. Ефименко, д. м. н., профессор (Пятигорск, Россия)

Е. В. Казакевич, д. м. н., профессор (Архангельск, Россия)

В. П. Катунцев, д. м. н., профессор (Москва, Россия)

В. А. Климанов, д. ф.-м. н., профессор (Москва, Россия)

Д. В. Клинов, к. ф.-м. н. (Москва, Россия)

Н. А. Кошурникова, д. м. н., профессор (Озерск, Россия)

И. П. Миннуллин, д. м. н., профессор (Санкт-Петербург, Россия)

И. Г. Мосягин, д. м. н., профессор (Санкт-Петербург, Россия)

О. М. Панасенко, д. б. н., профессор, член-корр. РАН (Москва, Россия)

В. А. Рогожников, д. м. н. (Москва, Россия)

С. А. Романов, к. б. н. (Озерск, Россия)

С. А. Сотниченко, д. м. н. (Владивосток, Россия)

Т. Г. Суранова, к. м. н., доцент (Москва, Россия)

Р. М. Тахауов, д. м. н., профессор (Северск, Россия)

Н. К. Шандала, д. м. н., профессор (Москва, Россия)

С. М. Шинкарев, д. т. н. (Москва, Россия)

Г. А. Шипулин, к. м. н. (Москва, Россия)

Т. В. Яковлева, д. м. н. (Москва, Россия)

ПОДАЧА РУКОПИСЕЙ editor@fmba.press

ПЕРЕПИСКА С РЕДАКЦИЕЙ editor@fmba.press

СОТРУДНИЧЕСТВО manager@fmba.press

АДРЕС РЕДАКЦИИ Волоколамское шоссе, д. 30, стр. 1, г. Москва, 123182, Россия

Журнал включен в Scopus в 2022 г.

Журнал включен в РИНЦ. IF 2018: 0,570

Журнал включен в Перечень 31.01.2020 (№ 1292)

Здесь находится открытый архив журнала



ВЫСШАЯ
АТТЕСТАЦИОННАЯ
КОМИССИЯ (ВАК)



DOI выпуска: 10.47183/mes.2022-02

Свидетельство о регистрации средства массовой информации № ФС77-25124 от 27 июля 2006 года

Учредитель и издатель: Федеральное медико-биологическое агентство fmba.gov.ru

Журнал распространяется по лицензии Creative Commons Attribution 4.0 International www.creativecommons.org



Подписано в печать 30.06.2022

Тираж 500 экз. Отпечатано в типографии Print.Formula
www.print-formula.ru

Contents

Содержание

REVIEW	5
<hr/>	
Role of LINC complex proteins in sperm formation Kurchashova SYu, Gasanova TV, Bragina EE	
Роль белков LINC-комплекса в формировании сперматозоидов С. Ю. Курчашова, Т. В. Гасанова, Е. Е. Брагина	
REVIEW	13
<hr/>	
Methods for prevention and treatment of convulsive disorders associated with cholinergic convulsant intoxication Zorina VN, Evdokimova EA, Rejniuk VL	
Методы профилактики и терапии судорожного синдрома при отравлении конвульсантами холинергического ряда В. Н. Зорина, Е. А. Евдокимова, В. Л. Рейнюк	
REVIEW	20
<hr/>	
Primary pre-hospital triage of patients with COVID-19 Cherkashin MA, Berezin NS, Berezina NA, Nikolaev AA, Kuplevatskaya DI, Kuplevatsky VI, Rakova TM, Shcheparev IS	
Первичная медицинская сортировка пациентов с COVID-19 на догоспитальном этапе М. А. Черкашин, Н. С. Березин, Н. А. Березина, А. А. Николаев, Д. И. Куплевацкая, В. И. Куплевацкий, Т. М. Ракова, И. С. Щепарев	
REVIEW	29
<hr/>	
Omics technologies in the diagnostics of <i>Mycobacterium tuberculosis</i> Bespyatykh JA, Basmanov DV	
Омиксные технологии в диагностике <i>Mycobacterium tuberculosis</i> Ю. А. Беспятых, Д. В. Басманов	
ORIGINAL RESEARCH	37
<hr/>	
Neurophysiological assessment of speech function in individuals having a history of mild COVID-19 Gulyaev SA, Voronkova YuA, Abramova TA, Kovrazhkina EA	
Нейрофизиологическое исследование речевой функции у лиц, перенесших легкую форму COVID-19 С. А. Гуляев, Ю. А. Воронкова, Т. А. Абрамова, Е. А. Ковражкина	
ORIGINAL RESEARCH	44
<hr/>	
Cerebral energy exchange in employees of hazardous nuclear facilities and productions with the low degree of psychophysiological adaptation Zvereva ZF, Torubarov FS, Vanchakova NP, Denisova EA	
Церебральный энергообмен у работников ядерно опасных предприятий и производств с низким уровнем психофизиологической адаптации З. Ф. Зверева, Ф. С. Торубаров, Н. П. Ванчакова, Е. А. Денисова	
ORIGINAL RESEARCH	50
<hr/>	
Dynamics of humoral immunity to SARS-CoV-2 in the professionally homogeneous group of people over a two-year period of COVID-19 outbreak Pomelova VG, Vychenkova TA, Bekman NI, Osin NS, Ishkov YuN, Styazhkin KK	
Динамика гуморального иммунного ответа к SARS-CoV-2 в профессионально однородной группе людей за двухлетний эпидемический период COVID-19 В. Г. Помелова, Т. А. Быченкова, Н. И. Бекман, Н. С. Осин, Ю. Н. Ишков, К. К. Стяжкин	
ORIGINAL RESEARCH	58
<hr/>	
Subpopulation composition of T-helpers in the peripheral blood of persons chronically exposed to radiation in the long term Kotikova AI, Blinova EA, Akleyev AV	
Субпопуляционный состав Т-хелперов в периферической крови хронически облученных лиц в отдаленном периоде А. И. Котикова, Е. А. Блинова, А. В. Аклеев	

ORIGINAL RESEARCH

67

Evaluation of the impact of COVID-19 pandemic on overall mortality in Ozyorsk urban district

Osipov MV, Sokolova VA, Kushnir AS

Оценка влияния пандемии COVID-19 на общий коэффициент смертности населения Озерского городского округа

М. В. Осипов, В. А. Соколова, А. С. Кушнир

ORIGINAL RESEARCH

73

Screening the activity of incorporated radionuclides in the research organization employees

Turlakov YuS, Grabsky YuV, Arefeva DV, Shayakhmetova AA, Firsanov VB, Petushok AV

Скрининг активности инкорпорированных радионуклидов у персонала научно-исследовательской организации

Ю. С. Турлаков, Ю. В. Грабский, Д. В. Арефьева, А. А. Шаяхметова, В. Б. Фирсанов, А. В. Петушок

ORIGINAL RESEARCH

79

Psychological well-being of the department heads at healthcare organizations

Kochubey AV, Yarotsky SYu, Kochubey VV

Психологическое благополучие заведующих отделениями медицинских организаций

А. В. Кочубей, С. Ю. Яроцкий, В. В. Кочубей

ORIGINAL RESEARCH

85

Medical rehabilitation of high performance athletes after reconstruction of anterior cruciate ligament of the knee

Boichenko RA, Gornov SV

Медицинская реабилитация в спорте высших достижений после реконструкции передней крестообразной связки коленного сустава

Р. А. Бойченко, С. В. Горнов

CLINICAL CASE

91

Early comprehensive rehabilitation of patient with postoperative dysphagia

Orlova OS, Magomed-Eminov MSh, Uklonskaya DV, Zborovskaya YuM

Ранняя комплексная реабилитация пациента с постоперационной дисфагией

О. С. Орлова, М. Ш. Магомед-Эминов, Д. В. Уклонская, Ю. М. Зборовская

ROLE OF LINC COMPLEX PROTEINS IN SPERM FORMATION

Kurchashova SYu¹ ✉, Gasanova TV³, Bragina EE^{1,2}

¹ Belozersky Institute of Physico-Chemical Biology, Lomonosov Moscow State University, Moscow, Russia

² Bochkov Medical Genetic Research Center, Moscow, Russia

³ Faculty of Biology, Lomonosov Moscow State University, Moscow, Russia

Spermatogenesis is characterized by the significant changes of three-dimensional organization of the nucleus in spermatocytes, spermatides and spermatozoa. The functional cooperation between the nuclear envelope proteins and the acroplaxome/manchette is essential for nuclear elongation, acrosome biogenesis, formation of the flagellum. Furthermore, the nuclear envelope ensures the non-random chromosome arrangement within the nucleus. The LINC (linker of nucleoskeleton and cytoskeleton) complex proteins are involved in interaction between the cytoskeleton and the nucleoskeleton, as well as in the control of mechanotransduction. The LINC complex contains proteins of the outer and inner nuclear membranes: KASH and SUN, respectively. The LINC complex proteins are involved in formation of the sperm head and flagellum, and are, therefore, essential for male fertility. This review will consider the issues of the LINC complex protein localization in cells during the successive stages of spermatogenesis, the role in regulation of sperm maturation, and mutations of the LINC complex proteins resulting in male infertility.

Keywords: LINC complex, nuclear lamina, nuclear pores, globozoospermia, male infertility

Funding: this research was supported by the Interdisciplinary Scientific and Educational School of Lomonosov Moscow State University "Molecular Technologies of the Living Systems and Synthetic Biology".

✉ **Correspondence should be addressed:** Svetlana Yu. Kurchashova
Leninskie gory, 1–40, Moscow, 119992, Russia; svetak99@mail.ru

Received: 27.05.2022 **Accepted:** 11.06.2022 **Published online:** 30.06.2022

DOI: 10.47183/mes.2022.023

РОЛЬ БЕЛКОВ LINC-КОМПЛЕКСА В ФОРМИРОВАНИИ СПЕРМАТОЗОИДОВ

С. Ю. Курчашова¹ ✉, Т. В. Гасанова³, Е. Е. Брагина^{1,2}

¹ Научно-исследовательский институт физико-химической биологии имени А. Н. Белозерского Московского государственного университета имени М. В. Ломоносова, Москва, Россия

² Медико-генетический научный центр имени Н. П. Бочкова, Москва, Россия

³ Биологический факультет Московского государственного университета имени М. В. Ломоносова, Москва, Россия

Процесс сперматогенеза характеризуется значительными изменениями в трехмерной организации ядер в сперматоцитах, сперматиде и сперматозоидах. Элонгация ядра, биогенез акросомы, формирование жгутика требуют функциональной кооперации между белками ядерной оболочки и акроплаксомы/манжеты. Помимо этого, ядерная оболочка обеспечивает неслучайное распределение хромосом в ядре. Белки комплекса, связывающего нуклеоскелет и цитоскелет (linker of nucleoskeleton and cytoskeleton, LINC), участвуют во взаимодействии цито- и нуклеоскелета, а также управляют механотрансдукцией. В состав LINC-комплекса входят белки внешней и внутренней мембраны KASH и SUN соответственно. Белки LINC-комплекса вовлечены в формирование головки и жгутика сперматозоида, таким образом, они необходимы для мужской фертильности. В обзоре представлены вопросы локализации белков LINC-комплекса в клетках на последовательных стадиях сперматогенеза, роль в регуляции созревания сперматозоидов и мутации белков LINC-комплекса, приводящие к мужскому бесплодию.

Ключевые слова: LINC-комплекс, ядерная ламина, ядерные поры, глобулозооспермия, бесплодие

Финансирование: работа была выполнена при поддержке Научно-образовательной школы МГУ им. М. В. Ломоносова «Молекулярные технологии живых систем и синтетическая биология».

✉ **Для корреспонденции:** Светлана Юрьевна Курчашова
Ленинские горы, д. 1, стр. 40, г. Москва, 119992; svetlanak@belozersky.msu.ru svetak99@mail.ru

Статья получена: 27.05.2022 **Статья принята к печати:** 11.06.2022 **Опубликована онлайн:** 30.06.2022

DOI: 10.47183/mes.2022.023

Spermatogenesis, which is responsible for sperm differentiation, is coordinated in space and time. During the process, male germ cells undergo changes when going through three fundamental phases: spermatogonial stem cell self-renewal, spermatogonial proliferation, meiotic division of spermatocytes to produce haploid round spermatids, and transformation of spermatids into spermatozoa. Spermatozoa acquire optimal architecture; the nuclear structures undergo changes that ensure the pairing of homologous chromosomes during meiosis, formation of haploid cells, extremely marked chromatin condensation to protect the parental genome from chemical and physical stress, and sperm head size reduction. Spermatogenesis involves formation of the acrosome and the flagellum in round spermatids, cytoplasm elimination, and nuclear condensation that requires histone replacement by protamines. The nuclear envelope alterations affect both inner and outer nuclear membranes. The outer membrane is involved in nuclear positioning and movement;

the inner membrane is associated with the nuclear lamina, the 3-dimensional protein meshwork of lamins together with lamina-associated proteins and chromatin. This regulates a broad range of functions of the nucleus, such as chromatin organization, DNA transcription and replication. Chromosomes occupy specific regions of cell nucleus, called "chromosome territories". Chromosomes in sperm nuclei are characterized by radial arrangement that affects gene expression. The nuclear envelope and integral proteins of the inner nuclear membrane play a key role in chromosome positioning and sperm head formation [1]. Nuclear reorganization is typical for both spermatocytes and spermatids. During meiotic prophase, the nuclear envelope proteins together with cytoskeletal elements control chromosome positioning. The nuclear envelope provides a platform for assembly of multiprotein complexes involved in gene expression regulation that results in morphological alterations of cells, such as nuclear elongation, acrosome

biogenesis, and flagellum formation [2]. A physical link is formed between the nucleoskeleton and cytoskeleton, which is essential for the nuclear positioning and motion. The LINC protein complex, the linker of nucleoskeleton and cytoskeleton, is formed by two transmembrane protein systems: the Nuclear Envelope Spectrin repeat proteins (NESPRIN), located in the outer nuclear membrane, and Sad1p-UNC84 (SUN), located in the inner nuclear membrane [3–5]. The central domains of NESPRIN proteins are of various lengths. C-terminal KASH (Klarsicht, ANC-1, Syne homology) transmembrane domain promotes the nuclear envelope localization and N-terminal domain is linked to the cytoskeleton [6–8]. On the contrary, SUN protein has a nucleoplasmic N-terminal domain linked to the nucleoskeleton, and a C-terminal domain located to the perinuclear space [2]. Nesprins include four proteins identified as KASH proteins, encoded by four genes, known as SYNE1, SYNE2, SYNE3, and SYNE4. The SUN family is comprised of five proteins (SUN1–5) [6, 9, 10]. The most common Nesprin isoforms, KASH1 and KASH2, are able to interact with F-actin. KASH3 is associated with intermediate filaments through the plectin-binding sequence [11]. KASH 4 interacts with kif5b, the microtubule-dependent motor kinesin-1 subunit, and, therefore, with microtubules [2]. In addition to these four members, KASH5 is the most divergent one; the KASH5 N-terminal domain interacts with dynein-dynactin. KASH5 mediates attachments between microtubules and chromosomes, and contributes to the rapid movement of chromosomes in the nuclei, thus facilitating chromosome pairing. Furthermore, this protein plays an important role in human fertility [12]. Among SUN proteins, SUN1 and SUN2 are expressed in somatic cells, while SUN3, SUN4 (the alternative name is SPAG4), and SUN5 (the alternative name is SPAG4L) are expressed exclusively in the testis [2, 9, 13]. The intracellular signaling pathways involve not only the LINC complex, but also the nuclear pore complex [14]. Firstly, SUN proteins located in the inner nuclear membrane require protein import into the nucleus, i.e. the properly functioning nuclear pores are necessary. Secondly, SUN1, colocalized with nucleoporin Nup153, affects the arrangement of the nuclear pore complexes [15]. The combination of SUN1 and SUN2 interacts with the mRNA particles, directly involved in the mRNA export through the nuclear pores in mammalian cells [16]. The regulatory function of the LINC complex during spermatogenesis was assessed in a number of studies. It has been shown that the LINC complex proteins are involved in proper chromosome pairing, meiotic chromosome recombination, telomere motion and attachment. SUN1 deficiency in mice prevents telomere attachment to the nuclear envelope, effective pairing of homologous chromosomes, and synapsis formation during prophase of meiosis. KASH5, being a specific partner of SUN1, is also involved in these events. SUN2 binds to KASH5 to form the SUN1-SUN2-KASH5 complex involved in meiotic telomere attachment to the nuclear envelope [2, 17]. SUN5 is involved in meiotic recombination as well. It is assumed that the SUN5-KASH2-LINC complex is involved in meiotic division of murine spermatocytes [18]. This function is associated with the presence in the cells of the properly functioning nuclear lamina, the fibrous layer underlying the inner nuclear membrane. In mouse cells, KASH5, colocalized with lamin B1, is involved in the nuclear motion during meiosis [19]. The LINC complex is also involved in sperm head formation and head-to-tail linkage. Thus, the LINC complex proteins play important role in male fertility [13, 20, 21]. Further study of characteristics of proteins of this complex will make it possible to create a relevant express test system, allowing us to

assess the contribution of each protein to the development of spermatozoa, impaired spermatogenesis and infertility treatment adjustment.

The issues regarding the role of proteins in the development of mature spermatozoa and the role of the LINC complex protein mutations in male infertility are discussed in this review.

Role of LINC complex in mechanotransduction

Mechanobiology describes how mechanical forces influence cell morphology and physiology. Such exposure is involved in regulation of cell development and differentiation. The majority of mechanical effects result in nuclear motion, alterations in the nuclear shape, chromatin structure, and gene expression. The LINC complex plays a crucial role in these processes. Via mechanotransduction, cells convert mechanical stimuli to biochemical signals, thus providing the link between the cytoskeleton and the nucleoskeleton. Mechanical forces applied to cells are converted to biochemical signals transmitted from the cytoskeleton to the nucleus, providing modulation of the nuclear envelope composition, nuclear shape, and gene expression. The LINC complex is hub for signal transduction from the cytoskeleton to the cell nucleus. This idea emerged after the study of the isolated nuclei exposed to mechanical stimuli. This experiment showed that the LINC complex disruption or impaired communication between the LINC complex and the nuclear lamina caused cytoskeletal disorganization and affected both signal transduction through the cytoskeleton to the nucleus together with gene expression [22]. Actin plays a key role in mechanotransduction. Actin is involved in cellular motility, signal transduction and response to mechanical stress. Some other functions of actin have been reported recently: the network formed by actin filaments near the nuclear envelope may be involved in regulation of the nuclear motion and may affect gene expression [23]. The LINC complex provides mechanical coupling between the nucleus and the actin cytoskeleton that affects nuclear motion and positioning. Binding between actin and LINC complex is mediated by KASH proteins, which on the one hand interact with SUN proteins of the nuclear envelope, and on the other, interact with the cytoskeleton via the actin-binding domain [24]. Actin forms thread-like structures that cover the surface of the nucleus. In these structures, actin interacts with KASH2 or KASH3 by contributing to the nuclear orientation and shaping, and protects the nucleus from mechanical deformation. Mutations of KASH2/KASH3 are associated with inhibition of the perinuclear actin cap assembly and adversely affect mechanotransduction [26]. Hippo kinase signaling cascade is one of the major pathways for signal transduction from mechanoreceptors. This evolutionary conservative pathway is involved in regulation of cell proliferation and tissue differentiation, as well as in specifying the organ size. The cascade of reactions induces activation of actin. The signaling pathway involves Yes-associated protein (YAP) and the homologous TAZ protein (transcription co-activator) with PDZ binding motif. PDZ motif is a sequence of 80–90 amino acids, arranged in six β -sheets (β A– β F) and two α -helices (α A, α B). Moving between the nucleus and the cytoplasm, YAP and TAZ transmit signals from mechanoreceptors to the nucleus [26]. During mitosis, actin and the LINC complex proteins regulate centrosome and chromosome positioning; during meiosis, actin is also involved in nuclear motion [27]. Actin and the LINC complex proteins control gene expression. Thus, actin is involved in the determination of the nuclear volume, chromatin conformation, and chromatin accessibility for transcription factors responsible for gene expression. Alterations in gene

expression result from the LINC complex abnormalities and the LINC complex-dependent mechanisms. KASH protein downregulation leads to gene expression alterations in epithelial cells [28]. In other words, transcription is not only regulated via mechanosignaling, but also depends directly on the LINC complex protein integrity. Currently, it is still unclear whether the LINC complex proteins are directly bound with chromatin, or interaction is realized via the nuclear lamina. Furthermore, histones are replaced by protamines in the post-meiotic germ cells. In somatic cells, the Lamin B receptor (LBR), the integral protein of the inner nuclear membrane, interacts with lamin B1 and provides the link between the nuclear lamina and chromatin. The interaction involves heterochromatin protein 1 (HP1) and BAF protein (barrier to autointegration factor) [29, 30]. In germ cells, LBR can temporarily bind to protamine 1. During mammalian spermatogenesis, protamines are phosphorylated to ensure the binding of chromatin in spermatids and are completely dephosphorylated during sperm maturation [31]. In elongated spermatids, phosphorylation is required to ensure the temporary association of protamine P1 and LBR [32]. Localization of a number of the nuclear envelope proteins during spermatogenesis in humans was studied [30]. Polymerase chain reaction and immunofluorescence analysis revealed LEMD1 protein, together with ANKLE2, LAP2 β and the short isoform of protein LEMD2 in spermatids. However, no emerin, LBR, full-length forms of LEMD2 and LEMD3 were found in the samples. Proteins LEMD1, ANKLE2, LAP2 β , emerin, LBR, full-length forms of LEMD2 and LEMD3, lamins A, C and B2 were not found in ejaculated spermatozoa. Thus, the nuclear envelope proteins involved in interaction with chromatin in somatic cells change their localization in the nuclei of spermatids and spermatozoa in accordance with the chromosome positioning and stabilization in specific areas of the nucleus. In humans, such alterations in the composition of the nuclear envelope in spermatids may provide chromatin detachment from the nuclear envelope and lamina that increases the potential of the histone-to-protamine transition [30]. BAF and BAF-L (BAF-like) proteins were found in spermatozoa [33]. BAF homodimers are involved in chromatin condensation, BAF/BAF-like heterodimers are able to increase the massive histone-to-protamine transition due to more "open" chromatin conformation [30]. Actin, being the conventional cytoskeletal component that provides communication with the LINC complex, circulates between the nucleus and the cytoplasm. In the nucleus, actin regulates the activity of transcription factors, contributes to the assembly of some chromatin remodeling complexes, and appears to be associated with three different RNA polymerase complexes [34]. One of the mechanisms underlying mechanotransduction functions as follows: mechanical stimuli are able to induce physical alterations in the nuclear pore complexes regardless of the LINC complex [35]. Mechanical alterations can also modulate the phosphorylation status of the nuclear envelope proteins. Lamins A and C are examples of proteins, whose phosphorylation define nuclear stiffness in response to mechanical stimuli [36]. Chromatin organization can be changed under the influence of cell exposure to environmental factors and cytoskeletal reorganization; such alterations of the chromatin status affect gene expression. Perinuclear actin provides the LINC complex protein-mediated regulation of the lamins A and C hyperacetylation, chromatin decondensation, and gene expression activation. The nuclear import is an alternative mechanism designed for regulation of gene expression induced by mechanotransduction. Import of histone-lysine N-methyltransferase EZH2 causes gene silencing due to histone methylation, while import of histone deacetylase (HDAC) leads to gene repression due to hypoacetylation [37, 38].

LINC proteins and sperm head

Acrosomal and postacrosomal segments are distinguished in the sperm head. The nucleus containing highly compacted chromatin occupies almost the entire sperm head. It is covered partially by the acrosome, a cap-shaped organelle derived from the Golgi apparatus that contains enzymes and receptors for oocyte binding. The acroplaxome is a structure located between the acrosomal membrane and the nuclear membrane that surrounds the developing acrosome and attaches it to the nuclear envelope. The acroplaxome contains keratin 5, F-actin and profilin IV. The manchette is a transient structure containing microtubules of centrosome [39]. Sperm capacitation occurs in the female genital tract. Capacitation involves biochemical modifications essential for oocyte fertilization. The testis-specific form of the SUN protein (SUN1 η is the most interesting component of this cascade [20]. SUN1 η is located at the anterior pole of the nucleus and points to the acrosomal membrane instead of the inner nuclear membrane. This protein participates in assembly of the extranuclear LINC-KASH3 complex involved in the plectin-mediated interaction with the acroplaxome. The same complex is assembled on the posterior pole of the nucleus (except for the area of the implantation fossa) [40]. Recent studies have shown that SUN3 and SUN4 are essential for sperm head formation. During spermatogenesis, the expression of SUN3 increases when the round spermatids are formed, and further increases during formation of elongated spermatids. SUN3 is localized in the lateral and posterior parts of the spermatid nucleus, however, no SUN3 was found in the implantation fossa and the rearmost part of the nucleus. KASH1 is the partner of SUN3 in the sperm head. KASH1, colocalized with SUN3, is involved in the LINC complex assembly. The LINC complex is capable of interacting with actin by the actin-binding domain or with microtubules via the dynein–dynactin complex. It can improve the interaction between the manchette and the outer nuclear membrane [20]. SUN4 is expressed only during spermatogenesis. It is localized to the posterior poles of the round and elongated spermatids. The protein complex SUN3-SUN4-KASH1 provides the link between the manchette and the nuclear envelope. Abnormal numbers of round spermatids, impaired sperm head elongation, and nuclear envelope disintegration with subsequent production of the deformed spermatozoa could be observed in the Sun4 knockout mice. The decrease in the level of SUN4 induces the SUN3 protein migration to the cytoplasm and manchette disorganization. This indicates that SUN4 is essential for normal SUN3 and KASH1 localization in the cell [13]. In humans, SUN4 forms the complex with the cytoskeletal protein septin (SEPT12) expressed specifically in testes and lamin B1 involved in the sperm head formation in post-meiotic germ cells, as well as in the sperm flagellum arrangement [41]. Along with actin filaments, microtubules, and intermediate filaments, the cytoskeleton also contains septins engaged in various physiological functions. In particular, SEPT12 is involved in mammalian spermatogenesis: it is expressed around the manchette, in the necks of elongated spermatids and annuli of mature spermatozoa [42]. In the study of the role of the LINC complex in acrosome biogenesis, the new testis-specific protein SPAG4L-2 of the family SPAG4L was characterized. High level of protein expression was observed during spermatogenesis; the protein was localized in the apical region of the round spermatid nucleus that points at the acrosome [43]. During nuclear elongation, SUN5 progressively migrates to the posterior pole of the nucleus in elongated spermatids to finally reach the implantation fossa. Such redistribution of protein excludes the protein from

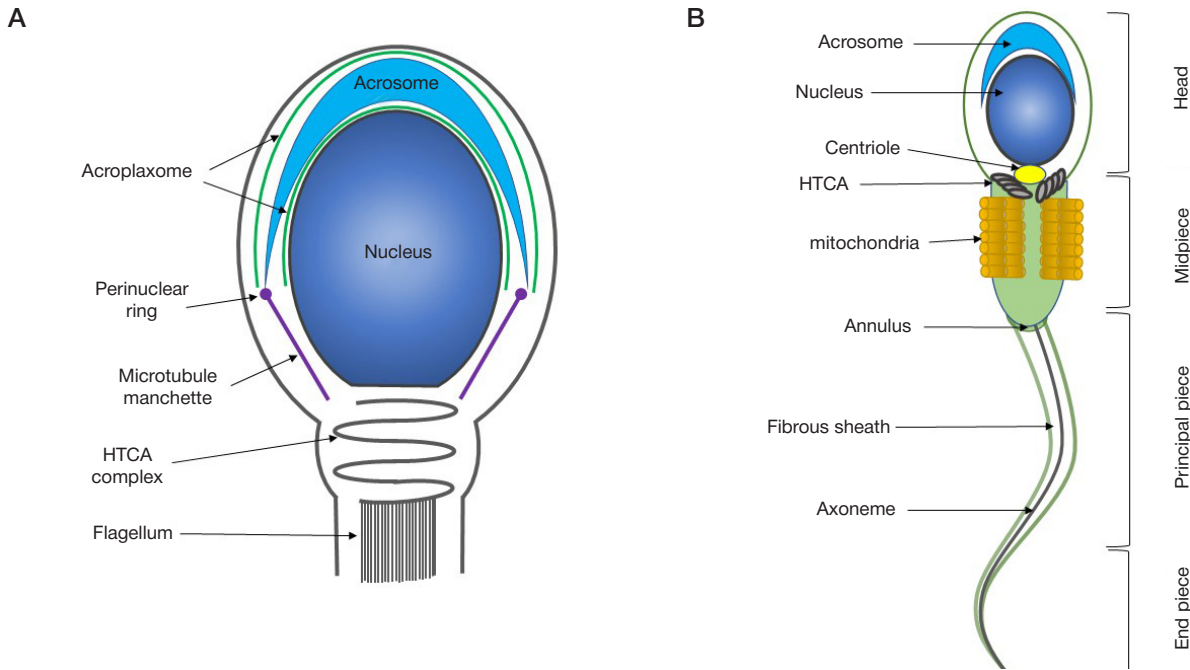


Fig. A. Spermatid structure. B. Structure of spermatozoon

the sperm head formation process. Sun5 knockout mice showed no disturbances of acrosomal development, however, abnormalities of the sperm flagella were found [44, 45]. Lamins are also involved in acrosome biogenesis. Lamins A and C were characterized as the components of the acroplaxome that is essential for acrosome biogenesis and spermatid head formation. Phosphorylation is an important mechanism responsible for the localization of lamins A/C in the cytoplasm, nucleoplasm or nuclear lamina [46]. Lamin B1 interacts with the testis-specific protein DRY19L2 synthesized mainly in spermatids. Disruption of DRY19L2 results in the altered localization of lamin B1 during spermatogenesis, as well as in the disturbed communication between the nuclear envelope and the acroplaxome during acrosome biogenesis. The sperm nucleus seems to be poorly compacted, and histones are not replaced by protamines. This results in globozoospermia, the condition characterized by abnormal sperm with rounded heads [47]. No KASH2 and KASH4 were found at any stage of the post-meiotic sperm development. The germ cell-specific protein KASH5 is localized to the cytoplasm. KASH5, forming complexes with SUN1 and SUN2, mediates telomere attachment to the cytoskeleton and chromosome movement in spermatocytes [2, 20, 48].

LINC complex and sperm flagellum

The sperm flagellum is divided into the connecting piece, the midpiece, the principal piece, and the end piece (see Figure). The axoneme that comprises two central and nine pairs of peripheral microtubules, is the core structure of the flagellum. The axoneme is surrounded by periaxonemal structures: nine longitudinally oriented outer dense fibers in the midpiece and principal piece, the fibrous sheath in the principal piece, and mitochondria that form a mitochondrial sheath surrounding the outer dense fibers in the midpiece of the flagellum. The flagellum is responsible for sperm motility that is essential for fertilization. Flagellar motility is ensured by the normally functioning cytoskeleton, ATP production by mitochondria, and correct arrangement of the axonemal components. ATP synthesis is ensured by both glycolysis and oxidative phosphorylation. Implantation fossa,

i.e. the segment providing the head-to-tail connection, plays a vital part in sperm function. The coupling apparatus is an asymmetric structure formed during spermatogenesis that contains centrioles (proximal and distal), dense fibrous structure (capitulum), and segmented columns [2]. The LINC complex proteins are involved in interaction between the coupling apparatus and the sperm head: particularly, SUN4 and SUN5 are involved in the head-to-tail anchorage [21]. SUN4 protein contributes to the outer dense fiber positioning, providing a link between axonemal microtubules and outer dense fibers. The researchers studied the mechanisms responsible for such interactions [9]. Sun4 knockout mice have been reported [13]: the flagellum is wrapped around the murine sperm head, suggesting incorrect connection of these structures. Coupling apparatus abnormalities associated with the SUN4 deficiency were not found, however, the lower head-to-tail linkage efficiency was observed [48]. The coupling apparatus is to a lesser extent attached to the lateral areas of the nucleus, suggesting that SUN4 is involved in the interaction. Such proteins as ODF1, SEPT12 and lamin B1 are the partners of SUN4. SEPT12 is involved in formation of the flagellum; together with SUN4 and lamin B1, SEPT12 is associated with the sperm neck [49]. According to available data, SUN5 is essential for the head-tail anchoring. SUN5 is localized in the nuclear envelope during spermatogenesis, however, in mature sperm, SUN5 is found exclusively in the head-tail coupling apparatus (HTCA) in the implantation fossa essential for the head-tail connection. Destroyed connection of the coupling apparatus to the sperm head with subsequent releasing of the flagellum into the lumen of the seminiferous tubule and retention of sperm head within the tubular epithelium was found in elongated spermatids of the Sun5 knockout mice [45]. A similar disorder was discovered in men with homozygous deletions of Sun5 associated with the emergence of decapitated spermatozoa [50]. To ensure interaction, SUN5 can co-operate with the heat shock protein DNAJB13, the structural component of axoneme found in spermatids and spermatozoa. It is believed that SUN5 prevents separation of the sperm head from the flagellum during sperm migration into the lumen of the seminiferous tubule [45].

Table. Nuclear envelope proteins involved in human spermatogenesis

Protein	Cells	Localization	Functions	Reference
Lamin B1	Spermatocytes	Nuclear envelope (NE)	The decreasing levels of lamin B1 are essential to reduce mechanical forces of NE, which is necessary to ensure chromosome movement during meiotic prophase. Ensures the specific non-random arrangement of chromosomes in the nuclei during cell maturation. Progressive decrease in lamin B1 is essential for the sperm head formation	[51]
	Round spermatids	Nuclear envelope, posterior pole of the nucleus Nucleoplasm		
	Elongating spermatids	Posterior pole of the nucleus		
	Elongated spermatids	Posterior pole of the nucleus		
	Mature sperm	Posterior pole of the nucleus		
LAP1	Spermatogonia	Nuclear envelope	Ensures the specific non-random arrangement of chromosomes in the nuclei during cell maturation. Ensures manchette formation	[52]
	Spermatocytes	Nuclear envelope, cytoplasm		
	Round spermatids	Posterior pole of the nucleus		
	Elongating spermatids	Posterior pole of the nucleus		
	Elongating spermatids	Posterior pole of the nucleus		
LAP2	Round spermatids	Nuclear envelope, nucleoplasm (for LAP2beta)	Ensures the specific non-random arrangement of chromosomes in the nuclei during cell maturation. Ensures chromatin compaction (together with BAF, BAF-L)	[30]
LEMD1	Round spermatids	Nucleoplasm, posterior pole of the nucleus	Ensures chromatin compaction (together with BAF, BAF-L)	[30]
	Elongating spermatids	Posterior pole of the nucleus		
	Elongated spermatids	Posterior pole of the nucleus		
SUN4	Round spermatids	Nuclear envelope	Ensures manchette microtubule attachment to the nucleus together with SUN3 and nesprin-1. Lateral binding of the coupling complex in the implantation fossa essential for the tight head-to-tail anchorage. Ensures sperm flagellum arrangement during spermiogenesis together with ODF1	[13]
	Elongating spermatids	Neck		
	Elongated spermatids	Neck		
	Mature sperm	Axoneme		

LINC complex and infertility

The LINC complex proteins are crucial for sperm differentiation. Impaired SUN and KASH protein interactions result in significantly lower sperm quality.

1. Knockout of Sun1 in mice results in infertility due to impaired interactions between SUN1 and telomeres during recombination in primary spermatocytes. Since the SUN1–KASH5 complex regulates telomere motion, KASH5 mutations result in inefficient telomere attachment to the nuclear envelope, and compromises homologous chromosome pairing [17]. It was shown that Sun1 knockout mice were infertile. Furthermore, cells of testes of such mice contained no coding or non-coding RNAs essential for spermatogenesis. This fact shows the new role played by the SUN1 protein in gene regulation [2].

2. Sun3 knockout mice are infertile; they display disruption of both flagellum and head. The main defects emerge during formation of elongated spermatids, since spermatid nuclei are unable to elongate due to impaired signal transduction between the cytoskeleton and the nuclear envelope. Animals producing a low concentration of spermatozoa are characterized by acrosome defects, low motility, and globozoospermic phenotype. It has been shown that SUN3 is engaged in the manchette attachment to the nuclear envelope via SUN3-SUN4-KASH1 [13]. Sun3 knockout mice demonstrate lower expression of SUN4 protein in association with abnormal

manchette formation. Spermatogenesis of SUN4-deficient mice progresses normally before meiosis. However, impaired post-meiotic differentiation results in infertility. Spermatid nuclei are round-shaped or altered, impaired chromatin remodeling is observed. The disorganized manchette is unable to ensure the nuclear envelope attachment necessary for the sperm head formation; acrosomal alterations occur and formed spermatozoa show signs of globozoospermia. Sun4 knockout mice show the reduced amount of SUN3 in spermatids along with abnormal sperm head elongation. Instead of the typical distribution of SUN3 polarized to the posterior pole of the nuclear envelope, this protein moves to the cytoplasm. The altered amounts of SUN4 correlate with inefficient sperm head-to-tail anchorage. In particular, spermatids of the Sun4 knockout mice show detachment of the coupling apparatus from the nuclear membrane that adversely affects the head-to-tail anchorage [48]. Taking into account the SUN4 capability of binding to SEPT12, the need to study the role of SEPT12 in infertility becomes clear. Indeed, Sept12 knockout mice produce sperm with multiple defects of flagella and heads, disrupted nuclei, premature chromosome condensation. Spermatozoa obtained from such mice cause preimplantation embryo developmental failure [2].

3. Sun5 knockout mice produce acephalic spermatozoa. SUN5 protein is essential for the sperm head-to-tail anchorage; knockout leads to their separation in elongated spermatids, thus causing infertility [51].

CONCLUSION

Male infertility remains a pressing issue of human reproduction. Infertility affects 15% of couples of reproductive age in the world. Quantitative, kinematic and morphological characteristics of sperm are assessed in order to estimate the fertilization potential of spermatozoa. According to the current WHO Manual for human semen analysis (WHO, 2021), in 95% of fertile men, ejaculate contains at least 4% of spermatozoa with the morphology typical for the potentially fertile subpopulation, that penetrated through cervical mucus *in vivo* after the coitus. The rest of the sperm subpopulation is characterized by morphological heterogeneity: spermatozoa have various structural defects of the head, acrosome, neck, and flagella. In particular, globozoospermia is diagnosed when the sperm morphology assessment reveals head defects, such as round head

(100% of spermatozoa for type 1 globozoospermia, and 40–80% for type 2 globozoospermia), along with no acrosomes or pronounced acrosomal defects [53].

Studying the disorders associated with male infertility is a challenge. Testicular integrity and sperm quality depend on both genetic and epigenetic factors. The effects of harmful chemicals, stress, and diets can be critical for spermatogenesis and embryo formation. Various protein complexes and hormones control the process of sperm differentiation. In particular, the LINC complex proteins ensure the functions of spermatozoa and their precursor cells throughout the entire differentiation process (see Table). The use of knockout animal models is required for exact determination of the function of each protein. It is also necessary to analyse the composition of the nuclear envelope during the sperm differentiation. This will make possible to identify new therapeutic targets in animals and later in humans to overcome the problem of infertility.

References

- Hazzouri M, Rousseaux S, Monegelard F, Usson Y, Pelletier R, Faure AK, et al. Genome organization in the human sperm nucleus studied by FISH and confocal microscopy. *Mol Reprod Dev.* 2000; 55: 307–315.
- Manfrevola F, Guillou F, Fasano S, Pierantoni R, Chianese R. LINCKing the Nuclear Envelope to Sperm Architecture. *Genes.* 2021; 12: 658.
- Crisp M, Liu Q, Roux K, Rattner JB, Shanahan C, Burke B, et al. Coupling of the nucleus and cytoplasm: Role of the LINC complex. *J Cell Biol.* 2006; 172: 41–53.
- Stewart-Hutchinson PJ, Hale CM, Wirtz D, Hodzic D. Structural requirements for the assembly of LINC complexes and their function in cellular mechanical stiffness. *Exp Cell Res.* 2008; 314: 1892–905.
- Sosa BA, Rothballer A, Kutay U, Schwartz TU. LINC complexes form by binding of three KASH peptides to domain interfaces of trimeric SUN proteins. *Cell.* 2012; 149: 1035–47.
- Hodzic DM, Yeater DB, Bengtsson L, Otto H, Stahl PD. Sun2 is a novel mammalian inner nuclear membrane protein. *J Biol Chem.* 2004; 279: 25805–12.
- Padmakumar VC, Libotte T, Lu W, Zaim H, Abraham S, Noegel AA, et al. The inner nuclear membrane protein Sun1 mediates the anchorage of Nesprin-2 to the nuclear envelope. *J Cell Sci.* 2005; 118: 3419–30.
- Starr DA. A nuclear–envelope bridge positions nuclei and moves chromosomes. *J Cell Sci.* 2009; 122: 577–86.
- Shao X, Tarnasky HA, Lee J.P, Oko R, van der Hoorn FA. Spag4, a Novel Sperm Protein, Binds Outer Dense-Fiber Protein Odf1 and Localizes to Microtubules of Manchette and Axoneme. *Dev Biol.* 1999; 211: 109–23.
- Kim DI, Kc B, Roux KJ. Making the LINC: SUN and KASH protein interactions. *Biol Chem.* 2015; 396: 295–310.
- Wilhelmsen K, Litjens SH, Kuikman I, Tshimbalanga N, Janssen H, van den Bout I, Raymond K et al, Nesprin-3, a novel outer nuclear membrane protein, associates with the cytoskeletal linker protein plectin. *J Cell Biol.* 2005; 171: 799–810.
- Gurusaran M, Davies OR. A molecular mechanism for LINC complex branching by structurally diverse SUN-KASH 6:6 assemblies. *eLife.* 2021; 10: e60175.
- Pasch E, Link J, Beck C, Scheuerle S, Alsheimer M. The LINC complex component Sun4 plays a crucial role in sperm head formation and fertility. *Biol Open.* 2015; 4: 1792–802.
- Jahed Z, Soheilypour M, Peyro M, Mofrad MR. The LINC and NPC relationship—it's complicated! *J Cell Sci.* 2016; 129: 3219–29.
- Liu Q, Pante N, Misteli T, Elsagga M, Crisp M, Hodzic D, et al. Functional association of Sun1 with nuclear pore complexes. *J Cell Biol.* 2007; 178: 785–98.
- Li P, Noegel AA. Inner nuclear envelope protein SUN1 plays a prominent role in mammalian mRNA export. *Nucleic Acids Res.* 2015; 43: 9874–88.
- Horn HF, Kim DI, Wright GD, Wong ESM, Stewart CL, Burke B, et al. A mammalian KASH domain protein coupling meiotic chromosomes to the cytoskeleton. *J Cell Biol.* 2013; 202: 1023–39.
- Li X, Wu Y, Huang L, Yang L, Xing X. SPAG4L/SPAG4L β interacts with Nesprin2 to participate in the meiosis of spermatogenesis. *Acta Biochim Biophys Sin.* 2019; 51: 669–76.
- Jiang XZ, Yang MG, Huang LH, Li CQ, Xing XW. SPAG4L, a novel nuclear envelope protein involved in the meiotic stage of spermatogenesis. *DNA Cell Biol.* 2011; 30: 875–82.
- Göb E, Schmitt J, Benavente R, Alsheimer M. Mammalian Sperm Head Formation Involves Different Polarization of Two Novel LINC Complexes. *PLoS ONE.* 2010; 5: e12072.
- Kmonickova V, Frolkova M, Steger K, Komrskova K. The Role of the LINC Complex in Sperm Development and Function. *Int J Mol Sci.* 2020; 21: 9058.
- Ramdas NM, Shivashankar GV. Cytoskeletal control of nuclear morphology and chromatin organization. *J Mol Biol.* 2015; 427: 695–706.
- Davidson PP, Bruno Cadot B. Actin on and around the Nucleus. *Trends Cell Biol.* 2021; 31: 211–23.
- Palazzo AF, Joseph HL, Chen YJ, Dujardin DL, Alberts AS, Pfister KK, et al. Cdc42, dynein, and dynactin regulate MTOC reorientation independent of Rho-regulated microtubule stabilization. *Curr Biol.* 2001; 11: 1536–41.
- Chambliss AB, Khatau SB, Erdenberger N, Robinson DK, Hodzic D, Longmore GD, et al. The LINC-anchored actin cap connects the extracellular milieu to the nucleus for ultrafast mechanotransduction. *Sci Rep.* 2013; 3: 1087.
- Ramos A, Camargo FD. The Hippo signaling pathway and stem cell biology. *Trends Cell Biol.* 2012; 22: 339–46.
- Booth AJ, Yue Z, Eykelenboom JK, Stiff T, Luxton GG, Hochegger H, et al. Contractile acto-myosin network on nuclear envelope remnants positions human chromosomes for mitosis. *eLife.* 2019; 8: e46902.
- Déjardin T, Carollo PS, Sipieter F, Davidson PM, Seiler C, Cuvelier D et al. Nesprins are mechanotransducers that discriminate epithelial–mesenchymal transition programs. *J Cell Biol.* 2020; 219: e201908036.
- Segura-Totten M, Wilson KL. BAF: Roles in chromatin, nuclear structure and retrovirus integration. *Trends Cell Biol.* 2004; 14: 261–26.
- Elkhatib RA, Paci M, Boissier R, Longepied G, Auguste Y, Achard V et al. LEM-domain proteins are lost during human spermiogenesis but BAF and BAF-L persist. *Reproduction.* 2017; 154: 387–401.
- Wu JY, Ribar TJ, Cummings DE, Brton KA, McKnight GS, Means AR. Spermiogenesis and exchange of basic nuclear proteins are impaired in male germ cells lacking Camk4. *Nat Genet.* 2000; 25: 448–52.

32. Mylonis I, Drosou V, Brancorsini S, Nikolakaki E, Sassone-Corsi P, Giannakourou T. Temporal association of protamine 1 with the inner nuclear membrane protein lamin B receptor during spermiogenesis. *J Biol Chem*. 2004; 279: 11626–31.
33. Skoko D, Li M, Huang Y, Mizuuchi M, Cai M, Bradley CM, et al. Barrier-to-autointegration factor (BAF) condenses DNA by looping. *Proc Natl Acad Sci. USA*. 2009; 106: 16610–15.
34. Dopie J, Skarp KP, Rajakylä EK, Tanhuanpää K, Vartiainen MK. Active maintenance of nuclear actin by importin 9 supports transcription. *Proc Natl Acad Sci. USA*. 2012; 109: E544–E552.
35. García-González A, Jacchetti E, Marotta R, Tunesi M, Rodríguez Matas JF, Raimondi MT. The Effect of Cell Morphology on the Permeability of the Nuclear Envelope to Diffusive Factors. *Front Physiol*. 2018; 9: 925.
36. Swift J, Ivanovska IL, Buxboim A, Harada T, Dingal PCDP, Pinter J, et al. Nuclear lamin-A scales with tissue stiffness and enhances matrix-directed differentiation. *Science*. 2013; 341: 1240104.
37. Li Y, Chu JS, Kurpinski K, Li X, Bautista DM, Yang L et al. Biophysical regulation of histone acetylation in mesenchymal stem cells. *Biophys J*. 2011; 100: 1902–9.
38. Le HQ, Ghatak S, Yeung CYC, Tellkamp F, Günschmann C, Dieterich C, et al. Mechanical regulation of transcription controls Polycomb-mediated gene silencing during lineage commitment. *Nat Cell Biol*. 2016; 18: 864–75.
39. Russell LD, Russell JA, MacGregor GR, Meistrich ML. Linkage of manchette microtubules to the nuclear envelope and observations of the role of the manchette in nuclear shaping during spermiogenesis in rodents. *Am J Anat*. 1991; 192: 97–120.
40. Pereira CD, Serrano JB, Martins F, da Cruz E Silva OAB, Rebelo S. Nuclear envelope dynamics during mammalian spermatogenesis: New insights on male fertility. *Biol Rev Camb Philos Soc*. 2019; 94: 1195–219.
41. Lin YH, Lin YM, Wang YY, Yu IS, Lin YW, Wang YH, et al. The expression level of septin12 is critical for spermiogenesis. *Am J Pathol*. 2009; 174: 1857–68.
42. Mostowy S, Cossart P. Septins: The fourth component of the cytoskeleton. *Nat Rev Mol Cell Biol*. 2012; 13: 183–94.
43. Frohnert C, Schweizer S, Hoyer-Fender S. SPAG4L/SPAG4L-2 are testis-specific SUN domain proteins restricted to the apical nuclear envelope of round spermatids facing the acrosome. *Mol Hum Reprod*. 2011; 17: 207–18.
44. Yassine S, Escoffier J, Abi Nahed R, Pierre V, Karaouzene T, Ray PF, et al. Dynamics of Sun5 localization during spermatogenesis in wild type and Dpy19l2 knock-out mice indicates that Sun5 is not involved in acrosome attachment to the nuclear envelope. *PLoS ONE*. 2015; 10: e0125452.
45. Shang Y, Yan J, Tang W, Liu C, Xiao S, Guo Y, Yuan L, Chen L, Jiang H, Guo X, et al. Mechanistic insights into acephalic spermatozoa syndrome-associated mutations in the human SUN5 gene. *J Biol Chem*. 2018; 293: 2395–407.
46. Shen J, Chen W, Shao B, Qi Y, Xia Z, Wang F, et al. Lamin A/C proteins in the spermatid acroplaxome are essential in mouse spermiogenesis. *Reproduction*. 2014; 148: 479–87.
47. Pierre V, Martinez G, Coutton C, Delarochette J, Yassine S, Novella C et al. Absence of Dpy19l2, a new inner nuclear membrane protein, causes globozoospermia in mice by preventing the anchoring of the acrosome to the nucleus. *Development*. 2012; 139: 2955–65.
48. Yang K, Adham IM, Meinhardt A, Hoyer-Fender S. Ultra-structure of the sperm head-to-tail linkage complex in the absence of the spermatid-specific LINC component SPAG4. *Histochem Cell Biol*. 2018; 150: 49–59.
49. Yeh CH, Kuo PL, Wang YY, Wu YY, Chen MF, Lin DY, et al. SEPT12/SPAG4/LAMINB1 complexes are required for maintaining the integrity of the nuclear envelope in postmeiotic male germ cells. *PLoS ONE*. 2015; 10: e0120722.
50. Elkhatib RA, Paci M, Longepied G, Saias-Magnan J, Courbière B, Guichaoua MR et al. Homozygous deletion of SUN5 in three men with decapitated spermatozoa. *Hum Mol Genet*. 2017; 26: 3167–71.
51. Elkhatib R, Longepied G, Paci M, Achard V, Grillo JM, Levy N et al. Nuclear envelope remodeling during human spermiogenesis involves somatic B-type lamins and a spermatid-specific B3 lamin isoform. *Mol Hum Reprod*. 2015; 21 (3): 225–36.
52. Serrano JB, Martins F, Sousa JC, Pereira CD, van Pelt AMM, Rebelo S, et al. Descriptive Analysis of LAP1 Distribution and That of Associated Proteins throughout Spermatogenesis. *Membranes (Basel)*. 2017; 7 (2): 22.
53. Litvinov VV, Sulima AN, Xaritonova MA, Klepukov AA, Ermilova IYu, Maklygina YuYu. Klinicheskij sluchaj preodoleniya besplodiya, obuslovlennogo muzhskim faktorom (globozoospermiej 1-go tipa), metodom intracitoplazmaticheskoj in'ekcii morfologicheski normal'nogo spermatozoida s aktivacijej oocitov Ca⁺ - ionoforom. *Andrologiya i genital'naya xirurgiya* 2019; 20 (3): 78–85. Russian.

Литература

1. Hazzouri M, Rousseaux S, Monegelard F, Usson Y, Pelletier R, Faure AK, et al. Genome organization in the human sperm nucleus studied by FISH and confocal microscopy. *Mol Reprod Dev*. 2000; 55: 307–315.
2. Manfrevola F, Guillou F, Fasano S, Pierantoni R, Chianese R. LINCking the Nuclear Envelope to Sperm Architecture. *Genes*. 2021; 12: 658.
3. Crisp M, Liu Q, Roux K, Rattner JB, Shanahan C, Burke B, et al. Coupling of the nucleus and cytoplasm: Role of the LINC complex. *J Cell Biol*. 2006; 172: 41–53.
4. Stewart-Hutchinson PJ, Hale CM, Wirtz D, Hodzic D. Structural requirements for the assembly of LINC complexes and their function in cellular mechanical stiffness. *Exp Cell Res*. 2008; 314: 1892–905.
5. Sosa BA, Rothballer A, Kutay U, Schwartz TU. LINC complexes form by binding of three KASH peptides to domain interfaces of trimeric SUN proteins. *Cell*. 2012; 149: 1035–47.
6. Hodzic DM, Yeater DB, Bengtsson L, Otto H, Stahl PD. Sun2 is a novel mammalian inner nuclear membrane protein. *J Biol Chem*. 2004; 279: 25805–12.
7. Padmakumar VC, Libotte T, Lu W, Zaim H, Abraham S, Noegel AA, et al. The inner nuclear membrane protein Sun1 mediates the anchorage of Nesprin-2 to the nuclear envelope. *J Cell Sci*. 2005; 118: 3419–30.
8. Starr DA. A nuclear-envelope bridge positions nuclei and moves chromosomes. *J Cell Sci*. 2009; 122: 577–86.
9. Shao X, Tarnasky HA, Lee J.P, Oko R, van der Hoorn FA. Spag4, a Novel Sperm Protein, Binds Outer Dense-Fiber Protein Odf1 and Localizes to Microtubules of Manchette and Axoneme. *Dev Biol*. 1999; 211: 109–23.
10. Kim DI, Kc B, Roux KJ. Making the LINC: SUN and KASH protein interactions. *Biol Chem*. 2015; 396: 295–310.
11. Wilhelmson K, Litjens SH, Kuikman I, Tshimbalanga N, Janssen H, van den Bout I, Raymond K et al, Nesprin-3, a novel outer nuclear membrane protein, associates with the cytoskeletal linker protein plectin. *J Cell Biol*. 2005; 171: 799–810.
12. Gurusaran M, Davies OR. A molecular mechanism for LINC complex branching by structurally diverse SUN-KASH 6:6 assemblies. *eLife*. 2021; 10: e60175.
13. Pasch E, Link J, Beck C, Scheuerle S, Alsheimer M. The LINC complex component Sun4 plays a crucial role in sperm head formation and fertility. *Biol Open*. 2015; 4: 1792–802.
14. Jahed Z, Soheilypour M, Peyro M, Mofrad MR. The LINC and NPC relationship—it's complicated! *J Cell Sci*. 2016; 129: 3219–29.
15. Liu Q, Pante N, Misteli T, Elsagga M, Crisp M, Hodzic D, et al. Functional association of Sun1 with nuclear pore complexes. *J Cell Biol*. 2007; 178: 785–98.
16. Li P, Noegel AA. Inner nuclear envelope protein SUN1 plays a prominent role in mammalian mRNA export. *Nucleic Acids Res*. 2015; 43: 9874–88.
17. Horn HF, Kim DI, Wright GD, Wong ESM, Stewart CL, Burke B, et al. A mammalian KASH domain protein coupling meiotic chromosomes to the cytoskeleton. *J Cell Biol*. 2013; 202: 1023–39.
18. Li X, Wu Y, Huang L, Yang L, Xing X. SPAG4L/SPAG4Lβ interacts

- with Nesprin2 to participate in the meiosis of spermatogenesis. *Acta Biochim Biophys. Sin.* 2019; 51: 669–76.
19. Jiang XZ, Yang MG, Huang LH, Li CQ, Xing XW. SPAG4L, a novel nuclear envelope protein involved in the meiotic stage of spermatogenesis. *DNA Cell Biol.* 2011; 30: 875–82.
 20. Göb E, Schmitt J, Benavente R, Alsheimer M. Mammalian Sperm Head Formation Involves Different Polarization of Two Novel LINC Complexes. *PLoS ONE.* 2010; 5: e12072.
 21. Kmonickova V, Frolikova M, Steger K, Komrskova K. The Role of the LINC Complex in Sperm Development and Function. *Int J Mol Sci.* 2020; 21: 9058.
 22. Ramdas NM, Shivashankar GV. Cytoskeletal control of nuclear morphology and chromatin organization. *J Mol Biol.* 2015; 427: 695–706.
 23. Davidson PP, Bruno Cadot B. Actin on and around the Nucleus. *Trends Cell Biol.* 2021; 31: 211–23.
 24. Palazzo AF, Joseph HL, Chen YJ, Dujardin DL, Alberts AS, Pfister KK, et al. Cdc42, dynein, and dynactin regulate MTOC reorientation independent of Rho-regulated microtubule stabilization. *Curr Biol.* 2001; 11: 1536–41.
 25. Chambliss AB, Khatau SB, Erdenberger N, Robinson DK, Hodzic D, Longmore GD, et al. The LINC-anchored actin cap connects the extracellular milieu to the nucleus for ultrafast mechanotransduction. *Sci Rep.* 2013; 3: 1087.
 26. Ramos A, Camargo FD. The Hippo signaling pathway and stem cell biology. *Trends Cell Biol.* 2012; 22: 339–46.
 27. Booth AJ, Yue Z, Eykelenboom JK, Stiff T, Luxton GG, Hohegger H, et al. Contractile acto-myosin network on nuclear envelope remnants positions human chromosomes for mitosis. *eLife.* 2019; 8: e46902.
 28. Déjardin T, Carollo PS, Sipieter F, Davidson PM, Seiler C, Cuvelier D et al. Nesprins are mechanotransducers that discriminate epithelial-mesenchymal transition programs. *J Cell Biol.* 2020; 219: e201908036.
 29. Segura-Totten M, Wilson KL. BAF: Roles in chromatin, nuclear structure and retrovirus integration. *Trends Cell Biol.* 2004; 14: 261–6.
 30. Elkhatib RA, Paci M, Boissier R, Longepied G, Auguste Y, Achard V et al. LEM-domain proteins are lost during human spermiogenesis but BAF and BAF-L persist. *Reproduction.* 2017; 154: 387–401.
 31. Wu JY, Ribar TJ, Cummings DE, Brton KA, McKnight GS, Means AR. Spermiogenesis and exchange of basic nuclear proteins are impaired in male germ cells lacking Camk4. *Nat Genet.* 2000; 25: 448–52.
 32. Mylonis I, Drosou V, Brancorsini S, Nikolakaki E, Sassone-Corsi P, Giannakouros T. Temporal association of protamine 1 with the inner nuclear membrane protein lamin B receptor during spermiogenesis. *J Biol Chem.* 2004; 279: 11626–31.
 33. Skoko D, Li M, Huang Y, Mizuuchi M, Cai M, Bradley CM, et al. Barrier-to-autointegration factor (BAF) condenses DNA by looping. *Proc Natl Acad Sci. USA.* 2009; 106: 16610–15.
 34. Dopic J, Skarp KP, Rajakylä EK, Tanhuanpää K, Vartiainen MK. Active maintenance of nuclear actin by importin 9 supports transcription. *Proc Natl Acad Sci. USA.* 2012; 109: E544–E552.
 35. García-González A, Jacchetti E, Marotta R, Tunesi M, Rodríguez Matas JF, Raimondi MT. The Effect of Cell Morphology on the Permeability of the Nuclear Envelope to Diffusive Factors. *Front Physiol.* 2018; 9: 925.
 36. Swift J, Ivanovska IL, Buxboim A, Harada T, Dingal PCDP, Pinter J, et al. Nuclear lamin-A scales with tissue stiffness and enhances matrix-directed differentiation. *Science.* 2013; 341: 1240104.
 37. Li Y, Chu JS, Kurpinski K, Li X, Bautista DM, Yang L et al. Biophysical regulation of histone acetylation in mesenchymal stem cells. *Biophys J.* 2011; 100: 1902–9.
 38. Le HQ, Ghatak S, Yeung CYC, Tellkamp F, Günschmann C, Dieterich C, et al. Mechanical regulation of transcription controls Polycomb-mediated gene silencing during lineage commitment. *Nat Cell Biol.* 2016; 18: 864–75.
 39. Russell LD, Russell JA, MacGregor GR, Meistrich ML. Linkage of manchette microtubules to the nuclear envelope and observations of the role of the manchette in nuclear shaping during spermiogenesis in rodents. *Am J Anat.* 1991; 192: 97–120.
 40. Pereira CD, Serrano JB, Martins F, da Cruz E Silva OAB, Rebelo S. Nuclear envelope dynamics during mammalian spermatogenesis: New insights on male fertility. *Biol Rev Camb Philos Soc.* 2019; 94: 1195–219.
 41. Lin YH, Lin YM, Wang YY, Yu IS, Lin YW, Wang YH, et al. The expression level of septin12 is critical for spermiogenesis. *Am J Pathol.* 2009; 174: 1857–68.
 42. Mostowy S, Cossart P. Septins: The fourth component of the cytoskeleton. *Nat Rev Mol Cell Biol.* 2012; 13: 183–94.
 43. Frohnert C, Schweizer S, Hoyer-Fender S. SPAG4L/SPAG4L-2 are testis-specific SUN domain proteins restricted to the apical nuclear envelope of round spermatids facing the acrosome. *Mol Hum Reprod.* 2011; 17: 207–18.
 44. Yassine S, Escoffier J, Abi Nahed R, Pierre V, Karaouzene T, Ray PF, et al. Dynamics of Sun5 localization during spermatogenesis in wild type and Dpy19l2 knock-out mice indicates that Sun5 is not involved in acrosome attachment to the nuclear envelope. *PLoS ONE.* 2015; 10: e0125452.
 45. Shang Y, Yan J, Tang W, Liu C, Xiao S, Guo Y, Yuan L, Chen L, Jiang H, Guo X, et al. Mechanistic insights into acephalic spermatozoa syndrome-associated mutations in the human SUN5 gene. *J Biol Chem.* 2018; 293: 2395–407.
 46. Shen J, Chen W, Shao B, Qi Y, Xia Z, Wang F, et al. Lamin A/C proteins in the spermatid acroplaxome are essential in mouse spermiogenesis. *Reproduction.* 2014; 148: 479–87.
 47. Pierre V, Martinez G, Coutton C, Delaroché J, Yassine S, Novella C et al. Absence of Dpy19l2, a new inner nuclear membrane protein, causes globozoospermia in mice by preventing the anchoring of the acrosome to the nucleus. *Development.* 2012; 139: 2955–65.
 48. Yang K, Adham IM, Meinhardt A, Hoyer-Fender S. Ultra-structure of the sperm head-to-tail linkage complex in the absence of the spermatid-specific LINC component SPAG4. *Histochem Cell Biol.* 2018; 150: 49–59.
 49. Yeh CH, Kuo PL, Wang YY, Wu YY, Chen MF, Lin DY, et al. SEPT12/SPAG4/LAMINB1 complexes are required for maintaining the integrity of the nuclear envelope in postmeiotic male germ cells. *PLoS ONE.* 2015; 10: e0120722.
 50. Elkhatib RA, Paci M, Longepied G, Saias-Magnan J, Courbière B, Guichaoua MR et al. Homozygous deletion of SUN5 in three men with decapitated spermatozoa. *Hum Mol Genet.* 2017; 26: 3167–71.
 51. Elkhatib R, Longepied G, Paci M, Achard V, Grillo JM, Levy N et al. Nuclear envelope remodelling during human spermiogenesis involves somatic B-type lamins and a spermatid-specific B3 lamin isoform. *Mol Hum Reprod.* 2015; 21 (3): 225–36.
 52. Serrano JB, Martins F, Sousa JC, Pereira CD, van Pelt AMM, Rebelo S, et al. Descriptive Analysis of LAP1 Distribution and That of Associated Proteins throughout Spermatogenesis. *Membranes (Basel).* 2017; 7 (2): 22.
 53. Литвинов В. В., Сулима А. Н., Харитоновна М. А., Клепуков А. А., Ермилова И. Ю., Маклыгина Ю. Ю. Клинический случай преодоления бесплодия, обусловленного мужским фактором (глобозооспермией 1-го типа), методом интрацитоплазматической инъекции морфологически нормального сперматозоида с активацией ооцитов Са⁺-ионофором. *Андрология и генитальная хирургия.* 2019; 20 (3): 78–85.

METHODS FOR PREVENTION AND TREATMENT OF CONVULSIVE DISORDERS ASSOCIATED WITH CHOLINERGIC CONVULSANT INTOXICATION

Zorina VN , Evdokimova EA, Rejniuk VL

Golikov Scientific and Clinical Center of Toxicology of the Federal Medical and Biological Agency, Saint-Petersburg, Russia

Organophosphates (OPs) and carbamates are a common cause of intoxication associated with convulsive disorders. These cholinergic substances form a bond with acetylcholinesterase (AChE), thus contributing to accumulation of acetylcholine in synapses and causing typical manifestations of toxicity, including seizures. Standard antidote therapy provides sufficient symptom control, reduces seizures and decreases mortality only in case of prescription at the early stage of poisoning or preventive administration. Traditionally, atropine is used, that blocks the activity of the muscarinic cholinergic receptors in the parasympathetic nervous system and reduce the smooth muscle contraction activity, along with oximes that reactivate the reversibly inhibited AChE in the nicotinic acetylcholine receptors found in skeletal muscle. If these are not sufficient, benzodiazepines that interact with γ -aminobutyric acid receptors are used to jugulate seizures, prevent organic brain disease and post-traumatic epilepsy. There are no unified guidelines for the cases of antidotes having no effect or insufficient efficacy of antidotes. Unwanted side effects of the existing drugs and progressive decrease of efficiency within 30 min after exposure to OPs necessitate the search for new agents. Combination therapy, new dosage forms, developing original molecules or modifying the existing ones are among the developed approaches discussed in our review.

Keywords: convulsive syndrome, neurotoxicants, organophosphates, cholinergic, anticonvulsant, antidotes, therapy, prevention

Author contribution: Zorina VN — literature analysis, manuscript writing; Evdokimova EA — compliance check, compilation of reference list; Rejniuk VL — additions and amendments to the manuscript.

 **Correspondence should be addressed:** Veronika N. Zorina
Bekhtereva, 1, Saint-Petersburg, 192019, Russia; uchsovet@toxicology.ru

Received: 21.04.2022 **Accepted:** 15.05.2022 **Published online:** 05.06.2022

DOI: 10.47183/mes.2022.019

МЕТОДЫ ПРОФИЛАКТИКИ И ТЕРАПИИ СУДОРОЖНОГО СИНДРОМА ПРИ ОТРАВЛЕНИИ КОНВУЛЬСАНТАМИ ХОЛИНЕРГИЧЕСКОГО РЯДА

В. Н. Зорина , Е. А. Евдокимова, В. Л. Рейнюк

Научно-клинический центр токсикологии имени академика С. Н. Голикова Федерального медико-биологического агентства, Санкт-Петербург, Россия

Фосфорорганические соединения (ФОС) и карбаматы — распространенная причина отравлений, ассоциированных с развитием судорожного синдрома. Эти холинергические вещества образуют связь с ацетилхолинэстеразой (АХЭ), что способствует накоплению ацетилхолина в нервных синапсах и приводит к характерным токсическим проявлениям, в том числе к развитию судорог. Стандартная антидотная терапия обеспечивает достаточный контроль симптомов, ослабляет судороги и снижает смертность только при назначении на самой ранней стадии отравления либо при профилактическом введении. Традиционно применяют атропин, который блокирует мускариновые холинергические рецепторы в парасимпатической нервной системе и уменьшает активность сокращения гладких мышц, а также оксимы, реактивирующие обратимо ингибированную АХЭ в никотиновых холинергических синапсах скелетных мышц. Если их недостаточно, для купирования судорог и профилактики развития органических повреждений головного мозга, посттравматической эпилепсии применяют средства бензодиазепинового ряда, взаимодействующие с рецепторами γ -аминомасляной кислоты. Единых официальных руководств на случай, когда антидоты не действуют или действуют недостаточно эффективно, не существует. Нежелательные побочные эффекты и прогрессирующее снижение эффективности существующих средств через 30 мин после воздействия ФОС обуславливают необходимость поиска новых средств. Среди разрабатываемых подходов — комбинированные схемы лечения, новые лекарственные формы, создание оригинальных или модификация существующих молекул, рассмотрению которых посвящен настоящий обзор.

Ключевые слова: судорожный синдром, нейротоксиканты, фосфорорганические соединения, холинергические вещества, антиконвульсант, антидоты, терапия, профилактика

Вклад авторов: В. Н. Зорина — анализ литературных данных, написание статьи; Е. А. Евдокимова — нормоконтроль, составление списка литературы; В. Л. Рейнюк — внесение дополнений и уточнений в текст рукописи.

 **Для корреспонденции:** Вероника Николаевна Зорина
ул. Бехтерева, д. 1, г. Санкт-Петербург, 192019, Россия; uchsovet@toxicology.ru

Статья получена: 21.04.2022 **Статья принята к печати:** 15.05.2022 **Опубликована онлайн:** 05.06.2022

DOI: 10.47183/mes.2022.019

Prevalence and pathogenetic mechanisms of intoxication with cholinergic convulsants

Intoxication with chemical convulsant agents is associated with generalized seizures in the form of single/repeated seizures or symptomatic status epilepticus [1]. The mechanisms underlying the development of seizure activity include stimulation of excitation or inhibition of inhibitory pathways in the central nervous system (CNS) [2]. Neurotoxicants

can affect neurotransmitters (synthesis, storage, release, reuptake), receptors (structure, expression levels, affinity for neurotransmitters), and the mechanisms underlying coupling with the cellular effector system involved in the receptor-ligand interactions [3].

Organophosphates (OPs), produced in the form of the ester, amide or thiol derivatives of phosphoric, phosphonic or phosphinic acid are the greatest contributors to intoxication associated with seizures. Prohibition of the use and disposal

of chemical weapons have reduced, but not nullified the risk of the population exposure to OPs, since OPs are extensively used for production of agrochemicals (pesticides); OPs are components of medicines [4, 5], plasticizers, and many polymeric materials; OPs are still used for terrorist attacks [6]. Pesticides, herbicides and insecticides are key contributors to the structure of acute toxicity in the developing world [4, 6, 7], and constitute over 40% in the structure of occupational disorders in rural areas. The working-age population is mainly affected, and the percentage of cases of the long-term loss of earning capacity and disability is high. Up to million people all over the world suffer from OP poisoning every year, of them about 300,000 die. In 2020, 3 million and even 5 million cases were reported [4, 5]. Approximately 100,000 people every year die from only insecticide poisoning. Self-poisoning with high-dose insecticides often causes death from cardiovascular shock. Only 22% of poisoned patients with an out-of-hospital cardiac arrest survive to admission, and 10% survive to discharge [8].

Based on the mechanism of action, OPs are classified as cholinergic substances. When a nerve impulse is transmitted, acetylcholine, stored in the presynaptic vesicles of neurons, is released into the synaptic cleft to interact with cholinergic receptors of two types: nicotinic (directly interacting with ion channels) and muscarinic (indirectly affecting the ion channel permeability). Acetylcholine is broken down by the enzyme, acetylcholinesterase (AChE), which quickly terminates signal transmission and ensures the AChE molecule release required for the new reaction [2]. OPs are structurally similar to acetylcholine, but are able to form a strong bond with AChE, blocking its functions. OP poisoning occurs in two phases: reversible AChE inhibition, when the bond hydrolysis is still possible (spontaneous or antidote-induced), which results in the enzyme function restoration, and subsequent bond "maturation" or "aging" associated with irreversible inhibition of the enzyme [4, 7]. The heavier radicals (R⁻) contained in OPs, the faster is aging [6]. AChE deficiency associated with OP poisoning contributes to excessive accumulation of acetylcholine in synapses and neuromuscular junctions of the peripheral and central nervous systems that eventually results in typical manifestations of toxicity (cholinergic syndrome), seizures, bradycardia, bronchoconstriction or even death [4, 7, 9]. The early stage of a seizure is followed by the mixed cholinergic and noncholinergic stage, which transforms into the noncholinergic stage associated with the glutamate excitotoxicity and neuronal death [2, 9].

Inflammatory mediators that increase the severity of subsequent seizures and enhance epileptogenesis are released upon exposure to OPs. A significant increase in the levels of pro-inflammatory cytokines (IL1b, TNF α , IL6) and prostaglandin E₂ 2–24 h after exposure to OP has been reported [10]. Glutamate releasing actively from presynaptic terminals increases intracellular calcium concentration due to inhibition of the KCNQ2/3 potassium channels, promotes other physiological and metabolic effects. Acute OP poisoning may be followed by chronic neuropathological complications resulting from initiation of neurodegenerative processes caused by excitotoxicity and neuroinflammatory responses [9, 11–13]. In addition to cholinergic and glutamatergic effects, insecticides inhibit monoacylglycerol lipase activity, which results in the increased brain levels of 2-arachidonoyl glycerol, being the cannabinoid receptor agonist. Insecticides also inhibit the endocannabinoid-degrading enzyme, fatty acid amide hydrolase (FAAH) [8]. OPs can directly sensitize cholinergic receptors.

Biological activity of carbamates (carbamic acid derivatives), that are constituents of pesticides, herbicides, fungicides,

insecticides, and medicines, including drugs for treatment of Alzheimer's disease, myasthenia gravis, glaucoma, is similar to that of OPs [7]. Carbamate poisoning, similar to OP intoxication based on the underlying mechanism, has some features [7, 8]. Carbamate activation requires no metabolic transformations [7]; clinical manifestations of intoxication are observed almost immediately after absorption [14]. The carbamate-AChE bond is weaker than that formed by OPs: the enzyme hydrolyzes spontaneously more rapidly, and there is no aging of the bond [7]. However, carbamates are comparable to OPs in terms of toxicity: cases of respiratory failure 12 h after poisoning have been reported [14]. In addition to anticholinesterase effect, carbamates have a direct cholinomimetic effect on the cholinergic receptors of synapses [3].

Analysis of the social status of individuals poisoned with OPs and carbamates produced unexpected results: 23% of victims were farmers, 27% were daily wagers, 21% were housewives, 11% were salaried employees, and 8% were students [5]. Thus, along with the risk of occupational poisoning due to harmful working conditions or terrorist poisoning, accidental and deliberate self-poisoning is rather widespread, together with toxic effects resulting from drug overdose. This determines the relevance of developing agents for jugulation of seizures.

The review was aimed to analyze published data on the existing and developed methods for prevention and treatment of convulsive disorders associated with the cholinergic convulsant intoxication, and to define the most promising areas for further development of medicines and comprehensive approaches to treatment. The RISC and PubMedNet databases were used. The search by keywords (antidote, organophosphorus compounds, anticonvulsant, antiepileptic agent, etc.) among the reports published over the last ten years was performed.

Standard treatment methods

In case of OP poisoning, it is extremely important to provide timely care to the affected person. Treatment with standard antidotes provides adequate symptom management, reduces seizures, and decreases mortality only in case of prescription at the early stage of poisoning or preventive administration [4].

Comprehensive treatment is commonly used: oxygen therapy, decontamination of skin and mucous membranes, and, if possible, hemodialysis. Atropine administration is started prior to administration of oxygen, since the lack of secretion management hinders oxygenation [7]. Moreover, atropine blocks the activity of the muscarinic cholinergic receptors in the parasympathetic nervous system, thus reducing the smooth muscle contraction activity [2, 4], however, it has no pronounced therapeutic effect in case of the CNS toxicity [11] due to difficulty crossing the blood–brain barrier (BBB). It also has no prominent effect on the cholinergic synapses of the skeletal muscle. Atropine cannot relieve nicotinic effects of OPs (spasms and fasciculation) [9]. In case of severe hypoxia, administration of atropine may be fatal due to blockade of the vagal nerve terminals and ventricular fibrillation [3].

The use of oximes (obidoxime, methoxime, azoxime, etc.) is recommended to reactivate AChE; pralidoxime chloride (2-PAM) is most commonly used [4, 6, 13, 15]. At an early stage of poisoning, oximes effectively reactivate the reversibly inhibited AChE in the nicotinic acetylcholine receptors found in skeletal muscle. However, oximes become almost useless after the bond maturation and irreversible AChE inactivation. Furthermore, oximes have difficulty crossing the BBB [9, 11]. First generation oximes are toxic, their interaction with OPs

may result in accumulation of the toxic OP-oxime complex in the body [3, 6]. Second generation oximes (H oximes, including HI-6, HLo-7, HGG-42) show better biological activity and bioavailability together with lower toxicity, however, many of them are unstable in aqueous solutions [6]. Among second generation oximes, levetiracetam has a good history of clinical use [16]. Carboxim, which has been developed in the USSR, is more stable in aqueous solutions and more easily crosses the BBB. It is much more effective compared to first generation oximes. New AChE reactivators are developed based on amidines and hydrazones. However, none of AChE reactivators are the broad-spectrum antidotes effective against poisoning with OPs of any type. Experimental studies of the oxime combinations, such as 2-PAM/carboxime, carboxime/atropine, are conducted in order to increase the protection index [6]. Reversible AChE inhibitors are also used (pyridostigmine, aminostigmine, physostigmine, galantamine) [3, 4, 9, 12], which have low toxicity, but are effective only in case of preventive administration.

When the effectiveness of first-line antidotes is insufficient, these are supplemented by anticonvulsants, including for prevention of the organic brain disease and post-traumatic epilepsy [4, 15]. Benzodiazepine are used, most often high-dose diazepam or lorazepam. Pharmacological efficacy of benzodiazepines results from interaction with the γ -aminobutyric acid (GABA) receptors and modulation of neurotransmission [17]. These days, the use of midazolam, the new drug that has shown benefits based on the comparative analysis of pharmacokinetics, is recommended [4, 13, 15], new drugs are developed [4, 18]. In case of OP-induced damage, benzodiazepines should be used as early as possible: benzodiazepine administration within 30 min jugulates seizures in the majority of cases [4, 19]; after 40 min their efficacy decreases significantly [4, 15], and after 60 min after the OP exposure benzodiazepines are ineffective, regardless of the total dose and amount that have passed through the BBB [9]. Despite high anticonvulsant activity and broad therapeutic range of benzodiazepines, elimination of convulsive disorder does not protect the victim's life: death may occur even in case of the complete seizure termination [3]. The cases of diazepam and midazolam resistance have been reported, which is considered to be associated with the OP-mediated disorders of binding with the target receptors or the receptor loss (benzodiazepine receptors disappear in more than 50% of neurons within 10–20 min), with the neuronal death and concomitant inflammation [9, 15, 20]. In case of BBB dysfunction, leukocytes and albumin enter the CNS. Albumin activates astrocytes, production of the seizure-provoking cytokine IL1 β is increased, and excessive TGF β is produced, which has a negative effect on the signal transmission in the CNS. The resulting inflammation affects neuromodulators, regulatory transport proteins, thus promoting seizures that cannot be managed using benzodiazepines [21].

Single administration of atropine, oximes (obidoxime, 2-PAM, HI-6) and drugs affecting GABA (diazepam, avizafone) is used for prevention or emergency therapy of the OP intoxication. In addition, pyridostigmine is sometimes used as a component of preventive antidotes [22]. Antidote auto-injectors have been designed: for example, the dual-chamber MARK-1 and DuoDote auto-injectors contain atropine (2.1 mg/0.7 mL) and 2-PAM (600 mg/2 mL), IM auto-injector contains 2 mg of atropine and 200 mg of obidoxime chloride; triple-chamber auto-injectors are available (atropine, oxime and diazepam) [4, 13, 23]. The use of the atropine sulfate and obidoxime mixture is acceptable [23], the release of auto-injectors containing midazolam instead of diazepam has been announced [13]. However, even the combination and preventive regimens for

administration of antidotes that reduce immediate fatality do not necessarily suppress seizure activity, unless high-dose atropine is administered very quickly [22]. Auto-injectors have some limitations: for example, adult doses of atropine could be administered to children, however, the adult dose of pralidoxime is too much for a child [23].

Currently, there are no unified official guidelines for the cases of antidotes having no effect or insufficient efficacy of antidotes. In case of failure to respond to prehospital treatment with benzodiazepines, the status epilepticus clinical protocols are most often used for treatment [19]. Antiepileptic drugs, such as levetiracetam, phenobarbital, phenytoin, fosphenytoin and valproates, are used in clinical practice. It is known that phenytoin (fosphenytoin) stabilizes the inactivated state of the neuronal voltage-gated sodium channels, but has such side effects as arrhythmogenicity. Phenobarbital (the long-acting barbiturate) affects GABA and AMPA ionotropic glutamate receptors, inhibits the release of neurotransmitters, but is capable of providing excessive inhibition of the CNS functions, including respiratory function. Levetiracetam suppresses neurotransmitter release by means of binding to the synaptic vesicle protein 2A (SV2A); the possibility of the glutamate receptor (mainly AMPA) modulation is assumed. Lacosamide enhances slow inactivation in voltage-gated sodium channels, however, the drug is capable of causing conduction disorders [21]. Pregabalin and tiagabine block calcium channels [24]. There is no clear understanding of these drugs comparative efficacy. According to a number of clinical trials, these drugs have virtually the same efficacy of about 50% [4, 19].

In the experiment that involved rats exposed to OPs, administration of high-dose midazolam and lorazepam (four times the therapeutic dose) suppressed seizures only in 10 and 6% of cases. In another experiment, phenobarbital first showed higher efficacy against persistent or recurrent convulsive disorder compared to valproic acid (35% vs. 56%), however, the drug ensured long lasting relief only in 19% of cases [19]. When testing pregabalin, levetiracetam and valproic acid as second-line drugs (in cases of refractory status epilepticus), the rats' behavioral response was delayed by 30–60 min (compared to diazepam and ketamine). Seizures stopped only when the levels of acetylcholine decreased by more than 50%. Pregabalin and valproic acid jugulated seizures, however, animals did not regain awareness. Levetiracetam stopped seizures, rats regained awareness, but experienced tremor. Furthermore, levetiracetam was more long-acting than pregabalin and valproic acid. The mechanism of action of these drugs is unclear. It is assumed that the drugs are capable of reducing the release of acetylcholine and glutamate [16].

When antiepileptic drugs are unable to terminate seizure activity, general anesthetics, such as ketamine, pentobarbital, or propofol, are administered within 24–48 h [4, 19]. The efficiency of ketamine (inhibits ion channels of the NMDA-type glutamate receptors, interacts with opioid, monoaminergic, muscarinic and nicotinic receptors, affects L-type calcium and sodium channels, and provides cytokine modulation, including IL1, IL6, IL8, IL10, THF α) supplementation has been confirmed after using first-line antidotes and benzodiazepines. The experiment showed that the use of ketamine and propofol made it possible to jugulate seizures in benzodiazepine-resistant rats [19, 21].

Valproic (2-propyl-pentanoic) acid [16] and its derivatives (valproates) deserve special attention. Their mechanism of action involves presynaptic and postsynaptic modulation of GABAergic transmission (valproates increase synthesis, release and therefore the inhibiting activity of GABA,

potentiate GABAergic transmission, show direct effects on GABA receptors due to reduced activity of β -hydroxybutyric acid (possessing excitatory effects) [25–27]. Valproic acid directly affects cell membranes, thus reducing paroxysmal discharges from neurons, provides modulation of sodium, calcium and potassium ion channels. Furthermore, valproic acid modulates glutamate activity. Valproates are capable of increasing the hippocampal extracellular levels of serotonin and dopamine. Suggestions have been also made that valproic acid has epigenetic effects and can modulate neurogenesis. Neuroprotective properties of valproates have been reported. The efficiency of valproic acid during generalized seizures in patients with epilepsy has been shown [25, 26]. However, the effective dose of valproic acid is significantly higher compared to that of benzodiazepines. During the experiments aimed at assessing the valproic acid efficiency, only high doses administered (≥ 150 mg/kg) to rats by intraperitoneal injection suppressed generalized seizures [28]. In case of OP-induced status epilepticus that was resistant to benzodiazepines, intravenous administration of the significantly lower dose valproic acid derivatives to experimental rats was effective [19].

Alternative treatment methods

Unwanted side effects of the existing drugs and progressive decrease of efficiency within 30 min after exposure to OPs necessitate the search for new agents. Since OPs are fast-acting agents, emergency care is often delayed, that is why versatile and fast-acting anticonvulsants are required that could be delivered via the most easy administration routes [25]. Combined treatment regimens, new dosage forms, development of original molecules and modification of existing molecules are among the approaches.

Combination therapy

Early polytherapy (for example, combining benzodiazepines with second-line drugs or NMDA receptor antagonists) may improve seizure control associated with the slightly enhanced side effects, however, there are just a few completed clinical trials [21]. Polytherapy is also capable of reducing the number of side effects due to reduction in drug dosage and drug synergism [29]. Particularly, the combination of midazolam, ketamine and valproate significantly reduced seizure severity and duration in experimental rats compared to monotherapy with higher doses [20]. The combined use of valproate and diazepam contributes to activation of neurogenesis [10]; there have been also attempts to combine valproates with carnitine [21]. The efficiency of reducing seizure activity in rats by using the combination of midazolam and dexmedetomidine ($\alpha 2$ adrenergic receptor antagonist) was higher compared to that of midazolam monotherapy, including when administered 60 min after initiation of seizures [29]. Prescription of sodium valproate to experimental rats after using midazolam reduced seizure frequency and duration, and supplementation of losartan (anesthetic agent) reduced the amount of brain damage [30]. In experimental rats, the combination of 3 mg/kg midazolam, 30 mg/kg ketamine and 90 mg/kg valproate showed the significant decrease in the number and duration of seizures compared to monotherapy with high-dose midazolam. The effects persisted 40 min after exposure to OPs, when midazolam became ineffective [20].

The efficiency of procyclidine supplementation was studied in experimental rats poisoned with OPs by intraperitoneal administration of triple (procyclidine 6 mg/kg, diazepam

10 mg/kg and pentobarbital 30 mg/kg) and dual (procyclidine 10 mg/kg and propofol 50 mg/kg) combinations. In the first case seizures stopped within 30–40 min after poisoning, however, mortality was 43%, and survivors had neurological disorders. In the second case seizures stopped, but 17% of rats died in 24 h. When using the combination of levetiracetam (50 mg/kg) with procyclidine (10 mg/kg) or caramiphen (10 mg/kg), seizures stopped in the majority of rats, however, mecamlamine supplementation was sometimes required. Procyclidine had a better effect than caramiphen, and preventive administration (20 min before OP intoxication) was far more effective than administration after poisoning. The combination of atropine and ketamine showed anticonvulsive effect when administered 30–120 min after poisoning [22].

In experimental animals, the effects of diazepam (10 mg/kg) were enhanced due to flupirtine supplementation (50 mg/kg) [12]. The use of memantine (neuroprotective agent) in addition to benzodiazepines showed a very narrow therapeutic index [4].

Novel non-invasive dosage forms

Increasing bioavailability and simplifying administration of the registered substances by means of developing non-invasive dosage forms (nasal dosage forms, aerosols, buccal solutions) are considered promising approaches. When using intranasal drug administration, adequate circulation in the nasal mucosa can provide pharmacokinetic benefits: the drug travels directly to the CNS and systemic circulation. Delayed absorption requires dosage increase, thus increasing the risk of overdose. However, benzodiazepine-containing sprays are recommended for pediatric use as sedatives. According to meta-analysis of the experience of using nasal dosage forms in children as sedatives, midazolam is more effective than diazepam. Bioavailability of lorazepam is 80%, and the time of peak concentration is 30 min, which is almost two times faster compared to that observed after intramuscular injection; there are no significant differences in the drug effect timing and duration when comparing with the intravenous infusion dosage form. When jugulating seizures, no differences in efficiency between the nasal dosage form of midazolam and intravenous infusion or rectal dosage form of diazepam were revealed. On average, seizures terminated within 3–4 min after the midazolam administration; maximum plasma concentration was achieved in 25 min, and clinically relevant concentration was reached within 10 min [31]. The majority of nasal dosage forms of benzodiazepines and buccal form of midazolam were registered as sedatives and hypnotics only. However, the VALTOCO diazepam-containing nasal spray was registered in the USA, which was indicated to be used as anticonvulsant.

Atropine-containing nasal sprays that have been tested on rats demonstrate efficiency comparable with that of parenteral drug administration, and rapid systemic absorption. The limited clinical trial of the atropine–chitosan nasal drops was carried out, during which peak concentration was achieved within 30 min. The nano-atropine dry powder inhaler turned out to be ineffective: only a small peak in the blood was observed in volunteers after 15 min, the second peak observed after 60 min was associated with the intestinal substance absorption. During the experiment involving volunteers, six atropine powder inhalations (in a dose of 0.4 mg per inhalation) were required to reach blood levels equivalent to single intramuscular injection (2 mg), which was considered not a promising avenue [4].

Atropine fast-disintegrating sublingual tablets were developed, comparable with the solution in terms of permeation rate.

However, bioequivalence of the sublingually administered atropine has not been defined [4].

Developing new valproic acid derivatives

The use of valproic acid as antidote is hardly acceptable due to high dose required for effective seizure termination. However, amide derivatives (for example, new derivative of valproic acid and 1,3,4-thiadiazole (valprazolamide)) demonstrate higher anticonvulsant activity and lower neurotoxicity in experimental settings. After intraperitoneal injection of valprazolamide to mice, DL_{50} and TD_{50} were 924.8 (756.9–1063.7) mg/kg and 456.7 (325.4–603.6) mg/kg [32].

Valnoctamide is more effective and has fewer side effects than sodium valproate [21]. It was tested on rats of various ages (21, 28 and 70 days), ED_{50} was 34–165 mg/kg. Only 9% of animals experienced sporadic short seizure episodes 2–3 h after the treatment initiation. The efficiency of valnoctamide intraperitoneal injection was shown in rats and guinea pigs (ED_{50} 62–80 mg/kg), including in case of delayed administration and the use in combination with diazepam in a dose of 2.2 mg/kg (monotherapy with the same dose of diazepam was ineffective) [28].

Sec-butyl-propyl-acetamide (SPD) is a more powerful homologue of valnoctamide, which has been shown in experimental rats [21]. ED_{50} of both SPD and valnoctamide is about 65 mg/kg, while ED_{50} of valproic acid is 366 mg/kg. The drug was tested on mice, rats and guinea pigs. Diazepam, valproic acid, valnoctamide were ineffective in the rat model of convulsive disorder when administered by intraperitoneal injection 30 min after exposure to OPs, and SPD suspension administered in a dose of 84 mg/kg suppressed seizures [33].

Anticonvulsant efficacy of the intraperitoneal injection of N-substituted valpromides was shown in mice [26]. The extended-release dosage form of valproic acid (metabolically activated prodrug) selectively bound to L-amino acid transporter 1 (LAT1) in experimental animals, thus contributing to more effective penetration into the CNS and slow release of the active ingredient [34]. Amide derivatives of valproic acid (RDG1-RDG8) are more active than sodium valproate in experimental settings [27].

Other treatment methods

Among the developed antiepileptic drugs, brivaracetam inhibits neurotransmitter release, more effectively binds to SV2A protein, is more fast-acting and has fewer side effects than levetiracetam during the preclinical testing. Preclinical studies have shown high efficiency of perampnel (selective antagonist of AMPA glutamate receptor) [21]. New antagonist of AMPA and KAR ionotropic glutamate receptors is developed [29].

It is suggested to use neurosteroids in cases OP exposure took place more than 30 min ago [9]. It is believed that neurosteroids act as positive allosteric modulators (nanomolar concentrations) and direct activators (micromolar concentrations) of all isoforms of GABA receptors (synaptic and

extrasynaptic receptors). The use of endogenous neurosteroids (allopregnanolone) is not economically feasible, however, synthetic neurosteroids (alfaxalone, ganaxolone) are more active in case of oral administration and have a 4–6 times longer half-life. The efficiency of ganaxolone administered by intramuscular injection was shown in experimental rats: monotherapy prevented neuronal death, reduced the loss of inhibitory interneurons; the combination with midazolam increased the efficiency. Ganaxolone analogues SGE-516 increased GABA-evoked currents [9, 21].

The efficiency of diphenhydramine in OP poisoning was similar to that of atropine. Antidote activity of chlorpheniramine and promethazine was revealed during the experiment. It was suggested to use antihistamines that possess central antimuscarinic effects. Monotherapy with glycopyrrolate, acting through peripheral receptors, or combining glycopyrrolate with atropine makes it possible to reduce mortality. However, there are no alterations in the toxic effects severity [4, 7].

Experiments on affecting cytokine profile by administration of IL1PA in addition to diazepam were conducted. Cannabinoids enhanced the effects of valproates. However, direct anticonvulsant effects had not been proven [21].

Histone deacetylase inhibitor supplementation was studied, aimed at affecting the expression of certain genes, including increasing the expression of the heat shock proteins and brain-derived neurotrophic factor to provide neuroprotection. It was suggested to use the heat shock proteins (for example, HSP-70) preventing protein denaturation and unwanted polypeptide aggregation; certain anti-inflammatory drugs were tested [10]. Among other agents tested in order to improve seizure control there were 2-deoxyglucose, huperzine A, imepitoin, minocycline, pitolisant, glibenclamide, P2X7 receptor antagonist, bumetanide, sodium bicarbonate, infusion of calcium channel blockers, and drugs with unknown mechanisms underlying anticonvulsant effects, such as clonidine [3, 4, 8, 21]. However, all these methods are not sufficient.

CONCLUSION

Thus, standard antidote therapy of OP poisoning is effective only when started very early. There are no unified guidelines on care provision to victims with convulsive disorders in case of no response to standard therapy. There are no unified recommendations on jugulating recurrent seizures occurring during the long distance transportation of the victim. None of the registered drugs provide comprehensive protection against neurotoxicants. This dictates the need for further research aimed at developing new agents for treatment of convulsive disorders associated with the cholinergic convulsant intoxication. Developing new medications based on the combinations of registered substances in order to provide cumulative effects, creating new dosage forms to enhance bioavailability of drugs, and developing novel original substances by means of modifying chemical synthesis of compounds that possess anticonvulsant effects are considered the most promising.

References

1. Razrabotka metodologii diagnostiki i farmakologicheskoy korrektsii posledstviy otravlenij veshchestvami sudorozhnogo dejstviya. Metodicheskie rekomendatsii MR FMBA Rossii 12.08-18. M., 2018; 44 p. Russian.
2. Phillips HN, Tormoehlen L. Toxin-induced seizures. *Neurol Clin.* 2020; 38 (4): 867–79.
3. Kucenko SA, editor. Voennaja toksikologija, radiobiologija i medicinskaja zashhita. SPb.: Foliant, 2004; 528 p. Russian.

4. Alozi M, Rawas-Qalaji M. Treating organophosphates poisoning: management challenges and potential solutions. *Crit Rev Toxicol.* 2020; 50 (9): 764–79.
5. Reddy BS, Skaria TG, Polepalli S, Vidyasagar S, Rao M, Kunhikatta V, et al. Factors associated with outcomes in organophosphate and carbamate poisoning: a retrospective study. *Toxicol Res.* 2020; 36 (3): 257–66.
6. Gladkih VD, Nazarov VB. Cholinesterase reactivators in the therapy of intoxication with neurotrophic physiologically active substances. *Extreme Medicine.* 2014; 1 (47): 54–6. Russian.
7. King AM, Aaron CK. Organophosphate and carbamate poisoning. *Emerg Med Clin North Am.* 2015; 33 (1): 133–51.
8. Eddleston M. Novel clinical toxicology and pharmacology of organophosphorus insecticide self-poisoning. *Annu Rev Pharmacol Toxicol.* 2019; 59: 341–60.
9. Reddy DS. Mechanism-based novel antidotes for organophosphate neurotoxicity. *Curr Opin Toxicol.* 2019; 14: 35–45.
10. Araujo Furtado M, Rossetti F, Chanda S, Yourick D. Exposure to nerveagents: from status epilepticus to neuroinflammation, brain damage, neurogenesis and epilepsy. *Neurotoxicology.* 2012; 33 (6): 1476–90.
11. Jett DA, Spriggs SM. Translational research on chemical nerve agents. *Neurobiol Dis.* 2020; 133: 104335.
12. Williamson J, Singh T, Kapur J. Neurobiology of organophosphate-induced seizures. *Epilepsy Behav.* 2019; 101 (Pt B): 106426.
13. Newmark J. Therapy for acute nerve agent poisoning: an update. *Neurol Clin Pract.* 2019; 9 (4): 337–42.
14. Lamb T, Selvarajah LR, Mohamed F, Jayamanne S, Gawarammana I, Mostafa A, et al. High lethality and minimal variation after acute self-poisoning with carbamate insecticides in Sri Lanka — implications for global suicide prevention. *Clin Toxicol (Phila).* 2016; 54 (8): 624–31.
15. Wu X, Kuruba R, Reddy DS. Midazolam-resistant seizures and brain injury after acute intoxication of diisopropylfluorophosphate, an organophosphate pesticide and surrogate for nerve agents. *J Pharmacol Exp Ther.* 2018; 367 (2): 302–21.
16. Imran I, Koch K, Schöfer H, Lau H, Klein J. Effects of three anti-seizure drugs on cholinergic and metabolic activity in experimental status epilepticus. *J Pharm Pharm Sci.* 2019; 22 (1): 340–51.
17. Benzodiazepines. *LiverTox: clinical and research information on drug-induced liver injury.* National Institute of Diabetes and Digestive and Kidney Diseases. Bethesda (MD) [Internet]. 2012. Available from: <https://www.ncbi.nlm.nih.gov/books/NBK548298>.
18. Arora N, Dhiman P, Kumar S, Singh G, Monga V. Recent advances in synthesis and medicinal chemistry of benzodiazepines. *Bioorg Chem.* 2020; 97: 103668.
19. Morgan JE, Wilson SC, Travis BJ, Bagri KH, Pagarigan KT, Belski HM, et al. Refractory and super-refractory status epilepticus in nerve agent-poisoned rats following application of standard clinical treatment guidelines. *Front Neurosci.* 2021; 15: 732213.
20. Niquet J, Lumley L, Baldwin R, Rossetti F, Suchomelova L, Naylor D, et al. Rational polytherapy in the treatment of cholinergic seizures. *Neurobiol Dis.* 2020; 133: 104537.
21. Amengual-Gual M, Sánchez Fernández I, Wainwright MS. Novel drugs and early polypharmacotherapy in status epilepticus. *Seizure.* 2019; 68: 79–88.
22. Myhrer T, Aas P. Choice of approaches in developing novel medical countermeasures for nerve agent poisoning. *Neurotoxicology.* 2014; 44: 27–38.
23. Vijayaraghavan R. Autoinjector device for rapid administration of drugs and antidotes in emergency situations and in mass casualty management. *J Int Med Res.* 2020; 48 (5): 300060520926019.
24. Al-Otaibi F. An overview of structurally diversified anticonvulsant agents. *Acta Pharm.* 2019; 69 (3): 321–44.
25. Romoli M, Mazzocchetti P, D'Alonzo R, Siliquini S, Rinaldi VE, Verrotti A, et al. Valproic acid and epilepsy: from molecular mechanisms to clinical evidences. *Curr Neuropharmacol.* 2019; 17 (10): 926–46.
26. Tasso SM, Moon SCh, Bruno-Blancha LE, Estiu GL. Characterization of the anticonvulsant profile of valpromide derivatives. *Bioorg Med Chem.* 2004; 12 (14): 3857–69.
27. Upmanyu N, Gupta S, Grover J, Mishra P. Synthesis of valproic acid derivatives and their evaluation for anticonvulsant activity. *The Internet Journal of Alternative Medicine.* 2008; 7 (1): 1–6. Available from: <https://ispub.com/IJAM/7/1/5721>.
28. Haines KM, Matson LM, Dunn EN, Ardinger CE, Stubbs RL, Bibi D, et al. Comparative efficacy of valnoctamide and secbutylpropylacetamide (SPD) in terminating nerve agent-induced seizures in pediatric rats. *Epilepsia.* 2019; 60 (2): 315–21.
29. Tsai YH, Lein PJ. Mechanisms of organophosphate neurotoxicity. *Curr Opin Toxicol.* 2021; 26: 49–60.
30. Swissa E, Bar-Klein G, Serlin Y, Weissberg I, Kamintsky L, Eisenkraft A, et al. Midazolam and isoflurane combination reduces late brain damage in the paraoxon-induced status epilepticus rat model. *Neurotoxicology.* 2020; 78: 99–105.
31. Bailey AM, Baum RA, Horn K, Lewis T, Morizio K, Schultz A, et al. Review of intranasally administered medications for use in the emergency department. *J Emerg Med.* 2017; 53 (1): 38–48.
32. Malygin AS. Research of the antiepileptic activity of the new amydic derivative valproic acid and 1,3,4-thiadiazole. *Medicine.* 2019; 3: 37–46. Russian.
33. White HS, Alex AB, Pollock A, Hen N, Ahmad T, Wilcox KS, et al. A new derivative of valproic acid amide possesses a broad-spectrum antiseizure profile and unique activity against status epilepticus and organophosphate neuronal damage. *Epilepsia.* 2012; 53 (1): 131–46.
34. Mikko Gynther M, Peura L, Vernerová M, Leppänen J, Kärkkäinen J, Lehtonen M, et al. Amino acid promoieties alter valproic acid pharmacokinetics and enable extended brain exposure. *Neurochem Res.* 2016; 41: 2797–809.

Литература

1. Разработка методологии диагностики и фармакологической коррекции последствий отравлений веществами судорожного действия. Методические рекомендации МР ФМБА России 12.08-18. М., 2018; 44 с.
2. Phillips HN, Tormoehlen L. Toxin-induced seizures. *Neurol Clin.* 2020; 38 (4): 867–79.
3. Куценко С. А., редактор. Военная токсикология, радиобиология и медицинская защита. СПб.: Фолиант, 2004; 528 с.
4. Alozi M, Rawas-Qalaji M. Treating organophosphates poisoning: management challenges and potential solutions. *Crit Rev Toxicol.* 2020; 50 (9): 764–79.
5. Reddy BS, Skaria TG, Polepalli S, Vidyasagar S, Rao M, Kunhikatta V, et al. Factors associated with outcomes in organophosphate and carbamate poisoning: a retrospective study. *Toxicol Res.* 2020; 36 (3): 257–66.
6. Gladkih В. Д., Назаров В. Б. Реактиваторы холинэстеразы в терапии отравлений нейротропными физиологически активными веществами. Медицина экстремальных ситуаций. 2014; 1 (47): 54–6.
7. King AM, Aaron CK. Organophosphate and carbamate poisoning. *Emerg Med Clin North Am.* 2015; 33 (1): 133–51.
8. Eddleston M. Novel clinical toxicology and pharmacology of organophosphorus insecticide self-poisoning. *Annu Rev Pharmacol Toxicol.* 2019; 59: 341–60.
9. Reddy DS. Mechanism-based novel antidotes for organophosphate neurotoxicity. *Curr Opin Toxicol.* 2019; 14: 35–45.
10. Araujo Furtado M, Rossetti F, Chanda S, Yourick D. Exposure to nerveagents: from status epilepticus to neuroinflammation, brain damage, neurogenesis and epilepsy. *Neurotoxicology.* 2012; 33 (6): 1476–90.
11. Jett DA, Spriggs SM. Translational research on chemical nerve agents. *Neurobiol Dis.* 2020; 133: 104335.
12. Williamson J, Singh T, Kapur J. Neurobiology of organophosphate-induced seizures. *Epilepsy Behav.* 2019; 101 (Pt B): 106426.
13. Newmark J. Therapy for acute nerve agent poisoning: an update. *Neurol Clin Pract.* 2019; 9 (4): 337–42.

14. Lamb T, Selvarajah LR, Mohamed F, Jayamanne S, Gawarammana I, Mostafa A, et al. High lethality and minimal variation after acute self-poisoning with carbamate insecticides in Sri Lanka — implications for global suicide prevention. *Clin Toxicol (Phila)*. 2016; 54 (8): 624–31.
15. Wu X, Kuruba R, Reddy DS. Midazolam-resistant seizures and brain injury after acute intoxication of diisopropylfluorophosphate, an organophosphate pesticide and surrogate for nerve agents. *J Pharmacol Exp Ther*. 2018; 367 (2): 302–21.
16. Imran I, Koch K, Schöfer H, Lau H, Klein J. Effects of three anti-seizure drugs on cholinergic and metabolic activity in experimental status epilepticus. *J Pharm Pharm Sci*. 2019; 22 (1): 340–51.
17. Benzodiazepines. LiverTox: clinical and research information on drug-induced liver injury. National Institute of Diabetes and Digestive and Kidney Diseases. Bethesda (MD) [Internet]. 2012. Available from: <https://www.ncbi.nlm.nih.gov/books/NBK548298>.
18. Arora N, Dhiman P, Kumar S, Singh G, Monga V. Recent advances in synthesis and medicinal chemistry of benzodiazepines. *Bioorg Chem*. 2020; 97: 103668.
19. Morgan JE, Wilson SC, Travis BJ, Bagri KH, Pagarigan KT, Belski HM, et al. Refractory and super-refractory status epilepticus in nerve agent-poisoned rats following application of standard clinical treatment guidelines. *Front Neurosci*. 2021; 15: 732213.
20. Niquet J, Lumley L, Baldwin R, Rossetti F, Suchomelova L, Naylor D, et al. Rational polytherapy in the treatment of cholinergic seizures. *Neurobiol Dis*. 2020; 133: 104537.
21. Amengual-Gual M, Sánchez Fernández I, Wainwright MS. Novel drugs and early polypharmacotherapy in status epilepticus. *Seizure*. 2019; 68: 79–88.
22. Myhrer T, Aas P. Choice of approaches in developing novel medical counter measures for nerve agent poisoning. *Neurotoxicology*. 2014; 44: 27–38.
23. Vijayaraghavan R. Autoinjector device for rapid administration of drugs and antidotes in emergency situations and in mass casualty management. *J Int Med Res*. 2020; 48 (5): 300060520926019.
24. Al-Otaibi F. An overview of structurally diversified anticonvulsant agents. *Acta Pharm*. 2019; 69 (3): 321–44.
25. Romoli M, Mazzocchetti P, D'Alonzo R, Siliquini S, Rinaldi VE, Verrotti A, et al. Valproic acid and epilepsy: from molecular mechanisms to clinical evidences. *Curr Neuropharmacol*. 2019; 17 (10): 926–46.
26. Tasso SM, Moon SCh, Bruno-Blancha LE, Estiu GL. Characterization of the anticonvulsant profile of valpromide derivatives. *Bioorg Med Chem*. 2004; 12 (14): 3857–69.
27. Upmanyu N, Gupta S, Grover J, Mishra P. Synthesis of valproic acid derivatives and their evaluation for anticonvulsant activity. *The Internet Journal of Alternative Medicine*. 2008; 7 (1): 1–6. Available from: <https://ispub.com/IJAM/7/1/5721>.
28. Haines KM, Matson LM, Dunn EN, Ardinger CE, Stubbs RL, Bibi D, et al. Comparative efficacy of valnoctamide and sec-butylpropylacetamide (SPD) in terminating nerve agent-induced seizures in pediatric rats. *Epilepsia*. 2019; 60 (2): 315–21.
29. Tsai YH, Lein PJ. Mechanisms of organophosphate neurotoxicity. *Curr Opin Toxicol*. 2021; 26: 49–60.
30. Swissa E, Bar-Klein G, Serlin Y, Weissberg I, Kamintsky L, Eisenkraft A, et al. Midazolam and isoflurane combination reduces late brain damage in the paraoxon-induced status epilepticus rat model. *Neurotoxicology*. 2020; 78: 99–105.
31. Bailey AM, Baum RA, Horn K, Lewis T, Morizio K, Schultz A, et al. Review of intranasally administered medications for use in the emergency department. *J Emerg Med*. 2017; 53 (1): 38–48.
32. Малыгин А. С. Оценка острой токсичности и нейротоксичности нового амидного производного вальпроевой кислоты и 1,3,4-тиадиазола. *Медицина*. 2019; 3: 37–46.
33. White HS, Alex AB, Pollock A, Hen N, Ahmad T, Wilcox KS, et al. A new derivative of valproic acid amide possesses a broad-spectrum antiseizure profile and unique activity against status epilepticus and organophosphate neuronal damage. *Epilepsia*. 2012; 53 (1): 131–46.
34. Mikko Gynther M, Peura L, Vernerová M, Leppänen J, Kärkkäinen J, Lehtonen M, et al. Amino acid promoieties alter valproic acid pharmacokinetics and enable extended brain exposure. *Neurochem Res*. 2016; 41: 2797–809.

PRIMARY PRE-HOSPITAL TRIAGE OF PATIENTS WITH COVID-19

Cherkashin MA¹✉, Berezin NS², Berezina NA¹, Nikolaev AA¹, Kuplevatskaya DI¹, Kuplevatsky VI¹, Rakova TM¹, Shcheparev IS³¹ Berezin Diagnostic and Treatment Center of International Institute of Biological Systems, St. Petersburg, Russia² International Institute of Biological Systems, St. Petersburg, Russia³ Pirogov National Medical and Surgical Center, Moscow, Russia

The COVID-19 pandemic affected every sector of society, radically altering the work of health systems throughout the world. In the situation of the mass influx of patients seeking medical care that was hard to control, the issue of the widespread adoption of the medical sorting (triage) principles became urgent within weeks. The review provides analysis of 49 publications dealing with various aspects of arranging pre-hospital triage. The dynamic changes in approaches to triage, its objectives and technologies, as well as in the contribution of various X-ray imaging methods depending on the evolving experience of working with the novel infection, are of great interest. The search for literature in Russian and English published before March 10, 2022 was performed in a number of databases (Embase, Medline/PubMed, Researchgate, medrxiv.org, RISC). The search was performed using the following keywords: COVID-19, coronavirus, *коронавирус*, SARS-CoV-2, 2019nCoV, lung ultrasound, computed tomography, computerized tomography, *компьютерная томография*, CT, triage, *сортировка*. The strategy of establishing pre-hospital triage centers or stations in case of pandemic makes it possible to reduce both the burden on the emergency departments and the occupancy rate for inpatient services. Quick access to various imaging methods (X-ray imaging, lung ultrasound or computed tomography) greatly facilitates taking clinical decisions, and could be considered beneficial in the current extraordinary situation.

Keywords: novel coronavirus infection, COVID-19, triage, computed tomography

Author contribution: Cherkashin MA — article planning, literature collecting and analysis, manuscript writing, editing; Berezina NA — literature collecting and analysis, manuscript writing; Berezin NS — article planning, manuscript writing, editing; Nikolaev AA, Kuplevatskaya DI, Kuplevatsky VI, Rakova TM, Shcheparev IS — literature collecting and analysis, manuscript writing.

✉ **Correspondence should be addressed:** Mikhail A. Cherkashin
6-ya Sovetskaya, 24–26b, St. Petersburg, 191144, Russia; mc@ldc.ru

Received: 14.04.2022 **Accepted:** 29.04.2022 **Published online:** 25.05.2022

DOI: 10.47183/mes.2022.015

ПЕРВИЧНАЯ МЕДИЦИНСКАЯ СОРТИРОВКА ПАЦИЕНТОВ С COVID-19 НА ДОГОСПИТАЛЬНОМ ЭТАПЕ

М. А. Черкашин¹✉, Н. С. Березин², Н. А. Березина¹, А. А. Николаев¹, Д. И. Куплевацкая¹, В. И. Куплевацкий¹, Т. М. Ракова¹, И. С. Щепарев³¹ Лечебно-диагностический центр международного института биологических систем имени С. Березина, Санкт-Петербург, Россия² Международный институт биологических систем, Санкт-Петербург, Россия³ Национальный медико-хирургический центр имени Н. И. Пирогова, Москва, Россия

Пандемия COVID-19 затронула все сферы жизни и кардинально изменила работу систем здравоохранения во всех странах. В условиях массового, трудно контролируемого обращения пациентов за медицинской помощью, с первых недель остро встал вопрос широкого внедрения в рутинную практику принципов медицинской сортировки (триажа). В обзоре дан анализ 49 публикаций, посвященных разным аспектам организации догоспитальной медицинской сортировки. Значительный интерес представляет динамика изменений подходов к триажу, его целей и технологий, а также роли разных методов лучевой диагностики, в зависимости от того, как накапливался опыт работы с новой инфекцией. Поиск литературы на русском и английском языках проведен за период до 10 марта 2022 г. с использованием различных баз данных и репозитория (Embase, Medline/PubMed, Researchgate, medrxiv.org, РИНЦ). Поиск осуществляли по ключевым словам «COVID-19», «coronavirus», «коронавирус», «SARS-CoV-2», «2019nCoV», «lung ultrasound», «computed tomography», «computerized tomography», «компьютерная томография», «СТ», «triage», «сортировка». Стратегия создания центров или пунктов догоспитальной сортировки в случае пандемии позволяет снизить нагрузку на приемные отделения больниц и загруженность стационаров. Быстрый доступ к различным методам медицинской визуализации (рентгенография, ультразвуковое исследование легких или компьютерная томография) значительно облегчает принятие клинического решения и в сложившихся нестандартных условиях может быть признан полезным.

Ключевые слова: новая коронавирусная инфекция, COVID-19, медицинская сортировка, компьютерная томография

Вклад авторов: М. А. Черкашин — планирование статьи, сбор и анализ литературы, подготовка рукописи, редактирование; Н. С. Березин — сбор и анализ литературы, подготовка рукописи; Н. А. Березина — планирование статьи, подготовка рукописи, редактирование; А. А. Николаев, Д. И. Куплевацкая, В. И. Куплевацкий, Т. М. Ракова, И. С. Щепарев — сбор и анализ литературы, подготовка рукописи.

✉ **Для корреспонденции:** Михаил Александрович Черкашин
ул. 6-я Советская, д. 24–26б, г. Санкт-Петербург, 191144, Россия; mc@ldc.ru

Статья получена: 14.04.2022 **Статья принята к печати:** 29.04.2022 **Опубликована онлайн:** 25.05.2022

DOI: 10.47183/mes.2022.015

At the end of 2019, the spread of the novel coronavirus infection began in China with an epicenter in the city of Wuhan, Hubei province [1, 2]. The virus was soon identified, and was given the name SARS-CoV-2 by the Coronaviridae Study Group (CSG) of the International Committee on Taxonomy of Viruses [3]. Acute infection caused by SARS-CoV-2 was named COVID-19 (Coronavirus disease 2019) [1]. In early 2020, the active global spread of COVID-19 began [4]. In March 2020, the epidemic also affected the Russian Federation. On March 11, 2020, the World Health Organization (WHO) classified COVID-19 as a pandemic due to the growing number of new cases.

As the experience of foreign countries had proved, the mass influx of patients revealed a severe mismatch between the needs and capabilities of inpatient services. Accumulation of patients potentially not in need of admission in emergency departments resulted in the shortage of beds and increased mortality among seriously ill patients [5, 6]. Within weeks of the novel coronavirus infection outbreak, there was an urgent need in the methods for identification of individuals with COVID-19 and their distribution based on the prognosis.

The obvious solution was the widespread application of medical sorting (triage) principles normally implemented

in case of a major catastrophe or natural disaster. The main principle of triage is as follows: when resources are insufficient, one has to segregate between patients who are in need of immediate inpatient care, and patients who can be referred to the outpatient clinic or treated less urgently.

The paper provides an analytical review of the data on the pre-hospital triage arrangement for patients with suspected COVID-19 and the role of various medical imaging methods in clinical decision-making published over the past two years. The approaches to X-ray diagnostics vary from country to country, and the attitude towards these diagnostic techniques has changed during the pandemic. The authors have focused on using chest computed tomography (CT), since this method remains most widely available in our country.

The search for literature in Russian and English published before March 10, 2022 was performed in a number of databases (Embase, Medline/PubMed, Researchgate, medrxiv.org, RISC). The following keywords were used for search: COVID-19, coronavirus, коронавирус, SARS-COV-2, 2019nCoV, computed tomography, computerized tomography, компьютерная томография, CT, triage, сортировка. Given the lack of knowledge and the great importance of the issue, available preprints, in-press articles and abstracts for scientific conferences were also included in analysis. At least two authors rated each of the 156 reports that were found from a scale of 1 to 5 (methods, the use of at least X-ray diagnostic method, results, clinical significance). In case of disagreement, the author team took a decision by vote. Finally, 49 reports were included.

Triage and its implementation

Pre-hospital triage of patients with suspected novel coronavirus infection in the environment of emergency department is a key to further strategy of the patient management and routing [7]. In the context of the ongoing pandemic, outpatient triage is a complex of diagnostic procedures aimed at assessing the patient's condition severity and making a decision as objective as possible on urgency and need for the patient's admission to the specialized hospital. Medical institutions can move on to triage in exceptional cases, generally in case of multiple simultaneous admissions. The main purpose of triage is to provide optimum care to the maximum number of victims or patients [7].

Low availability of PCR-based laboratory tests for primary diagnosis of patients with suspected COVID-19 was a common pressure faced by all countries during the first months of the pandemic [8–10]. The average delay after swabbing in the emergency department was 573 ± 327 min (189–2,812 min) [10].

It is necessary to promptly filter out the conventionally “zero-infection” patients, who should be provided care in outpatient clinics, and to deduce a group of patients with coronavirus infection to be referred to the conventionally “red zone” hospitals. Furthermore, it is important to perform primary pre-hospital differential diagnosis of the causes of respiratory failure, since this may result from the noncommunicable somatic disorder [10–12].

Initially, triage involved the patients' separation into COVID+ and COVID–; the majority of reports published in 2020 described exactly that strategy [10, 13]. However, this goal was soon supplemented with sorting based on the disease severity, since the hospitals were overloaded, and the need to establish clear criteria for admission in the context of acute shortage of beds became apparent.

In such circumstances, the search for diagnostic methods capable of affecting clinical decision-making on a short-term

basis began. Since damage to the respiratory system prevailed, some authors proposed the use of various X-ray imaging modalities for additional quick assessment of the patient's condition, such as chest computed tomography, ultrasound investigation, conventional X-ray imaging [11, 14–17].

As a result, by February 2020 there was a consensus opinion that the triage protocol had to include clinical, laboratory, and radiological data (usually the chest CT results) [18–20].

X-ray imaging

Conventional diagnostic X-ray imaging methods, being the most accessible and widely used, were adopted in patients with COVID-19 since the first days of the pandemic. However, it was found that CT was more sensitive [17, 21]. Nevertheless, X-ray imaging provides some advantages over CT: lower radiation burden, faster data acquisition, possible use in the intensive care units, portability. The method is still meaningful and useful for follow-up and quick diagnosis of possible complications in patients already admitted to hospital [20, 22]. The data of the retrospective comparative study aimed to assess the efficiency of CT and chest X-ray for the hospital admission triage were published [17]. A total of 113 patients with suspected COVID-19-associated pneumonia admitted to the university clinic in Izmir (Turkey) from March 15 to September 1, 2020 were enrolled. The inclusion criteria were as possible: positive PCR test result, availability of chest X-ray images with the preliminary diagnosis of pneumonia, availability of chest CT images in addition to X-ray images. The Brixia scoring system modified by the authors was used to assess lung injury: each lung was divided into 6 zones, each lung field was evaluated based on the presence and the grade of the ground glass opacities, reticular densities, and areas of consolidation. The scoring system details are provided in Table 1.

The authors noted that at an earlier stage of the disease, when the ground glass opacities prevailed, X-ray imaging was characterized by low sensitivity, that is why CT was more effective in this situation. However, at the progressive stages, the methods showed comparable sensitivity, thus allowing to suggest the use of X-ray imaging not for triage, but for assessing the dynamic changes in the condition of patients admitted to the intensive care unit [17].

Diagnostic ultrasound

Lung ultrasound (LU) is widely used for rapid assessment of patients with respiratory failure within the framework of the BLUE protocol [23]. The potential of using LU for differential diagnosis of viral and bacterial pneumonia was described during the pandemic of the H1N1 influenza (2009) [24]. To date, portable ultrasound units are widely used, that is why LU is applied at all stages of care provision, from outpatient clinics to intensive care units, in the context of the ongoing pandemic [14, 25, 26]. In contrast to X-ray imaging and CT, ultrasound imaging enables rapid assessment (the BLUE protocol duration is less than 3 min), there is no radiation burden, assessment can be repeated many times at any moment, there is no need to transport the patient [14–16]. LU makes it possible to promptly assess pulmonary lesion and the presence of pneumothorax or pleural effusion in severe patients with severe hypoxemia, when the patient's transfer to the CT unit is associated with organizational difficulties [14, 27].

The first recorded case of using LU to assess the pulmonary lesion grade in patient with COVID-19 was published in 2020 by the group of Italian physicians. The authors concluded that the

Table 1. Scoring system for assessment of radiographic findings and CT results (Brixia scoring system modified by Çinkooğlu)

Radiographic feature	CT feature	Grade (X-ray)	Score (CT)
No	No	0	0
Hazy density	Ground glass opacity	1	1
Reticular density	Crazy paving, reticular density	2	2
Consolidation	Consolidation	3	3

method could be used for primary screening in the emergency department since it allowed to divide patients into low-risk (no pathological findings; the patients can wait for the next-level X-ray imaging if necessary) and high-risk (pathological findings; the patients need further investigation and the decision whether to start therapy) group [25]. It was also mentioned that ultrasound imaging simplicity and availability of portable devices made it possible to use ultrasound for pre-triage screening in outpatient clinics.

Other authors proposed an ultrasound classification system based on the clinical trial data for assessing the lung injury severity, the need of patient's admission to ICU, and the need for mechanical ventilation [16]. Classification was based on the scoring system: damage to 12 areas (two anterior, two posterior and two lateral for each lung) was visually assessed (0–4 points). Classification was named LUZ (lung ultrasound Zaragoza score) by the authors. The LUZ score of 22 points or more was a predictor of the patient's need for mechanical ventilation [16].

Other authors suggest a pre-hospital triage algorithm based on the respiratory distress (RD) assessment, saturation measurement and ultrasound findings [26]. The patients should be divided into 4 groups:

- self-quarantine at home (no symptoms of RD, $SpO_2 \geq 93\%$, no pathological ultrasound findings);
- self-quarantine at home with subsequent follow-up (no symptoms of RD, $SpO_2 \geq 93\%$, pathological ultrasound findings);
- oxygen therapy at home with straight follow-up, or hospital admission for patients at risk (symptoms of RD, $SpO_2 < 93\%$, no pathological ultrasound findings);
- hospital admission (symptoms of RD, $SpO_2 < 93\%$, pathological ultrasound findings) [26].

A number of comparative clinical trials revealed that LU and CT showed similar sensitivity and specificity when used for primary diagnosis of the COVID-19-associated pneumonia [19].

In general, ultrasound imaging can be used both at the pre-hospital stage and in emergency departments for primary triage of patients, as well as for assessment of the disease severity and course in pulmonology departments and ICUs [14].

Computed tomography

Chest CT in patients with COVID-19 is used for the instrumental clinical decision support when performing triage, as well as

for primary X-ray diagnostics and assessment of the disease pattern (in outpatient and hospital settings, including intensive care units) [28]. Initially, the data on the CT sensitivity and specificity in the diagnosis of the COVID-19-associated viral pneumonia were quite controversial, however, situation had improved significantly after standardization and establishing clear criteria [29].

As early as April 2020, a number of clinical guidelines were issued by various medical associations (Fleischner Society, Society of Thoracic Radiology, American College of Radiology, Radiological Society of North America), which discussed the use of CT for the diagnosis of coronavirus pneumonia [30, 31].

Initially, great hope was placed on CT in terms of the COVID-19 diagnosis. The study is quite illustrative, during which a series of telephone interviews with seven emergency department clinical leads from across England were taken in April 2020 [32]. Triage of patients during the pandemic was one of the themes. All the surveyed leads reported that they often faced situations when asymptomatic patients in the emergency department with such presentations as trauma were unexpectedly demonstrating incidental viral pneumonia on CT. That is why undertaking chest radiography and significantly increasing the use of chest CT even in asymptomatic patients were started in order to promptly exclude lung injury [32]. French researchers reported the experience of three university hospitals of Lyon, France, gained from March to April 2020 [10]. Chest CT was performed in all patients regardless of the cause of the visit for triage and further transfer of patients to the COVID+ or COVID- hospital unit [10].

However, it quickly became apparent that radiographic features of all types of interstitial pneumonia caused by respiratory viruses were quite the same; in actual practice, it was almost impossible to distinguish between the COVID-associated lesion and, for example, influenza. It was only possible to evaluate the lung injury severity [33]. As a consequence, the agreement was reached to avoid using both X-ray imaging and CT for screening of asymptomatic patients, since the changes revealed had low specificity [28]. Thus, currently there is only one recommendation: to use X-ray methods in moderate to severe patients showing symptoms of respiratory distress with clinical suspicion of COVID-19, even in case of negative PCR test results. The interim guidelines issued by the Ministry of Health also suggest that pre-hospital X-ray diagnostics in patients with acute respiratory infections for the

Table 2. CO-RADS classification [7, 38]

CO-RADS	Suspicion for COVID-19	CT imaging results
CO-RADS 1	No	Normal or non-infectious disease
CO-RADS 2	Low	Pathological features typical for other infections but not COVID-19
CO-RADS 3	Medium	Equivocal findings for COVID-19
CO-RADS 4	High	Suspicious for COVID-19
CO-RADS 5	Very high	Typical COVID-19
CO-RADS 6	PCR+	COVID-19

Table 3. Classification of the CT scan results based on the changes revealed

Score	Radiological findings	Changes
CT-0 (zero)	Normal or no CT signs of viral pneumonia in patient with typical clinical manifestations and relevant exposure history	
CT-1 (mild)	Ground glass opacities with no other signs	Lung parenchymal involvement below 25%
CT-2 (moderate)	Ground glass opacities with no other signs	Lung parenchymal involvement 25–50%
CT-3 (severe)	Ground glass opacities and areas of consolidation	Lung parenchymal involvement 50–75% or lesion increase by 50% within 24–48 h in patient with respiratory distress
CT-4 (critical)	Diffuse ground glass opacification and areas of consolidation in combination with reticular pattern. Hydrothorax	Lung parenchymal involvement over 75%

purpose of triage is indicated only for moderate, severe and critical cases [1].

Features of CT performed in patients with suspected COVID-19

In most cases, low-dose CT scan is the best option, which allows to reduce radiation exposure without compromising the quality of assessment [34, 35]. The procedure is performed without intravenous contrast; the contrast could be additionally used in case of suspected pulmonary embolism or necrotizing pneumonia [1, 34–37].

Classifications have been developed by various radiological associations, that are currently widely used all over the world.

The CO-RADS classification system for assessment of the viral pneumonia likelihood, developed by the Dutch Radiological Society in March 2020, was the first effort for standardization of the criteria [7, 38].

Based on the number of radiological symptoms, according to this classification, the likelihood of having COVID-19 varies between very low (CO-RADS-1) and very high (CO-RADS-5), and the maximum score of CO-RADS-6 provides laboratory confirmation (Table 2).

At the stage of the CO-RADS clinical implementation, it turned out that this classification made it impossible to confirm reliably the diagnosis of COVID-19, despite of the high hopes.

Meanwhile, in early spring of 2020, the colleagues from China and USA proposed a number of variants for classification of lung involvement severity in patients with viral pneumonia [39].

Four groups are distinguished based on the percentage of pulmonary parenchymal involvement: normal lung (0%), less than 25%, 25–50%, more than 50% involved [39].

The modified version of this scoring system was included in the consensus of the Russian Society of Roentgenologists and Radiologists and approved in our country (Table 3) [37, 40].

The proposed scale greatly simplified characterization of findings and became a tool for preliminary assessment of the patient's condition severity by clinicians. In the context of the lack of hospital beds, this pneumonia severity scoring system provided the basis of the outpatient and emergency department triage. To date, hospitalization of patients assigned CT-3 and CT-4 scores has become a routine approach. The patients with pneumonia scores of CT-0-2 and no risk factors (age over 60, diabetes mellitus, pregnancy, etc.) are returned to the outpatient clinics [7, 40].

Organization of a pre-hospital triage center

During the initial phase of the pandemic, the burden of working with the majority of first admitted symptomatic patients fell on emergency departments making them considerably overburdened [32, 41–45].

The growing number of patients, difficulties in ensuring infection control, insufficient preparedness of hospitals for the large number of daily admissions, limited resources, difficulties in rapid obtaining the PCR test results resulted in implementation of strategies of both expanding the capacity of existing emergency departments and performing pre-hospital triage.

Thus, in April 2020, a group of authors from Milano published an article describing preparation of their hospital for patient admissions [44]. Primary assessment (pre-triage) was performed in the ambulance car or in a shelter unit created at the entrance of the emergency department, where body temperature, SpO₂, and respiratory system were assessed. The patients with suspected COVID-19 and SpO₂ < 94% were referred to CT and swabbing in the “red zone” of the emergency department; symptomatic patients with SpO₂ > 94% were referred to swabbing only. After obtaining the results, each patient was re-examined by the physician who decided whether he/she required admission. In case a severe patient arrived in need of immediate critical care, an isolated area with the necessary equipment was prepared in the emergency department. The patients of this category were admitted to the dedicated intensive care unit after CT and received respiratory support pending laboratory confirmation of COVID-19. The patients with positive swab test results were transferred to the COVID-19+ department, and the patients with negative results were transferred to the specialized COVID-19– department [44].

A group of authors from the universities of Milano and Parma proposed a diagnostic algorithm based on the experience in working with the first 702 patients in 2020. The algorithm included primary patient assessment in the shelter unit created at the entrance of the emergency department followed by CT referral to address the issue of admission [46].

In September 2020, a survey of heads of 283 Spanish emergency departments was published [43]. In the majority of emergency departments, triage was launched, observation beds were provided, and patient flow separation was introduced. The nursing staff was increased by 83%, and the number of physicians increased by 59% [43].

The following measures were proposed to increase the emergency department efficiency [32]:

1. Splitting patients into five cohorts based on clinical observations and investigations:
 - suitable for outpatient discharge;
 - suitable for outpatient discharge after in-depth assessment;
 - admit to medical ward;
 - admit to critical care;
 - commence end of life care.
2. Early escalation of care decisions in the emergency department.
3. Deployment of mobile emergency rapid intubation teams enabling early airway care in high-risk patients [32].

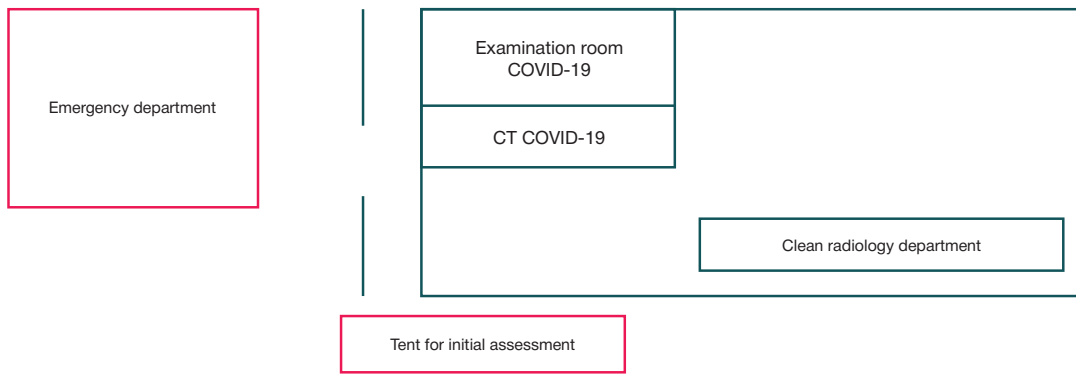


Fig. 1. Layout of the Sichuan university clinic triage station (adapted from [49])

In addition, the decision to establish pre-hospital pre-triage and triage centers was taken by a number of hospitals. Thus, on April 14, 2020, the first experience of creating such center in the indoor ambulance bay of the Massachusetts General Hospital, Boston, USA was reported [12]. The following areas were allocated and equipped:

- waiting area;
- desk;
- triage desk;
- swabbing area.

After assessment the patient was referred for home treatment under the supervision of general practitioner or admitted to hospital [12]. It was found that patients arrived via two main pathways: 75% of patients were referred from primary care offices, the other 25% were walk-ins. Over the first three weeks of operation, the center saw a total of 2667 patients (160 people daily on average), of them only 1% were transferred to the emergency department [12].

The strategy of using outpatient centers (OCTCs) for screening, routing, and follow-up of patients with suspected COVID-19 was implemented in Moscow in late March — early April [40]. A total of 47 centers equipped with CT scanners were deployed in city outpatient clinics. All the scanners were merged into unified digital space, thus enabling remote image assessment by radiologists and thus reducing the risk of infection in medical personnel. In addition, OCTCs were segregated into “red,” “buffer,” and “green” zones. The “red” zone contained CT scanners. All medical personnel assigned to this zone were provided with grade 3 personal protective gear. “Buffer” zone was used to put on personal protective gear. In the “green” zone there were consulting rooms and staff rooms. The outpatient centers saw over 268,000 patients by October 2020 [40].

The experience of the outpatient triage centers deployment in St. Petersburg was reported [7, 47]. During the first 6 months of operation, the centers saw only those patients admitted by ambulance, about 400 cases daily. Then the routing of patients changed, resulting in 80% of patients referred from outpatient clinics. The major goal was to provide preliminary assessment of the patient's condition severity and decide on hospitalization.

The standard algorithm of assessment was as follows:

- history taking;
- contactless temperature measurement;
- assessment of patient complaints;
- respiratory rate assessment and pulse oximetry;
- obtaining information on comorbidities and additional risks;
- in addition, taking the history of vaccination against

COVID-19 was started from June 2021 [48]. The authors noted that auscultation was impossible when wearing protective equipment, and such components of physical examination as palpation and percussion were severely limited. However, the data obtained were usually enough for primary assessment of the disease severity. The patient's physical examination was followed by CT. Then re-examination was performed using the image assessment results, and the decision of admission was made. Respiratory support and monitoring of vital functions were provided when necessary [7].

The time spent on triage is a key issue. The long patient's stay in the emergency department or triage center adversely affects his psychological state. However, in case of severe disease, the necessary care provision is delayed. Thus, analysis of 1,945 emergency department visits showed that the mean delay between CT appointment, CT scanning, and CT report was 187 ± 148 min [10]. However, taking into account the fact that the delay for PCR test results was several times longer at a

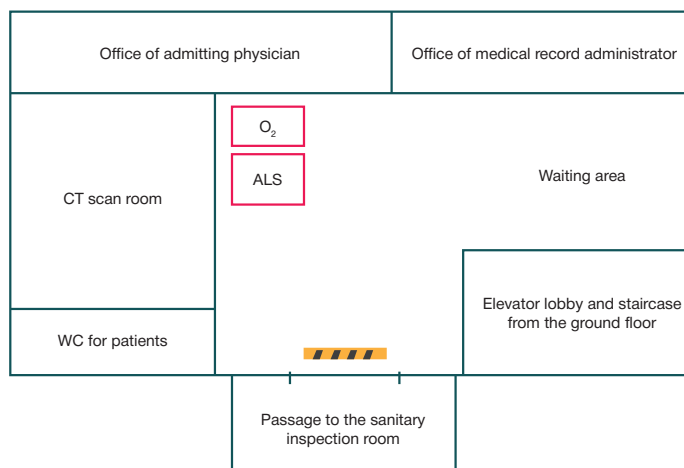


Fig. 2. Layout of the floor with CT scanner. O₂ — oxygen source, ALS — emergency trolley [7]

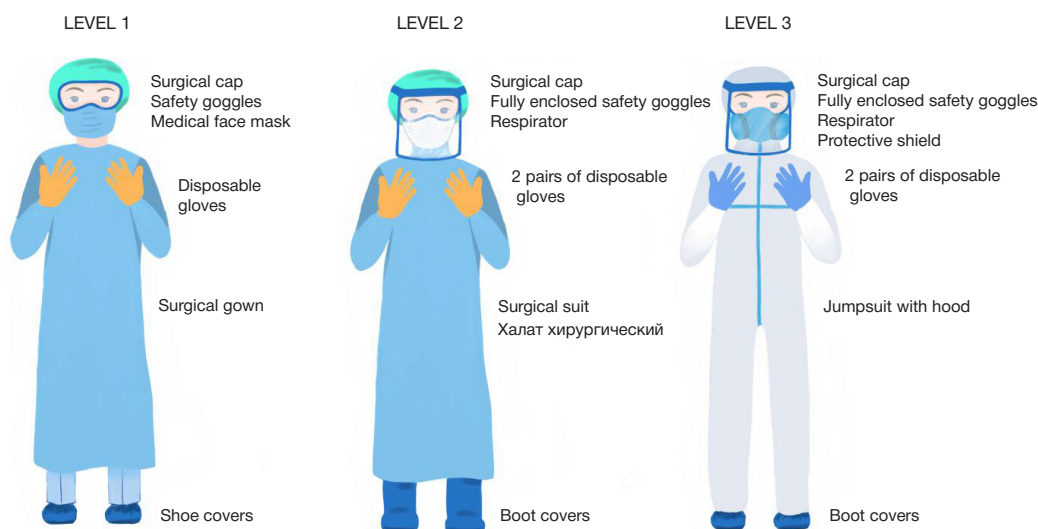


Fig. 3. Levels of protection depending on working conditions [7]

moment, the authors concluded that CT was a fast and simple method facilitating patient triage [10].

In general, implementation of pre-hospital triage was effective. According to the data from St. Petersburg obtained from April to November 2020, triage centers saw a total of 37,537: pneumonia was found in 21,986 cases, 5,532 patients needed hospitalization due to severe disease and severe lung injury, 32,005 patients were referred to outpatient clinics [47].

Providing infection control

To ensure adequate infection control, in practice it is necessary not only to modify the procedures, but also to perform some engineering and organizational operations, reconfigure units and facilities [32, 44].

In June 2020, the authors from the West China Hospital (Sichuan, China) reported the experience of the radiology department reconfiguration for primary triage [49]. There were 4,300 beds in the Sichuan university clinic. The clinic was reconfigured to handle cases of COVID-19 on January 21, 2020. Tents, in which the patients with suspected COVID-19 were assessed, were set up in front of the emergency department. After assessment the patients were sent to the emergency department for CT. To ensure infection control, the department was divided into four areas: contaminated, semicontaminated, buffer, and clean areas (Fig. 1) [49].

The authors of another article described another zoning variant: CT scan room, examination room, emergency cases and oxygen sources are in the contaminated area (Fig. 2) [7].

The patients are admitted to the center by ambulance, medical records are processed in the waiting area. Then physical examination, CT scan, and re-examination based on the CT results are performed. After that physician decides on evacuation to the specialized hospital or referral to the outpatient clinic [7].

Rearrangement of the routine diagnostic procedures is required to reduce the risk of infection in the staff. Thus, elective procedures (screening, etc.) must be delayed, the number of the first-line personnel must be reduced; it is recommended to perform radiography with a portable device at the bedside to avoid the movement of patients. Only a radiographer should be in the CT room, while radiologists should assess the images in the clean area [20].

High risk of the personnel contamination with viral aerosol, the need for regular treatment and disinfection of the rooms,

the use of personal protective equipment, and other factors make CT scan much more difficult and require thorough planning [34, 49]. The rational use of personal protective equipment seems to be a serious matter. In the beginning of the pandemic, information was extremely controversial, the majority of healthcare professionals were not trained to use PPE, that is why special training was required. For example, a three-step training scheme was implemented in one large regional hospital in Italy: lectures with live demonstration of the PPE donning and doffing, in-situ simulation of the PPE donning, use, and doffing, surprise individual assessment after the beginning of work [44]. Currently, all domestic and foreign regulatory agencies (Rosпотребнадзор, Ministry of Health, CDC, NHS и т. д.) distinguish the following levels of PPE protection [1, 7]:

— level 1: possibility of contact with the patient with suspected infection (emergency department staff; ambulance units; hospital ward staff; outpatient clinics personnel; diagnostic department personnel, etc.);

— level 2: prolonged contact with the patient in the unit of the infectious disease/reconfigured hospital;

— level 3: prolonged contact with the patients with suspected infection or infection confirmed by laboratory tests in the intensive care unit, invasive respiratory interventions in patients of this category.

Possible sets for various levels of PPE are provided in Fig. 3.

Thus, to date, the use of level 1 PPE is enough when working in the pre-hospital triage stations [1, 7].

CONCLUSION

The concept of establishing pre-hospital triage centers or stations in case of pandemic makes it possible to reduce both the burden on the emergency departments and the occupancy rate for inpatient services as a whole. Quick access to various imaging methods (X-ray imaging, lung ultrasound or CT) greatly facilitates taking clinical decisions, and could be considered beneficial in the current extraordinary situation. However, it is necessary to strictly follow the clinical practice guidelines in order to avoid the excessive use of chest CT without medical reasons. Organization of the activities of such centers requires careful preparation in terms of infection control, creation of safe routes, and patient flow separation.

References

- Vremennye metodicheskie rekomendacii «Profylaktika, diagnostika i lechenie novoj koronavirusnoj infekcii (COVID-19). Versiya 12 ot 21.09.2021 Ministerstvo zdravooxraneniya Rossijskoj Federacii. Russian.
- Zhu N, Zhang D, Wang, et al. A novel coronavirus from patients with pneumonia in china, 2019. *The New England Journal of Medicine*. 2020; 382 (8): 727–73.
- Ciotti M, Angeletti S, Minieri M, et al. COVID-19 Outbreak: an overview. *Chemotherapy*. 2019;64: 215–23. DOI: 10.1159/000507423.
- Ye Q, Wang B, Mao J, et al. Epidemiological analysis of COVID-19 and practical experience from China. *Journal of medical virology*. 2020; 92 (7): 755–69.
- Orfali K. What Triage Issues Reveal: Ethics in the COVID-19 Pandemic in Italy and France. *J Bioeth Inq*. 2020; 17 (4): 675–9. DOI: 10.1007/s11673-020-10059-y.
- Herreros B, Gella P, Real de Asua D. Triage during the COVID-19 epidemic in Spain: better and worse ethical arguments. *Journal of medical ethics*. 2020; 46 (7): 455–8. Available from: <https://doi.org/10.1136/medethics-2020-106352>.
- Berezina NA, Cherkashin MA, Kuplevackij VI, Kuplevackaya DI, Rakova TM, Nikolaev AA, i dr. Organizaciya raboty ambulatornogo centra komp'yuternoj tomografii dlya okazaniya ehkstretnoj pomoshhi pacientam s podozreniem na novuyu koronavirusnyu infekciyu. *Uchebnoe posobie. M.: Infra-M, 2020; 78 s.* DOI: 10.12737/1222384. Russian.
- Ai T Yang Z Hou H, et al. Correlation of chest CT and RT-PCR testing for Coronavirus Disease 2019 (COVID-19) in China: a Report of 1014 Cases. *Radiology*. 2020; 296: E32–E40.
- Xie X, Zhong Z, Zhao W, et al. Chest CT for typical Coronavirus Disease 2019 (COVID-19) pneumonia: relationship to negative RT-PCR testing. *Radiology*. 2020; 296: E41–E45.
- Ducray V, Vlachomitrou AS, Bouscambert-Duchamp M, et al. Chest CT for rapid triage of patients in multiple emergency departments during COVID-19 epidemic: experience report from a large French university hospital. *Eur Radiol*. 2021; 31: 795–803. Available from: <https://doi.org/10.1007/s00330-020-07154-4>.
- Cao Y, Li Q, Chen J, et al. Hospital Emergency Management Plan During the COVID-19 Epidemic. *Acad Emerg Med*. 2020; 27 (4): 309–11. DOI: 10.1111/acem.13951.
- Baugh JJ, Yun BJ, Searle E, et al. Creating a COVID-19 surge clinic to offload the emergency department. *Am J Emerg Med*. 2020; 38 (7): 1535–7. DOI: 10.1016/j.ajem.2020.04.057.
- Bai HX, Hsieh B, Xiong Z, et al. Performance of radiologists in differentiating COVID-19 from viral pneumonia on chest CT. *Radiology*. 2020; 200823. Available from: <https://doi.org/10.1148/radiol.2020200823>.
- Ciurba BE, Sárközi HK, Szabó IA, et al. Advantages of lung ultrasound in triage, diagnosis and monitoring COVID-19 patients: review. *Acta Marisiensis — Seria Medica*. 2021; 67 (2): 73–76. DOI:10.2478/amma-2021-0019.
- Lieveld AWE, Kok B, Schuit FH, et al. Diagnosing COVID-19 pneumonia in a pandemic setting: Lung Ultrasound versus CT (LUVCT) — a multicenter, prospective, observational study. *ERJ Open Res*. 2020; 6 (4): 00539–2020.
- Garcia-Rubio J, Lopez-Gimenez I, Horna-Garces V, et al. Point-of-care lung ultrasound assessment for risk stratification and therapy guiding in COVID-19 patients. A prospective non-interventional study. *Eur Respir J*. 2021; 2004283.
- Çinkooğlu A, Bayraktaroğlu S, Ceylan N, et al. Efficacy of chest X-ray in the diagnosis of COVID-19 pneumonia: comparison with computed tomography through a simplified scoring system designed for triage. *Egypt J Radiol Nucl Med*. 2021; 52: 166. Available from: <https://doi.org/10.1186/s43055-021-00541-x>.
- Bernheim A, Mei X, Huang M, et al. Chest CT Findings in Coronavirus Disease-19 (COVID-19): Relationship to Duration of Infection. *Radiology*. 2020 295 (3): 200463. DOI: 10.1148/radiol.2020200463.
- Alcantara ML, Bernardo MPL, Autran TB, et al. Lung ultrasound as a triage tool in an emergency setting during the Covid-19 outbreak: comparison with CT findings. *Int J Cardiovasc Sci*. 2020; 33 (5): 479–87 DOI: 10.36660/ijcs.20200133.
- Sverzellati N, Milone F, Balbi M. How imaging should properly be used in COVID-19 outbreak: an Italian experience. *Diagn Interv Radiol*. 2020; 26 (3): 204–6. Available from: <https://doi.org/10.5152/dir.2020.30320>.
- Wong HYF, Lam HYS, Fong AH, et al Frequency and distribution of chest radiographic findings in patients positive for COVID-19. *Radiology*. 2020; 296 (2): E72–E78. Available from: <https://doi.org/10.1148/radiol.2020201160>.
- Güneyli S, Atçeken Z, Doğan H, et al Radiological approach to COVID-19 pneumonia with an emphasis on chest CT. *Diagn Interv Radiol*. 2020; 26 (4): 323–32. Available from: <https://doi.org/10.5152/dir.2020.20260>.
- Liechtenstein DA, Meziere GA. Relevance of Lung Ultrasound in the Diagnosis of Acute Respiratory Failure, The BLUE Protocol. *Chest*. 2008; 134: 117–25.
- Tsung JW, Kessler DO, Shah VP. Prospective application of clinician performed lung ultrasonography during the 2009 H1N1 influenza A pandemic: distinguishing viral from bacterial pneumonia. *Crit Ultrasound J*. 2012; 4–16.
- Buonsenso D, Piano A, Raffaelli F, et al. Point-of-Care Lung Ultrasound findings in novel coronavirus disease-19 pneumoniae: a case report and potential applications during COVID-19 outbreak. *Eur Rev Med Pharmacol Sci*. 2020; 24 (5): 2776–80.
- Pilięgo C, Strumia A, Stone MB, Pascarella G. The Ultrasound-Guided Triage: A New Tool for Prehospital Management of COVID-19 Pandemic. *Anesth Analg*. 2020; 131 (2): e93–e94.
- Bello G, Blanco P. Lung ultrasonography for assessing lung aeration in acute respiratory distress syndrome: a narrative review. *J Ultrasound Med*. 2019; 38: 27–37.
- Machnicki S, Patel D, Singh A, et al. The Usefulness of Chest CT Imaging in Patients With Suspected or Diagnosed COVID-19. *CHEST*. 2021; 160 (2): 652–70. Available from: <https://doi.org/10.1016/j.chest.2021.04.004>.
- Salameh J, Leeflang M., Hooft L, et al. Thoracic imaging tests for the diagnosis of COVID-19. *Cochrane Database Syst Rev*. 2020; 9: Cd013639.
- Rubin GD, Ryerson CJ, Haramati LB, et al. The role of chest imaging in patient management during the COVID-19 pandemic: a multinational consensus statement from the Fleischner Society. *Radiology*. 2020; 296 (1): 172–80.
- Simpson S, Kay FU, Abbara S, et al. Radiological Society of North America expert consensus document on reporting chest CT findings related to COVID-19: endorsed by the Society of Thoracic Radiology, the American College of Radiology, and RSNA. *Radiol Cardiothorac Imaging*. 2020; 2 (2): e200152.
- Walton H, Navaratnam AV, Ormond M, et al. Emergency medicine response to the COVID-19 pandemic in England: a phenomenological study. *Emerg Med J*. 2020; 37 (12): 768–72. DOI: 10.1136/emermed-2020-210220.
- Wang W, Xu Y, Gao R, et al Detection of SARS-CoV-2 in different types of clinical specimens. *JAMA*. 2020; 323 (18): 1843–44. DOI:10.1001/jama.2020.3786
- Kwee TC, Kwee RM. Chest CT in COVID-19: what the radiologist needs to know. *RadioGraphics*. 2020; 40 (7): 1848–65.
- Dangis A, Gieraerts C, Bruecker YD, et al. Accuracy and reproducibility of low-dose submillisievert chest CT for the diagnosis of COVID-19. *Radiol Cardiothorac Imaging*. 2020; 2 (2): e200196.
- Homayounieh F, Holmberg O, Umairi RA, et al. Variations in CT utilization, protocols, and radiation doses in COVID-19 pneumonia: results from 28 Countries in the IAEA Study. *Radiology*. 2021; 298 (3): E141–E151. DOI: 10.1148/radiol.2020203453.
- Sinicyn VE, Tyurin IE, Mitkov VV. Vremennye soglasitel'nye metodicheskie rekomendacii Rossijskogo obshhestva rentgenologov i radiologov (RORR) i Rossijskoj associacii specialistov ul'trazvukovoj diagnostiki v medicine (RASUDM) «Metody luchevoj diagnostiki pnevmonii pri novoi koronavirusnoj infekcii COVID-19» (versiya 2). *Vestnik rentgenologii i radiologii*. 2020; 101 (2): 72–89. Available from: <https://doi.org/10.20862/0042-4676-2020-101-2-72-89>. Russian.
- Prokop M, van Everdingen W, van Rees Vellinga T, et al. CO-RADS: A Categorical CT Assessment Scheme for Patients Suspected

- of Having COVID-19-Definition and Evaluation. *Radiology*. 2020; 296 (2), E97–E104. Available from: <https://doi.org/10.1148/radiol.2020201473>.
39. Yang R, Li X, Liu H, et al. Chest CT severity score: an imaging tool for assessing severe COVID-19. *Radiol Cardiothorac Imaging*. 2020; 2:e200047.
 40. Morozov SP, Kuzmina ES, Ledixova NV, i dr. Mobilizaciya nauchno-prakticheskogo potentsiala sluzhby luchevoj diagnostiki g. Moskvy v pandemiyu COVID-19. *Digital Diagnostics*. 2020; 1 (1): 5–12. DOI: 10.17816/DD51043. Russian.
 41. Mitchell R, Banks C. On behalf of authoring working party Emergency departments and the COVID-19 pandemic: making the most of limited resources *Emergency Medicine Journal* 2020; 37: 258–9.
 42. Mareiniss DP. The impending storm: COVID-19, pandemics and our overwhelmed emergency departments. *Am J Emerg Med*. 2020; 38 (6): 1293–4. DOI: 10.1016/j.ajem.2020.03.033.
 43. Alquézar-Arbé A, Piñera P, Jacob J, et al. Impact of the COVID-19 pandemic on hospital emergency departments: results of a survey of departments in 2020 — the Spanish ENCOVUR study. *Emergencias*. 2020; 32 (5): 320–1.
 44. Carenzo L, Costantini E, Greco M, et al. Hospital surge capacity in a tertiary emergency referral centre during the COVID-19 outbreak in Italy. *Anaesthesia*. 2020; 75 (7): 928–34. DOI: 10.1111/anae.15072. Erratum in: *Anaesthesia*. 2020; 75 (11): 1540.
 45. Spina S, Marrazzo F, Migliari M, et al. The response of Milan's Emergency Medical System to the COVID-19 outbreak in Italy. *Lancet*. 2020; 395: e49–50.
 46. Sverzellati N, Milanese G, Milone F, et al. Integrated Radiologic Algorithm for COVID-19 Pandemic. *J Thorac Imaging*. 2020; 35 (4): 228–33. DOI: 10.1097/RTI.0000000000000516.
 47. Cherkashin M, Berezina N, Nikolaev A, et al. Outpatient CT-centre for emergency triage of COVID-19 patients: local experience from Saint Petersburg. *Insights into Imaging*. 2021; 12 (75): 80. DOI:10.1186/s13244-021-01014-5.
 48. Barchuk A, Cherkashin M, Bulina A, et al. Vaccine Effectiveness against Referral to Hospital and Severe Lung Injury Associated with COVID-19: A Population-based Case-control Study in St. Petersburg, Russia. *medRxiv* 2021.08.18.21262065; DOI: <https://doi.org/10.1101/2021.08.18.21262065>.
 49. Huang Z, Zhao S, Li Z, et al, The Battle Against Coronavirus Disease 2019 (COVID-19): Emergency Management and Infection Control in a Radiology Department. *J Am Coll Radiol*. 2020; 24 (5): 2776–80.

Литература

1. Временные методические рекомендации «Профилактика, диагностика и лечение новой коронавирусной инфекции (COVID-19). Версия 12 от 21.09.2021 Министерство здравоохранения Российской Федерации.
2. Zhu N, Zhang D, Wang, et al. A novel coronavirus from patients with pneumonia in china, 2019. *The New England Journal of Medicine*. 2020; 382 (8): 727–73.
3. Ciotti M, Angeletti S, Minieri M, et al. COVID-19 Outbreak: an overview. *Chemotherapy*. 2019;64: 215–23. DOI: 10.1159/000507423.
4. Ye Q, Wang B, Mao J, et al. Epidemiological analysis of COVID-19 and practical experience from China. *Journal of medical virology*. 2020; 92 (7): 755–69.
5. Orfali K. What Triage Issues Reveal: Ethics in the COVID-19 Pandemic in Italy and France. *J Bioeth Inq*. 2020; 17 (4): 675–9. DOI: 10.1007/s11673-020-10059-y.
6. Herreros B, Gella P, Real de Asua D. Triage during the COVID-19 epidemic in Spain: better and worse ethical arguments. *Journal of medical ethics*. 2020; 46 (7): 455–8. Available from: <https://doi.org/10.1136/medethics-2020-106352>.
7. Бerezina Н. А., Черкашин М. А., Куплевацкий В. И., Куплевацкая Д. И., Ракова Т. М., Николаев А. А., и др. Организация работы амбулаторного центра компьютерной томографии для оказания экстренной помощи пациентам с подозрением на новую коронавирусную инфекцию. Учебное пособие. М.: Инфра-М, 2020; 78 с. DOI: 10.12737/1222384.
8. Ai T Yang Z Hou H, et al. Correlation of chest CT and RT-PCR testing for Coronavirus Disease 2019 (COVID-19) in China: a Report of 1014 Cases. *Radiology*. 2020; 296: E32–E40.
9. Xie X, Zhong Z, Zhao W, et al. Chest CT for typical Coronavirus Disease 2019 (COVID-19) pneumonia: relationship to negative RT-PCR testing. *Radiology*. 2020; 296: E41–E45.
10. Ducray V, Vlachomitrou AS, Bouscambert-Duchamp M, et al. Chest CT for rapid triage of patients in multiple emergency departments during COVID-19 epidemic: experience report from a large French university hospital. *Eur Radiol*. 2021; 31: 795–803. Available from: <https://doi.org/10.1007/s00330-020-07154-4>.
11. Cao Y, Li Q, Chen J, et al. Hospital Emergency Management Plan During the COVID-19 Epidemic. *Acad Emerg Med*. 2020; 27 (4): 309–11. DOI: 10.1111/acem.13951.
12. Baugh JJ, Yun BJ, Searle E, et al. Creating a COVID-19 surge clinic to offload the emergency department. *Am J Emerg Med*. 2020; 38 (7): 1535–7. DOI: 10.1016/j.ajem.2020.04.057.
13. Bai HX, Hsieh B, Xiong Z, et al. Performance of radiologists in differentiating COVID-19 from viral pneumonia on chest CT. *Radiology*. 2020; 200823. Available from: <https://doi.org/10.1148/radiol.2020200823>.
14. Ciurba BE, Sárközi HK, Szabó IA, et al. Advantages of lung ultrasound in triage, diagnosis and monitoring COVID-19 patients: review. *Acta Marisiensis — Seria Medica*. 2021; 67 (2): 73–76. DOI:10.2478/amma-2021-0019.
15. Lieveld AWE, Kok B, Schuit FH, et al. Diagnosing COVID-19 pneumonia in a pandemic setting: Lung Ultrasound versus CT (LUVCT) — a multicenter, prospective, observational study. *ERJ Open Res*. 2020; 6 (4): 00539–2020.
16. Garcia-Rubio J, Lopez-Gimenez I, Horna-Garces V, et al. Point-of-care lung ultrasound assessment for risk stratification and therapy guiding in COVID-19 patients. A prospective non-interventional study. *Eur Respir J*. 2021; 2004283.
17. Çinkooğlu A, Bayraktaroglu S, Ceylan N, et al. Efficacy of chest X-ray in the diagnosis of COVID-19 pneumonia: comparison with computed tomography through a simplified scoring system designed for triage. *Egypt J Radiol Nucl Med*. 2021; 52: 166. Available from: <https://doi.org/10.1186/s43055-021-00541-x>.
18. Bernheim A, Mei X, Huang M, et al. Chest CT Findings in Coronavirus Disease-19 (COVID-19): Relationship to Duration of Infection. *Radiology*. 2020 295 (3): 200463. DOI: 10.1148/radiol.2020200463.
19. Alcantara ML, Bernardo MPL, Autran TB, et al. Lung ultrasound as a triage tool in an emergency setting during the Covid-19 outbreak: comparison with CT findings. *Int J Cardiovasc Sci*. 2020; 33 (5): 479–87 DOI: 10.36660/ijcs.20200133.
20. Sverzellati N, Milone F, Balbi M. How imaging should properly be used in COVID-19 outbreak: an Italian experience. *Diagn Interv Radiol*. 2020; 26 (3): 204–6. Available from: <https://doi.org/10.5152/dir.2020.30320>.
21. Wong HYF, Lam HYS, Fong AH, et al Frequency and distribution of chest radiographic findings in patients positive for COVID-19. *Radiology*. 2020; 296 (2): E72–E78. Available from: <https://doi.org/10.1148/radiol.2020201160>.
22. Güneşli S, Atçeken Z, Doğan H, et al Radiological approach to COVID-19 pneumonia with an emphasis on chest CT. *Diagn Interv Radiol*. 2020; 26 (4): 323–32. Available from: <https://doi.org/10.5152/dir.2020.20260>.
23. Liechtenstein DA, Meziere GA. Relevance of Lung Ultrasound in the Diagnosis of Acute Respiratory Failure, The BLUE Protocol. *Chest*. 2008; 134: 117–25.
24. Tsung JW, Kessler DO, Shah VP. Prospective application of clinician performed lung ultrasonography during the 2009 H1N1 influenza A pandemic: distinguishing viral from bacterial pneumonia. *Crit Ultrasound J*. 2012; 4–16.
25. Buonsenso D, Piano A, Raffaelli F, et al. Point-of-Care Lung Ultrasound findings in novel coronavirus disease-19 pneumoniae: a

- case report and potential applications during COVID-19 outbreak. *Eur Rev Med Pharmacol Sci.* 2020; 24 (5): 2776–80.
26. Pilego C, Strumia A, Stone MB, Pascarella G. The Ultrasound-Guided Triage: A New Tool for Prehospital Management of COVID-19 Pandemic. *Anesth Analg.* 2020; 131 (2): e93–e94.
 27. Bello G, Blanco P. Lung ultrasonography for assessing lung aeration in acute respiratory distress syndrome: a narrative review. *J Ultrasound Med.* 2019; 38: 27–37.
 28. Machnicki S, Patel D, Singh A, et al. The Usefulness of Chest CT Imaging in Patients With Suspected or Diagnosed COVID-19. *CHEST.* 2021; 160 (2): 652–70. Available from: <https://doi.org/10.1016/j.chest.2021.04.004>.
 29. Salameh J, Leeflang M., Hoof L, et al. Thoracic imaging tests for the diagnosis of COVID-19. *Cochrane Database Syst Rev.* 2020; 9: Cd013639.
 30. Rubin GD, Ryerson CJ, Haramati LB, et al. The role of chest imaging in patient management during the COVID-19 pandemic: a multinational consensus statement from the Fleischner Society. *Radiology.* 2020; 296 (1): 172–80.
 31. Simpson S, Kay FU, Abbara S, et al. Radiological Society of North America expert consensus document on reporting chest CT findings related to COVID-19: endorsed by the Society of Thoracic Radiology, the American College of Radiology, and RSNA. *Radiol Cardiothorac Imaging.* 2020; 2 (2): e200152.
 32. Walton H, Navaratnam AV, Ormond M, et al. Emergency medicine response to the COVID-19 pandemic in England: a phenomenological study. *Emerg Med J.* 2020; 37 (12): 768–72. DOI: 10.1136/emermed-2020-210220.
 33. Wang W, Xu Y, Gao R, et al. Detection of SARS-CoV-2 in different types of clinical specimens. *JAMA.* 2020; 323 (18): 1843–44. DOI:10.1001/jama.2020.3786
 34. Kwee TC, Kwee RM. Chest CT in COVID-19: what the radiologist needs to know. *RadioGraphics.* 2020; 40 (7): 1848–65.
 35. Dangis A, Gieraerts C, Bruecker YD, et al. Accuracy and reproducibility of low-dose submillisievert chest CT for the diagnosis of COVID-19. *Radiol Cardiothorac Imaging.* 2020; 2 (2): e200196.
 36. Homayounieh F, Holmberg O, Umairi RA, et al. Variations in CT utilization, protocols, and radiation doses in COVID-19 pneumonia: results from 28 Countries in the IAEA Study. *Radiology.* 2021; 298 (3): E141–E151. DOI: 10.1148/radiol.2020203453.
 37. Синицын В. Е., Тюрин И. Е., Митьков В. В. Временные согласительные методические рекомендации Российского общества рентгенологов и радиологов (РОПР) и Российской ассоциации специалистов ультразвуковой диагностики в медицине (РАСУДМ) «Методы лучевой диагностики пневмонии при новой коронавирусной инфекции COVID-19» (версия 2). *Вестник рентгенологии и радиологии.* 2020; 101 (2): 72–89. Available from: <https://doi.org/10.20862/0042-4676-2020-101-2-72-89>.
 38. Prokop M, van Everdingen W, van Rees Vellinga T, et al. CO-RADS: A Categorical CT Assessment Scheme for Patients Suspected of Having COVID-19-Definition and Evaluation. *Radiology.* 2020; 296 (2), E97–E104. Available from: <https://doi.org/10.1148/radiol.2020201473>.
 39. Yang R, Li X, Liu H, et al. Chest CT severity score: an imaging tool for assessing severe COVID-19. *Radiol Cardiothorac Imaging.* 2020; 2:e200047.
 40. Морозов С. П., Кузьмина Е. С., Ледихова Н. В., и др. Мобилизация научно-практического потенциала службы лучевой диагностики г. Москвы в пандемию COVID-19. *Digital Diagnostics.* 2020; 1 (1): 5–12. DOI: 10.17816/DD51043.
 41. Mitchell R, Banks C. On behalf of authoring working party Emergency departments and the COVID-19 pandemic: making the most of limited resources *Emergency Medicine Journal* 2020; 37: 258–9.
 42. Mareiniss DP. The impending storm: COVID-19, pandemics and our overwhelmed emergency departments. *Am J Emerg Med.* 2020; 38 (6): 1293–4. DOI: 10.1016/j.ajem.2020.03.033.
 43. Alquézar-Arbé A, Piñera P, Jacob J, et al. Impact of the COVID-19 pandemic on hospital emergency departments: results of a survey of departments in 2020 — the Spanish ENCOVUR study. *Emergencias.* 2020; 32 (5): 320–1.
 44. Carenzo L, Costantini E, Greco M, et al. Hospital surge capacity in a tertiary emergency referral centre during the COVID-19 outbreak in Italy. *Anaesthesia.* 2020; 75 (7): 928–34. DOI: 10.1111/anae.15072. Erratum in: *Anaesthesia.* 2020; 75 (11): 1540.
 45. Spina S, Marrazzo F, Migliari M, et al. The response of Milan's Emergency Medical System to the COVID-19 outbreak in Italy. *Lancet.* 2020; 395: e49–50.
 46. Sverzellati N, Milanese G, Milone F, et al. Integrated Radiologic Algorithm for COVID-19 Pandemic. *J Thorac Imaging.* 2020; 35 (4): 228–33. DOI: 10.1097/RTI.0000000000000516.
 47. Cherkashin M, Berezina N, Nikolaev A, et al. Outpatient CT-centre for emergency triage of COVID-19 patients: local experience from Saint Petersburg. *Insights into Imaging.* 2021; 12 (75): 80. DOI:10.1186/s13244-021-01014-5.
 48. Barchuk A, Cherkashin M, Bulina A, et al. Vaccine Effectiveness against Referral to Hospital and Severe Lung Injury Associated with COVID-19: A Population-based Case-control Study in St. Petersburg, Russia. *medRxiv* 2021.08.18.21262065; DOI: <https://doi.org/10.1101/2021.08.18.21262065>.
 49. Huang Z, Zhao S, Li Z, et al. The Battle Against Coronavirus Disease 2019 (COVID-19): Emergency Management and Infection Control in a Radiology Department. *J Am Coll Radiol.* 2020; 24 (5): 2776–80.

OMICS TECHNOLOGIES IN THE DIAGNOSTICS OF *MYCOBACTERIUM TUBERCULOSIS*

Bespyatykh JA^{1,2}✉, Basmanov DV¹

¹ Federal Research and Clinical Center of Physical-Chemical Medicine of Federal Medical Biological Agency, Moscow, Russia

² Mendeleev University of Chemical Technology of Russia, Moscow, Russia

Tuberculosis, caused by *Mycobacterium tuberculosis*, remains a global burden on our country and entire world. According to the World Health Organization, 10 million incident cases of tuberculosis were registered in 2019. A steady increase in the drug-resistant tuberculosis aggravates the situation and appears to be the major obstacle to the fight against the disease. A thorough understanding of the pathogen physiology and virulence properties is extremely important for the development of new diagnosis methods and treatment strategies. Multiomics approaches to studying the infectious agents are indispensable in understanding the nature of the disease. Despite the availability of sufficient genomic and transcriptomic data, pathogenic potential, survival rate, persistence, immunomodulation, mechanisms underlying drug resistance and host-pathogen interaction remain poorly understood. The use of proteomic approaches has been more informative, and provides more information about the true state of the cell in various conditions. Proteomic and bioinformatic approaches helped considerably in identification and characterization of target proteins that could be used for the development of new therapeutic options. Nevertheless, OMICs data integration with simultaneous use of the system approach to studying various clinically significant mycobacterial strains makes it possible to increase knowledge about the disease mechanisms and infection control methods. The review outlines various OMICs technologies and their role in the development of the *M. tuberculosis* diagnostic panels.

Keywords: tuberculosis, diagnosis, system analysis

Funding: the study was supported by RSF grant № 20-75-10144.

Author contribution: Bespyatykh JA — study concept, manuscript writing and editing; Basmanov DV — analysis of raw data on biosensors and microarrays, manuscript writing.

✉ **Correspondence should be addressed:** Julia A. Bespyatykh
Malaya Pirogovskaya, 1a, Moscow, 119435, Russia; JuliaBes@rcpcm.org

Received: 12.04.2022 **Accepted:** 27.04.2022 **Published online:** 16.05.2022

DOI: 10.47183/mes.2022.013

ОМИКСНЫЕ ТЕХНОЛОГИИ В ДИАГНОСТИКЕ *MYCOBACTERIUM TUBERCULOSIS*

Ю. А. Беспятых^{1,2}✉, Д. В. Басманов¹

¹ Федеральный научно-клинический центр физико-химической медицины Федерального медико-биологического агентства, Москва, Россия

² Российский химико-технологический университет имени Д. И. Менделеева, Москва, Россия

Туберкулез, вызываемый бактериями *Mycobacterium tuberculosis*, продолжает оставаться глобальным бременем для нашей страны и всего мира. По данным Всемирной организации здравоохранения, 10 млн случаев впервые выявленного туберкулеза зарегистрировано в 2019 г. Постоянный рост лекарственно-устойчивого туберкулеза усугубляет ситуацию и оказывается основным препятствием в борьбе с заболеванием. Для разработки новых способов диагностики и стратегий лечения крайне важно максимально полное понимание физиологии патогена и его вирулентных свойств. Мультиомиксные подходы в изучении инфекционных агентов являются крайне полезными для понимания сути заболевания. Несмотря на наличие большого количества геномных и транскриптомных данных, патогенный потенциал, выживаемость, персистенция, иммуномодуляция, механизмы лекарственной устойчивости и взаимодействия между хозяином и патогеном остаются малоизученными. Использование протеомных подходов оказалось более информативным и предоставляет более подробную информацию об истинном состоянии клетки в различных условиях. Подходы протеомики и биоинформатики значительно помогли в идентификации и характеристике целевых белков, которые могут быть использованы для создания новых терапевтических средств. В то же время именно интеграция омиксных данных и одновременное использование системного подхода к изучению различных клинически значимых штаммов микобактерий позволяют существенно расширить знания в понимании механизма заболевания и способов борьбы с инфекцией. В обзоре описаны различные омиксные технологии и их роль в разработке диагностических панелей *M. tuberculosis*.

Ключевые слова: туберкулез, диагностика, системный анализ

Финансирование: работа выполнена при поддержке гранта РФФИ № 20-75-10144.

Вклад авторов: Ю. А. Беспятых — концепция, написание текста и финальное редактирование; Д. В. Басманов — анализ исходных материалов по биосенсорам и чипам, написание текста.

✉ **Для корреспонденции:** Юлия Андреевна Беспятых
ул. Малая пироговская, д. 1а, г. Москва, 119435, Россия; JuliaBes@rcpcm.org

Статья получена: 12.04.2022 **Статья принята к печати:** 27.04.2022 **Опубликована онлайн:** 16.05.2022

DOI: 10.47183/mes.2022.013

Mycobacterium tuberculosis is a causative agent of tuberculosis (TB) and holds one of the leading roles among the causes of the infectious disease deaths. The major issues of TB management include the increase in cases of infection with the multidrug-resistant (MDR) and extensively drug-resistant (XDR) strains, and human immunodeficiency virus (HIV) co-infection [1]. Currently, TB therapy includes first-line drugs taken for 6–9 months and has severe side effects [2]. MDR/XDR TB requires extended treatment with the second-line anti-TB drugs in addition to the first-line drugs, pyrazinamide and high-dose isoniazid [3]. Regardless of the current stage-by-stage

approach to treatment regimens, the increase in cases of MDR and XDR TB creates new obstacles to the available drug therapy [4]. Thus, the need to improve medicines and infection control methods together with the need to develop new vaccine preparations becomes apparent.

M. tuberculosis is transmitted mainly by airborne droplets, by inhaling an aerosol containing cells of the pathogen [5]. After entering the lungs, bacteria infect alveolar macrophages and escape the host's immune response [6]. To further spread through the body, mycobacteria suppress the protective mechanism of macrophages, including autophagy, phagosome

oxidation, reactive oxygen and nitrogen species release [7, 8]. Furthermore, infected macrophages produce chemokines, which attract inflammatory cells, such as neutrophils and natural killer cells, thus promoting the further development of inflammation and the formation of multinucleated giant cells known as granulomas [9]. Thus, these are precisely granulomas that provide the niche for bacteria and serve as a reservoir of infection.

Proteins secreted by *M. tuberculosis* (secretome) play a key role in the abnormal immune responses and intracellular growth progression [10, 11]. The early secreted antigenic target protein 6 (ESAT-6) being the major virulence factor of *M. tuberculosis* is known to regulate the host immune responses by inhibiting pro-inflammatory responses, such as interferon (IFN) γ [12] and interleukin-12 (IL12) production [13]. Moreover, ESAT-6 stimulates IL6 production by macrophages [14] and plays an important role in inducing macrophage polarization and macrophage transition to epithelioid macrophages being the main component of the tuberculous granuloma [15, 16]. It is shown that Rv1988, a secreted effector protein, methylates the host cell histones, thus providing epigenetic modulation of the anti-mycobacterial function of macrophages [17]. All of this confirms the important role of the *M. tuberculosis* proteins in virulence [18]. In addition, high-throughput proteome-wide screening of potential antigens of *M. tuberculosis* can be used to develop new vaccines [19].

Despite the fact that the *M. tuberculosis* genome was extensively studied in the early 2000s, analysis of its proteome lagged due to protein isolation protocol complexity and the need to use a complex and expensive equipment [20]. To date, more than 30% of proteome have not been characterized and are represented by hypothetical proteins [21]. Decoding the function of these proteins would contribute to better understanding of the *M. tuberculosis* physiology and virulence. Clearly, this is only possible with the use of other OMICs technologies, such as transcriptomics and proteogenomics. There is no doubt that it is important to identify and characterize all genes, however, special attention should be paid to gene products responsible for virulence and pathogenesis. Transcripts, protein products, and metabolites can be defined and quantified, thus allowing one to reveal the differences in the pathogenicity and drug resistance between the lineages and strains of *M. tuberculosis*. In general, the combination of such approaches could help to find new anti-TB drug targets and contribute to implementation of the WHO End TB Strategy.

Genomics

Currently, understanding the genetic potential of the studied object would determine the future strategy of any research. The *M. tuberculosis* H37Rv strain complete genome sequence was first published in 1998 [22], and the development of sequencing technologies has resulted in the fact that there are more than 13,000 genomes of *M. tuberculosis* currently available in the NCBI database. However, it is worth mentioning that the majority of those are not arranged in rings. Annotation of the *M. tuberculosis* H37Rv strain genome (version 27 according to the TuberculList database (<http://tuberculist.epfl.ch/>)) containing 4018 protein-encoding genes, of which 26% belong to the class of proteins with hypothetical functions, has been considered a reference system and the most complete sequence for a long time. In 2019, complete sequence of the RUS_B0 strain belong to the Beijing family was published [23].

Mycobacteria have all the genes necessary for synthesis of essential amino acids, vitamins, enzymes, and cofactors.

It was found that these bacteria have a high proportion of genes encoding enzymes involved in lipogenesis and lipolysis. Furthermore, *M. tuberculosis* has genes necessary for synthesis of glycolytic enzymes, enzymes involved in the anabolic pentose phosphate pathway, which generates NADPH and pentoses, enzymes of the tricarboxylic acid and glyoxylate cycles synthesizing carbohydrates from fats. The tubercle bacillus also has enzymes involved in the aerobic, microaerophilic and anoxic electron transfer. It is shown that mycobacteria are able to survive in various environments, including oxygen-rich lungs, macrophages, and the center of caseous granuloma [24].

Mycobacterial genome is rich with fatty acid metabolism-related genes, including mycolic acids containing acidic asparagine- and glycine-rich motif polypeptides. The major part of the genome is also constituted by genes encoding PE (proline-glutamate, $n = 99$) and PPE (proline-proline-glutamate, $n = 68$) protein family, variability of which provides the differences between antigens and the ability to inhibit immune response [25].

Large amounts of DNA sequences repeats are one of the *M. tuberculosis* genome features: for example, insertion sequences (IS), contributing to mycobacterial DNA polymorphism, and variable number of tandem repeats (VNTR). Along with the IS, there are direct repeat regions (DR) separated by variable sequences (spacers), major polymorphic tandem repeats (MPTR), and polymorphic GC-repetitive sequence (PGRS). All these features of the *M. tuberculosis* genome provide the basis for the pathogen diagnosis and typing techniques: IS6110-based restriction fragment length polymorphism (RFLP typing) [26], spoligotyping [27], VNTR typing [28]. In addition, prophage-like sequences, *phiRv1* and *phiRv2*, have been found in the genome of H37Rv. These are considered to be associated with the pathogenicity factors due to the fact that no prophages have been found in the genomes of avirulent H37Ra and *M. bovis* BCG strains.

The development of more specific typing methods, for example, including drug resistance and virulence in certain different lineages of *M. tuberculosis*, requires confirming the functions of certain genes, their contribution to cell metabolism, and especially realization of the unique features of the pathogen. Clearly, all of that could be defined only with the use of additional methods, such as transcriptome and proteome analysis.

Proteomics

Proteomics is an important tool for identification of both known and new protein targets that are a part of the virulence system and cell protective mechanisms, and are a key element of the host-pathogen interaction. The increased or decreased synthesis of various proteins related to the host immunity and pathogen virulence indicates the role of these proteins in the protective mechanisms or pathogenesis. Such upregulation or downregulation is useful for identification of proteins that could be considered the important targets for medications or the development of diagnostic tools representing various stages of pathogenesis and the level of infection. Starting with identification of any such protein in order to find out whether the protein is a drug target or a diagnostic marker, as well as to monitor protein kinetics in various organs in response to infection, it is necessary to use the approach that includes the following consistent steps: identification of new targets, *in vitro* verification of their role, comparative analysis of the target unicity and specificity, *in vivo* verification of the effects of the target in *in vivo* models.

The methods of proteome analysis were most comprehensively described earlier [20], including considering the key results of the proteome analysis of the TB causative agent. To date, these are supplemented by information about the proteomic and transcriptomic data integration. For example, system OMICs analysis of the Beijing B0/W148 cluster was performed [23] that made it possible to reveal additional unique features of the cluster members.

The relevance of using the system approach could be also attributed to the fact that the transcript (even the abundant one) availability does not always result in protein synthesis. Thus, if there is no proteome analysis, transcriptomics will not be fully suggestive. For its part, proteome analysis makes it possible to register the end product, and combining these data with transcriptomic data provides additional insights into cell physiology. Currently, the acquired data inconsistencies are also a major shortcoming. It is clear that when developing diagnostic panels, each finding should be dealt with in the context of other findings, and the system should be considered as a whole.

Transcriptomics

As mentioned above, bacteria must extremely quickly adapt to changing environmental conditions, that is why gene expression alterations occurring in response to the host protective mechanisms or the effects of medications are essential for the pathogen survival and functioning. Transcriptome (full set of transcripts produced by bacteria cell) studies performed using various approaches complement primarily the genome sequencing data. The methods used for transcriptome analysis of mycobacteria have been discussed in detail earlier [29]. Clearly, the main discoveries of transcriptomics are related to studying the resistance of the causative agent of TB. Advances in technology have facilitated the emergence of DNA-microarrays, which have provided a powerful tool to explore differential gene expression, including under *in vivo* conditions [30]. However, this method has not yet been extended to the diagnosis. The use of transcripts as the diagnostic targets has a number of critical disadvantages, foremost among which is their lifetime. Anyway, transcriptomics is extremely important for understanding of cell metabolism and the use of other OMICs data for the diagnosis, since it was system analysis that made it possible to reveal the complex changes in the abundance of proteins responsible for fatty acid biosynthesis in the *M. tuberculosis* virulent strains (at the transcriptome and proteome levels) [23, 31, 32]. For its part, the latter showed the relevance of understanding of how various molecular fragments of the genome (genes and transcripts) became integrated into networks representing metabolism, regulation, signaling, and protein-protein interactions.

Metabolomics

Metabolic pathways provide the basis for cell functioning. Studying metabolic pathways and metabolic reconstruction is an important step in modelling of cellular activities and, most important, in understanding the underlying mechanisms at the system level.

Mycobacteria owe much of their unique properties to mycolic acids being the components of the bacterial cell wall. Several studies demonstrate the importance of mycolic acids for bacterial growth, survival, and pathogenesis [33]. In this way biosynthesis of mycolic acids has become the subject of numerous biochemical and genetic studies [34]. Thus, the

detailed model of the mycolic acid synthesis in *M. tuberculosis* was constructed that included 197 metabolites involved in 219 reactions catalyzed by 28 proteins. Comparative analysis of the *M. tuberculosis* H37Rv strain and human metabolic pathways showed that AccD3, Fas, FabH, Pks13, DesA1/2, DesA3 were potential targets for development of anti-TB drugs [35].

Continuous accumulation of protein data, decoding of their enzymatic properties allowed modeling a number of metabolic networks of mycobacteria. Thus, genome-scale metabolic network (GSMN) includes 849 unique chemical reactions involving 739 metabolites and 726 genes [36]. It should be noted that there is currently a lot of confusion due to incomplete characterization of some proteins and incomplete information about the biochemical reactions these proteins are involved in. Meanwhile, the use of available metabolic networks has made it possible to define 318 proteins essential for mycobacterial growth [35]. Thus, it can be assumed that these 318 proteins play an important role in maintaining metabolism of mycobacteria.

Protein-protein interactions provide the basis for intracellular signaling pathways, as well as for various transcriptional regulatory networks. To date, the extended version of the *M. tuberculosis* H37Rv strain protein interaction network is represented by the STRING database [37]. STRING contains literature data that describe both empirical interactions and interactions explored by genome analysis with the use of bioinformatic algorithms. Thus, network covers various types of direct mediated interactions and linkages, such as: a) physical complex formation of two proteins essential for the functional unit formation; b) co-regulation of genes belonging to one operon or adjacent genes; c) interaction of proteins involved in certain metabolic pathway and therefore affecting each other; d) associations between proteins based on the predominant coexistence, co-expression or domain fusion. The network represents the first integrated view of linkages between various proteins similar to acquiring the road map of the city. Currently, the database is filled during integration of system analysis, including the main emphasis on experimental specification of predicted relationships. Based on this information, a functional distance matrix and a subsequent protein proximity index were obtained, which help to understand how the influence of a particular protein can distribute to the metabolic network as a whole. This index was used to predict the strategy of maximum metabolic disruption by inhibiting the least amount of proteins. The study found that simultaneous inhibition of the combination of four proteins could affect a total of 471 proteins involved in 33 pathways, which resulted in 75% metabolic disruption [38].

OMICs in diagnostics

The studies on finding TB biomarkers are conducted constantly. A lot of promising candidates for defining the risk of infection, disease risk, probability of cure, and protection against infection have been found [39]. The majority of such biomarkers are associated with the host immunity and include proteins, metabolites, cell markers, and transcripts [40]. Despite numerous reports of the correlations with various TB stages, especially in children [41], there are currently no commercially available predictive biomarkers. Clearly, this indicates insufficient clinical significance of the described markers and the need for further search.

Certainly the most success is seen in molecular testing using genomic data both for the presence of *M. tuberculosis* and drug resistance. Thus, Xpert XDR (Cepheid; CA, USA) allows one to detect the genetic material of *M. tuberculosis*

together with mutations associated with resistance to rifampicin, isoniazid, injectable drugs, and fluoroquinolones. For its part, the Russian equivalent, the hydrogel microarrays developed by the Engelhardt Institute of Molecular Biology of Russian Academy of Sciences [42], particularly TB-TEST, make it possible to perform typing and simultaneously determine resistance based on a total of 114 genetic determinants: of those 28 mutations in *rpoB* associated with rifampicin resistance; 11 mutations in *katG*, five in *inhA* and five in *ahpC* associated with isoniazid resistance; 18 mutations in *embB* associated with ethambutol resistance; 15 mutations in *gyrA*; 23 mutations in *gyrB* associated with resistance to fluoroquinolones; 4 mutations in *rrs*; 5 mutations in *eis* associated with resistance to aminoglycosides and capreomycin [43].

The whole-genome sequencing is becoming an increasingly attractive option for identification of drug resistance in *M. tuberculosis*, the method can be also used to improve understanding of the TB transmission [44]. This technique is based on detecting mutations associated with drug resistance in the *M. tuberculosis* genome, the data show the correlation between the genetic mutations and the results of the culture-based drug susceptibility tests performed at least for four first-line drugs (isoniazid, rifampicin, ethambutol, and pyrazinamide) [45, 46]. At the same time, some differences regarding phenotypic and genetic drug resistance profiles suggest that the use of genomic data does not always allow to define the drug susceptibility of the bacterium. Taking into account the fact that the structure of the *M. tuberculosis* population is heterogenous and has its own characteristics, one could speak of developing the local diagnostic test systems. It's been reported that Beijing family strains prevail in our country (50–80% of all cases) [47]. Strong association with the drug resistance and higher virulence compared to other genotypes have been proven for this genotype family [48]. The latter was shown by both studying *in vivo* models [49] and epidemiological research. The increased abundance of virulence factors in Beijing family strains has been shown at the molecular level, including through the system OMICs analysis [23, 32, 50].

Taking into account all of the above, it can be assumed that early diagnosis of the Beijing family strains is the most promising. To date, the use of the label-free microfluidic biosensor device based on the photonic crystal surface mode (PC SM) is the most common approach. The PC SM biosensor makes it possible to assess a broad range of interactions: from the formation of various protein–protein complexes to interaction between oligonucleotides with different sequences. The fact that chemical reactions occur in an isolated zone of minimum volume, thus precluding contamination, reducing analysis time, and making the analysis procedure more user-friendly, is the main advantage of the technique. Such interactions, which are registered in the real-time mode, require no pre-labeling of target biomolecules [51], thereby simplifying and speeding up the analysis.

Taking into account the potential of the PC SM biosensor with a two-dimensional spatial resolution [52], we have proposed a fundamentally new method for typing of the TB causative agent [53]: the photonic crystal surface was modified with dextran, and the oligonucleotide system was used to detect the

M. tuberculosis single-stranded DNA. It is worth mentioning that the surface modification method was optimized for detection of the *M. tuberculosis* DNA [54]. In addition, a simplified variant has been proposed for differential detection of the Beijing and LAM families, which are most common in our country. Such an approach would make it possible not only to simplify the diagnosis, but also to reduce the costs of the diagnostic test system development and production. Furthermore, the platform itself could be used for the *M. tuberculosis* proteome typing.

Currently, two main immunological approaches to the diagnosis of latent TB infection are used that are included in the WHO guidelines [55]: tuberculin skin test (TST) and interferon- γ release assay (IGRA). Despite the fact that IGRA is more specific than TST, none of these tests allow one to distinguish between latent TB infection and active TB. Both tests have reduced sensitivity in various immunocompromised subpopulations. Cohort studies have shown that both TST and IGRA have low predictive value for the latent TB infection progression to active TB [56], that is why it is important to test only people at high risk of the disease progression and use all the available clinical data to complement test results. There are a number of convenient estimation tools, such as Online TST/IGRA Interpreter. C-Tb skin test (Statens Serum Institut; Copenhagen, Denmark) based on the specific TB antigens ESAT-6 and CFP10 showed the safety profile and accuracy similar to those of IGRA during the third phase of the clinical trial [57, 58].

Several groups of researchers reported a possibility of using HspX protein as a marker of the disease, including the latent form [59, 60]. However, subsequent systemic analysis of various *M. tuberculosis* strains showed the insolvency of such approach [32]. Thus, the search for the infectious process biomarkers is still the most pressing task for researchers all over the world.

CONCLUSION

Tuberculosis remains one of the main health problems in our country. Despite the existence of various test systems, identification and particularly typing of the pathogen are still an urgent task both in Russia and abroad. Available technologies are based mostly on the use of the well-studied genomic data. In the recent decades, plenty of other OMICs technologies have been introduced worldwide, such as metagenomics, transcriptomics, proteomics, metabolomics, and culturomics, which play a key role in understanding the main mechanisms of the bacterial virulence, resistance, and pathogenicity. We have reviewed various OMICs technologies and the possibility of their use as diagnostic tools. According to the state-of-the-art knowledge, OMICs technologies should be used in concert rather than separately in order to obtain meaningful data on the pathogenesis of *Mycobacterium tuberculosis*. Furthermore, for the nuanced and holistic understanding, new technologies are needed, such as bioinformatics, nanotechnology, single-cell genomics, together with the new technologies of gene expression, such as nanostring, and imaging tools. The sets of the existing and new OMICs data considered together should create an integrated presentation of the *M. tuberculosis* gene regulation and promote the development of both diagnostic panels and new efficient treatment methods.

References

- Rachow A, Ivanova O, Wallis R, Charalambous S, Jani I, Bhatt N, et al. TB sequel: Incidence, pathogenesis and risk factors of long-term medical and social sequelae of pulmonary TB — A study protocol 11 Medical and Health Sciences 1117 Public Health and Health Services. *BMC Pulm Med.* 2019; 19: 1–9. DOI: 10.1186/S12890-018-0777-3/TABLES/2.
- Podany AT, Swindells S. Current strategies to treat tuberculosis. *F1000Research.* 2016; 5. DOI: 10.12688/F1000RESEARCH.7403.1/DOI.
- Tiberi S, Scardigli A, Centis R, D'Ambrosio L, Muñoz-Torrico M, Salazar-Lezama MÁ, et al. Classifying new anti-tuberculosis drugs: rationale and future perspectives. *Int J Infect Dis.* 2017; 56: 181–4. DOI: 10.1016/J.IJID.2016.10.026.
- Migliori GB, Tiberi S, Zumla A, Petersen E, Chakaya JM, Wejse C, et al. MDR/XDR-TB management of patients and contacts: Challenges facing the new decade. The 2020 clinical update by the Global Tuberculosis Network. *Int J Infect Dis.* 2020; 92S: S15–S25. DOI: 10.1016/J.IJID.2020.01.042.
- Patterson B, Wood R. Is cough really necessary for TB transmission? *Tuberculosis.* 2019; 117: 31–35. DOI: 10.1016/J.TUBE.2019.05.003.
- Chai Q, Wang L, Liu CH, Ge B. New insights into the evasion of host innate immunity by *Mycobacterium tuberculosis*. *Cell Mol Immunol.* 2020; 17: 901–13. DOI: 10.1038/s41423-020-0502-z.
- Bradfute SB, Castillo EF, Arko-Mensah J, Chauhan S, Jiang S, Mandell M, et al. Autophagy as an immune effector against tuberculosis. *Curr Opin Microbiol.* 2013; 16: 355. DOI: 10.1016/J.MIB.2013.05.003.
- Weiss G, Schaible UE. Macrophage defense mechanisms against intracellular bacteria. *Immunol Rev.* 2015; 264: 182–203. DOI: 10.1111/IMR.12266. PMID: 25703560.
- Ehlers S, Schaible UE. The granuloma in tuberculosis: dynamics of a host-pathogen collusion. *Front Immunol.* 2013; 3. DOI: 10.3389/FIMMU.2012.00411. PMID: 23308075.
- Qiang L, Wang J, Zhang Y, Ge P, Chai Q, Li B, et al. *Mycobacterium tuberculosis* Mce2E suppresses the macrophage innate immune response and promotes epithelial cell proliferation. *Cell Mol Immunol.* 2019; 16: 380–91. DOI: 10.1038/S41423-018-0016-0. PMID: 29572547.
- Su H, Zhu S, Zhu L, Kong C, Huang Q, Zhang Z, et al. *Mycobacterium tuberculosis* latent antigen Rv2029c from the multistage DNA vaccine A39 drives TH1 responses via TLR-mediated macrophage activation. *Front Microbiol.* 2017; 8: 2266. DOI: 10.3389/FMICB.2017.02266/BIBTEX.
- Peng H, Wang X, Barnes PF, Tang H, Townsend JC, Samten B. The *Mycobacterium tuberculosis* Early Secreted Antigenic Target of 6 kDa Inhibits T Cell Interferon- γ Production through the p38 Mitogen-activated Protein Kinase Pathway. *J Biol Chem.* 2011; 286: 24508–18. DOI: 10.1074/JBC.M111.234062. PMID: 21586573.
- Wang X, Barnes PF, Huang F, Alvarez IB, Neuenschwander PF, Sherman DR, et al. Early secreted antigenic target of 6-kDa protein of *Mycobacterium tuberculosis* primes dendritic cells to stimulate Th17 and inhibit Th1 immune responses. *J Immunol.* 2012; 189: 3092–103. DOI: 10.4049/JIMMUNOL.1200573. PMID: 22904313.
- Jung BG, Wang X, Yi N, Ma J, Turner J, Samten B. Early Secreted Antigenic Target of 6-kDa of *Mycobacterium tuberculosis* Stimulates IL6 Production by Macrophages through Activation of STAT3. *Sci Rep.* 2017; 7. DOI: 10.1038/SREP40984. PMID: 28106119.
- Refai A, Gritli S, Barbouche MR, Essafi M. *Mycobacterium tuberculosis* Virulent Factor ESAT-6 Drives Macrophage Differentiation Toward the Pro-inflammatory M1 Phenotype and Subsequently Switches It to the Anti-inflammatory M2 Phenotype. *Front Cell Infect Microbiol.* 2018; 8. DOI: 10.3389/FMICB.2018.00327. PMID: 30283745.
- Lin J, Jiang Y, Liu D, Dai X, Wang M, Dai Y. Early secreted antigenic target of 6-kDa of *Mycobacterium tuberculosis* induces transition of macrophages into epithelioid macrophages by downregulating iNOS / NO-mediated H3K27 trimethylation in macrophages. *Mol Immunol.* 2020; 117: 189–200. DOI: 10.1016/J.MOLIMM.2019.11.013. PMID: 31816492.
- Yaseen I, Kaur P, Nandicoori VK, Khosla S. *Mycobacteria* modulate host epigenetic machinery by Rv1988 methylation of a non-tail arginine of histone H3. *Nat Commun.* 2015 6: 1. 2015; 6: 1–13. DOI: 10.1038/ncomms9922. PMID: 26568365.
- Schubert OT, Mouritsen J, Ludwig C, Röst HL, Rosenberger G, Arthur PK, et al. The Mtb proteome library: A resource of assays to quantify the complete proteome of *mycobacterium tuberculosis*. *Cell Host Microbe.* 2013; 13: 602–12. DOI: 10.1016/j.chom.2013.04.008.
- Kunnath-Velayudhan S, Porcelli SA. Recent Advances in Defining the Immunoproteome of *Mycobacterium tuberculosis*. *Front Immunol.* 2013; 0: 335. DOI: 10.3389/FIMMU.2013.00335.
- Беспярых Ю. А., Шитиков Е. А., Ильина Е. Н. Протеомные подходы в изучении микобактерий. *Acta Naturae.* 2017; 9, 1 (32): 16–26. DOI: 10.32607/20758251-2017-9-1-15-25. PMID: 28461970.
- Uddin R, Siddiqui QN, Sufian M, Azam SS, Wadood A. Proteome-wide subtractive approach to prioritize a hypothetical protein of XDR-*Mycobacterium tuberculosis* as potential drug target. *Genes Genomics.* 2019; 41: 1281–92. DOI: 10.1007/S13258-019-00857-Z. PMID: 31388979.
- Cole ST, Brosch R, Parkhill J, Garnier T, Churcher C, Harris D, et al. Deciphering the biology of *mycobacterium tuberculosis* from the complete genome sequence. *Nature.* 1998; 393: 537–44.
- Bespyatykh J, Shitikov E, Guliaev A, Smolyakov A, Klimina K, Veselovsky V, et al. System OMICS analysis of *Mycobacterium tuberculosis* Beijing B0/W148 cluster. *Sci Rep.* 2019; 9. DOI: 10.1038/s41598-019-55896-z. PMID: 31848428.
- Upadhyay S, Mittal E, Philips JA. Tuberculosis and the art of macrophage manipulation. *Pathog Dis.* 2018; 76: 37. DOI: 10.1093/FEMSPD/FTY037. PMID: 29762680.
- Tientcheu LD, Koch A, Ndengane M, Andoseh G, Kampmann B, Wilkinson RJ. Immunological consequences of strain variation within the *Mycobacterium tuberculosis* complex. *Eur J Immunol.* 2017; 47: 432. DOI: 10.1002/EJI.201646562. PMID: 28150302.
- Van Embden JD, Cave MD, Crawford JT, Dale JW, Eisenach KD, Gicquel B, et al. Strain identification of *Mycobacterium tuberculosis* by DNA fingerprinting: recommendations for a standardized methodology. *J Clin Microbiol.* 1993; 31: 406–9. PMID: 8381814.
- Bespyatykh JA, Zimenkov DV, Shitikov EA, Kulagina EV, Lapa SA, Gryadunov DA, et al. Spoligotyping of *Mycobacterium tuberculosis* complex isolates using hydrogel oligonucleotide microarrays. *Infect Genet Evol.* 2014; 26. DOI: 10.1016/j.meegid.2014.04.024.
- Frothingham R, Meeker-O'Connell WA. Genetic diversity in the *Mycobacterium tuberculosis* complex based on variable numbers of tandem DNA repeats. *Microbiology.* 1998; 144 (Pt 5): 1189–96. DOI: 10.1099/00221287-144-5-1189. PMID: 9611793.
- Skvorcova TA, Azhikina TL. Analiz transkriptomov patogennyx bakterij v inficirovannom organizme: problema i sposoby ix resheniya (obzornaya stat'ya). *Bioorganicheskaya ximiya.* 2010; 36: 596–606. Russian.
- Coppola M, Lai RPJ, Wilkinson RJ, Ottenhoff THM. The In Vivo Transcriptomic Blueprint of *Mycobacterium tuberculosis* in the Lung. *Front Immunol.* 2021; 12: 5212. DOI: 10.3389/FIMMU.2021.763364/BIBTEX. PMID: 35003075.
- Bespyatykh J, Shitikov E, Butenko I, Altukhov I, Alexeev D, Mokrousov I, et al. Proteome analysis of the *Mycobacterium tuberculosis* Beijing B0/W148 cluster. *Sci Rep.* 2016; 6. DOI: 10.1038/srep28985.
- Bespyatykh J, Shitikov E, Bespyatykh D, Guliaev A, Klimina K, Veselovsky V, et al. Metabolic Changes of *Mycobacterium tuberculosis* during the Anti-Tuberculosis Therapy. *Pathog (Basel, Switzerland).* 2020; 9. DOI: 10.3390/PATHOGENS9020131. PMID: 32085490.
- Nataraj V, Varela C, Javid A, Singh A, Besra GS, Bhatt A. Mycolic acids: deciphering and targeting the Achilles' heel of the tubercle bacillus. *Mol Microbiol.* 2015; 98: 7. DOI: 10.1111/MMI.13101. PMID: 26135034.
- Takayama K, Wang C, Besra GS. Pathway to Synthesis and

- Processing of Mycolic Acids in *Mycobacterium tuberculosis*. *Clin Microbiol Rev*. 2005; 18: 81. DOI: 10.1128/CMR.18.1.81-101.2005. PMID: 15653820.
35. Chandra N, Kumar D, Rao K. Systems biology of tuberculosis. *Tuberculosis (Edinb)*. 2011; 91: 487–96. DOI: 10.1016/J.TUBE.2011.02.008. PMID: 21459043.
 36. Beste DJV, Hooper T, Stewart G, Bonde B, Avignone-Rossa C, Bushell ME, et al. GSMN-TB: A web-based genome-scale network model of *Mycobacterium tuberculosis* metabolism. *Genome Biol*. 2007; 8: 1–18. DOI: 10.1186/GB-2007-8-5-R89/FIGURES/5. PMID: 17521419.
 37. Von Mering C, Huynen M, Jaeggi D, Schmidt S, Bork P, Snel B. STRING: a database of predicted functional associations between proteins. *Nucleic Acids Res*. 2003; 31: 258–61. DOI: 10.1093/NAR/GKG034. PMID: 12519996.
 38. Raman K, Vashisht R, Chandra N. Strategies for efficient disruption of metabolism in *Mycobacterium tuberculosis* from network analysis. *Mol Biosyst*. 2009; 5: 1740–51. DOI: 10.1039/B905817F. PMID: 19593474.
 39. Goletti D, Lee MR, Wang JY, Walter N, Ottenhoff THM. Update on tuberculosis biomarkers: From correlates of risk, to correlates of active disease and of cure from disease. *Respirology*. 2018; 23: 455–66. DOI: 10.1111/RESP.13272. PMID: 29457312.
 40. La Manna MP, Orlando V, Li Donni P, Sireci G, Di Carlo P, Cascio A, et al. Identification of plasma biomarkers for discrimination between tuberculosis infection/disease and pulmonary non tuberculosis disease. *PLoS One*. 2018; 13: e0204029. DOI: 10.1371/JOURNAL.PONE.0192664. PMID: 29543810.
 41. Togun TO, MacLean E, Kampmann B, Pai M. Biomarkers for diagnosis of childhood tuberculosis: A systematic review. *PLoS One*. 2018; 13: e0204029. DOI: 10.1371/JOURNAL.PONE.0204029. PMID: 30212540.
 42. Zimenkov DV, Antonova OV, Kuzmin AV, Isaeva YD, Krylova LY, Popov SA, et al. Detection of second-line drug resistance in *Mycobacterium tuberculosis* using oligonucleotide microarrays. *BMC Infect Dis*. 2013; 13: 1–8. DOI: 10.1186/1471-2334-13-240/TABLES/4. PMID: 23705640.
 43. Bespyatykh YuA, Shitikov EA, Zimenkov DV, Kulagina EV, Gryadunov D. A, Nosova EYu, i dr. Opredelenie lekarstvennoj ustojchivosti i genotipirovanie klinicheskix shtammov *Mycobacterium tuberculosis* pri pomoshhi ehksperimental'nogo nabora «TB-TEST». *Pul'monologiya*. 2013; 4: 77–81. DOI: 10.18093/0869-0189-2013-0-4-77-81. Russian.
 44. Satta G, Lipman M, Smith GP, Arnold C, Kon OM, McHugh TD. *Mycobacterium tuberculosis* and whole-genome sequencing: how close are we to unleashing its full potential? *Clin Microbiol Infect*. 2018; 24: 604–9. DOI: 10.1016/J.CMI.2017.10.030. PMID: 29108952.
 45. Allix-Bequec C, Arandjelovic I, Lijun Bi, Beckert P, Bonnet M, Bradley P, et al. Prediction of Susceptibility to First-Line Tuberculosis Drugs by DNA Sequencing. *N Engl J Med*. 2018; 379: 1403–15. DOI: 10.1056/NEJMJA1800474. PMID: 30280646.
 46. Cox H, Mizrahi V. The Coming of Age of Drug-Susceptibility Testing for Tuberculosis. *N Engl J Med*. 2018; 379: 1474–5. DOI: 10.1056/NEJME1811861. PMID: 30256713.
 47. Shitikov E, Kolchenko S, Mokrousov I, Bespyatykh J, Ischenko D, Ilina E, et al. Evolutionary pathway analysis and unified classification of East Asian lineage of *Mycobacterium tuberculosis*. *Sci Rep*. 2017; 7: 9227. DOI: 10.1038/s41598-017-10018-5.
 48. Ribeiro SCM, Gomes LL, Amaral EP, Andrade MRM, Almeida FM, Rezende AL, et al. *Mycobacterium tuberculosis* strains of the modern sublineage of the Beijing family are more likely to display increased virulence than strains of the ancient sublineage. *J Clin Microbiol*. 2014; 52: 2615–24. DOI: 10.1128/JCM.00498-14. PMID: 24829250.
 49. Bespyatykh YuA, Vinogradova TI, Manicheva OA, Zabolotnyx NV, Dogonadze MZ, Vitovskaya ML, i dr. Virulentnost' *Mycobacterium tuberculosis* genotipa Beijing v usloviyax in vivo. *Infekciya i immunitet*. 2019; 9 (1): 173–82. DOI: 10.15789/2220-7619-2019-1-173-182. Russian.
 50. Bespyatykh J, Smolyakov A, Guliaev A, Shitikov E, Arapidi G, Butenko I, et al. Proteogenomic analysis of *Mycobacterium tuberculosis* Beijing B0/W148 cluster strains. *J Proteomics*. 2019; 192: 18–26. DOI: 10.1016/j.jprot.2018.07.002.
 51. Konopsky VN, Karakouz T, Alieva EV, Vicario C, Sekatskii SK, Dietler G. Photonic Crystal Biosensor Based on Optical Surface Waves. *Sensors*. 2013; 13: 2566–78. DOI: 10.3390/S130202566. PMID: 23429517.
 52. Konopsky V, Mitko T, Aldarov K, Alieva E, Basmanov D, Moskalets A, et al. Photonic crystal surface mode imaging for multiplexed and high-throughput label-free biosensing. *Biosens Bioelectron*. 2020; 168. DOI: 10.1016/J.BIOS.2020.112575. PMID: 32892115.
 53. Mitko TV, Shakurov RI, Shirshikov FV, Sizova SV, Alieva EV, Konopskij VN, i dr. Sozdanie mikroflyuidnogo biosensora dlya diagnostiki i tipirovaniya *Mycobacterium tuberculosis*. *Klinicheskaya praktika*. 2021; 12 (2): 14–20. DOI: <https://doi.org/10.17816/clinpract71815>. Russian.
 54. Sizova S, Shakurov R, Mitko T, Shirshikov F, Solovyeva D, Konopsky V, et al. The Elaboration of Effective Coatings for Photonic Crystal Chips in Optical Biosensors. *Polymers (Basel)*. 2021; 14. DOI: 10.3390/POLYM14010152. PMID: 35012173.
 55. WHO. Latent tuberculosis infection: updated and consolidated guidelines for programmatic management [cited 2022 Apr 11]. Available from: <https://apps.who.int/iris/handle/10665/260233>.
 56. Pai M, Denkinger CM, Kik SV, Rangaka MX, Zwerling A, Oxlade O, et al. Gamma interferon release assays for detection of *Mycobacterium tuberculosis* infection. *Clin Microbiol Rev*. 2014; 27: 3–20. DOI: 10.1128/CMR.00034-13. PMID: 24396134.
 57. Aggerbeck H, Ruhwald M, Hoff ST, Borregaard B, Hellstrom E, Malahleha M, et al. C-Tb skin test to diagnose *Mycobacterium tuberculosis* infection in children and HIV-infected adults: A phase 3 trial. *PLoS One*. 2018; 13: e0204554. DOI: 10.1371/JOURNAL.PONE.0204554. PMID: 30248152.
 58. Ruhwald M, Aggerbeck H, Gallardo RV, Hoff ST, Villate JI, Borregaard B, et al. Safety and efficacy of the C-Tb skin test to diagnose *Mycobacterium tuberculosis* infection, compared with an interferon — release assay and the tuberculin skin test: a phase 3, double-blind, randomised, controlled trial. *Lancet Respir Med*. 2017; 5: 259–68. DOI: 10.1016/S2213-2600(16)30436-2. PMID: 28159608.
 59. Castro-Garza J, García-Jacobo P, Rivera-Morales LG, Quinn FD, Barber J, Karls R, et al. Detection of anti-HspX antibodies and HspX protein in patient sera for the identification of recent latent infection by *Mycobacterium tuberculosis*. *PLoS One*. 2017; 12. DOI: 10.1371/JOURNAL.PONE.0181714. PMID: 28813434.
 60. Dhiman A, Haldar S, Mishra SK, Sharma N, Bansal A, Ahmad Y, et al. Generation and application of DNA aptamers against HspX for accurate diagnosis of tuberculous meningitis. *Tuberculosis (Edinb)*. 2018; 112: 27–36. DOI: 10.1016/J.TUBE.2018.07.004. PMID: 30205966.

Литература

1. Rachow A, Ivanova O, Wallis R, Charalambous S, Jani I, Bhatt N, et al. TB sequel: Incidence, pathogenesis and risk factors of long-term medical and social sequelae of pulmonary TB — A study protocol 11 Medical and Health Sciences 1117 Public Health and Health Services. *BMC Pulm Med*. 2019; 19: 1–9. DOI: 10.1186/S12890-018-0777-3/TABLES/2.
2. Podany AT, Swindells S. Current strategies to treat tuberculosis. *F1000Research*. 2016; 5. DOI: 10.12688/F1000RESEARCH.7403.1/DOI.
3. Tiberi S, Scardigli A, Centis R, D'Ambrosio L, Muñoz-Torrico M, Salazar-Lezama MÁ, et al. Classifying new anti-tuberculosis drugs: rationale and future perspectives. *Int J Infect Dis*. 2017; 56: 181–4. DOI: 10.1016/J.IJID.2016.10.026.
4. Migliori GB, Tiberi S, Zumla A, Petersen E, Chakaya JM, Wejse C, et al.

- MDR/XDR-TB management of patients and contacts: Challenges facing the new decade. The 2020 clinical update by the Global Tuberculosis Network. *Int J Infect Dis.* 2020; 92S: S15–S25. DOI: 10.1016/J.IJID.2020.01.042.
5. Patterson B, Wood R. Is cough really necessary for TB transmission? *Tuberculosis.* 2019; 117: 31–35. DOI: 10.1016/J.TUBE.2019.05.003.
 6. Chai Q, Wang L, Liu CH, Ge B. New insights into the evasion of host innate immunity by *Mycobacterium tuberculosis*. *Cell Mol Immunol.* 2020; 17: 901–13. DOI: 10.1038/s41423-020-0502-z.
 7. Bradfute SB, Castillo EF, Arko-Mensah J, Chauhan S, Jiang S, Mandell M, et al. Autophagy as an immune effector against tuberculosis. *Curr Opin Microbiol.* 2013; 16: 355. DOI: 10.1016/J.MIB.2013.05.003.
 8. Weiss G, Schaible UE. Macrophage defense mechanisms against intracellular bacteria. *Immunol Rev.* 2015; 264: 182–203. DOI: 10.1111/IMR.12266. PMID: 25703560.
 9. Ehlers S, Schaible UE. The granuloma in tuberculosis: dynamics of a host-pathogen collusion. *Front Immunol.* 2013; 3. DOI: 10.3389/FIMMU.2012.00411. PMID: 23308075.
 10. Qiang L, Wang J, Zhang Y, Ge P, Chai Q, Li B, et al. *Mycobacterium tuberculosis* Mce2E suppresses the macrophage innate immune response and promotes epithelial cell proliferation. *Cell Mol Immunol.* 2019; 16: 380–91. DOI: 10.1038/S41423-018-0016-0. PMID: 29572547.
 11. Su H, Zhu S, Zhu L, Kong C, Huang Q, Zhang Z, et al. *Mycobacterium tuberculosis* latent antigen Rv2029c from the multistage DNA vaccine A39 drives TH1 responses via TLR-mediated macrophage activation. *Front Microbiol.* 2017; 8: 2266. DOI: 10.3389/FMICB.2017.02266/BIBTEX.
 12. Peng H, Wang X, Barnes PF, Tang H, Townsend JC, Samten B. The *Mycobacterium tuberculosis* Early Secreted Antigenic Target of 6 kDa Inhibits T Cell Interferon- γ Production through the p38 Mitogen-activated Protein Kinase Pathway. *J Biol Chem.* 2011; 286: 24508–18. DOI: 10.1074/JBC.M111.234062. PMID: 21586573.
 13. Wang X, Barnes PF, Huang F, Alvarez IB, Neuenschwander PF, Sherman DR, et al. Early secreted antigenic target of 6-kDa protein of *Mycobacterium tuberculosis* primes dendritic cells to stimulate Th17 and inhibit Th1 immune responses. *J Immunol.* 2012; 189: 3092–103. DOI: 10.4049/JIMMUNOL.1200573. PMID: 22904313.
 14. Jung BG, Wang X, Yi N, Ma J, Turner J, Samten B. Early Secreted Antigenic Target of 6-kDa of *Mycobacterium tuberculosis* Stimulates IL6 Production by Macrophages through Activation of STAT3. *Sci Rep.* 2017; 7. DOI: 10.1038/SREP40984. PMID: 28106119.
 15. Refai A, Gritli S, Barbouche MR, Essafi M. *Mycobacterium tuberculosis* Virulent Factor ESAT-6 Drives Macrophage Differentiation Toward the Pro-inflammatory M1 Phenotype and Subsequently Switches It to the Anti-inflammatory M2 Phenotype. *Front Cell Infect Microbiol.* 2018; 8. DOI: 10.3389/FMICB.2018.00327. PMID: 30283745.
 16. Lin J, Jiang Y, Liu D, Dai X, Wang M, Dai Y. Early secreted antigenic target of 6-kDa of *Mycobacterium tuberculosis* induces transition of macrophages into epithelioid macrophages by downregulating iNOS / NO-mediated H3K27 trimethylation in macrophages. *Mol Immunol.* 2020; 117: 189–200. DOI: 10.1016/J.MOLIMM.2019.11.013. PMID: 31816492.
 17. Yaseen I, Kaur P, Nandicoori VK, Khosla S. *Mycobacteria* modulate host epigenetic machinery by Rv1988 methylation of a non-tail arginine of histone H3. *Nat Commun* 2015 6.1. 2015; 6: 1–13. DOI: 10.1038/ncomms9922. PMID: 26568365.
 18. Schubert OT, Mouritsen J, Ludwig C, Röst HL, Rosenberger G, Arthur PK, et al. The Mtb proteome library: A resource of assays to quantify the complete proteome of *mycobacterium tuberculosis*. *Cell Host Microbe.* 2013; 13: 602–12. DOI: 10.1016/j.chom.2013.04.008.
 19. Kunnath-Velayudhan S, Porcelli SA. Recent Advances in Defining the Immunoproteome of *Mycobacterium tuberculosis*. *Front Immunol.* 2013; 0: 335. DOI: 10.3389/FIMMU.2013.00335.
 20. Беспятых Ю. А., Шитиков Е. А., Ильина Е. Н. Протеомные подходы в изучении микобактерий. *Acta Naturae.* 2017; 9, 1 (32): 16–26. DOI: 10.32607/20758251-2017-9-1-15-25. PMID: 28461970.
 21. Uddin R, Siddiqui QN, Sufian M, Azam SS, Wadood A. Proteome-wide subtractive approach to prioritize a hypothetical protein of XDR-*Mycobacterium tuberculosis* as potential drug target. *Genes Genomics.* 2019; 41: 1281–92. DOI: 10.1007/S13258-019-00857-Z. PMID: 31388979.
 22. Cole ST, Brosch R, Parkhill J, Garnier T, Churcher C, Harris D, et al. Deciphering the biology of *mycobacterium tuberculosis* from the complete genome sequence. *Nature.* 1998; 537–44.
 23. Bespyatykh J, Shitikov E, Guliaev A, Smolyakov A, Klimina K, Veselovsky V, et al. System OMICs analysis of *Mycobacterium tuberculosis* Beijing B0/W148 cluster. *Sci Rep.* 2019; 9. DOI: 10.1038/s41598-019-55896-z. PMID: 31848428.
 24. Upadhyay S, Mittal E, Philips JA. Tuberculosis and the art of macrophage manipulation. *Pathog Dis.* 2018; 76: 37. DOI: 10.1093/FEMSPD/FTY037. PMID: 29762680.
 25. Tientcheu LD, Koch A, Ndengane M, Andoseh G, Kampmann B, Wilkinson RJ. Immunological consequences of strain variation within the *Mycobacterium tuberculosis* complex. *Eur J Immunol.* 2017; 47: 432. DOI: 10.1002/EJ.201646562. PMID: 28150302.
 26. Van Embden JD, Cave MD, Crawford JT, Dale JW, Eisenach KD, Gicquel B, et al. Strain identification of *Mycobacterium tuberculosis* by DNA fingerprinting: recommendations for a standardized methodology. *J Clin Microbiol.* 1993; 31: 406–9. PMID: 8381814.
 27. Bespyatykh JA, Zimenkov DV, Shitikov EA, Kulagina EV, Lapa SA, Gryadunov DA, et al. Spoligotyping of *Mycobacterium tuberculosis* complex isolates using hydrogel oligonucleotide microarrays. *Infect Genet Evol.* 2014; 26. DOI: 10.1016/j.meegid.2014.04.024.
 28. Frothingham R, Meeker-O'Connell WA. Genetic diversity in the *Mycobacterium tuberculosis* complex based on variable numbers of tandem DNA repeats. *Microbiology.* 1998; 144 (Pt 5): 1189–96. DOI: 10.1099/00221287-144-5-1189. PMID: 9611793.
 29. Скворцова Т. А., Ажикина Т. Л. Анализ транскриптомов патогенных бактерий в инфицированном организме: проблемы и способы их решения (обзорная статья). *Биоорганическая химия.* 2010; 36: 596–606.
 30. Coppola M, Lai RPJ, Wilkinson RJ, Ottenhoff THM. The In Vivo Transcriptomic Blueprint of *Mycobacterium tuberculosis* in the Lung. *Front Immunol.* 2021; 12: 5212. DOI: 10.3389/FIMMU.2021.763364/BIBTEX. PMID: 35003075.
 31. Bespyatykh J, Shitikov E, Butenko I, Altukhov I, Alexeev D, Mokrousov I, et al. Proteome analysis of the *Mycobacterium tuberculosis* Beijing B0/W148 cluster. *Sci Rep.* 2016; 6. DOI: 10.1038/srep28985.
 32. Bespyatykh J, Shitikov E, Bespyatykh D, Guliaev A, Klimina K, Veselovsky V, et al. Metabolic Changes of *Mycobacterium tuberculosis* during the Anti-Tuberculosis Therapy. *Pathog (Basel, Switzerland).* 2020; 9. DOI: 10.3390/PATHOGENS9020131. PMID: 32085490.
 33. Nataraj V, Varela C, Javid A, Singh A, Besra GS, Bhatt A. Mycolic acids: deciphering and targeting the Achilles' heel of the tubercle bacillus. *Mol Microbiol.* 2015; 98: 7. DOI: 10.1111/MMI.13101. PMID: 26135034.
 34. Takayama K, Wang C, Besra GS. Pathway to Synthesis and Processing of Mycolic Acids in *Mycobacterium tuberculosis*. *Clin Microbiol Rev.* 2005; 18: 81. DOI: 10.1128/CMR.18.1.81-101.2005. PMID: 15653820.
 35. Chandra N, Kumar D, Rao K. Systems biology of tuberculosis. *Tuberculosis (Edinb).* 2011; 91: 487–96. DOI: 10.1016/J.TUBE.2011.02.008. PMID: 21459043.
 36. Beste DJV, Hooper T, Stewart G, Bonde B, Avignone-Rossa C, Bushell ME, et al. GSMN-TB: A web-based genome-scale network model of *Mycobacterium tuberculosis* metabolism. *Genome Biol.* 2007; 8: 1–18. DOI: 10.1186/GB-2007-8-5-R89/FIGURES/5. PMID: 17521419.
 37. Von Mering C, Huynen M, Jaeggi D, Schmidt S, Bork P, Snel B. STRING: a database of predicted functional associations between proteins. *Nucleic Acids Res.* 2003; 31: 258–61. DOI: 10.1093/NAR/GKG034. PMID: 12519996.
 38. Raman K, Vashisht R, Chandra N. Strategies for efficient disruption of metabolism in *Mycobacterium tuberculosis* from network analysis. *Mol Biosyst.* 2009; 5: 1740–51. DOI: 10.1039/B905817F. PMID: 19593474.

39. Goletti D, Lee MR, Wang JY, Walter N, Ottenhoff THM. Update on tuberculosis biomarkers: From correlates of risk, to correlates of active disease and of cure from disease. *Respirology*. 2018; 23: 455–66. DOI: 10.1111/RESP.13272. PMID: 29457312.
40. La Manna MP, Orlando V, Li Donni P, Sireci G, Di Carlo P, Cascio A, et al. Identification of plasma biomarkers for discrimination between tuberculosis infection/disease and pulmonary non tuberculosis disease. *PLoS One*. 2018; 13. DOI: 10.1371/JOURNAL.PONE.0192664. PMID: 29543810.
41. Togun TO, MacLean E, Kampmann B, Pai M. Biomarkers for diagnosis of childhood tuberculosis: A systematic review. *PLoS One*. 2018; 13: e0204029. DOI: 10.1371/JOURNAL.PONE.0204029. PMID: 30212540.
42. Zimenkov DV, Antonova OV, Kuzmin AV, Isaeva YD, Krylova LY, Popov SA, et al. Detection of second-line drug resistance in *Mycobacterium tuberculosis* using oligonucleotide microarrays. *BMC Infect Dis*. 2013; 13: 1–8. DOI: 10.1186/1471-2334-13-240/TABLES/4. PMID: 23705640.
43. Беспятых Ю. А., Шитиков Е. А., Зименков Д. В., Кулагина Е. В., Грядун Д. А., Носова Е. Ю., и др. Определение лекарственной устойчивости и генотипирование клинических штаммов *Mycobacterium tuberculosis* при помощи экспериментального набора «ТБ-ТЕСТ». *Пульмонология*. 2013; 4: 77–81. DOI: 10.18093/0869-0189-2013-0-4-77-81.
44. Satta G, Lipman M, Smith GP, Arnold C, Kon OM, McHugh TD. *Mycobacterium tuberculosis* and whole-genome sequencing: how close are we to unleashing its full potential? *Clin Microbiol Infect*. 2018; 24: 604–9. DOI: 10.1016/J.CMI.2017.10.030. PMID: 29108952.
45. Allix-Beguec C, Arandjelovic I, Lijun Bi, Beckert P, Bonnet M, Bradley P, et al. Prediction of Susceptibility to First-Line Tuberculosis Drugs by DNA Sequencing. *N Engl J Med*. 2018; 379: 1403–15. DOI: 10.1056/NEJMOA1800474. PMID: 30280646.
46. Cox H, Mizrahi V. The Coming of Age of Drug-Susceptibility Testing for Tuberculosis. *N Engl J Med*. 2018; 379: 1474–5. DOI: 10.1056/NEJME1811861. PMID: 30256713.
47. Shitikov E, Kolchenko S, Mokrousov I, Bespyatykh J, Ischenko D, Ilna E, et al. Evolutionary pathway analysis and unified classification of East Asian lineage of *Mycobacterium tuberculosis*. *Sci Rep*. 2017; 7: 9227. DOI: 10.1038/s41598-017-10018-5.
48. Ribeiro SCM, Gomes LL, Amaral EP, Andrade MRM, Almeida FM, Rezende AL, et al. *Mycobacterium tuberculosis* strains of the modern sublineage of the Beijing family are more likely to display increased virulence than strains of the ancient sublineage. *J Clin Microbiol*. 2014; 52: 2615–24. DOI: 10.1128/JCM.00498-14. PMID: 24829250.
49. Беспятых Ю. А., Виноградова Т. И., Маничева О. А., Заболотных Н. В., Догондзе М. З., Витовская М. Л., и др. Вирулентность *Mycobacterium tuberculosis* генотипа Beijing в условиях *in vivo*. *Инфекция и иммунитет*. 2019; 9 (1): 173–82. DOI: 10.15789/2220-7619-2019-1-173-182.
50. Bespyatykh J, Smolyakov A, Guliaev A, Shitikov E, Arapidi G, Butenko I, et al. Proteogenomic analysis of *Mycobacterium tuberculosis* Beijing B0/W148 cluster strains. *J Proteomics*. 2019; 192: 18–26. DOI: 10.1016/j.jprot.2018.07.002.
51. Konopsky VN, Karakouz T, Alieva EV, Vicario C, Sekatskii SK, Dietler G. Photonic Crystal Biosensor Based on Optical Surface Waves. *Sensors*. 2013; 13: 2566–78. DOI: 10.3390/S130202566. PMID: 23429517.
52. Konopsky V, Mitko T, Aldarov K, Alieva E, Basmanov D, Moskalets A, et al. Photonic crystal surface mode imaging for multiplexed and high-throughput label-free biosensing. *Biosens Bioelectron*. 2020; 168. DOI: 10.1016/J.BIOS.2020.112575. PMID: 32892115.
53. Митько Т. В., Шакуров Р. И., Ширшиков Ф. В., Сизова С. В., Алиева Е. В., Конопский В. Н., и др. Создание микрофлюидного биосенсора для диагностики и типирования *Mycobacterium tuberculosis*. *Клиническая практика*. 2021; 12 (2): 14–20. DOI: <https://doi.org/10.17816/clinpract71815>.
54. Sizova S, Shakurov R, Mitko T, Shirshikov F, Solovyeva D, Konopsky V, et al. The Elaboration of Effective Coatings for Photonic Crystal Chips in Optical Biosensors. *Polymers (Basel)*. 2021; 14. DOI: 10.3390/POLYM14010152. PMID: 35012173.
55. WHO. Latent tuberculosis infection: updated and consolidated guidelines for programmatic management [cited 2022 Apr 11]. Available from: <https://apps.who.int/iris/handle/10665/260233>.
56. Pai M, Denkinger CM, Kik SV, Rangaka MX, Zwering A, Oxlade O, et al. Gamma interferon release assays for detection of *Mycobacterium tuberculosis* infection. *Clin Microbiol Rev*. 2014; 27: 3–20. DOI: 10.1128/CMR.00034-13. PMID: 24396134.
57. Aggerbeck H, Ruhwald M, Hoff ST, Borregaard B, Hellstrom E, Malahleha M, et al. C-Tb skin test to diagnose *Mycobacterium tuberculosis* infection in children and HIV-infected adults: A phase 3 trial. *PLoS One*. 2018; 13. DOI: 10.1371/JOURNAL.PONE.0204554. PMID: 30248152.
58. Ruhwald M, Aggerbeck H, Gallardo RV, Hoff ST, Villate JI, Borregaard B, et al. Safety and efficacy of the C-Tb skin test to diagnose *Mycobacterium tuberculosis* infection, compared with an interferon — release assay and the tuberculin skin test: a phase 3, double-blind, randomised, controlled trial. *Lancet Respir Med*. 2017; 5: 259–68. DOI: 10.1016/S2213-2600(16)30436-2. PMID: 28159608.
59. Castro-Garza J, García-Jacobo P, Rivera-Morales LG, Quinn FD, Barber J, Karls R, et al. Detection of anti-HspX antibodies and HspX protein in patient sera for the identification of recent latent infection by *Mycobacterium tuberculosis*. *PLoS One*. 2017; 12. DOI: 10.1371/JOURNAL.PONE.0181714. PMID: 28813434.
60. Dhiman A, Haldar S, Mishra SK, Sharma N, Bansal A, Ahmad Y, et al. Generation and application of DNA aptamers against HspX for accurate diagnosis of tuberculous meningitis. *Tuberculosis (Edinb)*. 2018; 112: 27–36. DOI: 10.1016/J.TUBE.2018.07.004. PMID: 30205966.

NEUROPHYSIOLOGICAL ASSESSMENT OF SPEECH FUNCTION IN INDIVIDUALS HAVING A HISTORY OF MILD COVID-19

Gulyaev SA [✉], Voronkova YuA, Abramova TA, Kovrazhkina EA

Federal Center for Brain and Neurotechnologies of Federal Medical and Biological Agency, Moscow, Russia

Establishing a link between the objective research data and the thought process is one of the major issues of modern neurophysiology. The study was aimed to find an opportunity to perform objective analysis of the causes of cognitive impairment in individuals having a history of mild novel coronavirus infection by solving the inverse EEG problem. A total of 38 COVID-19 survivors were assessed, who had returned to work. The control group included 33 healthy individuals. EEG was recorded using a 128-channel system with an average reference. The data obtained were subjected to the EEG microstate segmentation and converted using the algorithm for solving the inverse EEG problem implemented in the sLORETA software package. In individuals with no history of COVID-19 being in a state of relaxed wakefulness, the component of rhythmic activity within Brodmann area 47, responsible for perception and realization of music, was found in all classes of EEG microstates ($0.01 < p < 0.05$; χ^2 -test). Auditory-speech load was characterized by rhythmic activity within areas 22, 23, 37, 39, 40, 44, 45, and 47. In individuals having a history of novel coronavirus infection being in a state of relaxed wakefulness, rhythmic activity within areas 22, 37, 39, 40 was detected. Under auditory-speech load, there was rhythmic activity within areas 37, 39, and 41 ($p < 0.05$; χ^2 -test). Thus, alterations in realization of speech function in the form of the disordered sequence of switching on the main language centers were revealed in COVID-19 survivors.

Keywords: novel coronavirus infection, EEG, inverse problem solution

Author contribution: Gulyaev SA — data analysis, manuscript writing, editing; Voronkova YuA, Abramova TA — data acquisition; Kovrazhkina EA — editing.

Compliance with ethical standards: the study was approved by the Ethics Committee of the Federal Center for Brain and Neurotechnologies of FMBA (protocol № 148-1 dated June 15, 2021). All the subjects took part in the experiment on a voluntary basis with no extra benefit. The experiment was studied by employees of the Federal Center for Brain and Neurotechnologies of FMBA within the limits of scientific work conducted by the institution with no third party funding.

✉ **Correspondence should be addressed:** Sergey A. Gulyaev
Ostrovitianova, 1, str. 10, Moscow, 117997, Russia; sergruss@yandex.ru

Received: 24.03.2022 **Accepted:** 04.05.2022 **Published online:** 25.05.2022

DOI: 10.47183/mes.2022.016

НЕЙРОФИЗИОЛОГИЧЕСКОЕ ИССЛЕДОВАНИЕ РЕЧЕВОЙ ФУНКЦИИ У ЛИЦ, ПЕРЕНЕСШИХ ЛЕГКУЮ ФОРМУ COVID-19

С. А. Гуляев [✉], Ю. А. Воронкова, Т. А. Абрамова, Е. А. Ковражкина

Федеральный центр мозга и нейротехнологий Федерального медико-биологического агентства, Москва, Россия

Одной из наиболее важных проблем современной нейрофизиологии является установление связи между данными объективных исследований и мыслительным процессом. Целью исследования был объективный анализ причин развития когнитивных дисфункций у лиц, перенесших легкую форму новой коронавирусной инфекции, с помощью технологии решения обратной ЭЭГ-задачи. Проведено обследование 38 человек, перенесших COVID-19 и вернувшихся к выполнению профессиональных обязанностей. Контрольную группу составили 33 здоровых человека. ЭЭГ регистрировали с помощью 128-канальной системы с усредненным референтом. Полученные данные сегментировали с выделением отдельных ЭЭГ-микросостояний и преобразовывали с помощью алгоритма решения обратной задачи ЭЭГ, реализованном в пакете прикладных программ sLORETA. У лиц, не болевших COVID-19, в состоянии пассивного расслабленного бодрствования во всех классах ЭЭГ-микросостояний присутствует компонент ритмической активности 47-го поля Бродмана, ответственного за восприятие и реализацию музыки ($0,01 < p < 0,05$; χ^2 -test). Слухоречевая нагрузка характеризовалась появлением ритмической активности над полями 22, 23, 37, 39, 40, 44, 45 и 47. У переболевших новой коронавирусной инфекцией в состоянии пассивного расслабленного бодрствования ритмическая активность была зарегистрирована над полями 22, 37, 39, 40. При слухоречевой нагрузке ритмическая активность выделялась над полями 37, 39 и 41 ($p < 0,05$; χ^2 -test). Таким образом, у лиц, перенесших COVID-19, выявлены изменения реализации речевой функции в виде дезорганизации последовательности включения основных речевых центров.

Ключевые слова: новая коронавирусная инфекция, ЭЭГ, решение обратной задачи

Вклад авторов: С. А. Гуляев — анализ данных, написание текста, оформление; Ю. А. Воронкова, Т. А. Абрамова — получение данных; Е. А. Ковражкина — оформление.

Соблюдение этических стандартов: исследование одобрено этическим комитетом ФЦМН ФМБА России (протокол № 148-1 от 15 июня 2021 г.). Все лица приняли участие в эксперименте на добровольных началах, без дополнительного поощрения. Исследования эксперимента проводили сотрудники ФГБУ ФЦМН ФМБА России в рамках научной работы учреждения без привлечения сторонних средств.

✉ **Для корреспонденции:** Сергей Александрович Гуляев
ул. Островитянова, д. 1, стр. 10, г. Москва, 117997, Россия; sergruss@yandex.ru

Статья получена: 24.03.2022 **Статья принята к печати:** 04.05.2022 **Опубликована онлайн:** 25.05.2022

DOI: 10.47183/mes.2022.016

Establishing a link between the objective research data and the thought process is one of the major issues of modern neurophysiology. Currently, activity in the neural structures of the brain is studied by functional brain imaging methods, such as functional magnetic resonance imaging (fMRI) and positron emission tomography (PET), and neurophysiological techniques based on the electroencephalography/magnetoencephalography (EEG/MEG) studies in various

modalities (continuous or discrete EEG). All these methods have disadvantages, resulting in difficulties in data interpretation. Thus, functional brain imaging methods detect the major changes in the neuronal activity over a rather long period of time. Regardless of the almost direct temporal relationship with brain activity, continuous EEG/MEG is so complex and diverse that it is unable to precisely answer the question, which neural structures are responsible for its formation. In case of discrete

recording widely used to study the neural structures responses to external stimuli (evoked potential (EP) tests), this method provides information on the nervous tissue direct response to the selected stimulus, which makes it impossible to study brain function as a whole even in case of recording long-latency EPs, resulting in determining recognition of a particular stimulus [1].

Thus, to study cognitive processes, a method is required for selection of different variants of continuous activity, which can currently be implemented by using clustering algorithms [2] with subsequent conversion of the results through solving the inverse EEG problem [3–5].

These studies are of particular interest in individuals having disorders that result in mild cognitive impairment, which is difficult to diagnose by common clinical assessment methods. The post-COVID syndrome observed in people having a history of novel coronavirus infection (COVID-19), even the mild form, is of interest as an example of the specific case of such disorder.

According to the current logic, the impact of COVID-19 on the central nervous system (CNS) is beyond question: like other coronaviruses, it can invade the CNS via both hematogenous and neuronal pathways. However, the virus is quickly neutralized, that is why there is usually no clinically significant damage to brain matter or meninges [6, 7]. At the same time, the reports of COVID-19-associated neurological manifestations show that cerebral symptoms, such as headache and dizziness (13.1–16.8% of cases), together with anosmia and hypogeusia/ageusia (up to 83% of observations) are most common in patients with novel coronavirus infection [8]. Cerebrovascular events are registered in 2–17%, and seizure in 1% of cases (similar to their prevalence in the population). This suggests that these secondary disorders result from hypoxia and electrolyte imbalance, as well as from the effects of the products of immune response. The rodent and neuronal cell culture studies have demonstrated viral RNA invading cells and subsequent massive deaths of neurons [9]. However, clinical reports of the direct damage to brain matter in the form of encephalitis are rare [10–12]. Nevertheless, autopsy of those who died from COVID-19 [13–16] revealed viral RNA transcripts in the tissue of cranial nerves in 40% of cases, as well as viral proteins in endothelial cells of the olfactory bulb. The main neurological manifestations of COVID-19 are represented by cerebral symptoms and/or damage to specific cranial nerves; it is necessary to exclude other causes in case of any structural brain tissue changes.

The nature of neuropsychiatric disorders observed in about 25% of patients with COVID-19 remains poorly understood. According to some reports, anxiety disorders/phobias (8.5–28.8%) and depression (9.5–16.5%) are the most common. However, in patients with severe COVID-19, these could be attributed not to the effects of the virus itself, but to stress related to the fact of infection, isolation, stay in the intensive care unit, fear of death or further development of various complications [17].

Under these circumstances, diagnostic methods capable of objectifying clinical manifestations are of some interest. However, meta-analysis of EEG recordings obtained from 308 patients with COVID-19 revealed non-specific changes in the majority of cases; paroxysmal EEG activity was detected in 20.3% of cases, the confirmed seizures and status epilepticus were observed in 2.05% [18]. Other authors, who had explained specific changes in EEG by the condition severity, hypoxia-ischemia, and the resulting secondary neurological disorder, reached almost the same conclusion [19].

These findings are entirely to be expected: regardless of the direct routes of invading the nervous tissue, the effects of

COVID-19 are characterized by diffuse processes with no focal destruction of nerve cells, accompanied by bioelectrical brain activity alterations associated with various neuropsychiatric syndromes. That is why objectifying such “cerebral” alterations requires the use of slightly different methods.

The study was aimed to find an opportunity to perform objective analysis of the causes of cognitive impairment in individuals having a history of mild COVID-19 by EEG and solving the inverse neurophysiological problem.

METHODS

Main group

A total of 38 COVID-19 survivors were assessed, who had returned to work. Inclusion criteria: all subjects were right-handed; no history of severe traumatic brain injury and mental disorders; the age of the subjects was 38.6 ± 2 years. Exclusion criteria: smoking; taking pharmacologically active substances due to chronic disorder.

All the participants were working people who had a relevant special educational background. A total of 35 (92%) individuals were employed at the time of the study. The majority of volunteers, 37 individuals (97%), lived in families. None of the subjects were disabled. The majority of subjects, 35 individuals (92%), were right-handed.

Neuropsychological testing was performed using the Montreal Cognitive Assessment score (MoCA), which was chosen due to scope of its coverage of various cognitive functions and sensitivity compared to other scores for detection of mild to moderate cognitive impairment [20]. However, the testing results defined the average score of 26 (variation 3, minimum score 25, maximum score 28), which confirmed no cognitive impairment.

T1- and T2-weighted MRI scans in the suppression and diffusion modes revealed alterations in only two subjects (5% of all cases). In the first case, the findings were represented by chronic cerebral venous sinus thrombosis, and in the second case these were represented by small vessel disease. Both findings were not associated with the history of COVID-19.

Control group

A total of 33 healthy people were enrolled who had volunteered to take part in the experiment. Their age ranged between 19–60 years; the average age was 32.37 ± 9.44 years; the volunteers' educational background was equivalent to that of the subjects in the index group.

General characteristics of methods

The eyes-closed resting state EEG was recorded in the darkened room using the 128 channel HydroCel-128 system (Magstim; USA) with an average reference, combined with the EGI-GES-300 bioamplifier (Magstim; USA). The resulting signal was converted into a digital form by discrete sampling with a sampling rate of 500 Hz, thus allowing to eliminate signal distortion in the frequency range of 1–250 Hz. The signal bandwidth with the applied 50-Hz notch filter was 0.5–70 Hz, which made it possible to integrate the main ranges of interest. No recording was performed within a minute after connecting a volunteer to the device in order to eliminate movement-related artifacts resulting from the subject's maladaptation.

Impedance, the total resistance of the neural interface electrodes, was maintained within 10 kOhm. It was

Table 1. Comparative characteristics of the class 1–6 EEG microstate duration in controls

	Class 1		Class 2		Class 3		Class 4		Class 5		Class 6	
	m	SD										
Resting state	0,02	0,01	0,02	0,01	0,03	0,01	0,02	0,01	0,03	0,01	0,02	0,01
Task state	0,04	0,01	0,04	0,01	0,04	0,01	0,04	0,01	0,05	0,01	0,04	0,01
<i>p</i> (<i>t</i> -test)	< 0,001		< 0,001		< 0,001		< 0,001		< 0,001		< 0,001	

Note: m — mean; SD — standard deviation.

continuously monitored throughout the study in accordance with the manufacturer's instructions.

A pool of functional tests included recording the eyes-closed resting state EEG that was considered the resting-state bioelectrical activity, and recording EEG under auditory-speech load (listening to a short story in the subject's native language). This made it possible to obtain environmental changes defined by activation of only one cognitive function with the relatively well understood architecture of cortical processing in accordance with the modern two-stream hypothesis [21].

The results were further processed and analyzed. Other electrical devices that created spurious electromagnetic emissions were turned off to minimize signal artifacts; we also controlled impedance of the interface, maintained room temperature, minimized facial muscle artifacts. The data pool obtained was filtered with the 1–70 Hz wide band filter. Standardization of electrode positioning to obtain single EEG electrode space and separation of the signal into independent components allowing one to remove various artifacts of physical and biological origin, that had not been eliminated from the EEG signal at the first stage, were performed. Subsequently, microstate segmentation of the EEG signal was performed by k-means clustering or the adhesion-spraying method to define six microstate classes taking into account variability of the classes 5 and 6 [22–24]. The final phase of research included analysis of the EEG source localization for each of the distinguished EEG microstate classes in accordance with the method by R. Pascual-Marqui with the use of the algorithm for solving the inverse EEG problem implemented in the sLORETA software package [25, 26].

The findings provided information on both the resting state and task state bioelectrical brain activity. Six classes of EEG microstates were assessed separately taking into account the following characteristics: 1) microstate duration, seconds; 2) microstate occurrence per second; 3) EEG microstate contribution to the total energy of the scalp field (coverage). The main cortical area was defined for each case of the EEG

microstate sequence and for each EEG microstate class in accordance with the Brodmann's map.

Statistical data processing

Statistical processing of the results was performed using the GNU-PSPP software package for GNU OC Linux Mate 10.10 (Canonical Ltd.; UK). Statistical analysis included the following steps: the data were tested for reliability or internal consistency by the Cronbach's alpha method ($0.05 < \alpha < 0.5$), after that factor analysis was used to define the main factors for further analysis. The results were compared using t-test to define the significance of changes due to the influence of the selected factor in one of the study groups and one-way analysis of variance (ANOVA) to define the influence of individual factors on different comparison groups. Pearson's chi-squared test (χ^2) was used to assess changes in the groups were the results obtained were in the form of qualitative characteristics. A single degree of freedom was used for all calculations; the accepted significance level was $\alpha > 0.05$.

The previously reported guidelines were used to develop a common method for statistical analysis [27].

RESULTS

Comparative characteristic of EEG microstates recorded during realization of speech function

Comparison of the EEG microstate characteristics under functional load using the paired *t*-test showed the following: in controls engaged in listening or active speech production, all three major indicators (duration, occurrence, and coverage) were significantly ($p < 0.05$) different from those obtained in a state of relaxed wakefulness. At the same time, in COVID-19 survivors, there were no such differences in the characteristics of bioelectrical activity between the resting state and the situation of auditory-speech load. In the vast majority of comparisons,

Table 2. Comparative characteristics of the class 1–6 EEG microstate duration in individuals having a history of novel coronavirus infection

	Class 1		Class 2		Class 3		Class 4		Class 5		Class 6	
	m	SD										
Resting state	0,04	0,02	0,04	0,02	0,04	0,01	0,05	0,02	0,04	0,02	0,05	0,01
Task state	0,04	0,02	0,04	0,02	0,04	0,01	0,04	0,01	0,05	0,01	0,04	0,02
<i>p</i> (<i>t</i> -test)	> 0,5		0,4		> 0,5		> 0,5		0,02		> 0,1	

Note: m — mean; SD — standard deviation.

Table 3. Comparative characteristics of the class 1–6 EEG microstate occurrence in controls

	Class 1		Class 2		Class 3		Class 4		Class 5		Class 5	
	m	SD										
Resting state	6,18	3,43	6,57	3,48	5,65	3,91	5,66	3,93	5,71	4,09	5,40	3,80
Task state	3,88	0,00	3,88	0,00	3,88	0,00	3,88	0,00	3,87	0,01	3,88	0,00
<i>p</i> (<i>t</i> -test)	< 0,01		< 0,001		0,01		0,01		0,01		0,02	

Note: m — mean; SD — standard deviation.

Table 4. Comparative characteristics of the class 1–6 EEG microstate occurrence in individuals having a history of novel coronavirus infection

	Class 1		Class 2		Class 3		Class 4		Class 5		Class 6	
	m	SD										
Resting state	3,88	0,00	3,88	0,01	3,88	0,00	3,88	0,00	3,88	0,00	3,88	0,01
Task state	3,88	0,01	3,88	0,00	3,88	0,00	3,88	0,01	3,88	0,01	3,63	0,95
p (t -test)	> 0,5		0,4		> 0,5		> 0,5		0,4		0,2	

Note: m — mean; SD — standard deviation.

the differences were nonsignificant ($p > 0.3$). Significant differences ($p = 0.02$) were revealed during assessment of the class 5 EEG microstate coverage only (Tables 1–6).

Microstates source analysis by solving the EEG inverse problem

The sources of distinct EEG microstates were assessed using the algorithm for solving the inverse EEG problem. However, the algorithm is based on defining the power of scalp potentials, since this parameter defines not the excitatory functional area, but the areas producing rhythmic activity, thus forcing us to use the general term “activity” that represents the area of interest for the algorithm to be used, but is not equivalent to the term “excitation of nervous tissue”.

However, the gradual transition from excitation of nerve centers to production of rhythmic activity was indicative of activity in distinct neuronal areas associated with the studied function realization. This made it possible to distinguish two main sequences, typical for cortical structures that produced rhythmic activity both in the state of relaxed wakefulness and under auditory-speech load, and locate the data obtained in accordance with the Brodmann’s map of cortical areas (see Figure).

The findings showed that no rhythmic activity was registered in controls within major Brodmann areas forming a cortical representation of speech (39, 40 and 44, 45), however, the components of rhythmic activity in the Brodmann area 47 responsible for perception and realization of music were found in all classes of EEG microstates. The auditory-speech load was characterized by rhythmic activity within areas 22 (class 2), 23 (class 6), 37 (classes 3–6), 39, 40 (classes 3–6), 44 (classes 3, 4 and 6), 45 (class 6), and 47 (class 5), which formed the following centers: center responsible for perception of noise, Wernicke’s area, Broca’s area, and center responsible for perception of music. This was in line with the common perceptions of the speech function realization via dorsal stream of the dual stream model of speech processing.

However, other sequences of the recorded rhythmic patterns within the recorded classes of EEG microstates were found in COVID-19 survivors (see Figure), along with the reduced total number of EEG microstates involved in realization of speech function.

Thus, no rhythmic activity within Brodmann area 47 typical for controls was revealed in the state of relaxed wakefulness. At the same time, rhythmic activity was revealed within areas 22 (classes 1, 5, 6), 37 (class 3), 39, 40 (all classes of EEG microstates). Under auditory-speech load, rhythmic activity was detected within areas 37 (classes 1 and 3), 39 (classes 4, 5, 6), and 41 (class 6).

DISCUSSION

The study of bioelectrical brain activity made it possible to substantially enhance the capabilities of EEG method and improve the accuracy of results, especially in the context of using a multichannel high density EEG system.

Comparative analysis of the changing characteristics of EEG microstates also confirmed the functional changes in bioelectrical activity, which were based on the changes in the patterns of activity in distinct groups of neurons. Thus, the lack of changes in the EEG microstate coverage in healthy individuals and COVID-19 survivors showed preserved neural structures involved in realization of functions. However, the differences in duration and occurrence of distinct classes of EEG microstates demonstrated the functional connectivity disruption, which, according to a number of authors, was indicative of mismatch in the joint activity of separate neural networks [23, 24].

An almost complete regression of variability in the EEG microstate occurrence in the COVID-19 survivors, detected in all the specified classes, was of particular interest. We considered this phenomenon a crude manifestation of low compensatory ability being the sequelae of the disease in such people.

However, the most complete characteristics of bioelectrical changes in the COVID-19 survivors were shown when solving the inverse EEG problem, which made it possible to detect

Table 5. Comparative characteristics of the class 1–6 EEG microstate coverage in controls

	Class 1		Class 2		Class 3		Class 4		Class 5		Class 6	
	m	SD										
Resting state	17%	14%	19%	13%	17%	14%	16%	15%	18%	16%	13%	12%
Task state	17%	3%	17%	4%	16%	3%	17%	3%	18%	4%	16%	4%
p (t -test)	0,8		0,4		0,6		0,9		0,9		0,2	

Note: m — mean; SD — standard deviation.

Table 6. Comparative characteristics of the class 1–6 EEG microstate coverage in individuals having a history of novel coronavirus infection

	Class 1		Class 2		Class 3		Class 4		Class 5		Class 6	
	m	SD										
Resting state	17%	7%	15%	7%	17%	6%	17%	6%	16%	6%	18%	6%
Task state	15%	6%	17%	7%	17%	5%	16%	8%	20%	3%	15%	7%
p (t -test)	> 0,5		> 0,4		> 0,5		> 0,5		0,02		0,1	

Note: m — mean; SD — standard deviation.

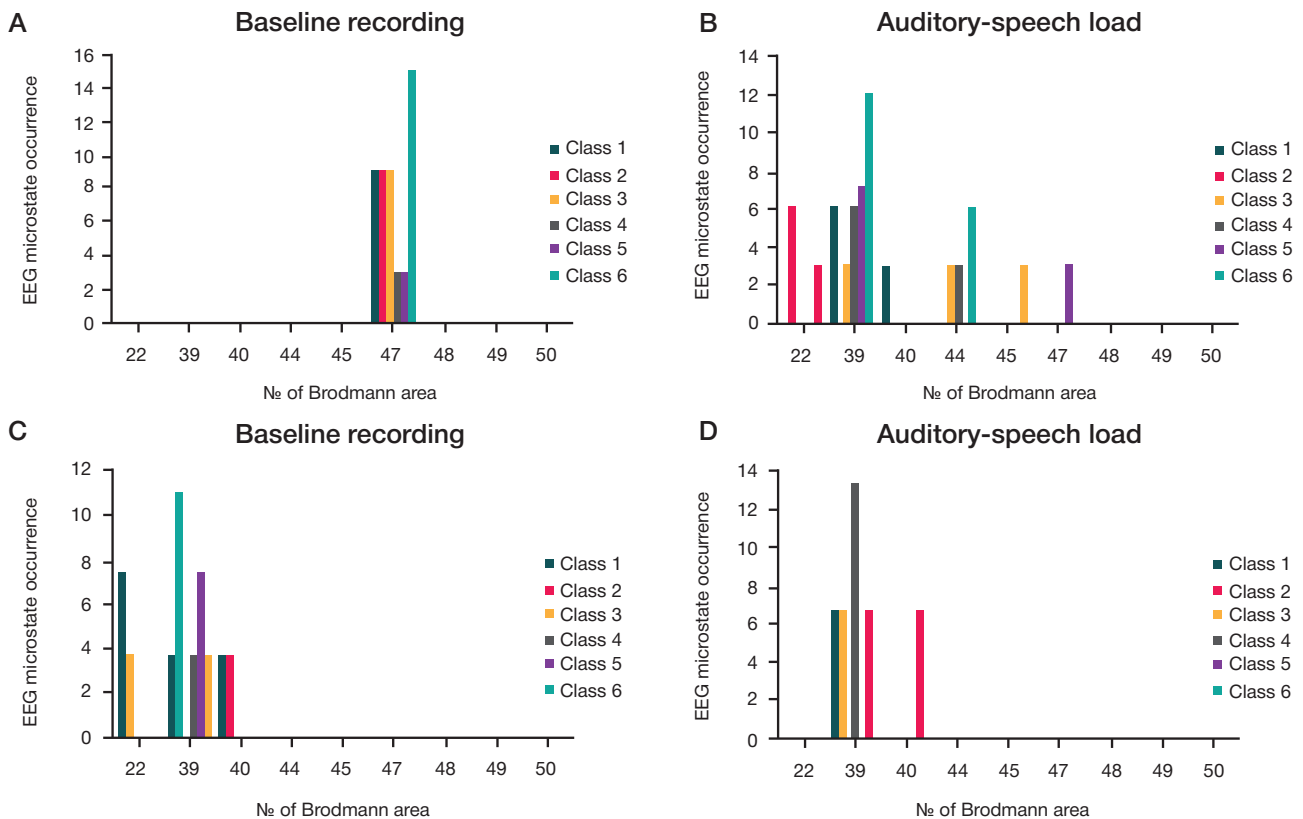


Fig. Rhythmic activity occurrence in accordance with the Brodmann area in controls (A, B) and individuals having a history of novel coronavirus infection (C, D) in the state of relaxed wakefulness and under auditory-speech load; $p < 0.05$ (χ^2 -test)

the disrupted sequences of the rhythmic activity registration within distinct brain structures and their association with the Brodmann's map of cortical areas.

According to the results, impaired speech function realization manifested itself in the disrupted information flow through the ventral stream and impaired communication between the areas within Wernicke's area and Broca's area (dorsal stream), which resulted in communication disorders in the form of impaired perception of new information and difficulties in implementing the decisions.

This is probably associated with the effects of COVID-19 on the neuronal structures, including those mediated by immunopathological processes, previously reported in experimental studies [19].

CONCLUSIONS

1. Individuals having a history of novel coronavirus infection who have returned to work after convalescence show

objective changes in bioelectrical brain activity associated with unexplored mechanisms, underlying functional damage to neural networks, involved in realization of the higher brain functions. 2. Recovery of general EEG characteristics in people having a history of novel coronavirus infection occurs over a long period of time (at least six months), which provides the basis for dysfunction known as post-COVID syndrome. 3. The results of solving the inverse EEG problem showed that COVID-19 survivors demonstrated alterations in realization of speech function in the form of the disordered sequence of switching on the main language centers. The study has shown that in people having a history of novel coronavirus infection, cognitive impairment undermining restoration of professional skills persists over a long time (up to six months). Such disorders are difficult to differentiate by clinical and brain imaging methods only, that is why recording and verification of these processes require developing the new multimodality neurophysiological assessment procedures.

References

- Qi G, Zhao S, Ceder AA, Guan W, Yan X. Wielding and evaluating the removal composition of common artefacts in EEG signals for driving behaviour analysis. *Accid Anal Prev.* 2021; 159: 106223. DOI: 10.1016/j.aap.2021.106223. Epub 2021 Jun 10. PMID: 34119819.
- Dittman Z, Munia TTK, Aviyente S. Graph Theoretic Analysis of Multilayer EEG Connectivity Networks. *Annu Int Conf IEEE Eng Med Biol Soc.* 2021; 2021: 475–9. DOI: 10.1109/EMBC46164.2021.9629514. PMID: 34891336
- Pascual-Marqui RD, Michel CM, Lehmann D. Segmentation of brain electrical activity into microstates: model estimation and validation. *IEEE Trans Biomed Eng.* 1995; 42 (7): 658–65. Available from: <https://doi.org/10.1109/10.391164>.
- Grech R, Cassar T, Muscat J, Camilleri KP, Fabri SG, Zervakis M, et al. Review on solving the inverse problem in EEG source analysis. *J Neuroeng Rehabil.* 2008; 5: 25. DOI: 10.1186/1743-0003-5-25. PMID: 18990257; PMCID: PMC2605581.
- Hecker L, Rupprecht R, Tebartz Van Elst L, Kornmeier J. ConvDip: A Convolutional Neural Network for Better EEG Source Imaging. *Front Neurosci.* 2021; 15: 569918. DOI: 10.3389/fnins.2021.569918. PMID: 34177438; PMCID: PMC8219905.
- Escaffre O, Borisevich V, Rockx B. Pathogenesis of Hendra and

- Nipah virus infection in humans. *J Infect Dev Ctries.* 2013; 7 (4): 308–11. Available from: <https://doi.org/10.3855/jidc.3648>.
7. Wang GF, Li W, Li K. Acute encephalopathy and encephalitis caused by influenza virus infection. *Curr Opin Neurol.* 2010; 23 (3): 305–11. Available from: <https://doi.org/10.1097/wco.0b013e328338f6c9>.
 8. Roy D, Ghosh R, Dubey S, Dubey MJ, Benito-León J, Kanti Ray B. Can Neurological and Neuropsychiatric Impacts of COVID-19 Pandemic. *J Neurol Sci.* 2021; 48 (1): 9–24. Available from: <https://doi.org/10.1017/cjn.2020.173>
 9. Song E, Zhang C, Israelow B, Lu-Culligan A, Prado AV, Skriabine S, et al. Neuroinvasion of COVID-19 in human and mouse brain. *J Exp Med.* 2021; 218 (3): e20202135. Available from: <https://doi.org/10.1084/jem.20202135>
 10. Moriguchi T, Harii N, Goto J, et al. A first case of meningitis/encephalitis associated with SARS-Coronavirus-2. *Int J Infect Dis.* 2020; 94: 55–58. Available from: <https://doi.org/10.1016/j.ijid.2020.03.06>
 11. Ye M, Ren Y, Lv T. Encephalitis as a clinical manifestation of COVID-19. *Brain Behav Immun.* 2020; S0889–1591 (20): 30465–7. Available from: <https://doi.org/10.1016/j.bbi.2020.04.017>.
 12. Duong L, Xu P, Liu A. Meningoencephalitis without respiratory failure in a young female patient with COVID-19 infection in Downtown Los Angeles, early April 2020. *Brain Behav Immun.* 2020; 87: 33. Available from: <https://doi.org/10.1016/j.bbi.2020.04.024>.
 13. Helms J, Kremer S, Merdji H, Clere-Jehl R, Schenck M, Kummerl C, et al. Neurologic Features in Severe COVID-19 Infection. *N Engl J Med.* 2020; 382 (23): 2268–70. Available from: <https://doi.org/10.1056/NEJMc2008597>.
 14. Puelles VG, Lütgehetmann M, Lindenmeyer MT, Sperhake JP, Wong MN, Allweiss L, et al. Multiorgan and Renal Tropism of COVID-19. *N Engl J Med.* 2020; 383 (6): 590–2. Available from: <https://doi.org/10.1056/NEJMc2011400>.
 15. Solomon IH, Normandin E, Bhattacharyya S, Mukerji SS, Keller K, Ali AS, et al. Neuropathological Features of Covid-19. *N Engl J Med.* 2020; 383 (10): 989–92. Available from: <https://doi.org/10.1056/NEJMc2019373>.
 16. Troyer EA, Kohn JN, Hong S. Are we facing a crashing wave of neuropsychiatric sequelae of COVID-19? Neuropsychiatric symptoms and potential immunologic mechanisms. *Brain Behav Immun.* 2020; 87: 34–39. Available from: <https://doi.org/10.1016/j.bbi.2020.04.027>
 17. Rogers JP, Chesney E, Oliver D, et al. Psychiatric and neuropsychiatric presentations associated with severe coronavirus infections: a systematic review and meta-analysis with comparison to the COVID-19 pandemic. *Lancet Psychiatry.* 2020; 7 (7): 611–27. Available from: [https://doi.org/10.1016/S2215-0366\(20\)30203-0](https://doi.org/10.1016/S2215-0366(20)30203-0).
 18. Kubota T, Gajera PK, Kuroda N. Meta-analysis of EEG findings in patients with COVID-19. *Epilepsy Behav.* 2021; 115: 107682. Available from: <https://doi.org/10.1016/j.yebeh.2020.107682>.
 19. Petrescu AM, Taussig D, Bouilleret V. Electroencephalogram (EEG) in COVID-19: A systematic retrospective study. *Neurophysiol Clin.* 2020; 50 (3): 155–65. Available from: <https://doi.org/10.1016/j.neucli.2020.06.001>.
 20. Pinto TCC, Machado L, Bulgacov TM, Rodrigues-Júnior AL, Costa MLG, Ximenes RCC, et al. Is the Montreal Cognitive Assessment (MoCA) screening superior to the Mini-Mental State Examination (MMSE) in the detection of mild cognitive impairment (MCI) and Alzheimer's Disease (AD) in the elderly? *Int Psychogeriatr.* 2019; 31 (4): 491–504. Available from: <https://doi.org/10.1017/S1041610218001370>.
 21. Mishkin M, Ungerleider LG. Contribution of striate inputs to the visuospatial functions of parieto-preoccipital cortex in monkeys. *Behav Brain Res.* 1982; 6 (1): 57–77. Available from: [https://doi.org/10.1016/0166-4328\(82\)90081-x](https://doi.org/10.1016/0166-4328(82)90081-x).
 22. Lehmann D, Strik WK, Henggeler B, Koenig T, Koukkou M. Brain electric microstates and momentary conscious mind states as building blocks of spontaneous thinking: I. Visual imagery and abstract thoughts. *Int J Psychophysiol.* 1998; 29 (1): 1–11. Available from: [https://doi.org/10.1016/s0167-8760\(97\)00098-6](https://doi.org/10.1016/s0167-8760(97)00098-6).
 23. Michel CM, Koenig T. EEG microstates as a tool for studying the temporal dynamics of whole-brain neuronal networks: A review. *Neuroimage.* 2018; 180 (Pt B): 577–93. Available from: <https://doi.org/10.1016/j.neuroimage.2017.11.062>.
 24. Van De Ville D, Britz J, Michel CM. EEG microstate sequences in healthy humans at rest reveal scale-free dynamics. *Proceedings of the National Academy of Sciences.* 2010; 107 (42): 18179–84; Available from: <https://doi.org/10.1073/pnas.1007841107>.
 25. Pascual-Marqui RD, Michel CM, Lehmann D. Segmentation of brain electrical activity into microstates: model estimation and validation. *IEEE Trans Biomed Eng.* 1995; 42 (7): 658–65. Available from: <https://doi.org/10.1109/10.391164>
 26. Vitali P, et al. Integration of multimodal neuroimaging methods: a rationale for clinical applications of simultaneous EEG-fMRI. *Funct Neurol.* 2015. PMID: 26214023.
 27. Sarter M, Fritschy JM. Reporting statistical methods and statistical results in *EJN*. *Eur J Neurosci.* 2008; 28 (12): 2363–4. Available from: <https://doi.org/10.1111/j.1460-9568.2008.06581.x>.

Литература

1. Qi G, Zhao S, Ceder AA, Guan W, Yan X. Wielding and evaluating the removal composition of common artefacts in EEG signals for driving behaviour analysis. *Accid Anal Prev.* 2021; 159: 106223. DOI: 10.1016/j.aap.2021.106223. Epub 2021 Jun 10. PMID: 34119819.
2. Dittman Z, Munia TTK, Aviyente S. Graph Theoretic Analysis of Multilayer EEG Connectivity Networks. *Annu Int Conf IEEE Eng Med Biol Soc.* 2021; 2021: 475–9. DOI: 10.1109/EMBC46164.2021.9629514. PMID: 34891336
3. Pascual-Marqui RD, Michel CM, Lehmann D. Segmentation of brain electrical activity into microstates: model estimation and validation. *IEEE Trans Biomed Eng.* 1995; 42 (7): 658–65. Available from: <https://doi.org/10.1109/10.391164>.
4. Grech R, Cassar T, Muscat J, Camilleri KP, Fabri SG, Zervakis M, et al. Review on solving the inverse problem in EEG source analysis. *J Neuroeng Rehabil.* 2008; 5: 25. DOI: 10.1186/1743-0003-5-25. PMID: 18990257; PMCID: PMC2605581.
5. Hecker L, Rupprecht R, Tebartz Van Elst L, Kornmeier J. ConvDip: A Convolutional Neural Network for Better EEG Source Imaging. *Front Neurosci.* 2021; 15: 569918. DOI: 10.3389/fnins.2021.569918. PMID: 34177438; PMCID: PMC8219905.
6. Escaffre O, Borisevich V, Rockx B. Pathogenesis of Hendra and Nipah virus infection in humans. *J Infect Dev Ctries.* 2013; 7 (4): 308–11. Available from: <https://doi.org/10.3855/jidc.3648>.
7. Wang GF, Li W, Li K. Acute encephalopathy and encephalitis caused by influenza virus infection. *Curr Opin Neurol.* 2010; 23 (3): 305–11. Available from: <https://doi.org/10.1097/wco.0b013e328338f6c9>.
8. Roy D, Ghosh R, Dubey S, Dubey MJ, Benito-León J, Kanti Ray B. Can Neurological and Neuropsychiatric Impacts of COVID-19 Pandemic. *J Neurol Sci.* 2021; 48 (1): 9–24. Available from: <https://doi.org/10.1017/cjn.2020.173>
9. Song E, Zhang C, Israelow B, Lu-Culligan A, Prado AV, Skriabine S, et al. Neuroinvasion of COVID-19 in human and mouse brain. *J Exp Med.* 2021; 218 (3): e20202135. Available from: <https://doi.org/10.1084/jem.20202135>
10. Moriguchi T, Harii N, Goto J, et al. A first case of meningitis/encephalitis associated with SARS-Coronavirus-2. *Int J Infect Dis.* 2020; 94: 55–58. Available from: <https://doi.org/10.1016/j.ijid.2020.03.06>
11. Ye M, Ren Y, Lv T. Encephalitis as a clinical manifestation of COVID-19. *Brain Behav Immun.* 2020; S0889–1591 (20): 30465–7. Available from: <https://doi.org/10.1016/j.bbi.2020.04.017>.
12. Duong L, Xu P, Liu A. Meningoencephalitis without respiratory failure in a young female patient with COVID-19 infection in Downtown Los Angeles, early April 2020. *Brain Behav Immun.* 2020; 87: 33. Available from: <https://doi.org/10.1016/j.bbi.2020.04.024>.

13. Helms J, Kremer S, Merdji H, Clere-Jehl R, Schenck M, Kummerlen C, et al. Neurologic Features in Severe COVID-19 Infection. *N Engl J Med.* 2020; 382 (23): 2268–70. Available from: <https://doi.org/10.1056/NEJMc2008597>.
14. Puelles VG, Lütgehetmann M, Lindenmeyer MT, Sperhake JP, Wong MN, Allweiss L, et al. Multiorgan and Renal Tropism of COVID-19. *N Engl J Med.* 2020; 383 (6): 590–2. Available from: <https://doi.org/10.1056/NEJMc2011400>.
15. Solomon IH, Normandin E, Bhattacharyya S, Mukerji SS, Keller K, Ali AS, et al. Neuropathological Features of Covid-19. *N Engl J Med.* 2020; 383 (10): 989–92. Available from: <https://doi.org/10.1056/NEJMc2019373>.
16. Troyer EA, Kohn JN, Hong S. Are we facing a crashing wave of neuropsychiatric sequelae of COVID-19? Neuropsychiatric symptoms and potential immunologic mechanisms. *Brain Behav Immun.* 2020; 87: 34–39. Available from: <https://doi.org/10.1016/j.bbi.2020.04.027>
17. Rogers JP, Chesney E, Oliver D, et al. Psychiatric and neuropsychiatric presentations associated with severe coronavirus infections: a systematic review and meta-analysis with comparison to the COVID-19 pandemic. *Lancet Psychiatry.* 2020; 7 (7): 611–27. Available from: [https://doi.org/10.1016/S2215-0366\(20\)30203-0](https://doi.org/10.1016/S2215-0366(20)30203-0).
18. Kubota T, Gajera PK, Kuroda N. Meta-analysis of EEG findings in patients with COVID-19. *Epilepsy Behav.* 2021; 115: 107682. Available from: <https://doi.org/10.1016/j.yebeh.2020.107682>.
19. Petrescu AM, Taussig D, Boullieret V. Electroencephalogram (EEG) in COVID-19: A systematic retrospective study. *Neurophysiol Clin.* 2020; 50 (3): 155–65. Available from: <https://doi.org/10.1016/j.neucli.2020.06.001>.
20. Pinto TCC, Machado L, Bulgacov TM, Rodrigues-Júnior AL, Costa MLG, Ximenes RCC, et al. Is the Montreal Cognitive Assessment (MoCA) screening superior to the Mini-Mental State Examination (MMSE) in the detection of mild cognitive impairment (MCI) and Alzheimer's Disease (AD) in the elderly? *Int Psychogeriatr.* 2019; 31 (4): 491–504. Available from: <https://doi.org/10.1017/S1041610218001370>.
21. Mishkin M, Ungerleider LG. Contribution of striate inputs to the visuospatial functions of parieto-preoccipital cortex in monkeys. *Behav Brain Res.* 1982; 6 (1): 57–77. Available from: [https://doi.org/10.1016/0166-4328\(82\)90081-x](https://doi.org/10.1016/0166-4328(82)90081-x).
22. Lehmann D, Strik WK, Henggeler B, Koenig T, Koukkou M. Brain electric microstates and momentary conscious mind states as building blocks of spontaneous thinking: I. Visual imagery and abstract thoughts. *Int J Psychophysiol.* 1998; 29 (1): 1–11. Available from: [https://doi.org/10.1016/s0167-8760\(97\)00098-6](https://doi.org/10.1016/s0167-8760(97)00098-6).
23. Michel CM, Koenig T. EEG microstates as a tool for studying the temporal dynamics of whole-brain neuronal networks: A review. *Neuroimage.* 2018; 180 (Pt B): 577–93. Available from: <https://doi.org/10.1016/j.neuroimage.2017.11.062>.
24. Van De Ville D, Britz J, Michel CM. EEG microstate sequences in healthy humans at rest reveal scale-free dynamics. *Proceedings of the National Academy of Sciences.* 2010; 107 (42): 18179–84. Available from: <https://doi.org/10.1073/pnas.1007841107>.
25. Pascual-Marqui RD, Michel CM, Lehmann D. Segmentation of brain electrical activity into microstates: model estimation and validation. *IEEE Trans Biomed Eng.* 1995; 42 (7): 658–65. Available from: <https://doi.org/10.1109/10.391164>
26. Vitali P, et al. Integration of multimodal neuroimaging methods: a rationale for clinical applications of simultaneous EEG-fMRI. *Funct Neurol.* 2015. PMID: 26214023.
27. Sarter M, Fritschy JM. Reporting statistical methods and statistical results in *EJN*. *Eur J Neurosci.* 2008; 28 (12): 2363–4. Available from: <https://doi.org/10.1111/j.1460-9568.2008.06581.x>.

CEREBRAL ENERGY EXCHANGE IN EMPLOYEES OF HAZARDOUS NUCLEAR FACILITIES AND PRODUCTIONS WITH THE LOW DEGREE OF PSYCHOPHYSIOLOGICAL ADAPTATION

Zvereva ZF¹✉, Torubarov FS¹, Vanchakova NP², Denisova EA¹

¹ Burnazyan Federal Medical Biophysical Center, Moscow, Russia

² Pavlov First Saint Petersburg State Medical University, St. Petersburg, Russia

Psychophysiological assessment of employees of 10 Russian nuclear power plants revealed a low degree of psychophysiological adaptation (PPA) in 30% of subjects. Studying the functional activity (FA) of the brain by EEG revealed the decline in FA in individuals with the low degree of PPA. The impaired cerebral energy exchange could be one of the factors contributing to the decline in the brain functional state. The study was aimed to assess the features of the cerebral energy exchange in the employees of the hazardous nuclear facilities and productions with the low degree of PPA. A total of 159 EEG recordings acquired from individuals with the low degree of PPA (50.8 ± 4.6), and 152 EEG recordings acquired from individuals with the high degree of PPA (48.8 ± 1.5) were studied. Energy exchange was assessed in individuals with the low FA of both brain as a whole and the following conditionally distinguished structural and functional units (SFUs) of the CNS: mainly cerebral cortex (SFU-1), cortical-subcortical interactions (SFU-2), central control of the cardiovascular system (SFU-3). EEG was recorded by standard method using the electroencephalography unit. The magnitude of the hemispheric differences (HD) in the power of biopotentials (BP) between the homologous EEG leads was used to assess the cerebral energy exchange. There is evidence of the cerebral energy exchange increase in the anterior cortical areas of individuals with the low degree of PPA. The increased cerebral energy exchange has been also revealed in SFU-1 and SFU-2 responsible for the mental and psychophysiological functions of the CNS. However, cerebral energy exchange remains unchanged in the SFU-3 reflecting the central control of the CVS.

Keywords: employees, hazardous nuclear facilities and productions, central nervous system, EEG, psychophysiological adaptation, cerebral energy exchange, functional state

Author contribution: Zvereva ZF, Torubarov FS, Vanchakova NP — data processing, manuscript writing; Denisova EA — psychophysiological assessment.

Compliance with ethical standards: the study was approved by the Ethics Committee of the A. I. Burnazyan Federal Medical Biophysical Center (protocol № 406 dated December 13, 2021).

✉ **Correspondence should be addressed:** Zoya F. Zvereva
Pestelya 9, k. 146, Moscow, 127490, Russia; zvereva01@yandex.ru

Received: 15.04.2022 **Accepted:** 29.04.2022 **Published online:** 03.05.2022

DOI: 10.47183/mes.2022.012

ЦЕРЕБРАЛЬНЫЙ ЭНЕРГООБМЕН У РАБОТНИКОВ ЯДЕРНО ОПАСНЫХ ПРЕДПРИЯТИЙ И ПРОИЗВОДСТВ С НИЗКИМ УРОВНЕМ ПСИХОФИЗИОЛОГИЧЕСКОЙ АДАПТАЦИИ

З. Ф. Зверева¹✉, Ф. С. Торубаров¹, Н. П. Ванчакова², Е. А. Денисова¹

¹ Федеральный медицинский биофизический центр имени А. И. Бурназяна, Москва, Россия

² Первый Санкт-Петербургский государственный медицинский университет имени И. П. Павлова, Санкт-Петербург, Россия

В результате психофизиологического обследования работников 10-й АЭС России у 30% обследованных выявлен низкий уровень психофизиологической адаптации (ПФА). Изучение функциональной активности (ФА) головного мозга с помощью ЭЭГ установило ее снижение у лиц с низким уровнем ПФА. Одним из факторов снижения функционального состояния головного мозга может быть нарушение церебрального энергообмена. Целью работы было изучить особенности церебрального энергообмена у работников ядерно опасных предприятий и производств с низким уровнем ПФА. Исследовали 159 ЭЭГ лиц с низким уровнем ПФА ($50,8 \pm 4,6$), 152 ЭЭГ лиц с высоким уровнем ПФА ($48,8 \pm 1,5$). Энергообмен изучали при низкой ФА как мозга в целом, так и отдельных условно выделенных нами структурно-функциональных образований (СФО) ЦНС: преимущественно коры (СФО-1), корково-подкоркового взаимодействия (СФО-2), центральной регуляции сердечно-сосудистой системы (СФО-3). ЭЭГ регистрировали общепринятым способом на электроэнцефалографе. Для оценки церебрального энергообмена использовали показатель величины межполушарных различий (ВМПР) мощности биопотенциалов (БП) ЭЭГ гомологичных отведений. Получены данные об усилении при низком уровне ПФА церебрального энергообмена в передних отделах коры головного мозга. Усиление церебрального энергообмена выявлено также в СФО-1 и СФО-2, ответственных за психические и психофизиологические функции ЦНС. При этом в СФО-3, отражающем центральную регуляцию ССС, церебральный энергообмен не менялся.

Ключевые слова: работники, ядерно опасные предприятия, центральная нервная система, ЭЭГ, психофизиологическая адаптация, церебральный энергообмен, функциональное состояние

Вклад авторов: З. Ф. Зверева, Ф. С. Торубаров, Н. П. Ванчакова — обработка данных и написание статьи; Е. А. Денисова — психофизиологическое обследование.

Соблюдение этических стандартов: исследование одобрено этическим комитетом Федерального медицинского биофизического центра им. А. И. Бурназяна (протокол № 406 от 13 декабря 2021 г.)

✉ **Для корреспонденции:** Зоя Фёдоровна Зверева
Пестеля, д. 9, к. 146, г. Москва, 127490, Россия; zvereva01@yandex.ru

Статья получена: 15.04.2022 **Статья принята к печати:** 29.04.2022 **Опубликована онлайн:** 03.05.2022

DOI: 10.47183/mes.2022.012

The work of operating personnel of the hazardous nuclear facilities and productions is associated with severe emotional strain and high responsibility. The employees' top priorities are as follows: timely and accurate perception of complex information, evaluation of information, decision making and adequate response. All the tasks are implemented by the central nervous

system (CNS). The impaired functional state (FS) of the CNS resulting in the low degree of psychophysiological adaptation (PPA) affects the professional activities reliability and can lead to the increased risk of accidents being the fault of the staff [1].

Psychophysiological assessment (PA) of employees of the hazardous nuclear facilities and productions performed

within the framework of the mandatory annual medical check-ups makes it possible to assess the CNS FS and the degree of PPA [2, 3]. The experience of PA has proven the feasibility of using a comprehensive approach to assess the degree of PPA by methods taking into account human mental, psychophysiological and physiological spheres [1, 3, 4].

Our conceptual model of PA, developed for the personnel of the hazardous nuclear facilities and productions, makes it possible to assess the functional activity (FA) of the allocated conditional structural and functional units (SFUs) of the CNS, the functional state of the entire CNS, and the degree of PPA [5]. The following SFUs of the CNS are considered: primarily cerebral cortex (SFU-1); cortical-subcortical interactions (SFU-2); central control of the cardiovascular system (SFU-3).

The functional activity of the CNS structural and functional units is assessed in the following way:

- SFU-1 is assessed by psychological techniques that reflect the mental sphere: personal characteristics, individual's mental state, character traits, intelligence level, the degree of internality-externality (individual's preparedness to take responsibility for what happens to him/her and around), which are mostly ensured by cerebral cortex [6];

- SFU-2 is assessed by psychophysiological techniques that reflect the dynamics of neural processes, switching between the processes, the level of eye-hand coordination, overall efficiency and activity of the CNS, which are ensured mostly by the cortical-subcortical interactions [7];

- SFU-3 is assessed by physiological technique for determining the heart rate variability (HRV) that reflects the central control of the cardiovascular system (CVS), which is ensured by subcortical structures, the diencephalic region of the brainstem [8].

The FA levels of the CNS SFUs are determined as high, medium or low. This makes it possible to define the degree of PPA as an integrated indicator, which could also be high, medium or low [2, 3, 4]. PA is performed with the PFS-CONTROL software-hardware complex (SHC) [2, 4].

The previously conducted PA of the operating personnel of 10 Russian nuclear power plants showed that 30% of employees had a low degree of PPA [9, 10]. When assessing the CNS FS in these employees by EEG given the low degree of PPA, abnormal parameters were detected significantly more often than in case of high degree of PPA [11, 12]. This suggested the decline in the CNS FS. The greatest number of abnormalities was revealed in individuals with the low degree of PPA in the SFU reflecting the central control of the CVS [9–12].

In matters of human adaptation to living conditions, including tense and responsible professional activity, studying brain energy metabolism [13] underlying the functional plasticity of the brain [14] is considered important. In the studies involving the use of neuroergometry for evaluation of the cerebral energy exchange by recording the brain direct current (DC) potentials [15], alterations in the CNS associated with the harsh living conditions and the development of adaptive response were defined. It was shown that the altered adaptive response in the form of the increased cerebral energy exchange was observed in migrants and individuals permanently residing in the harsh climate of the Arctic Zone of the Russian Federation (RF) [16]. The close correlation between the light pattern, cerebral energy exchange and anxiety was found in the residents of the Arctic Zone of the RF. The seasonal variation of the cerebral energy exchange in the form of the increase during the lighter periods of the year in people with high levels of anxiety is associated with the more prominent increase in energy exchange compared to people with low levels of anxiety [17]. When studying

the relationship between the brain activity and the energy metabolism, it was shown that heavier mental workloads were associated with the more prominent increase in the cerebral energy exchange compared to the less heavy workloads [13]. The differences in the cerebral energy exchange increase between various cortical areas under mental workloads of different types were also revealed [18].

Despite their importance, the issues of human brain energy metabolism associated with adaptive response in the employees of the hazardous nuclear facilities and productions are poorly understood. Cerebral energy exchange in the nuclear industry workers with the low degree of PPA has not yet been explored.

For electroencephalography, widely used in studying the mechanisms underlying the normal and abnormal rearrangements in the CNS FS, an indicator, the magnitude of the hemispheric differences (HD) in the power of biopotentials (BP) between the homologous EEG leads, was developed to be used during the study [19]. Matching this indicator with the DC potentials used in neuroergometry has revealed their similarity when assessing alterations in the CNS FS [20] and justified the use of the magnitude of the HD in the power of BP between the homologous EEG leads for analysis of the cerebral energy exchange in individuals with the low degree of PPA.

The study was aimed to assess the features of the cerebral energy exchange in the employees of the hazardous nuclear facilities and productions with the low degree of PPA.

METHODS

Archive EEG recordings obtained from the employees of the hazardous nuclear facilities and productions during the PA performed within the framework of medical check-up were studied. Inclusion criteria: EEG recordings of individuals with no contraindications to further work based on the results of medical check-up and PA. A total of 311 EEG were extracted, of those 159 EEG recordings of individuals with the low degree of PPA (50.8 ± 4.6 years; 146 males, 13 females), and 152 EEG recordings of individuals with the high degree of PPA (48.8 ± 1.5 years; 140 males, 12 females). Due to the low number of female subjects, the groups were recognized as homogenous.

PA was performed using the PFS-CONTROL SHC [2–4]. The following psychological techniques were used:

- multiphasic personality test (MPT; adapted version of MMPI [2, 3, 21, 22]);

- Raymond Cattell's 16 Personality Factors Questionnaire (16PF, form A) [2, 3, 23];

- John Raven's Progressive Matrices Test [2, 3, 24];

- questionnaire of the level of subjective control (USC) [2, 3, 25];

SFU-1 was distinguished based on the methods.

Psychophysiological methods:

- simple visual-motor reaction (SVMR), complex visual-motor reaction (CVMR), reaction to a moving object (RMO);

SFU-2 was distinguished based on the methods.

Physiological method: HRV; SFU-3 was distinguished based on the method.

Two groups were formed based on the degree of PPA in order to access the cerebral energy exchange:

- group 1 with the low degree of PPA ($n = 159$);

- group 2 with the high degree of PPA (comparison group; $n = 152$).

Two subgroups were also formed based on the FA of the CNS SFUs:

- subgroup 1 with the low FA: SFU-1 ($n = 48$), SFU-2 ($n = 53$), SFU-3 ($n = 110$);

Table 1. HD in the power of BP between the homologous EEG leads acquired from the anterior and posterior cortical areas associated with the high and low degree of PPA

Degree of PPA	HD in the power of BP between the homologous EEG leads (AU)		Test / <i>p</i>
	Cortical areas		
	anterior	posterior	
Low <i>n</i> = 159	18,1 ± 0,09**	15,9 ± 0,04*	<i>t</i> / 0,0089* <i>t</i> / 0,0034*
High <i>n</i> = 152	17,3 ± 0,05**	15,7 ± 0,02*	<i>t</i> / 0,0056*

Note: * — significant differences between the anterior and posterior cortical areas; ** — significant differences between the high and low degree of PPA.

– subgroup 2 with the high FA: SFU-1 (*n* = 117), SFU-2 (*n* = 71), SFU-3 (*n* = 87).

EEG recording was acquired with the EEGA-21/26 Encephalan-131-03 unit (Medicom MTD; Russia) using the standard 10–20% system with the subject in a state of passive wakefulness. Electrodes were placed over the following cortical zones: Fp1, Fp2, F3, F4, F7, F8, T3, T4, T5, T6, C3, C4, P3, P4, O1, O2. Monopolar montage was used with the reference electrodes placed on the earlobes. The signal digitization rate was 1024, and the reading speed was 30 mm/s. The following ranges were recorded: 0–3.5 Hz — δ ; 4.0–7.0 Hz — θ ; 8.0–13.0 Hz — α ; 14–24 Hz — β_1 ; 25–35 Hz — β_2 .

To calculate the cerebral energy exchange value:

– the artifact free sections of the recording (1.5–2 min) were processed with the EEGA-21/26 Encephalan-131-03 software to obtain the numerical values for 10 fragments of the EEG BP power spectrum in each of the leads placed over the hemispheres;

– to calculate the difference between two values (%), the values of the HD in the power of BP between the homologous EEG leads were calculated using the formula $(A-B)/(A+B) \times 100\%$, where A was the power of BP in the EEG lead set up over the left hemisphere, and B was the power of BP in the EEG lead set up over the right hemisphere, based on the conditional mean;

– the absolute values of the HD in the power of BP between the homologous EEG leads were averaged over all the ranges (α , δ , θ , β_1 , β_2) for each electrode pair; the resulting values were considered the indicators of the cerebral energy exchange measured in arbitrary units (AU);

– the average cerebral energy exchange values were calculated for the anterior (Fp1, Fp2, F3, F4, F7, F8, T3,

T4, T5, T6) and posterior cortical areas (C3, C4, P3, P4, O1, O2) [19].

Statistical data processing was performed with the STATISTICA 6 for Windows (StatSoft Inc.; USA) and Biostat (AnalystSoft; USA) software. The data set processing with the STATISTICA 6 software involved calculating the mean values (*M*) and errors (*m*). Student's *t*-test was used to assess the significance of differences between the mean values. The differences in the comparison groups were considered significant at $p < 0.05$. The data set processing with the Biostat software involved applying the χ^2 test, the significance level was set at 0.05 ($p < 0.05$).

RESULTS

Table 1 presents the values of the HD in the power of BP between the homologous EEG leads acquired from the anterior and posterior cortical areas in individuals with the high and low degree of PPA.

The values acquired from the anterior cortical areas were higher than those acquired from the posterior areas in individuals with both high and low degree of PPA. The cerebral energy exchange was higher in anterior than in posterior areas. These ratios are similar to normal ratios of healthy people [19].

In individuals with the low degree of PPA, HD in the power of BP between the homologous EEG leads increased in the anterior cortical areas (in relation to the high degree). There were no differences between the values of the HD in the power of BP between the homologous EEG leads obtained in individuals with the low and high degree of PPA.

From the above, it is clear that in individuals with the low degree of PPA, cerebral energy exchange increased in the

Table 2. HD in the power of BP between the homologous EEG leads acquired from the anterior and posterior cortical areas associated with the high and low degree of PPA

SFU of CNS	FA	HD in the power of BP between the homologous EEG leads (AU)		Test / <i>p</i>
		Cortical areas		
		anterior	posterior	
SFU-1	low <i>n</i> = 48	18,8 ± 0,07**	16,1 ± 0,08*	<i>t</i> / 0,0062* <i>t</i> / 0,0030***
	high <i>n</i> = 117	17,2 ± 0,02**	15,5 ± 0,05*	<i>t</i> / 0,0050*
SFU-2	low <i>n</i> = 53	18,2 ± 0,06**	15,9 ± 0,04*	<i>t</i> / 0,0058* χ^2 / 0,046***
	high <i>n</i> = 71	17,0 ± 0,02**	15,7 ± 0,05*	<i>t</i> / 0,0062*
SFU-3	low <i>n</i> = 110	17,9 ± 0,04*	15,9 ± 0,06*	<i>t</i> / 0,0052*
	high <i>n</i> = 87	17,2 ± 0,03*	15,7 ± 0,09*	<i>t</i> / 0,016*

Note: * — significant differences between the anterior and posterior cortical areas; ** — significant differences between the high and low FA of the SFUs.

anterior cortical areas and remained unchanged in the posterior areas.

Table 2 presents the values of the HD in the power of BP between the homologous EEG leads acquired from the anterior and posterior cortical areas associated with the high and low FA of the SFUs.

In the SFU-1 of individuals with the low FA, the values of the HD in the power of BP between the homologous EEG leads increased (in relation to the high FA) in the anterior cortical areas and remained unchanged in the posterior areas.

Similarly, in the SFU-2 of individuals with the low FA, the values of the HD in the power of BP between the homologous EEG leads increased (in relation to the high FA) in the anterior cortical areas and did not change in the posterior areas.

From the above, it is clear that in the SFU-1 and SFU-2 of individuals with the high FA, cerebral energy exchange increased in the anterior cortical areas and remained unchanged in the posterior areas.

In the SFU-2 of individuals with the low FA, the values of the HD in the power of BP between the homologous EEG leads acquired from the anterior and posterior cortical areas were similar to those acquired from individuals with the high FA. The cerebral energy exchange remained unchanged both in the anterior and posterior cortical areas.

Thus, in individuals with the low degree of PPA and low FA of the SFU-1 and SFU-2, cerebral energy exchange increased in the anterior cortical areas and never changed in the posterior areas. In individuals with the low FA of the SFU-3, cerebral energy exchange remained unchanged both in the anterior and posterior cortical areas.

DISCUSSION

The findings showed that the cerebral energy exchange increased in individuals with the low degree of PPA. In the past electroencephalographic studies of the nuclear power plant personnel it was found that the signs of the CNS FS decline in the form of the increase in indicators recognized as anomalous were found in EEG recordings of individuals with the low degree of PPA [9–12]. According to literature, the types of activity significantly different from normal and showing the CNS FS decline are revealed in EEG recordings of individuals with the low degree of adaptation almost in 80% of observations [9–12]. Based on the data provided it can be assumed that the increased cerebral energy exchange in the employees of the hazardous nuclear facilities and productions with the low level of PPA is the evidence of the CNS FS decline.

PPA is the body's systemic response to the impact of the external and internal factors aimed at adaptation [1, 4, 21, 26]. Stress is considered the main underlying mechanism [27, 28]. It was shown that stress developing as a non-specific body's response to the significant impact of the external and internal factors [27, 28] results naturally in the low degree of adaptation, CNS FS decline, and the increased cerebral energy metabolism [15]. These data have been confirmed by studying the cerebral energy exchange in individuals living in the harsh climate of the Arctic Zone of the RF [16], as well as in the Arctic Zone residents with the high anxiety levels [17]. It can be assumed that the increased cerebral energy exchange in individuals with the low degree of PPA revealed during our study results from stress developing in the nuclear industry workers in response to the significant impact of the external and internal factors during their tense and responsible professional activities.

The increased cerebral energy exchange indicates the probable switching to additional psychophysiological mechanisms allowing individuals with the low degree of PPA to cope with stress. However, this compensatory mechanism is not optimal, it results in fatigue and requires further recovery. That is why the emergence of such alterations should be considered the critical factor for the employees of the hazardous nuclear facilities and productions.

Based on the study results, the cerebral energy exchange increased in individuals with the low FA of the SFU-1 and SFU-2, reflecting human mental and psychophysiological spheres, and remained unchanged in individuals with the low FA of the SFU-3, reflecting human physiology.

In accordance with the conceptual model of PPA, SFU-1 is considered as mainly cortical, SFU-2 as the cortical-subcortical interactions, SFU-3 as the central control of the cardiovascular system [5]. Cerebral cortex is the main area responsible for the functions involving SFU-1 [6]. The cortical-subcortical interactions play a dominant role in the implementation of functions involving SFU-2 [7]. Subcortical structures, the diencephalic region of the brainstem, are the main areas responsible for functions involving SFU-3 [8]. Currently, PPA is believed to be a systemic process based on information processing [29]. Based on the above it can be assumed that the cerebral energy exchange processes are to the greatest extent involved in information processing associated with implementation of functions involving mainly cerebral cortex (SFU-1). The same for functions implemented with the dominant role of the cortical-subcortical interactions (SFU-2). The cerebral energy exchange processes are less involved in information processing associated with implementation of functions involving mostly subcortical structures, the diencephalic region of the brainstem (SFU-3).

It can be also assumed that the increase in the cerebral energy exchange is a compensatory neurochemical process aimed at increasing the FA of the most important SFUs of the brain.

The increased cerebral energy exchange in the anterior cortical areas associated both with low PPA and low FA of the CNS SFUs, involved in mental and psychophysiological functions, is related to the more dynamic nature of these functions in the context of the increased stress compared to physiological functions. SFUs related to regulation of the cardiovascular system are autonomous, and FA of these SFUs seems to involve different mechanisms.

CONCLUSIONS

In the employees of the hazardous nuclear facilities and productions with the low degree of psychophysiological adaptation, cerebral energy exchange increases in the anterior cortical areas and remains unchanged in the posterior areas. In individuals with the low functional activity of the structural and functional units reflecting both mental and psychophysiological spheres, cerebral energy exchange increases in the anterior cortical areas and does not change in the posterior areas. In individuals with the low functional activity of the structural and functional unit reflecting the central control of the cardiovascular system, cerebral energy exchange remains unchanged in both anterior and posterior cortical areas. Advanced research is required to define the cause of no changes in the cerebral energy exchange in this SFU. The findings are important not only for neuroscience but for practical application in medicine.

References

1. Samojlov AS, Bushmanov AYU, Bobrov AF, Shheblanov VYu, Sedin VI, Kalinina MYu. Psixofiziologicheskie aspekty obespecheniya nadezhnosti professional'noj deyatel'nosti rabotnikov organizacij atomnoj otrasli. V sbornike: Materialy III otraslevoj nauchno-prakticheskoy konferencii. ANO DPO «Texnicheskaya akademiya Rosatoma». M., 2018; s. 62–76. Russian.
2. Organizaciya i provedenie psixofiziologicheskix obsledovaniy rabotnikov organizacij, ehkspluatiruyushhix osobo radiacionno opasnye i yaderno opasnye proizvodstva i ob"ekty v oblasti ispol'zovaniya atomnoj ehnergii, pri proxozhdenii rabotnikami medicinskix osmotrov v medicinskix organizacijax FMBA Rossii. Metodicheskie rekomendacii R FMBA Rossii 2.2.9.84–2015. Moskva, 2015. Russian.
3. Rukovodstvo po ocenke i interpretacii rezul'tatov monitoringa psixofiziologicheskogo sostoyaniya rabotnikov organizacij, ehkspluatiruyushhix osobo radiacionno opasnye i yaderno opasnye proizvodstva i ob"ekty v oblasti ispol'zovaniya atomnoj ehnergii. FMBA Rossii 2.2.9. 2014; 40 s. Russian.
4. Bobrov AF, Bushmanov AYU, Sedin VI, Shheblanov Vyu. Sistemnaya ocenka rezul'tatov psixofiziologicheskix obsledovaniy. Medicina ehkstreml'nyx situacij. 2015; (3): 13–9. Russian.
5. Torubarov FS, Bushmanov AYU, Zvereva ZF, Kretov AS, Lukyanova SN, Denisova EA. Konceptiya psixofiziologicheskogo obsledovaniya personala ob"ektov ispol'zovaniya atomnoj ehnergii v medicinskix organizacijax. Medicina ehkstreml'nyx situacij. 2021; 23 (1): 13–8. Russian.
6. Luriya AR. Vysshie korkovye funkcii cheloveka i ix narushenie pri lokal'nyx porazheniyax mozga. M.: Akadem. proekt, 2000; 433 s. Russian.
7. Loskutova TD. Ocenka funkcional'nogo sostoyaniya central'noj nervnoj sistemy cheloveka po parametram prostoj dvigatel'noj reakcii. Fiziologicheskij zhurnal SSSR. 1975; 61 (1): 3–12. Russian.
8. Baevsij RM. Konceptiya fiziologicheskoy normy i kriterii zdorov'ya. Rossijskij fiziologicheskij zhurnal im. I. M. Sechenova. 2003; (4): 473–87. Russian.
9. Isaeva NA, Torubarov FS, Zvereva ZF, Lukyanova SN, Denisova EA. Bioelektricheskaya aktivnost' golovnogogo mozga u rabotnikov Novovoronezhskoj i Beloyarskoj AEHS s raznym urovnem adaptacii k usloviyam ix trudovoj deyatel'nosti. Medicinskaya radiologiya i radiacionnaya bezopasnost'. 2016; 61 (5): 5–12. Russian.
10. Torubarov FS, Zvereva ZF, Lukyanova SN. EhEhG pokazateli sostoyaniya central'noj nervnoj sistemy u lic s razlichnymi urovnymi psixofiziologicheskoy adaptacii. Saratovskij nauchno-meditsinskij zhurnal. Prilozhenie oktyabr'-dekabr'. 2019; 15 (4): 965–7. Russian.
11. Torubarov FS, Zvereva ZF, Lukyanova SN. Bioelektricheskaya aktivnost' golovnogogo mozga u operativnogo personala AEHS Rossii s nizkim urovnem psixofiziologicheskoy adaptacii. Medicinskaya radiologiya i radiacionnaya bezopasnost'. 2021; 66 (2): 23–35. Russian.
12. Zvereva ZF, Torubarov FS, Denisova EA, Miroshnik E. Prognosticheskie kriterii psixofiziologicheskoy adaptacii po dannym sravnitel'noj karakteristiki vizual'nogo analiza i pokazatelej moshhnosti biopotencialov EhEhG u rabotnikov yaderno opasnyx predpriyatij i proizvodstv. Medicina truda i promyshlennaya ehkologiya. 2021; 61 (9): 588–94. Russian.
13. Kirsanov VM. Ocenka stepeni adaptacii individa na osnove pokazatelej ehnergeticheskogo potenciala golovnogogo mozga i psixodiagnosticheskogo obsledovaniya. Innovacii v nauke. 2012. (8): 64–8. Russian.
14. Foster C, Steventon JJ, Helme D, Tomassini V, Wise RG. Cerebral Metabolic Changes During Visuomotor Adaptation Assessed Using Quantitative fMRI. Front Physiol. 2020 May 8; 11: 428.
15. Fokin VF, Ponomareva NV. Ehnergeticheskaya fiziologiya mozga. Moskva: «Antidor», 2003; 288 s. Russian.
16. Gribanov AV, Anikina NYu, Gudkov AB. Cerebral'nyj ehnergoobmen kak marker adaptivnyx reakcij cheloveka v prirodno-klimaticheskix usloviyax Arkticheskoy zony Rossijskoj Federacii. Ehkologiya cheloveka. 2018; (8): 32–40. Russian.
17. Gribanov AV, Kocova ON, Anikina NYu, Pankov MN, Korelskaya IE. Sezonnnye izmeneniya cerebral'nogo ehnergoobmena pri raznom urovne trevozhnosti u molodyx lyudej v arkticheskoy zone rossijskoj federacii. Chelovek. Sport. Medicina. 2021; 21 (4): 73–80. Russian.
18. Timmel M, Strässler F, Knerer K. Brain DC potential changes of computerized tasks and paper/pencil tasks. Int J Psychophysiol. 2001; 40 (3): 187–94.
19. Zvereva Z. F. Xarakter mezhpolutsharnogo raspredeleniya moshhnosti biopotencialov golovnogogo mozga v norme i pri ego lateralizovannom porazhenii [dissertaciya]. M., 2004. Russian.
20. Miroshnik EV, Zvereva ZF, Bobrov AF, Baskakov IS, Vanchakova NP, Elanskaya OV. Sopostavlenie pokazatelej bioelektricheskoy aktivnosti golovnogogo mozga i ehnergeticheskix processov v tkani mozga (Velichiny mezhpolutsharnyx razlichij gomologichnyx otvedenij i urovnya postoyannogo potenciala golovnogogo mozga). Medicina ehkstreml'nyx situacij. 2017; 60 (2): 49–59. Russian.
21. Berezin FB. Psixicheskaya i psixofiziologicheskaya adaptaciya cheloveka. L.: Nauka, 1988; 270 s. Russian.
22. Berezin FB, Miroshnikov MP, Sokolova ED, Metodika mnogostoronnego issledovaniya lichnosti (MMML): struktura, osnovy interpretacii, nekotorye oblasti primeneniya. M.: Izd-vo «Berezin Feliks Borisovich», 2011; 320 s. Russian.
23. Cattell RB, Eber HW. Handbook for the Sixteen Personality factor Questionnaire. Illinois, 1964.
24. Raven JC. A manual for Raven's progressive matrices and vocabulary tests. London: H.K. Levis @ Go. Ltd, 1988.
25. Sekoyan I. Eh. «Lokus kontrolya» Dzhuliana Rottera s pozicij psixometrii. Nezavisimyj psixiatricheskij zhurnal. 2008; 3: 18–25. Russian.
26. Anoxin PK. Ocherki po fiziologii funkcional'nyx sistem. M.: Nauka, 1975; 447 s. Russian.
27. Sele G. Stress bez distressa. M.: Progress, 1979; 124 s. Russian.
28. Yunusova SG, Rozental AN, Baltina TV. Stress. Biologicheskij i psixologicheskij aspekty. Uchenye zapiski Kazanskogo universiteta. ser. gumanitarnye nauki. 2008; (3): 139–150. Russian.
29. Sudakov KV. Informaciya v deyatel'nosti funkcional'nyx sistem organizma. Vestnik Chelyabinskogo gosudarstvennogo universiteta. Filosofiya. Sociologiya. Kul'turologiya. 2009; 149 (11): 35–46. Russian.

Литература

1. Самойлов А. С., Бушманов А. Ю., Бобров А. Ф., Щебланов В. Ю., Седин В. И., Калинина М. Ю. Психофизиологические аспекты обеспечения надежности профессиональной деятельности работников организаций атомной отрасли. В сборнике: Материалы III отраслевой научно-практической конференции. АНО ДПО «Техническая академия Росатом». М., 2018; с. 62–76.
2. Организация и проведение психофизиологических обследований работников организаций, эксплуатирующих особо радиационно опасные и ядерно опасные производства и объекты в области использования атомной энергии, при прохождении работниками медицинских осмотров в медицинских организациях ФМБА России. Методические рекомендации Р ФМБА России 2.2.9.84 - 2015. Москва, 2015.
3. Руководство по оценке и интерпретации результатов мониторинга психофизиологического состояния работников организаций, эксплуатирующих особо радиационно опасные и ядерно опасные производства и объекты в области использования атомной энергии. ФМБА России 2.2.9. 2014; 40 с.
4. Бобров А. Ф., Бушманов А. Ю., Седин В. И., Щебланов В. Ю. Системная оценка результатов психофизиологических обследований. Медицина экстремальных ситуаций. 2015; (3):

- 13–9.
5. Торубаров Ф. С., Бушманов А. Ю., Зверева З. Ф., Кретов А. С., Лукьянова С. Н., Денисова Е. А. Концепция психофизиологического обследования персонала объектов использования атомной энергии в медицинских организациях. Медицина экстремальных ситуаций. 2021; 23 (1): 13–8.
 6. Лурия А. Р. Высшие корковые функции человека и их нарушение при локальных поражениях мозга. М.: Академ. проект, 2000; 433 с.
 7. Лоскутова Т. Д. Оценка функционального состояния центральной нервной системы человека по параметрам простой двигательной реакции. Физиологический журнал СССР. 1975; 61 (1): 3–12.
 8. Баевский Р. М. Концепция физиологической нормы и критерии здоровья. Российский физиологический журнал им. И. М. Сеченова. 2003; (4): 473–87.
 9. Исаева Н. А., Торубаров Ф. С., Зверева З. Ф., Лукьянова С. Н., Денисова Е. А. Биоэлектрическая активность головного мозга у работников Нововоронежской и Белоярской АЭС с разным уровнем адаптации к условиям их трудовой деятельности. Медицинская радиология и радиационная безопасность. 2016; 61 (5): 5–12.
 10. Торубаров Ф. С., Зверева З. Ф., Лукьянова С. Н. ЭЭГ показатели состояния центральной нервной системы у лиц с различными уровнями психофизиологической адаптации. Саратовский научно-медицинский журнал. Приложение октябрь-декабрь. 2019; 15 (4): 965–7.
 11. Торубаров Ф. С., Зверева З. Ф., Лукьянова С. Н. Биоэлектрическая активность головного мозга у оперативного персонала АЭС России с низким уровнем психофизиологической адаптации. Медицинская радиология и радиационная безопасность. 2021; 66 (2): 23–35.
 12. Зверева З. Ф., Торубаров Ф. С., Денисова Е. А., Мирошник Е. Прогностические критерии психофизиологической адаптации по данным сравнительной характеристики визуального анализа и показателей мощности биоэлектрических потенциалов ЭЭГ у работников ядерно опасных предприятий и производств. Медицина труда и промышленная экология. 2021; 61 (9): 588–94.
 13. Кирсанов В. М. Оценка степени адаптации индивида на основе показателей энергетического потенциала головного мозга и психодиагностического обследования. Инновации в науке. 2012; (8): 64–8.
 14. Foster C, Steventon JJ, Helme D, Tomassini V, Wise RG. Cerebral Metabolic Changes During Visuomotor Adaptation Assessed Using Quantitative fMRI. *Front Physiol.* 2020 May 8; 11: 428.
 15. Фокин В. Ф., Пономарева Н. В. Энергетическая физиология мозга. Москва: «Антидор», 2003; 288 с.
 16. Грибанов А. В., Аникина Н. Ю., Гудков А. Б. Церебральный энергообмен как маркер адаптивных реакций человека в природно-климатических условиях Арктической зоны Российской Федерации. Экология человека. 2018; (8): 32–40.
 17. Грибанов А. В., Котцова О. Н., Аникина Н. Ю., Панков М. Н., Корельская И. Е. Сезонные изменения церебрального энергообмена при разном уровне тревожности у молодых людей в арктической зоне российской федерации. Человек. Спорт. Медицина. 2021; 21 (4): 73–80.
 18. Trimmel M, Strässler F, Knerer K. Brain DC potential changes of computerized tasks and paper/pencil tasks. *Int J Psychophysiol.* 2001; 40 (3): 187–94.
 19. Зверева З. Ф. Характер межполушарного распределения мощности биопотенциалов головного мозга в норме и при его латерализованном поражении [диссертация]. М., 2004.
 20. Мирошник Е. В., Зверева З. Ф., Бобров А. Ф., Баскаков И. С., Ванчакова Н. П., Еланская О. В. Сопоставление показателей биоэлектрической активности головного мозга и энергетических процессов в ткани мозга (Величины межполушарных различий гомологичных отведений и уровня постоянного потенциала головного мозга). Медицина экстремальных ситуаций. 2017; 60 (2): 49–59.
 21. Березин Ф. Б. Психическая и психофизиологическая адаптация человека. Л.: Наука, 1988; 270 с.
 22. Березин Ф. Б., Мирошников М. П., Соколова Е. Д., Методика многостороннего исследования личности (ММИЛ): структура, основы интерпретации, некоторые области применения. М.: Изд-во «Березин Феликс Борисович», 2011; 320 с.
 23. Cattell RB, Eber HW. Handbook for the Sixteen Personality factor Questionnaire. Illinois, 1964.
 24. Raven JC. A manual for Raven's progressive matrices and vocabulary tests. London: H.K. Levis @ Go. Ltd, 1988.
 25. Секоян И. Э. «Локус контроля» Джулиана Роттера с позиций психометрии. Независимый психиатрический журнал. 2008; 3: 18–25.
 26. Анохин П. К. Очерки по физиологии функциональных систем. М.: Наука, 1975; 447 с.
 27. Селье Г. Стресс без дистресса. М.: Прогресс, 1979; 124 с.
 28. Юнусова С. Г., Розенталь А. Н., Балтина Т. В. Стресс. Биологический и психологический аспекты. Ученые записки Казанского университета. сер. гуманитарные науки. 2008; (3): 139–150.
 29. Судаков К. В. Информация в деятельности функциональных систем организма. Вестник Челябинского государственного университета. Философия. Социология. Культурология. 2009; 149 (11): 35–46.

DYNAMICS OF HUMORAL IMMUNITY TO SARS-COV-2 IN THE PROFESSIONALLY HOMOGENEOUS GROUP OF PEOPLE OVER A TWO-YEAR PERIOD OF COVID-19 OUTBREAK

Pomelova VG , Bychenkova TA, Bekman NI, Osin NS, Ishkov YuN, Styazhkin KK

State Research Institute of Biological Instrumentation of the Federal Medical Biological Agency, Moscow, Russia

It is important to control the levels of specific IgG against SARS-CoV-2 to ensure the timely monitoring of immunity in patients with COVID-19. Yet it is unclear what antibody levels protect against new infection and how long the protection is maintained. The study was aimed to assess the dynamic changes in the levels of IgG against SARS-CoV-2 by the two-year controlled observation. Healthy individuals ($n = 70$), COVID-19 survivors ($n = 42$), and people vaccinated with Sputnik V ($n = 43$) were enrolled. They were followed-up from April 2020 to April 2022. Serum IgG levels were defined ($n = 312$) using immunochip and the commercially available test system. Significance of differences was estimated using the Mann-Whitney U test for $p \leq 0.05$. IgG levels in the disease survivors (median 97.1; 95% CI: 80–162 BAU/mL) and vaccinated individuals (103.1; 78–139 BAU/mL) were significantly higher than in healthy people (4.3; 4.1–4.5 BAU/mL). Intensity of immune response significantly increased after vaccination of the disease survivors (up to 1023; 657–1191 BAU/mL) or administration of booster dose to vaccinated individuals (413; 213–545 BAU/mL). In elderly convalescents (60+), IgG levels were significantly higher, and in vaccinated people these were significantly lower, than in people under the age of 60. IgG levels decreased faster in vaccinated individuals (after 3–4 months), than in the disease survivors, and stabilized at <100 BAU/mL in 60% of subjects within 5–9 months. Thus, intensity and duration of immune response in COVID-19 survivors and vaccinated people vary significantly depending on age, observation period, and additional vaccinations/revaccinations. Three cases of infection after full vaccination were reported over the entire follow-up period, including infection in a patient having a history of the disease and subsequent vaccination.

Keywords: COVID-19, IgG, SARS-CoV-2, dynamics of immune response, patients, age, Sputnik V vaccine, immunochip

Acknowledgements: we would like to thank staff members of the State Research Institute of Biological Instrumentation: Kanaeva TA for carrying out immunochip-based analysis, Balaban AS for antigen printing with nanoplotter and immunochip preparation for analysis, Stadnik OB for management of the serum samples acquisition and testing using commercially available immunoassay kit.

Author contribution: Pomelova VG — concept, experimental design, manuscript writing; Bychenkova TA — management of immunochip-based immunochemistry studies, data processing; Bekman NI — statistical analysis, preparation of illustrations; Osin NS — providing technical assistance, data analysis and discussion, manuscript editing; Ishkov YuN, Styazhkin KK — data analysis and discussion, manuscript editing.

Compliance with ethical standards: the study was approved by the Ethics Committee of the State Research Institute of Biological Instrumentation (protocol № 4 dated June 09, 2021). The informed consent was submitted by all subjects.

 **Correspondence should be addressed:** Vera G. Pomelova
Volokolamskoe shosse, 75, corp. 1, Moscow, 125424, Russia; v.pomelova@immunoscreen.ru

Received: 19.05.2022 **Accepted:** 04.06.2022 **Published online:** 16.06.2022

DOI: 10.47183/mes.2022.020

ДИНАМИКА ГУМОРАЛЬНОГО ИММУННОГО ОТВЕТА К SARS-COV-2 В ПРОФЕССИОНАЛЬНО ОДНОРОДНОЙ ГРУППЕ ЛЮДЕЙ ЗА ДВУХЛЕТНИЙ ЭПИДЕМИЧЕСКИЙ ПЕРИОД COVID-19

В. Г. Помелова , Т. А. Быченкова, Н. И. Бекман, Н. С. Осин, Ю. Н. Ишков, К. К. Стяжкин

Государственный научно-исследовательский институт биологического приборостроения Федерального медико-биологического агентства, Москва, Россия

Для оперативного мониторинга состояния системы иммунитета при COVID-19 важно контролировать уровень специфических IgG к SARS-CoV-2. Однако неясно, какой уровень антител и насколько долго может обеспечить защиту от нового заражения. Целью работы было оценить в двухлетнем контролируемом обследовании динамику уровней IgG к SARS-CoV-2. В исследовании участвовали здоровые лица ($n = 70$), переболевшие COVID-19 ($n = 42$) и вакцинированные «Спутником V» ($n = 43$). Период наблюдения: апрель 2020 г. — апрель 2022 г. IgG выявляли в сыворотке крови ($n = 312$) на иммуночипе и в коммерческом тесте. Достоверность различий оценивали по критерию Манна-Уитни для $p \leq 0,05$. Уровни IgG у переболевших (медиана 97,1; 95% ДИ: 80–162 BAU/мл) и вакцинированных (103,1; 78–139 BAU/мл) были достоверно выше, чем у здоровых людей (4,3; 4,1–4,5 BAU/мл). Напряженность иммунного ответа значительно возросла после вакцинации переболевших (до 1023; 657–1191 BAU/мл) или введения бустера вакцинированным (413; 213–545 BAU/мл). У реконвалесцентов старшего возраста (60+) уровень IgG достоверно выше, у вакцинированных — достоверно ниже, чем у людей моложе 60. IgG у вакцинированных снижались быстрее (через 3–4 месяца), чем у переболевших, а через 5–9 месяцев стабилизировались на уровне <100 BAU/мл у 60% обследованных. Таким образом, показатели напряженности и продолжительности иммунного ответа у переболевших COVID-19 и вакцинированных людей сильно варьируют в зависимости от возраста, срока наблюдения, дополнительной вакцинации / ревакцинации. За весь период наблюдений отмечено три случая заболевания после полного цикла вакцинации, в том числе у ранее переболевшего (а затем вакцинированного) человека.

Ключевые слова: COVID-19, IgG, SARS-CoV-2, динамика иммунного ответа, пациенты, возраст, вакцина «Спутник V», иммуночип

Благодарности: сотрудникам ФГУП «ГосНИИБП» Т. А. Канаевой — за постановку анализа на иммуночипе; А. С. Балабану — за печать антигенов на наноплоттере и подготовку иммуночипа к работе; О. Б. Стаднику — за организацию сбора и тестирования образцов сывороток в коммерческом тесте.

Вклад авторов: В. Г. Помелова — идея, дизайн экспериментов, подготовка рукописи; Т. А. Быченкова — руководство проведением иммунохимических исследований на иммуночипе, обработка результатов; Н. И. Бекман — статистический анализ, подготовка иллюстративного материала; Н. С. Осин — организация технической части исследований, анализ и обсуждение результатов, корректировка рукописи; Ю. Н. Ишков, К. К. Стяжкин — анализ и обсуждение результатов, корректировка рукописи.

Соблюдение этических стандартов: исследование одобрено этическим отделом ФГУП «ГосНИИБП» (протокол № 4 от 09 июня 2021 г.). Все участники подписали добровольное согласие на участие в исследовании.

 **Для корреспонденции:** Вера Гавриловна Помелова
Волоколамское шоссе, д. 75, корпус 1, г. Москва, 125424, Россия; v.pomelova@immunoscreen.ru

Статья получена: 19.05.2022 **Статья принята к печати:** 04.06.2022 **Опубликована онлайн:** 16.06.2022

DOI: 10.47183/mes.2022.020

The pandemic of novel Coronavirus Disease 2019 (COVID-19), declared by the WHO in March 2020, required a substantial effort on the part of the health systems of different countries, including Russia, to provide morbidity surveillance and the measures to reduce the risk of infection. From an epidemiological standpoint, the most effective protection is ensured by herd immunity developing naturally due to the growing proportion of insusceptible people having a history of infection in the population, or due to vaccination.

It is recommended to control the levels of circulating IgG antibodies to ensure timely monitoring of immunity [1, 2]. For that purpose, it is necessary to use the registered test systems for quantification of antibodies against various coronavirus antigens (S, S1, RBD, N). It is believed that there is a strong correlation between the levels of antibodies against the spike protein S1 receptor-binding domain (RBD) of SARS-CoV-2 and the neutralizing antibody titers measured using neutralization test [3].

However, it is still unclear what antibody levels ensure sufficient protection of the patient against the same and especially against new variants of SARS-CoV-2, and how long the necessary protection is maintained, that results from infection or vaccination [4]. The intensity and duration of immune response vary significantly among patients [5] and are largely dependent on gender, age, and COVID-19 severity [6–9].

The dynamic changes in humoral immunity are studied mainly within 6–8 months after the disease onset or vaccination [5, 8, 9]. That is why a longer follow-up is needed to assess individual characteristics of the developing protective immunity, which provide the basis for forecasting future trends of the pandemic [10], and developing personalized protocols for vaccination [8] and treatment.

It is of interest to obtain data on IgG formation and maintaining the level of IgG antibodies against SARS-CoV-2 over the two-year observation period, the longest-ever reported in the literature.

The study was aimed to assess the dynamic changes in the levels of IgG against SARS-CoV-2 in the two-year controlled observation of the State Research Institute of Biological Instrumentation staff members, and to define the factors affecting the intensity and duration of humoral immunity.

METHODS

Patients

The study was carried out in the molecular diagnostic laboratory of the State Research Institute of Biological Instrumentation from April 2020 to April 2022. A total of 77 research institute staff members and 8 members of their families were enrolled, who had COVID-19 or were vaccinated during the period. Inclusion of family disease history was justified by the possibility of expanding the age range (16–88 years) when assessing IgG levels and dynamic changes in people who had recovered from or were vaccinated against the disease, and by identification of possible disease features in cohabiting family members. Inclusion criteria: well-documented case of COVID-19 or vaccination/revaccination (discharge summary, vaccination certificate). Exclusion criteria: incomplete information about the patient, error in labeling or inadequate appearance of serum samples (hemolysis, drying, microbial germination).

The subjects (a total of 155 people) were divided into three groups (Table 1): control group H that included healthy donors (70 people; serum samples were collected before the

pandemic in order to perform another study [11]); group D that included convalescents (COVID-19 survivors, who had not been vaccinated before the disease onset); group V that included vaccinated people (who had no COVID-19 before vaccination and were vaccinated with two doses of Sputnik V).

In group D, 24 out of 42 disease survivors (57.1%) were fully vaccinated with Sputnik V 6–22 months (13.5 on average) after the disease onset; among them 3 individuals were later vaccinated with Sputnik Light (subgroup D + V).

In group V, 14 out of 43 people (32.6%) were revaccinated (RV). They received a booster dose of one of the vaccines (6–9 months after receiving the first dose of Sputnik V): two doses of Sputnik V (8 people) or CoviVac (2 people), and a single dose of Sputnik Light (4 people) (subgroup V + RV).

All the listed above vaccines, Sputnik V, Sputnik Light (N. F. Gamaleya National Research Center for Epidemiology and Microbiology; Russia), CoviVac (Chumakov Federal Scientific Center for Research and Development of Immune-and-Biological Products; Russia), were registered and approved in the Russian Federation. Vaccination was performed by healthcare professionals in accordance with the manufacturer's instructions.

There were no significant differences between the groups in gender (there were 71 males and 84 females) or age (the average age was 52 years, the age range was 16–88 years).

A total of 1–12 serum samples were obtained from each subject, including before the disease onset (or vaccination) and on various dates after the disease onset (or administration of the first vaccine dose); a total of 312 serum samples were collected (Table 1). Serum aliquots were stored at –20 °C prior to analysis.

Based on medical records (taking into account the length of hospital stay and the extent of lung damage based on the computed tomography results), moderate to severe COVID-19 was diagnosed in 11 out of 42 infected people (26.2%) in the group D; the others had a mild disease.

Assessment of IgG against SARS-CoV-2

In 99 out of 312 serum samples (31.7%), IgG levels were measured by chemiluminescence immunoassay with the ARCHITECT i1000sr immunoassay analyzer (Abbott Laboratories; USA) using the SARS-CoV-2 IgG II Quant Reagent Kit (Abbott Ireland Diagnostic Division; Ireland). Analysis was performed by INVITRO (Moscow).

In 312 serum samples (100%), IgG levels were measured using the experimental immunoassay-based test system (State Research Institute of Biological Instrumentation), based on the domestic patented PHOSPHAN phosphorescence analysis technology for identification of the infectious and somatic disease markers [11–13]. Immunoassay was performed in the wells of standard polystyrene microplates by the method similar to the enzyme-linked immunosorbent assay (ELISA). In contrast to ELISA, eight microzones (0.5 mm in diameter each) were printed on the bottom of each well, four microzones per each of two antigens: recombinant SARS-CoV-2 spike protein, RBD, Wuhan variant (catalog number ATMP02479COV; AtaGenix, China), and recombinant SARS-CoV-2 spike protein, RBD (L452R, T478K), variant B.1.617.2, Delta (code YP-009724390.1, catalog number ATMP02527COV; AtaGenix, China).

Serum samples diluted 1 : 100 were injected into the wells of the microplate 50 µL per well. After the 1.5-hour incubation, 50 µL of biotinylated (100 ng/50 µL, 1-hour incubation) monoclonal antibody against human IgG (SORBENT; Russia), and 40 µL of streptavidin (Sigma-Aldrich; USA) conjugated

Table 1. General characteristics of blood sera donors

Group (number) of subjects	Code of the group	Time range of the registered disease cases or vaccination events	Number		Average age (range), years	Number of assessed serum samples
			males	females		
Healthy people (70)	H	No	30	40	50 (20–64)	70
COVID-19 survivors (42)	D	04.2020 – 10.2021	22	20	50 (16–78)*	132
Of them vaccinated with Sputnik V 6–22 months after the disease onset (24)**	D + V	02.2021 – 11.2021	12	12	49 (21–78)*	32
Vaccinated people (43)	V	12.2020 – 09.2021	19	24	55 (26–88)*	110
Of them revaccinated (14)***	V + RV	07.2021 – 01.2022	8	6	61 (38–76)*	14
Total (155)		04.2020 – 01.2022	71	84	52 (16–88)*	312

Note: * — extreme points of the age range (16, 76, 78, 88 years) are represented by relatives of the research institute staff members; ** — including 3 people revaccinated with Sputnik Light about 6 months after receiving the first dose of Sputnik V; *** — booster vaccination with Sputnik V, 2 doses (8 people), Sputnik Light (4 people) or CoviVac, 2 doses (2 people) 6–9 months after receiving the first dose of Sputnik V.

to platinum coproporphyrin (13 ng/40 μ L, 30-min incubation) were added to each well. All steps were performed at room temperature with the samples shaken in a shaker. Microplate was three times washed with buffer solution between the steps, and at the final stage it was additionally three times washed with distilled water. Microplate was dried, and then fluorescence intensity was measured with the IPI-05 indicator unit (Immunoscreen, Russia; MA number RZN, January 21, 2022) by time-resolved scanning of the microplate well bottoms.

IgG levels (measured in BAU/mL) were calculated using calibration curves for each of two antigens of the immunochip. Calibration samples were certified based on the first WHO International Standard. The measurement range was 0–10000 BAU/mL. Quality control measurements involved the use of the positive control serum (obtained from the COVID-19 survivor) with the IgG level of about 500 BAU/mL, and the negative control serum (made of serum obtained from healthy donor before the pandemic; according to the commercially available immunoassay, contained no IgG against SARS-CoV-2), which were included in the assay settings. Test results were considered positive (antibody detected) when IgG levels exceeded 10.0 BAU/mL.

Statistical analysis

Statistical processing of the results was performed using the standard Microsoft Office Professional Plus Excel 2013

v. 15.0.4727.1000 (Microsoft; USA) and MedCalc v. 10 (MedCalc Software; Belgium) software using the parametric and non-parametric techniques for data analysis. The Pearson correlation method was used to assess the degree of correlation; significance of differences was estimated using the Mann–Whitney U test for the significance level of 0.05 ($p \leq 0.05$).

RESULTS

There was a high degree of correlation between IgG levels measured by commercially available immunoassay and with the use of immunochip containing SARS-CoV-2 Wuhan variant ($r = 0.928544$; $N = 99$) or Delta variant ($r = 0.933363$; $N = 99$); correlation coefficient for the results obtained for two variants of the virus was 0.978057 ($N = 312$). Against this background, the results of IgG identification are provided only for immunochip containing a Wuhan variant of the virus.

Distribution of the COVID-19 cases among the subjects is presented in Fig. 1. The first cases were reported in April 2020, and the maximum number of infected people was reported in May. The second wave of infection took place from September 2020 to January 2021: 27 out of 42 group D members (64.3%) were infected; of them five people were unvaccinated, and one was a COVID-19 survivor who had been vaccinated with Spnitnik V 10 months after recovery.

Vaccination campaign was launched in late December 2020. By April 2021, 30 out of 43 people (69.8%) were fully

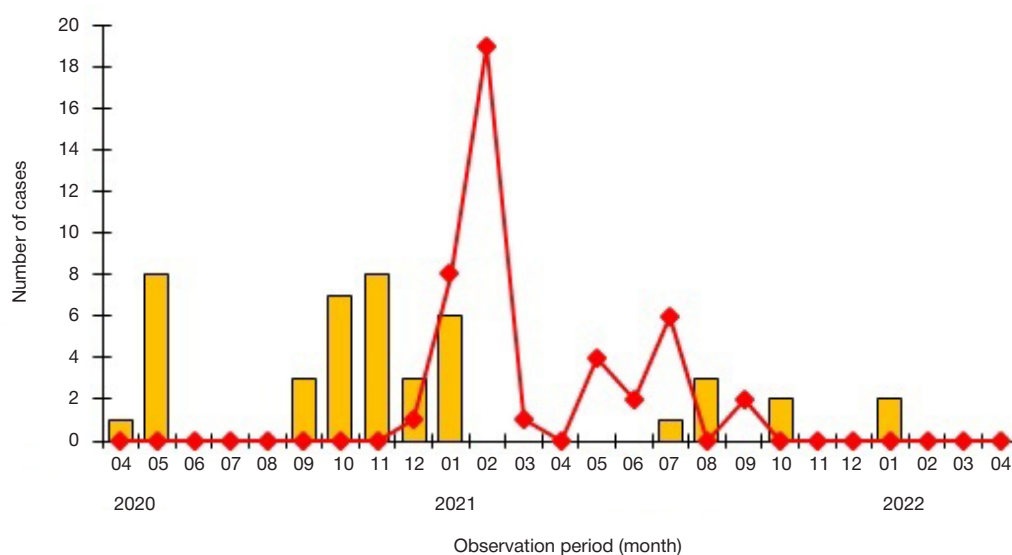


Fig. 1. Monthly distribution of people getting COVID-19 (histograms) and vaccinated with Sputnik V (curve) over the two-year observation period

Table 2. Serum anti-SARS-CoV-2 IgG levels as a function of gender and age

Group	Indicator	Number of samples	Median [95% CI] IgG levels, BAU/mL	<i>p</i>
D: COVID-19 survivors	Gender: male female	44	83,1 [56,5–106,7]	0,2099
		39	160,1 [85,9–225,7]	
	Age, years: ≥ 60 < 60	26	162,8 [95,9–241,2]*	0,0268
		57	84,4 [55,6–128,5]*	
V: vaccinated	Gender: male female	19	79,7 [35,7–143,4]	0,1104
		33	117,7 [86,6–224,5]	
	Age, years: ≥ 60 < 60	22	77,4 [25,9–99,6]*	0,0191
		30	137,0 [101,8–228,1]*	

Note: CI — Confidence Interval; * — the difference between the groups is statistically significant.

vaccinated with Sputnik V, and by October 100% of the group V members were vaccinated. Two members of this group were infected in January 2022, six months after administration of the first vaccine dose (Fig. 1).

In elderly COVID-19 survivors (aged 60+), IgG levels were significantly higher ($p = 0.0268$) than in people under the age of 60. On the contrary, significant negative correlation with age was revealed in fully vaccinated people who had no COVID-19 ($p = 0.0191$). The patients' gender had no significant effect on the antibody levels (Table 2).

The majority of infected individuals (73.8%) had a mild disease. Moderate to severe course of infection was reported in 11 people (26.2%). These cases were evenly distributed over the months of the observation period. Males were severely ill more frequently than females (eight out of 22 (36.4%) vs. three out of 20 (15%)); however, the differences were non-significant due to small sample size. The age

of individuals with severe COVID-19 was 35–77 years (on average, 58 years). Among eight severely ill males, only three were elderly (70–77 years), and the others were 53 years of age or younger.

High heterogeneity of antibody levels was noted in both COVID-19 survivors (Fig. 2A) and people vaccinated with two doses of Sputnik V (Fig. 2B), especially shortly after the disease onset or administration of the first vaccine dose (Fig. 2A, B).

In vaccinated people, IgG levels gradually declined (Fig. 2C). The maximum value (median 195.3; 95% CI: 45.5–403.2 BAU/mL) was reported on day 37–55 after administration of the first vaccine dose. By month 3–4, antibody levels declined by half (median 108.7; 95% CI: 75.1–147.2 BAU/mL), and by month 7–9 these decreased by four times (median 48.7; 95% CI: 29.8–145.7 BAU/mL). The same trend of the IgG decrease was observed in convalescents (Fig. 2C). The exception were antibody levels observed by month 3–4 after the disease onset.

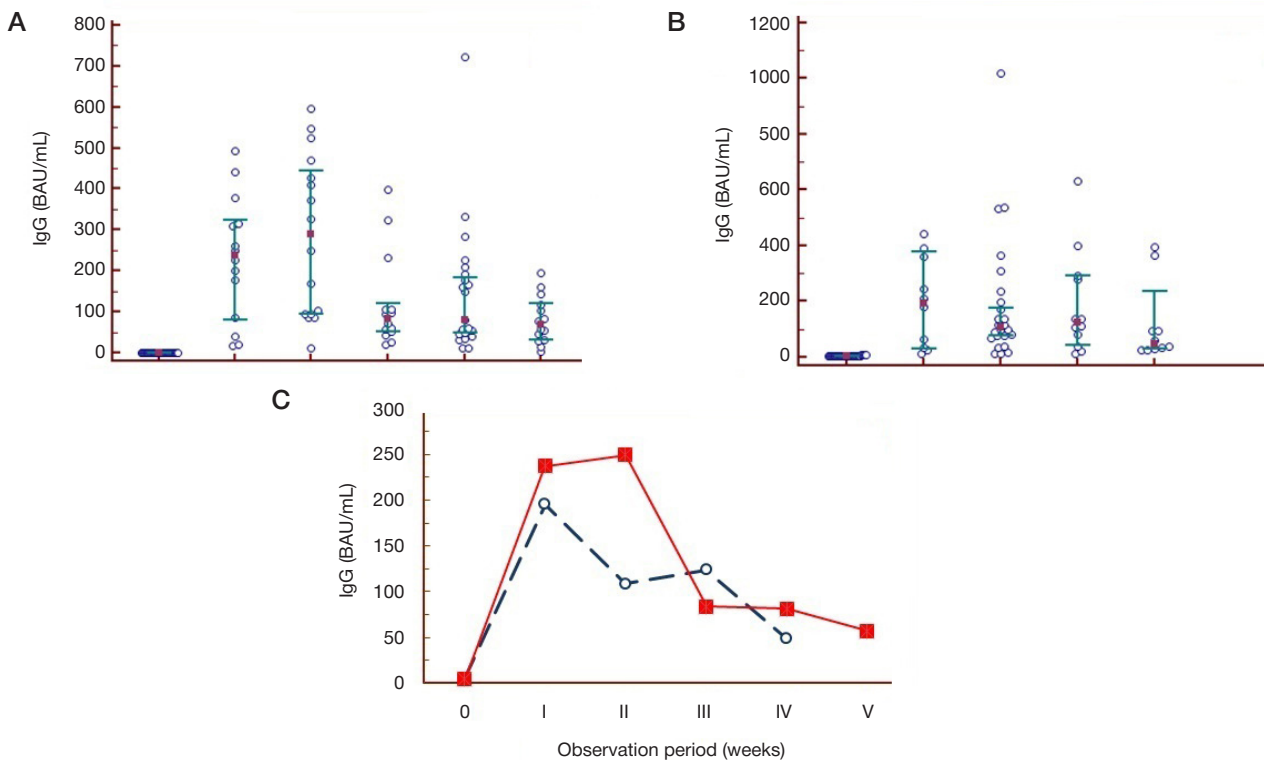


Fig. 2. A. Distribution of the serum levels of antibodies against SARS-CoV-2 in COVID-19 survivors. 0 — before the disease onset ($n = 16$); I — 2–8 ($n = 14$); II — 9–16 ($n = 17$); III — 17–24 ($n = 14$); IV — 25–36 ($n = 22$); V — 37–68 ($n = 15$). **B.** Distribution of the serum levels of antibodies against SARS-CoV-2 in people vaccinated with Sputnik V. 0 — before vaccination ($n = 38$); I — 6–8 ($n = 10$); II — 9–16 ($n = 24$); III — 17–24 ($n = 12$); IV — 25–36 ($n = 12$). Median values with 95% CI are provided for **A** and **B** (red dot). **C.** Median IgG levels for the observation period. 0 — before the disease onset or vaccination; I — 2–8 (survivors) or 6–8 (vaccinated individuals); II — 9–16; III — 17–24; IV — 25–36; V — 37–68. Median IgG levels are provided for the disease survivors (red line) and vaccinated people (blue dotted line)

These values (median 249.8; 95% CI: 94.9–427.5 BAU/mL) were significantly higher ($p = 0.029$) compared to those of vaccinated people observed within the same period after receiving the first vaccine dose. After 5–9 months, antibody levels stabilized at less than 100 BAU/mL (Fig. 2C) in about 60% of the subjects.

In general, antibody levels measured in the group D convalescents (median 97.1; 95% CI: 80–162 BAU/mL) and group V vaccinated individuals (median 103.1; 95% CI: 78–139 BAU/mL) were comparable; these values were significantly higher ($p < 0.0001$) than that of healthy donors (median 4.3; 95% CI: 4.1–4.5 BAU/mL). Vaccination of the disease survivors (subgroup D + V) or administration of booster dose to vaccinated people (subgroup V + RV) resulted in the significantly ($p < 0.0001$) increased immunity: up to median values of 1023 BAU/mL (95% CI: 657–1191) and 413 BAU/mL (95% CI: 213–545 BAU/mL), respectively (Fig. 3).

Three new COVID-19 cases confirmed by positive PCR test results were revealed during the whole observation period (Fig. 1, Table 3). Three women aged 40–43 were infected. Among them two women had no history of COVID-19, and one woman had COVID-19 about 16 months before the new infection. All of them were infected after full vaccination with Sputnik V, about six months after receiving the first vaccine dose; mild course of the disease was observed in all the women.

DISCUSSION

Significant effects of age on IgG levels were found (Table 2). In elderly convalescents (60+), antibody levels were significantly higher than in people under the age of 60. On the contrary, negative correlation with age was observed in fully vaccinated people who had no history of the disease. Similar patterns were revealed in other studies [6, 7].

No significant effects of gender on the antibody levels in COVID-19 patients could be determined due to small sample size. However, it is obvious that endocrine profile associated with biological differences between men and women can affect the immune response. According to our data, antibody levels in men are almost twice lower compared to those in women (Table 2). Furthermore, men have moderate to severe COVID-19 twice as frequently as women.

These observations are consistent with the results of assessing representative patient samples [6, 14, 15]. According to some reports, men have lower levels of CD4+ T cells and CD19+ B cells, which play a vital part in humoral and cellular immunity providing protection against COVID-19 [6]. This could result in delayed formation of protective antibodies against the coronavirus S1 protein receptor-binding domain. In women, IgG levels dramatically increased and reached peak

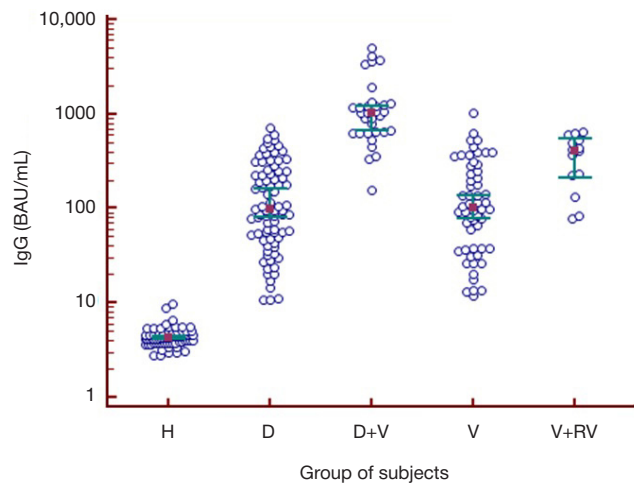


Fig. 3. Distribution of the serum levels of antibodies against SARS-CoV-2 in groups H ($n = 70$), D ($n = 84$), D + V ($n = 32$), V ($n = 58$), and V + RV ($n = 14$). Median values with 95% CI are provided (red dot)

values during the fourth week after the emergence of clinical symptoms, and in men antibody levels increased gradually and reached peak values during the seventh week [6, 14]. The fact of delayed antibody formation in combination with the clinical and biochemical data set made it possible to consider the patient's male gender a risk factor of more severe COVID-19 and death [6, 9].

We have failed to trace the influence of the disease severity on the protective immunity levels and dynamic changes, despite the availability of evidence of such relationship [7]. Unfortunately, we had only later samples collected mainly not earlier than 7–12 months after the disease onset, because staff members having a history of moderate to severe COVID-19 refused to provide samples shortly after recovery.

Analysis of family history of the disease in three research institute staff members revealed no patterns in the COVID-19 course in their cohabiting relatives (six people), who were infected with an interval of 2–3 days. Two staff members (woman aged 63 and man aged 58) had a mild disease; among their relatives (three people aged 26–78 and two people aged 16 and 42, respectively) only one person (aged 78) was admitted to hospital due to moderate disease. The third female employee (aged 62) was critically ill, however, her husband (aged 65) had a mild disease.

The intensity of humoral immunity was dependent on the time passed since the disease onset or administration of the first vaccine dose. IgG levels in vaccinated people decreased rapidly by month 3–4 of follow-up (Fig. 2B), which was in line with the literature data [8]. Antibody levels observed in convalescents during month 3–4 of follow-up were significantly

Table 3. Characteristics of new COVID-19 cases in staff members having a history of the disease and vaccinated individuals

Name (group)	Gender	Age	Date of previous COVID-19 infection	Vaccination date, vaccine type (dose)	IgG levels, BAU/mL	Date of new COVID-19 infection
RAA (V)	F	43	No	Sputnik V: 02.05.2021 (1) 23.05.2021 (2)	360,5*	15.10.2021
ZhOA (D + V)	F	40	15.10.2020	Sputnik V: 18.07.2021 (1) 08.08.2021 (2)	617,2**	31.01.2022
ZYuN (V)	F	43	No	Sputnik V: 23.07.2021 (1) 07.08.2021 (2)	37,2***	26.01.2022

Note: * — IgG level on day 42 after administration of the first vaccine dose; ** — IgG level on day 90 after administration of the first vaccine dose; *** — IgG level at the time of the disease onset.

higher ($p = 0.029$) than those observed in vaccinated people (Fig. 2B). This was due to the contribution of sera with high antibody levels obtained from elderly patients of both genders, especially males, whose antibody levels reached maximum values during this period (no data reported). The findings support the conclusion that there is a positive correlation between age and IgG levels in COVID-19 survivors (Table 2) and are probably an indirect evidence of the delayed protective immunity formation in men, as noted earlier [6].

In general, antibody levels decreased by month 5–9 and stabilized at less than 100 BAU/mL (Fig. 2B) in about 60% of surveyed patients, as noted by other researchers [10]. At the same time, significant individual differences in the dynamics of humoral immune response between the study participants were revealed given that at least two serum samples had been collected from each subject. In vaccinated people, IgG levels gradually decreased, as previously reported for the integral indicator of this group (Fig. 2B, 2C), however, in some COVID-19 survivors the levels of protective immunity remained unchanged until the end of the follow-up period (no data reported).

Only three new cases of infection after full vaccination with Sputnik V were revealed over the entire observation period (Fig. 1, Table 3). The subjects were infected and had a mild disease in October 2021 and January 2022, i.e. during the period when the highly contagious Delta and Omicron coronavirus variants predominated in Moscow, and the daily cases increase reached 9,000 and 26,000, respectively [16, 17]. Taking into account the total number (Table 1) of vaccinated people with no history of the disease (43 people) and vaccinated disease survivors (24 people), the prevalence of COVID-19 among vaccinated people was 4.5%. These findings were in line with the available data supporting the fact that Sputnik V vaccine never provided 100% protection [18, 19], but contributed to the milder COVID-19 course in vaccinated people [20].

It should be noted that in one infected female patient out of three, IgG level was low at the time of the disease onset (37.2 BAU/mL). In the other two female patients, antibody levels were 360.5 and 617.2 BAU/mL on days 42 and 90 after receiving the first vaccine dose, respectively (i.e. 3–4.5 months before the disease onset) (Table 3); however, these levels could be reduced in half or more at the time of the new infection, given the dynamics of IgG levels in vaccinated people (Fig. 2B). Although until now there is no clear understanding of what antibody levels are capable of providing sufficient protection against the same and especially against new variants of the SARS-CoV-2 coronavirus [4], the presence of antibodies is clearly not the only factor of protection against COVID-19 [9]. No new cases of infection in 95.5% of the surveyed people, the majority of them having the circulating antibody levels below 100 BAU/mL (Fig. 2C), support the view that the long-term protective immunity is largely ensured by complex interactions between the humoral and cellular immunity factors [5].

An important feature of the study is the use of immunochip allowing us to simultaneously assess the levels of antibodies against the receptor-binding domains of two SARS-CoV-2 variants (Wuhan and Delta). The data for the first variant are provided, since antibody levels measured for both variants are almost identical ($r = 0.978057$). This suggests that immune response in COVID-19 survivors and people vaccinated with Sputnik V provides effective protection against both variants, as noted earlier [21]. However, such overlapping results were obtained only for sera collected from patients, who had been

infected from April 2020 to January 2021, i.e. during the first two waves of infection among staff members (Fig. 1), when the majority of COVID-19 cases were caused by Wuhan (reference) variant and local Russian variants of the virus [22, 23]. People infected in July–October 2021 (the third wave of infection presented in Fig. 1) had at least twice as high levels of antibodies against the Delta variant, that prevailed in the population during this period [17, 23].

The increase in the analysis multiplexity, and, as a consequence, in informativeness is a global trend related to the possibility of combining several tests in a common format by means of miniaturization and development of high-density microarrays. Advanced multiplex technologies based on chemiluminescence methods and flow cytometry (for example, test systems manufactured by Merck, Luminex, etc.) provide an opportunity for simultaneous detection of up to 100 various markers and are best suited to assess the composite immune response when studying various aspects of COVID-19 [24, 25]. However, such tests are expensive; sophisticated equipment and highly qualified operator are required.

In our opinion, more simple and cost-effective tests, such as PHOSPHAN, are more beneficial when used for monitoring. Indeed, the resulting data set (high degree of correlation with the commercially available test, and possibility of detecting specific features of the specific antibody binding to the receptor-binding domains of two variants of novel coronavirus) taking into account the fundamental possibility of constructing multiplex tests of various design depending on the research tasks (for example, the use of a wider range of diagnostically significant antigens, internal positive and negative controls in immunochip) supports the assumption that PHOSPHAN technology platform may be beneficial when used to monitor the levels of circulating antibodies in COVID-19 survivors and vaccinated people. The immunochip developed can make it possible not only to detect specific antibodies, but also to distinguish between variants of the virus based on the significant differences in antibody titers, at least in people with no history of COVID-19 and unvaccinated patients. The detailed analysis of this situation is beyond the current scope of this study and will be reported later.

CONCLUSIONS

1. The intensity and duration of immune response in COVID-19 survivors and vaccinated people varied significantly depending on age, observation period, and additional vaccinations/revaccinations.
2. IgG levels were significantly higher in the following groups: elderly people (60+) having a history of COVID-19 compared to individuals under the age of 60; COVID-19 survivors and individuals vaccinated with Sputnik V compared to people with no disease history and unvaccinated individuals; disease survivors after vaccination and vaccinated individuals after receiving the booster dose.
3. IgG levels were significantly lower in vaccinated elderly people (60+) compared to individuals under the age of 60.
4. IgG levels in vaccinated individuals decreased faster (within 3–4 months), than in COVID-19 survivors; after 5–9 months IgG levels were stabilized at less than 100 BAU/mL in about 60% of subjects.
5. The prevalence of COVID-19 among vaccinated people was 4.5% (three vaccinated people out of 67 were infected).
6. Multiplex immunochip analysis is a promising method for simultaneous quantification of antibodies against two or even more variants of the novel SARS-CoV-2 coronavirus.

References

- Popova AY, Ezhlova EB, Melnikova AA, Andreeva EE, Kombarova SY, Lyalina LV, et al. Kollektivnyy immunitet k SARS-CoV-2 zhitelej Moskvy v ehpidemicheskij period COVID-19. *Infekcionnye bolezni*. 2020; 18(4): 8–16. DOI: 10.20953/1729-9225-2020-4-8-16. Russian.
- Ahmed ZB, Razu MH, Akter F, Rabby RI, Karmaker P, Kha M. Seropositivity of SARS-CoV-2 IgG Antibody among People in Dhaka City during the Prevaccination Period. *Hindawi BioMed Research International*. 2022; 2022: 6. Available from: <https://doi.org/10.1155/2022/4451144>.
- Santiago L, Uranga-Murillo I, Arias M, González-Ramírez AM, Macías-León J, Moreo E, et al. Determination of the Concentration of IgG against the Spike Receptor-Binding Domain That Predicts the Viral Neutralizing Activity of Convalescent Plasma and Serum against SARS-CoV-2. *Biology*. 2021; 10: 208. Available from: <https://doi.org/10.3390/biology10030208>.
- Karmishin AM., Nosov NYu, Postupajlo VB, Zhigarlovskij BA, Kruglov AA, Petuxov AN. Method for quantitative assessment of protective immunity against SARS-COV-2, its duration and antibody dynamics. *Extreme Medicine*. 2021; 2(23): 5–12. DOI: 10.47183/mes.2021.019. Russian.
- Dan JM, Mateus J, Kato Yu, Hastie KM, Yu ED, Faliti CE, et al. Immunological memory to SARS-CoV-2 assessed for up to 8 months after infection. *Science*. 2021; 371: eabf4063 (2021). DOI: 10.1126/science.abf4063.
- Huang B, Cai Yu, Li N, Li K, Wang Z, Li L, et al. Sex-based clinical and immunological differences in COVID-19. *BMC Infectious Diseases*. 2021; 21: 647. Available from: <https://doi.org/10.1186/s12879-021-06313-2>.
- Schlickeiser S, Schwarz T, Steiner S, Wittke K, Al Beshar N, Meyer O, et al. Disease severity, fever, age, and sex correlate with SARS-CoV-2 neutralizing antibody responses. *Front Immunol*. 2021; 11: 628971. DOI: 10.3389/fimmu.2020.628971.
- Naaber P, Tserel L, Kangro K, Sepp E, Jürjenson V, Adamson A, et al. Dynamics of antibody response to BNT162b2 vaccine after six months: a longitudinal prospective study. *The Lancet Regional Health — Europe*. 2021; 10: 1–10. Available from: <https://doi.org/10.1016/j.lanpe.2021.100208>.
- Markewitz R, Torge A, Wandinger K-P, Pauli D, Franke A, Bujanda L, et al. Clinical correlates of anti SARS CoV 2 antibody profiles in Spanish COVID 19 patients from a high incidence region. *Scientific Reports*. 2021; 11: 4363. Available from: <https://doi.org/10.1038/s41598-021-83969-5>.
- Li C, Yu D, Wu X, Liang H, Zhou Z, Xie Y, et al. Twelve-month specific IgG response to SARS-CoV-2 receptor-binding domain among COVID-19 convalescent plasma donors in Wuhan. *Nature Communications*. 2021; 12: 4846. Available from: <https://doi.org/10.1038/s41467-021-25109-1> | www.nature.com/naturecommunications.
- Pomelova VG, Korenberg EI, Kuznetsova TI, Bychenkova TA, Bekman NI, Osin NS. C6 Peptide-Based Multiplex Phosphorescence Analysis (PHOSPHAN) for Serologic Confirmation of Lyme Borreliosis. *PLoS ONE*. 2015; 10(7): e0130048. DOI: 10.1371/journal.pone.0130048.
- Bekman NI, Pomelova VG, Osin NS. Mul'tipleksnyj analiz narkoticheskix sredstv na osnove texnologii immunochipov FOSFAN. *Klinicheskaya laboratornaya diagnostika*. 2018; 63(3): 178–83. Available from: <http://dx.doi.org/10.18821/0869-2084-2018-63-3-178-183>. Russian.
- Bekman NI, Laricheva SYu, Bychenkova TA, Pomelova VG, Osin NS. Odnovremennoe opredelenie tireotropnogo gormona i svobodnogo tiroksina v suxix pyatnax krovi cheloveka s ispol'zovaniem fosforescentnyx nanochastic. *Biorganicheskaya ximiya*. 2020; 46(2): 170–9. DOI: 10.31857/s0132341320020074. Russian.
- Markmann AJ, Giallourou N, Bhowmik DR, Hou YJ, Lerner A, Martinez DR, et al. Sex disparities and neutralizing-antibody durability to SARS-CoV-2 infection in convalescent individuals. *mSphere*. 2021; 6: e00275-21. Available from: <https://doi.org/10.1128/mSphere.00275-21>.
- Zeng F, Dai C, Cai P, Wang J, Xu L, Li J, et al. A comparison study of SARS-CoV-2 IgG antibody between male and female COVID-19 patients: A possible reason underlying different outcome between sex. *J Med Virol*. 2020; 1–5. DOI: 10.1002/jmv.25989.
- Statistika koronavirusa v Moskve. Available from: <http://russian-trade.com/coronavirus-russia/Moskva>.
- Knorre DD, Nabieva E, Garushyanc SK. Rossijskij konsorcium po sekvenirovaniyu genomov koronavirusov (CORGI). Dostupno po ssylke: <http://taxameter.ru>. Russian.
- Logunov DY, Dolzhikova IV, Zubkova OV, Tuchvatullin AI, Shcheblyakov DV, Dzharullaeva AS, et al. Safety and immunogenicity of an rAd26 and rAd5 vector-based heterologous prime-boost COVID-19 vaccine in two formulations: two open, non-randomised phase — studies from Russia. *The Lancet*. 2020; 396(10255): 887–97. Available from: [https://doi.org/10.1016/S0140-6736\(20\)31866-3](https://doi.org/10.1016/S0140-6736(20)31866-3).
- Logunov DY, Dolzhikova IV, Shcheblyakov DV, Tuchvatullin AI, Zubkova OV, Dzharullaeva AS, et al. Safety and efficacy of an rAd26 and rAd5 vector-based heterologous prime-boost COVID-19 vaccine: an interim analysis of a randomised controlled phase 3 trial in Russia. *The Lancet*. 2021; 397(10275): 671. Available from: [https://doi.org/10.1016/S0140-6736\(21\)00234-8](https://doi.org/10.1016/S0140-6736(21)00234-8).
- Kolobuxina LV, Burgasova OA, Kruzhkova IS, Bakalin VV, Generalova LV, Shagaev AV, et al. Ocenka klinicheskogo techeniya COVID-19 u pacientov, vakcinirovannyx «Sputnik V», izmenchivosti RBD-domena S-belka SARS-COV-2 i virusnejtralizuyushhix svoystv syvorotki. *Vestnik RGMU*. 2021; 5: 66–75. DOI: 10.24075/vrgmu.2021.046. Russian.
- Gushchin VA, Dolzhikova IV, Shchetinin AM, Odintsova AS, Siniavin AE, Nikiforova MA, et al. Neutralizing activity of sera from Sputnik V-vaccinated people against variants of concern (VOC: B.1.1.7, B.1.351, P.1, B.1.617.2, B.1.617.3) and Moscow endemic SARS-CoV-2 variants. *Vaccines*. 2021; 9: 779. Available from: <https://doi.org/10.3390/vaccines9070779>.
- Garafutdinov RR, Mavzyutov AR, Nikonorov YuM, Chubukova OV, Matniyazov RT, Bajmiev AnX, et al. Betakoronavirus SARS-CoV-2, ego genom, raznoobrazie genotipov i molekulyarno-biologicheskie mery bor'by s nim. *Biomika*. 2020; 12(2): 242–71. DOI: 10.31301/2221-6197.bmcs.2020-15. Russian.
- Borisova NI, Kotov IA, Kolesnikov AA, Kaptelova VV, Speranskaya AS, Kondrasheva L.u, et al. Monitoring rasprostraneniya variantov SARS-CoV-2 (Coronaviridae: Coronavirinae: Betacoronavirus; Sarbecovirus) na territorii Moskovskogo regiona s pomoshh'yu targetnogo vysokoproizvoditel'nogo sekvenirovaniya. *Voprosy virusologii*. 2021; 66(4): 269–78. DOI: <https://doi.org/10.36233/0507-4088-72>. Russian.
- Wu J, Tang L, Ma Y, Zhang D, Li Q, Mei H, Hu Y. Immunological profiling of COVID-19 patients with pulmonary sequelae. 2021; *mBio* 12: e01599-21. Available from: <https://doi.org/10.1128/mBio.01599-21>.
- Grossberg AN, Koza LA, Ledreux A, Prusmack C, Krishnamurthy HK, Jayaraman V, et al. A multiplex chemiluminescent immunoassay for serological profiling of COVID-19-positive symptomatic and asymptomatic patients. *Nature Communications*. 2021; 12: 740. Available from: <https://doi.org/10.1038/s41467-021-21040-7>.

Литература

- Попова А. Ю., Ежлова Е. Б., Мельникова А. А., Андреева Е. Е., Комбарова С. Ю., Лялина Л. В. и др. Коллективный иммунитет к SARS-CoV-2 жителей Москвы в эпидемический период COVID-19. *Инфекционные болезни*. 2020; 18(4): 8–16. DOI: 10.20953/1729-9225-2020-4-8-16.
- Ahmed ZB, Razu MH, Akter F, Rabby RI, Karmaker P, Kha M. Seropositivity of SARS-CoV-2 IgG Antibody among People in Dhaka City during the Prevaccination Period. *Hindawi BioMed*

- Research International. 2022; 2022: 6. Available from: <https://doi.org/10.1155/2022/4451144>.
3. Santiago L, Uranga-Murillo I, Arias M, González-Ramírez AM, Macías-León J, Moreo E, et al. Determination of the Concentration of IgG against the Spike Receptor-Binding Domain That Predicts the Viral Neutralizing Activity of Convalescent Plasma and Serum against SARS-CoV-2. *Biology*. 2021; 10: 208. Available from: <https://doi.org/10.3390/biology10030208>.
 4. Кармишин А. М., Носов Н. Ю., Поступайло В. Б., Жигарловский Б. А., Круглов А. А., Петухов А. Н. Метод количественной оценки напряженности и длительности иммунитета к SARS-COV-2 и динамики изменения титров антител. *Медицина экстремальных ситуаций*. 2021; 2 (23): 5–12. DOI: 10.47183/mes.2021.019.
 5. Dan JM, Mateus J, Kato Yu, Hastie KM, Yu ED, Faliti CE, et al. Immunological memory to SARS-CoV-2 assessed for up to 8 months after infection. *Science*. 2021; 371: eabf4063 (2021). DOI: 10.1126/science.abf4063.
 6. Huang B, Cai Yu, Li N, Li K, Wang Z, Li L, et al. Sex-based clinical and immunological differences in COVID-19. *BMC Infectious Diseases*. 2021; 21: 647. Available from: <https://doi.org/10.1186/s12879-021-06313-2>.
 7. Schlickeiser S, Schwarz T, Steiner S, Wittke K, Al Beshar N, Meyer O, et al. Disease severity, fever, age, and sex correlate with SARS-CoV-2 neutralizing antibody responses. *Front Immunol*. 2021; 11: 628971. DOI: 10.3389/fimmu.2020.628971.
 8. Naaber P, Tserel L, Kangro K, Sepp E, Jürjenson V, Adamson A, et al. Dynamics of antibody response to BNT162b2 vaccine after six months: a longitudinal prospective study. *The Lancet Regional Health — Europe*. 2021; 10: 1–10. Available from: <https://doi.org/10.1016/j.lanepe.2021.100208>.
 9. Markewitz R, Torge A, Wandinger K-P, Pauli D, Franke A, Bujanda L, et al. Clinical correlates of anti SARS CoV 2 antibody profiles in Spanish COVID 19 patients from a high incidence region. *Scientific Reports*. 2021; 11: 4363. Available from: <https://doi.org/10.1038/s41598-021-83969-5>.
 10. Li C, Yu D, Wu X, Liang H, Zhou Z, Xie Y, et al. Twelve-month specific IgG response to SARS-CoV-2 receptor-binding domain among COVID-19 convalescent plasma donors in Wuhan. *Nature Communications*. 2021; 12: 4846. Available from: <https://doi.org/10.1038/s41467-021-25109-1> | www.nature.com/naturecommunications.
 11. Pomelova VG, Korenberg EI, Kuznetsova TI, Vychenkova TA, Bekman NI, Osin NS. C6 Peptide-Based Multiplex Phosphorescence Analysis (PHOSPHAN) for Serologic Confirmation of Lyme Borreliosis. *PLoS ONE*. 2015; 10 (7): e0130048. DOI: 10.1371/journal.pone.0130048.
 12. Бекман Н. И., Помелова В. Г., Осин Н. С. Мультиплексный анализ наркотических средств на основе технологии иммуночипов ФОСФАН. *Клиническая лабораторная диагностика*. 2018; 63 (3): 178–83. Available from: <http://dx.doi.org/10.18821/0869-2084-2018-63-3-178-183>.
 13. Бекман Н. И., Ларичева С. Ю., Быченкова Т. А., Помелова В. Г., Осин Н. С. Одновременное определение тиреотропного гормона и свободного тироксина в сухих пятнах крови человека с использованием фосфоресцентных наночастиц. *Биоорганическая химия*. 2020; 46 (2): 170–9. DOI: 10.31857/s0132341320020074.
 14. Markmann AJ, Giallourou N, Bhowmik DR, Hou YJ, Lerner A, Martinez DR, et al. Sex disparities and neutralizing-antibody durability to SARS-CoV-2 infection in convalescent individuals. *mSphere*. 2021; 6: e00275-21. Available from: <https://doi.org/10.1128/mSphere.00275-21>.
 15. Zeng F, Dai C, Cai P, Wang J, Xu L, Li J, et al. A comparison study of SARS-CoV-2 IgG antibody between male and female COVID-19 patients: A possible reason underlying different outcome between sex. *J Med Virol*. 2020; 1–5. DOI: 10.1002/jmv.25989.
 16. Статистика коронавируса в Москве. Доступно по ссылке: <http://russian-trade.com/coronavirus-russia/Moskva>.
 17. Кнопре Д. Д., Набиева Е., Гарушянц С. К. Российский консорциум по секвенированию геномов коронавирусов (CORGI). Доступно по ссылке: <http://taxameter.ru>.
 18. Logunov DY, Dolzhikova IV, Zubkova OV, Tuchvatullin AI, Shcheblyakov DV, Dzharullaeva AS, et al. Safety and immunogenicity of an rAd26 and rAd5 vector-based heterologous prime-boost COVID-19 vaccine in two formulations: two open, non-randomised phase — studies from Russia. *The Lancet*. 2020; 396 (10255): 887–97. Available from: [https://doi.org/10.1016/S0140-6736\(20\)31866-3](https://doi.org/10.1016/S0140-6736(20)31866-3).
 19. Logunov DY, Dolzhikova IV, Shcheblyakov DV, Tuchvatullin AI, Zubkova OV, Dzharullaeva AS, et al. Safety and efficacy of an RAD26 and RAD5 vector-based heterologous prime-boost COVID-19 vaccine: an interim analysis of a randomised controlled phase 3 trial in Russia. *The Lancet*. 2021; 397 (10275): 671. Available from: [https://doi.org/10.1016/S0140-6736\(21\)00234-8](https://doi.org/10.1016/S0140-6736(21)00234-8).
 20. Колобухина Л. В., Бургасова О. А., Кружкова И. С., Бакалин В. В., Генералова Л. В., Шагаев А. В. и др. Оценка клинического течения COVID-19 у пациентов, вакцинированных «Спутник V», изменчивости RBD-домена S-белка SARS-COV-2 и вируснейтрализующих свойств сыворотки. *Вестник РГМУ*. 2021; 5: 66–75. DOI: 10.24075/vrgmu.2021.046.
 21. Gushchin VA, Dolzhikova IV, Shchetinin AM, Odintsova AS, Siniavin AE, Nikiforova MA, et al. Neutralizing activity of sera from Sputnik V-vaccinated people against variants of concern (VOC: B.1.1.7, B.1.351, P.1, B.1.617.2, B.1.617.3) and Moscow endemic SARS-CoV-2 variants. *Vaccines*. 2021; 9: 779. Available from: <https://doi.org/10.3390/vaccines9070779>.
 22. Гарафутдинов Р. Р., Мавзютов А. Р., Никоноров Ю. М., Чубукова О. В., Матниязов Р. Т., Баймиев Ан. Х. и др. Бетакоронавирус SARS-CoV-2, его геном, разнообразие генотипов и молекулярно-биологические меры борьбы с ним. *Биомика*. 2020; 12 (2): 242–71. DOI: 10.31301/2221-6197.bmcs.2020-15.
 23. Борисова Н. И., Котов И. А., Колесников А. А., Каптелова В. В., Сперанская А. С., Кондрашева Л. Ю. и др. Мониторинг распространения вариантов SARS-CoV-2 (Coronaviridae: Coronavirinae: Betacoronavirus; Sarbecovirus) на территории Московского региона с помощью таргетного высокопроизводительного секвенирования. *Вопросы вирусологии*. 2021; 66 (4): 269–78. DOI: <https://doi.org/10.36233/0507-4088-72>.
 24. Wu J, Tang L, Ma Y, Zhang D, Li Q, Mei H, Hu Y. Immunological profiling of COVID-19 patients with pulmonary sequelae. 2021; *mBio* 12: e01599-21. Available from: <https://doi.org/10.1128/mBio.01599-21>.
 25. Grossberg AN, Koza LA, Ledreux A, Prusmack C, Krishnamurthy HK, Jayaraman V, et al. A multiplex chemiluminescent immunoassay for serological profiling of COVID-19-positive symptomatic and asymptomatic patients. *Nature Communications*. 2021; 12: 740. Available from: <https://doi.org/10.1038/s41467-021-21040-7>.

SUBPOPULATION COMPOSITION OF T-HELPERS IN THE PERIPHERAL BLOOD OF PERSONS CHRONICALLY EXPOSED TO RADIATION IN THE LONG TERM

Kotikova AI^{1,2} ✉, Blinova EA^{1,2}, Akleyev AV^{1,2}

¹ Urals Research Center for Radiation Medicine, Chelyabinsk, Russia

² Chelyabinsk State University, Chelyabinsk, Russia

Earlier, it has been convincingly established that exposure to ionizing radiation (IR) alters the T cell-mediated immunity in the long term. However, a search for papers describing the effect chronic exposure to radiation has on various subpopulations of T-helpers yielded no results. Therefore, we designed this study seeking to investigate the quantitative characteristics of various subpopulations of T-helpers in the peripheral blood of individuals chronically exposed to low-level radiation for a long period of time. The study involved 102 chronically exposed Techa Riverside residents (Russia) aged 60–87 years. The participants were divided into two groups, one comprised of exposed individuals with the average red bone marrow (RBM) irradiation dose of 567 ± 73 mGy, another, the control group, comprised of people with the irradiation dose below 70 mGy. With the help of flow cytometry, we identified the quantitative characteristics of T-helper subpopulations in the peripheral blood at various stages of their differentiation, as well as various T-helper subpopulations of central and effector memory. The study revealed no significant differences in the composition of T-helper subpopulations in the compared groups. We discovered a significant growth of the double positive follicular T-helper 17 subpopulation in the population of central memory T-helpers, which is associated with the increase of RBM ($p = 0.04$; $S = 0.19$), thymus and peripheral lymphoid organs ($p = 0.03$; $S = 0.22$) irradiation dose. In the group of exposed individuals, the number of naive T-helpers ($p = 0.009$) and double positive follicular T-helpers 17 in the T_{EM} subpopulation ($p = 0.04$) was decreasing as the age of participants increased, and the number of effector memory T-helpers, on the contrary, increased with age ($p = 0.04$). We have not registered similar phenomena in the comparison group.

Keywords: T-helpers, follicular T-helpers, immunity, chronic exposure

Funding: the work was carried out as part of the "State of human cellular immunity against manifestation of the long-term effects of chronic exposure to radiation" State Task (code 27.002.20.800).

Author contribution: Kotikova AI — methodology development, laboratory research, statistical processing, article authoring; Blinova EA — methodology development, article authoring; Akleyev AV — development of the research concept, scientific supervision, article authoring.

Compliance with ethical standards: the study was approved by the Ethics Committee of the Urals Research Center for Radiation Medicine (Minutes #1 of April 14, 2022). All participants signed a voluntary informed consent to participate in the study.

✉ **Correspondence should be addressed:** Alisa I. Kotikova
Vorovskogo, 68, str. A, Chelyabinsk, 454141, Russia; kotikovaalisa@gmail.com

Received: 15.04.2022 **Accepted:** 12.05.2022 **Published online:** 04.06.2022

DOI: 10.47183/mes.2022.018

СУБПОПУЛЯЦИОННЫЙ СОСТАВ Т-ХЕЛПЕРОВ В ПЕРИФЕРИЧЕСКОЙ КРОВИ ХРОНИЧЕСКИ ОБЛУЧЕННЫХ ЛИЦ В ОТДАЛЕННОМ ПЕРИОДЕ

А. И. Котикова^{1,2} ✉, Е. А. Блинова^{1,2}, А. В. Аклев^{1,2}

¹ Уральский научно-практический центр радиационной медицины Федерального медико-биологического агентства, Челябинск, Россия

² Челябинский государственный университет, Челябинск, Россия

К настоящему времени убедительно показано, что воздействие ионизирующего излучения (ИИ) вызывает долгосрочное изменение Т-клеточного иммунитета. Однако количественных исследований влияния хронического радиационного воздействия на различные субпопуляции Т-хелперов в доступной литературе найдено не было. Поэтому целью работы было исследовать количественные характеристики различных субпопуляций Т-хелперов в периферической крови лиц, подвергшихся хроническому низкоинтенсивному радиационному воздействию, в отдаленные сроки после начала облучения. В исследовании приняло участие 102 хронически облученных жителя прибрежных сел реки Течи (Россия) в возрасте 60–87 лет, которые были подразделены на облученных лиц (средняя накопленная доза облучения красного костного мозга составила 567 ± 73 мГр) и группу сравнения (доза облучения не превышала 70 мГр). Методом проточной цитометрии определяли количественные характеристики субпопуляций Т-хелперов в периферической крови на разной стадии их дифференцировки, а также различные субпопуляции Т-хелперов центральной и эффекторной памяти. В ходе исследования не выявлено статистически значимых различий в субпопуляционном составе Т-хелперов в сравниваемых группах. Отмечено статистически значимое повышение содержания субпопуляции «double positive» фолликулярных Т-хелперов 17 в популяции Т-хелперов центральной памяти с увеличением дозы облучения ККМ ($p = 0,04$; $S = 0,19$), а также тимуса и периферических лимфоидных органов ($p = 0,03$; $S = 0,22$). В группе облученных лиц зарегистрировано снижение количества наивных Т-хелперов ($p = 0,009$) и «double positive» фолликулярных Т-хелперов 17 в составе субпопуляции T_{EM} ($p = 0,04$) и увеличение количества Т-хелперов эффекторной памяти ($p = 0,04$) с увеличением возраста, чего не наблюдалось в группе сравнения.

Ключевые слова: Т-хелперы, фолликулярные Т-хелперы, иммунитет, хроническое облучение

Финансирование: работа выполнена в рамках государственного задания «Состояние клеточного иммунитета человека в период реализации отдаленных эффектов хронического радиационного воздействия» (код 27.002.20.800).

Вклад авторов: А. И. Котикова — разработка методики, лабораторные исследования, статистическая обработка, написание статьи; Е. А. Блинова — разработка методики, написание статьи; А. В. Аклев — концепция исследования, научное руководство, написание статьи.

Соблюдение этических стандартов: исследование одобрено этическим комитетом УНПЦ РМ (протокол № 1 от 14 апреля 2022 г.). Все участники подписывали добровольное информированное согласие на участие в исследовании.

✉ **Для корреспонденции:** Алиса Игоревна Котикова
ул. Воровского, д. 68, корп. А, г. Челябинск, 454141, Россия; kotikovaalisa@gmail.com

Статья получена: 15.04.2022 **Статья принята к печати:** 12.05.2022 **Опубликована онлайн:** 04.06.2022

DOI: 10.47183/mes.2022.018

Earlier, it has been convincingly established that exposure to ionizing radiation (IR) alters the T cell-mediated immunity in the long term. A number of studies have identified that irradiated individuals, including Techa Riverside residents, have more mutations in the genes of the T cell receptor (TCR mutations). An in-depth analysis of the immune status of such people allowed establishing the special role cytotoxic CD3⁺CD16⁺CD56⁺ lymphocytes play in the elimination of TCR mutant cells [1].

Regarding the impact of IR on T cell populations, there are data showing changes in the peripheral blood T helper indices. For example, 20 years after exposure, survivors of the Hiroshima and Nagasaki atomic bombing that received the dose greater than 1 Gy had the number of naive T helpers (CD4⁺CD45RA⁺ phenotype) decreasing [2]. The Chernobyl accident victims exhibited similar reactions: those who received high doses of radiation had less T-helpers in the peripheral blood [3]. A study that involved employees of Mayak Production Association (a nuclear industry production facility) has revealed a linear dose-dependent decrease in the number of peripheral blood T helpers [4]. A study of low dose occupational exposure that involved employees of Kozloduy, a Bulgarian nuclear power plant, yielded an assumption about a possible immune response shift from Th₁ to Th₂ [5]. However, a search for quantitative studies describing the effect chronic exposure to radiation has on various subpopulations of T helpers, including Th₁₇, Th₂₂, Th₉ etc., yielded no results.

This study aimed to investigate the quantitative characteristics of various subpopulations of T helpers in the peripheral blood of individuals chronically exposed to low-level radiation for a long period of time.

METHODS

The study of T helper subpopulations involved 102 people whose irradiation conditions and nature were described in detail earlier [6]. Techa Riverside residents were exposed to gamma radiation both externally and internally, mainly from ⁹⁰Sr and ¹³⁷Cs. The contamination came from the liquid radioactive waste discharged into the river by Mayak. The largest doses were absorbed by the red bone marrow (RBM) in 1950s–1960s; the associated key source of radiation was ⁹⁰Sr. We divided the chronically exposed people into two groups: exposed individuals (*n* = 54) and the control group (*n* = 48). It is important to note that currently, among the Techa Riverside residents, people with the accumulated radiation dose exceeding 100 mGy (localization — stomach and RBM) suffer and die from malignant neoplasms, including leukemia, more often [6].

Table 1. Characteristics of the studied groups

Group characteristics		Exposed individuals	Control group
		<i>n</i> = 54	<i>n</i> = 48
Age at the time of examination, years, M ± SE (min–max)		73.26 ± 0.58 (67–84)	68.73 ± 0.96 (60–87)
Gender, person (%)	male	22 (40.7)	17 (35.4)
	female	32 (59.3)	31 (64.6)
Ethnicity, people (%)	Slavs	17 (31.5)	21 (43.8)
	Turks	35 (64.8)	26 (54.2)
	Not established	2 (3.7)	1 (2)
Dose accumulated in the RBM, mGy, M ± SE (min–max)		567 ± 73 (80.20–2930)	17.20 ± 2.25 (1.89–55)
Dose accumulated in the thymus and peripheral lymphoid organs, mGy, M ± SE (min–max)		79.80 ± 10.70 (4.63–355)	7.35 ± 1.29 (0.21–39.5)

Note: *n* — the number of subjects; M ± SE — mean ± standard error.

The study inclusion criteria were: permanent residence in one of the 41 Techa River villages from 01.01.1950 to 12.31.1960; availability of data on the established doses accumulated in the RBM, thymus and peripheral lymphoid organs (as measured with the TRDST 2016 dosimetric system) [7]; absence of autoimmune, oncological, acute or chronic (exacerbating) inflammatory diseases, hemoblastoses, renal or hepatic insufficiency, acute cerebrovascular accidents in the previous three months; no intake of antibiotics, glucocorticoids and cytostatics in the previous six months; no X-ray examinations in the previous six months.

The control group included people living in the similar socio-economic conditions whose RBM radiation dose accumulated over their entire lives did not exceed 70 mGy [8] (Table 1).

For the study, we sampled 9 ml of fasting blood of the participants into vacuum tubes filled with K3-EDTA (Greiner Bio-One; Austria). Flow cytometry enabled assessment of the relative number of T helper subpopulations by the level of expression of CD45RA (naive T helpers marker), CD62L (marker of directed cell migration to the peripheral lymphoid organs), CCR4, CCR6, CXCR3, and CXCR5. Into the flow cytometer (Beckman Coulter; USA) tube, we added 100 µl of the test sample, 5 µl of CD3 and CD4 monoclonal antibodies (Beckman Coulter, USA; conjugated with Krome Orange and Pacific Blue, respectively), 20 µl of CD45RA and CD62L monoclonal antibodies (Beckman Coulter, USA; conjugated with PE and FITC, respectively), 5 µl of monoclonal antibodies CCR4, CCR6, CXCR3 and CXCR5 (Beckman Coulter, USA; conjugated with APC, Per-CP-eFluorTM710, PE-Cyanine7 and PE-eFluor® 610 respectively). The samples were incubated for 20 minutes in a dark place at room temperature. Then, we added 1 ml of VersaLyse Lysing Solution (Beckman Coulter; USA) to the tube to remove erythrocytes, and then left the samples to incubate for 10 more minutes under the same conditions. After incubation, the samples were analyzed in a Navios flow cytometer (Beckman Coulter; USA).

The gating tactic we employed in the context of T helper subpopulations analysis relied on the identification of T helpers by the presence of CD3 and CD4 markers on the cell surface. Next, we divided the population of CD3⁺CD4⁺ cells into subpopulations of T helpers at different stages of differentiation by the presence of surface markers CD45RA and CD62L. Namely, we differentiated between phenotype CD3⁺CD4⁺CD45RA⁺CD62L⁺ naive T helpers (T_{Naive}), central memory phenotype CD3⁺CD4⁺CD45RA⁺CD62L⁺ T helpers (T_{CM}), effector memory phenotype CD3⁺CD4⁺CD45RA⁺CD62L⁻ T helpers (T_{EM}) and terminally differentiated phenotype

Table 2. Phenotype characteristics of the studied T helper subpopulations, peripheral blood of exposed individuals

Cell phenotype	Population name
CXCR5 ⁻ CXCR3 ⁻ CCR6 ⁻ CCR4 ⁺	T helpers 2 (Th ₂)
CXCR5 ⁻ CXCR3 ⁻ CCR6 ⁺ CCR4 ⁻	T helpers 17 (Th ₁₇)
CXCR5 ⁻ CXCR3 ⁻ CCR6 ⁻ CCR4 ⁺	T helpers 17 and T helpers 22 (Th ₁₇ and Th ₂₂)
CXCR5 ⁻ CXCR3 ⁻ CCR6 ⁻ CCR4 ⁻	T helpers 1 and T helpers 9 (Th ₁ and Th ₉)
CXCR5 ⁻ CXCR3 ⁻ CCR6 ⁻ CCR4 ⁻	"Non-classical" Th17 (Th ₁ /Th ₁₇)
CXCR5 ⁺ CXCR3 ⁻ CCR6 ⁻ CCR4 ⁻	Follicular T helpers 2 (Tfh ₂)
CXCR5 ⁺ CXCR3 ⁻ CCR6 ⁻ CCR4 ⁺	Follicular T helpers 2 (Tfh ₂)
CXCR5 ⁺ CXCR3 ⁻ CCR6 ⁻ CCR4 ⁻	Follicular T helpers 17 double negative (double negative Tfh ₁₇)
CXCR5 ⁺ CXCR3 ⁻ CCR6 ⁻ CCR4 ⁺	Follicular T-helpers 17 (Tfh ₁₇)
CXCR5 ⁺ CXCR3 ⁻ CCR6 ⁻ CCR4 ⁻	Follicular T helpers 1 (Tfh ₁)
CXCR5 ⁺ CXCR3 ⁻ CCR6 ⁻ CCR4 ⁺	Follicular T helpers 17 double positive (double positive Tfh ₁₇)

CD3⁺CD4⁺CD45RA⁺CD62L⁻ T helpers (TEMRA). In the T_{CM} and T_{EM} populations, subpopulations of various T helpers were identified by the presence of CCR4, CCR6, CXCR3, and CXCR5 markers [9–11] (Table 2).

For statistical data processing we employed SigmaPlot software (SYSTAT Software; USA). Kolmogorov-Smirnov test enabled verification of normalcy of distribution of the indicators. To compare the arrays of nonparametric data, we applied the Mann–Whitney U-test. First of all, the above parameters were evaluated for T helpers at different levels of differentiation, then we processed the data describing subpopulations of central and effector memory T helpers.

To identify dependencies, we used the Spearman's rank correlation coefficient and the Pearson correlation coefficient, as well as linear regression. The results were considered reliable at 5% significance level.

RESULTS

The currently adopted approach is to rely on CD markers expression to identify T helpers at different stages of differentiation. The literature offers detailed descriptions of the ability of T_{Naive} not differentiated in the secondary lymphoid organs (antigen-dependent differentiation) to give rise to memory T cells and effector cells. T_{CM}s carry the CD62L adhesion molecule, which determines their ability to largely localize in the secondary lymphoid organs. T_{EM}s are not able to penetrate into the peripheral lymphoid organs, however, they carry a wide range of different adhesion and chemokine molecules on their surface, which aid their migration into tissues and organs. The

ability of T_{EM}s to proliferate and differentiate is reduced, and the cells part of this population are the main producers of effector cytokines, such as IFN γ and IL4. TEMRA effector cells are considered to be the final stage of T lymphocyte differentiation process in the peripheral blood. The effector properties of TEMRA require no costimulation; they manifest under the action of cytokines produced by the inflamed tissue [12].

At the first stage of the study, we relied on the expression of CD45RA (surface marker) and CD62L (marker of directed cell migration to the peripheral lymphoid organs) to investigate the relative number of T helpers at different stages of differentiation: T_{Naive}, T_{CM}, T_{EM}, and TEMRA (Table 3).

Comparison of the quantitative indicators of lymphocytes and T helpers at different stages of differentiation in the exposed and control groups revealed no significant differences (Table 3).

The expression of CCR4, CCR6, CXCR3, and CXCR5 chemokine receptors allowed estimating the number of T helper populations in the T_{CM} and T_{EM} subpopulations. The Th₁, Th₂, Th₁₇ and Th₂₂, Th₉ subpopulations, as well as follicular T helpers, are predominantly found in the T_{CM} and T_{EM} populations. All these cells have unique developmental and regulatory pathways and play different roles in the immunity and immunity-mediated pathologies [13].

Tables 4 and 5 present the results of estimation of representation of various subpopulations of T helpers in the T_{CM} and T_{EM} populations, as well as the ratio of Th₁/Th₂ and Th₁/Th₁₇ in the exposed individuals group.

We discovered no significant differences in the T_{CM} population T helper subpopulation values between the exposed individuals and control groups.

Table 3. The number of T helpers of different subpopulations in the compared groups

Indicator	Exposed individuals	Control group
	Me (Q ₁ –Q ₂)	
Lymphocytes, abs.	2.17 (1.49–2.76)	2.07 (1.62–2.55)
Lymphocytes, %	32.00 (22.00–36.80)	31.10 (26.00–38.75)
CD3 ⁺ CD4 ⁺ -cells, %	36.34 (31.83–41.54)	39.50 (33.15–45.22)
T _{Naive} , %	26.04 (14.89–39.66)	27.79 (17.46–36.77)
T _{CM} , %	36.83 (30.23–42.65)	36.74 (31.87–43.48)
T _{EM} , %	27.85 (20.35–38.58)	30.63 (23.24–38.09)
TEMRA, %	2.37 (1.15–4.18)	1.83 (1.22–5.72)

Table 4. Relative number (%) of T_{CM} population T helpers (data for the study participants)

Indicator, %	Exposed individuals	Control group
	Me (Q ₁ -Q ₂)	
Th ₂	2.51 (0.99–5.16)	4.33 (2.54–6.63)
Th ₁₇	2.43 (0.92–3.64)	2.58 (1.38–4.19)
Th ₁₇ и Th ₂₂	0.23 (0.07–0.75)	0.40 (0.07–0.97)
Th ₁ и Th ₉	32.79 (24.65–37.70)	33.03 (25.03–37.43)
Th ₁ /Th ₁₇	1.28 (0.58–2.61)	1.41 (0.36–3.05)
CXCR5 ⁺ CXCR3 ⁺ CCR6 ⁺ CCR4 ⁻ , Tfh ₂	8.46 (5.69–11.11)	8.03 (5.29–10.68)
CXCR5 ⁺ CXCR3 ⁺ CCR6 ⁺ CCR4 ⁺ , Tfh ₂	0.13 (0.05–0.39)	0.13 (0.06–0.31)
double negative Tfh ₁₇	5.98 (3.26–9.67)	7.56 (4.29–11.32)
Tfh ₁₇	0.14 (0.04–0.34)	0.21 (0.05–0.53)
Tfh ₁	6.11 (4.07–8.92)	6.54 (4.98–8.14)
double positive Tfh ₁₇	0.05 (0.00–0.16)	0.04 (0.00–0.08)
Th ₁ /Th ₂	11.70 (6.24–32.08)	7.73 (3.60–15.97)
Th ₁ /Th ₁₇	13.43 (7.65–38.59)	11.63 (7.51–22.32)

Comparison of the T_{EM} populations' T helper subpopulation indicators revealed no significant differences between the study groups.

To establish the long-term dependence of the number of different subpopulations of T helpers at different stages of differentiation in the peripheral blood of the exposed individuals we applied the Spearman's rank correlation coefficient and the Pearson correlation coefficient. "Long-term" here means that RBM, thymus, and peripheral lymphoid organs have accumulated the dose a long time ago. The analysis procedure covered both groups.

The correlation analysis did not reveal significant associations of the number of T helpers at different stages of differentiation in the peripheral blood of the exposed individuals with the dose accumulated by RBM, thymus and peripheral lymphoid organs.

Investigating the dependence of content of various T_{CM} population's T helper subpopulations on the radiation dose accumulated by the RBM, thymus and peripheral lymphoid organs, we discovered that the content of double positive Tfh₁₇ subpopulation depended significantly on the degree of irradiation of the thymus and peripheral lymphoid organs ($p = 0.02$; $S = 0.23$). However, linear regression analysis did not reveal significant dose-based dependences. As for

the remaining studied subpopulations of T helpers, we also discovered no significant dependences on the dose values.

A similar analysis was carried out to investigate the dependences of the content of various T_{EM} population's T helper subpopulations on the degree of irradiation of RBM, thymus and peripheral lymphoid organs. No statistically significant dependences of the studied parameters of the T_{EM} populations on the dose values were found.

It is known that with age, immune system of the human beings undergoes involutions changes: the number of some subpopulations of T helpers goes down [14], the direction of differentiation changes [15], and their functioning is disrupted [16]. With this in mind, we have also investigated dependence of the content of various peripheral blood T helper subpopulations on age (Table 6; the age was that reached by the participants at the time of the study).

Correlation analysis revealed a significant association between the decrease in the number of T_{Naive} and age in the exposed group. The values were $p = 0.009$, $S = -0.35$ and $p = 0.01$, $R = -0.34$ (Spearman's rank correlation coefficient and Pearson correlation coefficient, respectively). No such association was registered in the control group. In the exposed group, we have also found that the number of T_{EM} grows up significantly with age ($p = 0.04$, $S = 0.28$ and $p = 0.02$, $R = 0.33$,

Table 5. Relative number (%) of TEM population T helpers (data for the study participants)

Indicator, %	Exposed individuals	Control group
	Me (Q ₁ -Q ₂)	
Th ₂	0.67 (0.26–1.52)	0.94 (0.34–2.30)
Th ₁₇	4.29 (2.37–6.80)	5.22 (3.17–6.82)
Th ₁₇ и Th ₂₂	0.23 (0.03–0.52)	0.17 (0.05–0.59)
Th ₁ и Th ₉	45.96 (39.49–57.57)	51.51 (36.74–56.46)
Th ₁ /Th ₁₇	2.52 (1.08–5.52)	3.34 (1.35–7.23)
CXCR5 ⁺ CXCR3 ⁺ CCR6 ⁺ CCR4 ⁻ , Tfh ₂	2.29 (1.59–3.33)	2.22 (1.18–7.23)
CXCR5 ⁺ CXCR3 ⁺ CCR6 ⁺ CCR4 ⁺ , Tfh ₂	0.02 (0–0.09)	0 (0–0.04)
double negative Tfh ₁₇	2.11 (1.24–3.45)	2.75 (1.55–4.35)
Tfh ₁₇	0.02 (0–0.10)	0.04 (0–0.15)
Tfh ₁	2.48 (1.49–3.87)	2.42 (1.84–3.62)
double positive Tfh ₁₇	0 (0–0.03)	0 (0–0.02)
Th ₁ /Th ₂	62.63 (26.95–224.95)	44.66 (20.59–111.95)
Th ₁ /Th ₁₇	10.19 (6.13–21.56)	9.92 (6.15–15.25)

Table 6. Dependence of indicators of various subpopulations of T helpers on the age of participants (as of the time of the study)

Indicator, %	Exposed individuals		Control group	
	S (p)	R (p)	S (p)	R (p)
T _{Naive}	-0.35 (0.009)	-0.34 (0.01)	-	-
T _{EM}	0.28 (0.04)	0.33 (0.02)	-	-
Central memory T helpers				
double positive Tfh ₁₇	-	-	-	0.32 (0.03)
Effector memory T helpers				
double positive Tfh ₁₇	-0.28 (0.04)	-	0.37 (0.01)	0.39 (0.006)

Note: S (p) — the Spearman's rank correlation coefficient (correlation significance level); R (p) — Pearson linear correlation coefficient (correlation significance level).

Spearman's rank correlation coefficient and Pearson correlation coefficient, respectively). Nothing similar was discovered in the control group. These dependencies were investigated with a linear regression analysis (Figure 1; moving average graphs).

We discovered a significant dependence of the content of T_{EM} subpopulation's double positive Tfh₁₇ (peripheral blood) on age in both groups, but these associations were multidirectional: in the exposed individuals, the number of cells of this population decreased significantly with age (p = 0.04; S = -0.28), and in the control group, on the contrary, the said number increased (p = 0.003, S = 0.32 and p = 0.05, R = 0.29, Spearman's rank correlation coefficient and Pearson correlation coefficient, respectively). Moreover, in the control group we revealed an age-dependent increase in the T_{CM} subpopulation's double positive Tfh₁₇ counts (p = 0.009, R = 0.38), while in the exposed group no such dependence was registered.

Linear regression analysis of the dependence of number of T_{CM} and T_{EM} subpopulations' double positive Tfh₁₇ on the age of the exposed group participant revealed no significant correlations; for the control group, the results are shown on Fig. 2 (moving average graph).

The analysis of dependence of the content of various peripheral blood T helper subpopulations on the age of exposed individuals at the beginning of exposure showed the following correlations: the amount of T_{Naive} decreased as the age increased (p = 0.03, S = -0.34 and p = 0.04; R = -0.32, Spearman's rank correlation coefficient and Pearson correlation coefficient, respectively), while the number of T_{EM}s increased (p = 0.03, S = 0.35 and p = 0.04, R = 0.32, Spearman's rank correlation coefficient and Pearson correlation coefficient, respectively) (Fig. 3).

As for the remaining T helper populations, we discovered no significant dependences on the age reached at the time of the study and at the beginning of exposure.

DISCUSSION

T helper cells are critically important to the regulation of immune system: the range of their actions stretches from activating B-lymphocytes, cytotoxic T-lymphocytes and other cell populations to suppressing immune response.

However, in addition to supporting the functions of adaptive immunity, T helpers can also be involved in the development of autoimmune [17,18] and oncological diseases [19, 20]. The development of chronic lymphocytic leukemia was reported to be associated with the spread of abnormal follicular T helper cells that elevate levels of cytokines and produce costimulatory factors that promote tumor cell proliferation [21]. Other studies [22, 23] have shown protumor activity of Th₁₇, which manifests in the production of immunosuppressive cytokines and chemokines in the tumor microenvironment, thus stimulating its growth and metastasis.

The balance of various subpopulations of T helpers plays an important role in the immune response. For example, cytokines produced by Th₂ cells block production of Th₁ cytokines and are their natural killer cells. In addition, Th1 cells can inhibit the differentiation and proliferation of basophils and eosinophils, the activity of which is controlled by the synthesis of Th₂ cytokines [24]. Ionizing radiation compromises the Th₁/Th₂ immune balance and tilts it towards Th₂ dominance, the unbalanced state potentially contributing to immune system dysfunction after exposure [25]. A number of studies report a shift in the Th₁/Th₂ balance towards Th₂ in the cases of hematological

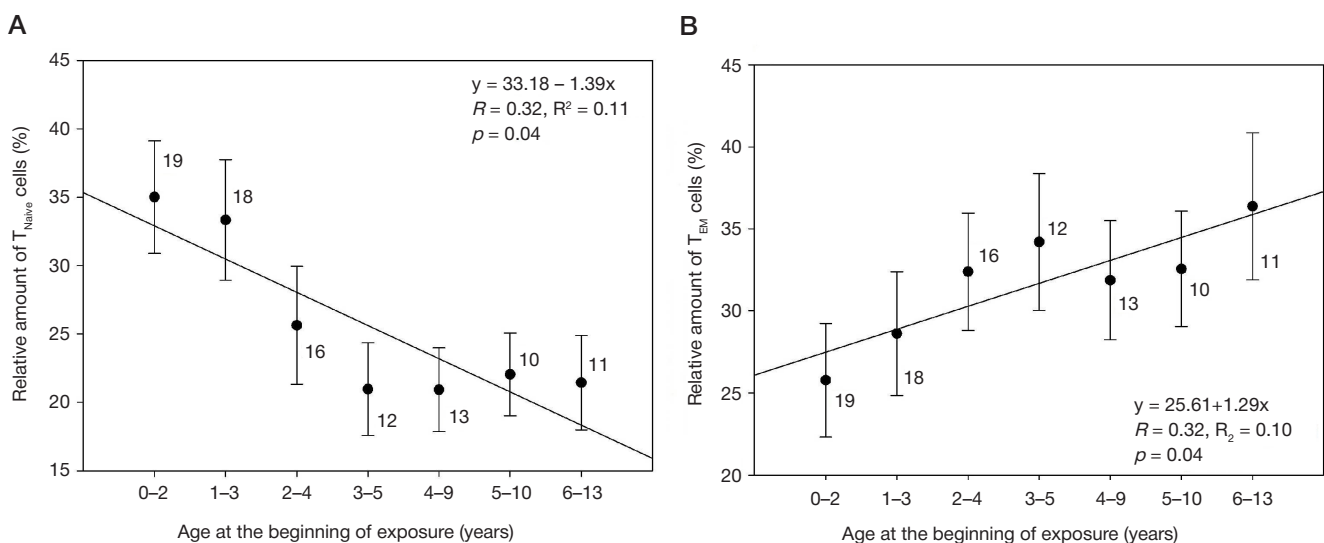


Fig. 1. Dependence of the relative amounts of peripheral blood TNaive (A) and TEM (B) on age, exposed individuals; linear regression

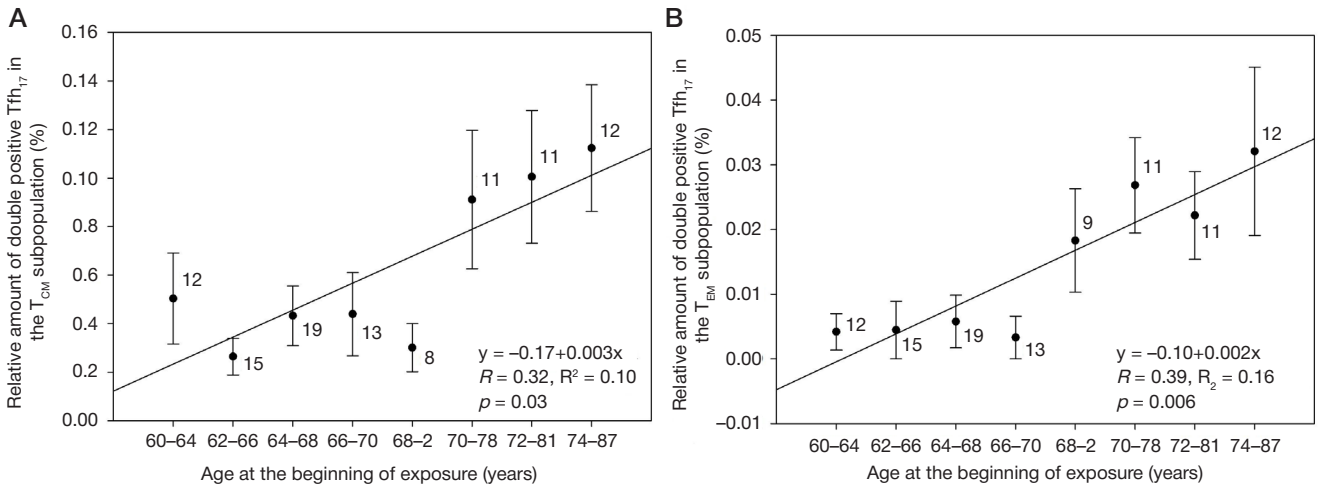


Fig. 2. Dependence of the content of double positive Tfh₁₇ in T_{CM} (A) and T_{EM} (B) subpopulations (peripheral blood) on age (as of the time of the study), control group; linear regression

malignant neoplasms [26–28]. More recent papers describe another association of immunocompetent cells, Th₁/Th₁₇, which, when unbalanced, contributes to the development of autoimmune diseases, primarily rheumatoid arthritis [29, 30].

Investigating the long-term effects of exposure to radiation, we discovered no significant differences in the relative content of various peripheral blood T helper subpopulations, as well as the Th₁/Th₂ and Th₁/Th₁₇ associations, between the exposed individuals and control groups. However, in the exposed group, we did reveal some peculiarities (differences from the control group indicator values) in the dependence of individual populations of peripheral blood T helpers on the degree of irradiation of thymus, peripheral lymphoid organs and age.

In the exposed group, we established that the increase in the amount of peripheral blood T_{CM} population's double positive Tfh₁₇ depends on the dose accumulated by the thymus and peripheral lymphoid organs. Other studies that involved people exposed to radiation have also registered dose-dependent changes in the number of T helpers and their functional properties. Thus, the Hiroshima and Nagasaki atomic bombing survivors exhibited a dose-dependent decrease in the number of CD4⁺ T cells in peripheral blood [3], a higher occurrence of T cell receptor mutations (mainly in CD4⁺ T cells population) [31], and a dose-dependent shortening of the T helper telomere length at doses above 0.5 Gy [32]. In Mayak employees that were chronically exposed to radiation the T helper part of the immune system was also changed:

a greater dose (2–4 Gy, external irradiation) translated into a smaller number of CD4⁺ cells [33]; the concentrations of some cytokines and chemokines changed, too. The results obtained allowed a conclusion that the identified changes in the parameters of immune systems of the examined individuals supported chronic inflammatory status and could contribute to the development of late radiation-induced pathologies, such as cardiovascular and malignant diseases [5, 34].

In addition to the dependences on radiation dose, age-related changes were found in the groups. We discovered that the number of T_{Naive} in the peripheral blood of the exposed individuals decreased with age, and the amount of T_{EM}s increased, the latter capable of migrating through the vascular and tissue endothelium to inflammation foci and triggering a rapid immune response with the synthesis of predominantly effector cytokines [12]. These results are consistent with the literature data describing the decrease of naive T helper cell numbers with age in people older than 70–75 years [14]. In addition, naive T cells in older people grow prone to effector differentiation [35]. It should be noted that no such correlations were found in the control group, where the number of double positive Tfh₁₇ in the T_{CM} and T_{EM} subpopulations increased with age, while in the exposed group, on the contrary, the T_{EM} subpopulation's double positive Tfh₁₇ content was growing down very slightly with age. Follicular T helper cells express CXCR5 chemokine receptor, which allows them to migrate to its CXCL13 ligand in the B-cell follicle. Normal follicular T helper

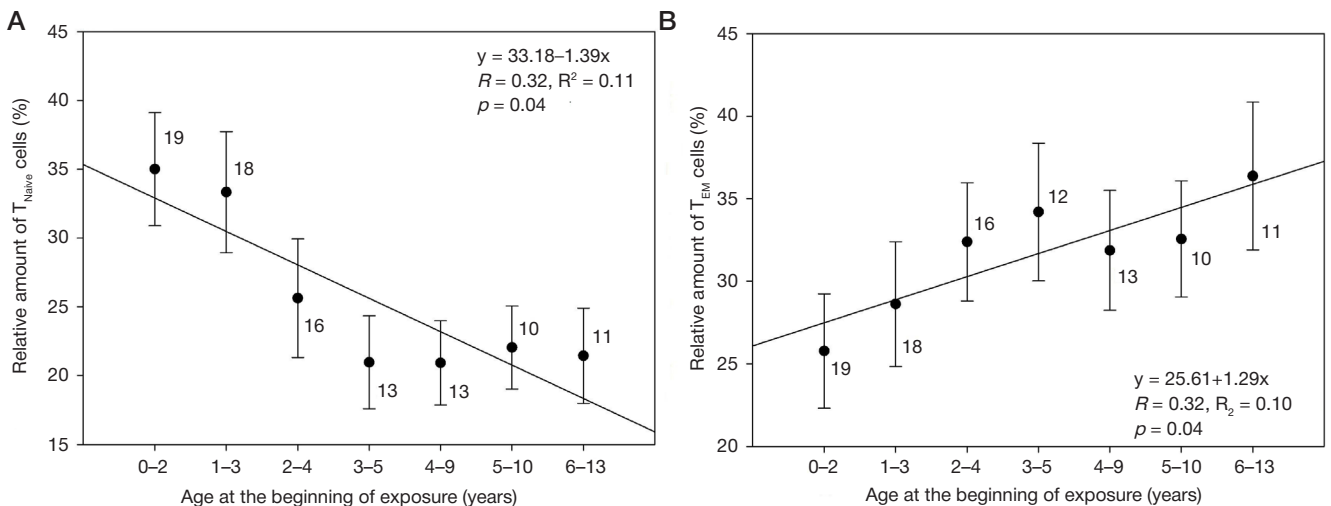


Fig. 3. Dependence of the relative amounts of peripheral blood T_{Naive} (A) and T_{EM} (B) on age, exposed individuals, at the beginning of exposure; linear regression

cells produce a unique range of cytokines and chemokines needed for supporting survival and proliferation of B-cells in the germinal centers [9, 21, 36, 37]. Thus, Tfh₁₇ produce IL21 and IL17, which are involved in enhancing the interaction between T and B cells and are necessary for the formation of germinal centers [38].

Thus, in the exposed individuals, the late effects after chronic exposure to radiation include some changes in the T helper part of the immune system, which depend both on the radiation dose and on the age reached at the time of the study. However, the limited sample recruited for this study disallows unequivocal conclusions at this stage and necessitates further research.

CONCLUSIONS

1. The long term effects of chronic exposure to radiation with the doses predominantly accumulated by the RBM (average

dose — 567 ± 73 mGy), as registered in the Techa Riverside residents aged 67 through 84, do not include changes in the relative content of various T helper subpopulations in peripheral blood. 2. The relative amount of double positive Tfh₁₇ contained in the peripheral blood T_{CM} population of the exposed individuals positively correlated with the degree of irradiation of thymus and peripheral lymphoid organs ($p = 0.02$); however, there was no linear regression dependence registered. 3. The data obtained indirectly indicate intensification of involutational processes in the exposed individuals due to the number of T_{Naive} decreasing with age and the number of T_{EM} increasing therewith. In the exposed individuals group, the following late age-related dependences were revealed: decreasing relative amount of T_{Naive} ($p = 0.009$) and double positive Tfh₁₇ in the T_{EM} subpopulation ($p = 0.04$), and increasing relative content of T_{EM} ($p = 0.04$) in the peripheral blood. However, no similar dependencies were found in the control group.

References

- Akleev AA, Blinova EA, Dolgushin II. TCR-mutacii v limfocitax perifericheskoy krovi i immunnyj status u lic, podverghshixsya xronicheskomu radiacionnomu vozdejstviyu, v otdalennye sroki. *Rossijskij immunologicheskij zhurnal*. 2019; 13 (22,1): 13–23. DOI: 10.31857/S102872210005016-2. Russian.
- Nalbant A. IL17, IL21, and IL22 Cytokines of T Helper 17 Cells in Cancer. *J Interferon Cytokine Res*. 2019; 39 (1): 56–60. DOI: 10.1089/jir.2018.0057.
- Akiyama M. Late effects of radiation on the human immune system: an overview of immune response among the atomic-bomb survivors. *Int J Radiat Biol*. 1995; 68: 497–508.
- Heylmann D, Rödel F, Kindler T, Kaina B. Radiation sensitivity of human and murine peripheral blood lymphocytes, stem and progenitor cells. *Biochimica et Biophysica Acta (BBA). Reviews on Cancer*. 2014; 1846 (1): 121–29. DOI: 10.1016/j.bbcan.2014.04.009.
- Rybkina VL, Bannikova MV, Adamova GV, Dörr H, Scherthan H, Azizova TV. Immunological markers of chronic occupational radiation exposure. *Health Phys*. 2018; 115 (1): 108–13. DOI:10.1097/HP.0000000000000855.
- Akleev AV, redaktor. *Posledstviya radioaktivnogo zagryazneniya reki Tечи*. Chelyabinsk: Kniga, 2016; 390 s. Russian.
- Degteva MO, Napier BA, Tolstykh EI, Shishkina EA, Bougrov NG, Krestinina LY, et al. Raspredelenie individual'nyx doz v kogorte lyudej, obluchennyx v rezul'tate radioaktivnogo zagryazneniya reki Tечи. *Medicinskaya radiologiya i radiacionnaya bezopasnost'*. 2019; 64 (3): 46–53. DOI: 10.12737/article_5cf2364cb49523.98590475. Russian.
- SanPin 2.6.1.2523-09 «Normy radiacionnoj bezopasnosti (NRB - 99/2009)». M., 2009; 225 s. Russian.
- Zurochka AV, Khaidukov SV, Kudryavtsev IV, Chereshnev VA. Protochnaya citometriya v biomedicinskix issledovaniyax. Ekaterinburg: RIO UrO RAN, 2018; 720 s. Russian.
- Kudryavtsev IV, Serebryakova MK, Totolyan AA. Znacheniya normy subpopulyacij T-xelperov razlichnogo urovnya differencirovki v perifericheskoy krovi. *Klinicheskaya laboratornaya diagnostika*. 2016; 61 (3): 179–84. DOI: 10.18821/0869-2084-2016-3-179-184. Russian.
- Kudryavtsev IV, Borisov AG, Krobinets II, Savchenko AA, Serebryakova MK, Totolyan AA. Xemokinovye receptory na T-xelperax razlichnogo urovnya differencirovki: osnovnye subpopulyacii. *Medicinskaya immunologiya*. 2016; 18 (3): 239–50. DOI: 10.15789/1563-0625-2016-3-239-250. Russian.
- Kudryavcev IV. T-kletki pamyati: osnovnye populyacii i stadii diferencirovki. *Rossijskij immunologicheskij zhurnal*. 2014; 8 (17): 947–64. Russian.
- Dong C. Cytokine Regulation and Function in T Cells. *Annu Rev Immunol*. 2021; 39: 51–76. DOI: 10.1146/annurev-immunol-061020-053702.
- Goronzy JJ, Lee WW, Weyand CM. Aging and T-cell diversity. *Exp Gerontol*. 2007; 42 (5): 400–6. DOI: 10.1016/j.exger.2006.11.016.
- Lefebvre JS, Lorenzo EC, Masters AR, et al. Vaccine efficacy and T helper cell differentiation change with aging. *Oncotarget*. 2016; 7 (23): 33581–94. DOI: 10.18632/oncotarget.9254.
- Haynes L, Lefebvre JS. Age-related Deficiencies in Antigen-Specific CD4 T cell Responses: Lessons from Mouse Models. *Aging Dis*. 2011; 2 (5): 374–81.
- Huang J, Xu X, Yang J. miRNAs Alter T Helper 17 Cell Fate in the Pathogenesis of Autoimmune Diseases. *Front Immunol*. 2021; 12: 593473. DOI: 10.3389/fimmu.2021.593473.
- Takeuchi Y, Hirota K, Sakaguchi S. Impaired T cell receptor signaling and development of T cell-mediated autoimmune arthritis. *Immunol Rev*. 2020; 294 (1): 164–76. DOI: 10.1111/imr.12841.
- Shao F, Zheng P, Yu D, Zhou Z, Jia L. Follicular helper T cells in type 1 diabetes. *FASEB J*. 2020; 34 (1): 30–40. DOI: 10.1096/fj.201901637R.
- Chang SH. T helper 17 (Th17) cells and interleukin-17 (IL17) in cancer. *Arch Pharm Res*. 2019; 42 (7): 549–59. DOI: 10.1007/s12272-019-01146-9.
- Wu X, Fajardo-Despaigne JE, Zhang C, et al. Altered T Follicular Helper Cell Subsets and Function in Chronic Lymphocytic Leukemia. *Front Oncol*. 2021; 11: 674492. DOI: 10.3389/fonc.2021.674492.
- Dahal LN. The dichotomy of T helper 17 cells in cancer. *Nat Rev Immunol*. 2017; 17 (9): 592. DOI: 10.1038/nri.2017.93.
- Marshall EA, Ng KW, Kung SH, et al. Emerging roles of T helper 17 and regulatory T cells in lung cancer progression and metastasis. *Mol Cancer*. 2016; 15 (1): 67. DOI: 10.1186/s12943-016-0551-1.
- Mazzarella G, Bianco A, Catena E, De Palma R, Abbate GF. Th1/Th2 lymphocyte polarization in asthma. *Allergy*. 2000; 55 (Suppl 61): 6–9. DOI: 10.1034/j.1398-9995.2000.00511.x.
- Chen R, Wang YW, Fornace AJ Jr, Li HH. Impairment of the Intrinsic Capability of Th1 Polarization in Irradiated Mice: A Close Look at the Imbalanced Th1/Th2 Response after Irradiation. *Radiat Res*. 2016; 186 (6): 559–67. DOI: 10.1667/RR14401.1.
- Zhang X-L, Komada Y, Chipeta J, Li Q-S, Inaba H, Azuma E, Yamamoto H, Sakurai M. Intracellular cytokine profile of T cells from children with acute lymphoblastic leukemia. *Cancer Immunol Immunother*. 2000; 49: 165–72.
- Yatnda P, Mintz P, Grigoriadou K, Lemonnier F, Vilmer E, Langlade-Demoyen P. Analysis of T-cell defects in the specific immune response against acute lymphoblastic leukemia cells. *Exp Hematol*. 1999; 27: 1375–83.
- De Totero D, Reato G, Mauro F, et al. IL-4 production and increased CD30 expression by a unique CD8 — T-cell subset in

- B-cell chronic lymphocytic leukaemia. *Br J Haematol.* 1999; 104: 589–99.
29. Pan B, Zeng L, Cheng H, et al. Altered balance between Th1 and Th17 cells in circulation is an indicator for the severity of murine acute GVHD. *Immunol Lett.* 2012; 142 (1–2): 48–54. DOI: 10.1016/j.imlet.2011.12.005.
 30. Bazzazi H, Aghaei M, Memarian A, Asgarian-Omran H., Behnampour N, Yazdani Y. Th1–Th17 ratio as a new insight in rheumatoid arthritis disease. *Iran J Allergy Asthma Immunol.* 2018; 17 (1): 68–77.
 31. Kusunoki Y, Yamaoka M, Kasagi F, Hayashi T, MacPhee DG, Kyoizumi S. Long-lasting changes in the T-cell receptor V beta repertoires of CD4 memory T-cell populations in the peripheral blood of radiation-exposed people. *Br J Haematol.* 2003; 122: 975–84. DOI: 10.1046/j.1365-2141.2003.04520.x.
 32. Yoshida K, Misumi M, Kubo Y, Yamaoka M, Kyoizumi S, Ohishi W, et al. Long-term effects of radiation exposure and metabolic status on telomere length of peripheral blood T cells in atomic bomb survivors. *Radiat Res.* 2016; 186: 367–76. DOI: 10.1667/RR14389.1.
 33. Kiselev SM, Sokolnikov ME, Lyss LV, Ilyina NI. Immunological monitoring of the personnel at radiation hazardous facilities. *Radiation Protection Dosimetry.* 2016; 173 (1–3): 124–30. DOI: 10.1093/rpd/ncw346.
 34. Rybkina VL, Azizova TV, Scherthan H, Meineke V, Doerr H, Adamova GV, et al. Expression of blood serum proteins and lymphocyte differentiation clusters after chronic occupational exposure to ionizing radiation. *Radiat Environ Biophys.* 2014; 53 (4): 659–70. DOI: 10.1007/s00411-014-0556-3.
 35. Zhang H, Weyand CM, Goronzy JJ. Hallmarks of the aging T-cell system. *FEBS J.* 2021; 288 (24): 7123–142. DOI: 10.1111/febs.15770.
 36. Bentebibel SE, Lopez S, Obermoser G, et al. Induction of ICOS+CXCR3+CXCR5+ TH cells correlates with antibody responses to influenza vaccination. *Sci Transl Med.* 2013; 5 (176): 176ra32. DOI: 10.1126/scitranslmed.3005191.
 37. Brenna E, Davydov AN, Ladell K, et al. CD4+ T Follicular Helper Cells in Human Tonsils and Blood Are Clonally Convergent but Divergent from Non-Tfh CD4+ Cells. *Cell Rep.* 2020; 30 (1): 137–52. DOI: 10.1016/j.celrep.2019.12.016.
 38. Olatunde AC, Hale JS, Lamb TJ. Cytokine-skewed Tfh cells: functional consequences for B cell help. *Trends Immunol.* 2021; 42 (6): 536–50. DOI: 10.1016/j.it.2021.04.006.

Литература

1. Аклеев А. А., Блинова Е. А., Долгушин И. И. TCR-мутации в лимфоцитах периферической крови и иммунный статус у лиц, подвергшихся хроническому радиационному воздействию, в отдаленные сроки. *Российский иммунологический журнал.* 2019; 13 (22,1): 13–23. DOI: 10.31857/S102872210005016-2.
2. Nalbant A. IL17, IL21, and IL22 Cytokines of T Helper 17 Cells in Cancer. *J Interferon Cytokine Res.* 2019; 39 (1): 56–60. DOI: 10.1089/jir.2018.0057.
3. Akiyama M, Late effects of radiation on the human immune system: an overview of immune response among the atomic-bomb survivors. *Int J Radiat Biol.* 1995; 68: 497–508.
4. Heylmann D, Rödel F, Kindler T, Kaina B. Radiation sensitivity of human and murine peripheral blood lymphocytes, stem and progenitor cells. *Biochimica et Biophysica Acta (BBA). Reviews on Cancer.* 2014; 1846 (1): 121–29. DOI: 10.1016/j.bbcan.2014.04.009.
5. Rybkina VL, Bannikova MV, Adamova GV, Dörr H, Scherthan H, Azizova TV. Immunological markers of chronic occupational radiation exposure. *Health Phys.* 2018; 115 (1): 108–13. DOI: 10.1097/HP.0000000000000855.
6. Аклеев А. В., редактор. Последствия радиоактивного загрязнения реки Течи. Челябинск: Книга, 2016; 390 с.
7. Дегтева М. О., Напье Б. А., Толстых Е. И., Шишкина Е. А., Бугров Н. Г., Крестинина Л. Ю., Аклеев А. В. Распределение индивидуальных доз в когорте людей, облученных в результате радиоактивного загрязнения реки Течи. *Медицинская радиология и радиационная безопасность.* 2019; 64 (3): 46–53. DOI: 10.12737/article_5cf2364cb49523.98590475.
8. СанПин 2.6.1.2523-09 «Нормы радиационной безопасности (НРБ - 99/2009)». М., 2009; 225 с.
9. Зурочка А. В., Хайдуков С. В., Кудрявцев И. В., Черешнев В. А. Проточная цитометрия в биомедицинских исследованиях. Екатеринбург: РИО УрО РАН, 2018; 720 с.
10. Кудрявцев И. В., Серебрякова М. К., Тотолян А. А. Значения нормы субпопуляций Т-хелперов различного уровня дифференцировки в периферической крови. *Клиническая лабораторная диагностика.* 2016; 61 (3): 179–84. DOI: 10.18821/0869-2084-2016-3-179-184.
11. Кудрявцев И. В., Борисов А. Г., Кробинец И. И., Савченко А. А., Серебрякова М. К., Тотолян А. А. Хемокиновые рецепторы на Т-хелперах различного уровня дифференцировки: основные субпопуляции. *Медицинская иммунология.* 2016; 18 (3): 239–50. DOI: 10.15789/1563-0625-2016-3-239-250.
12. Кудрявцев И. В. Т-клетки памяти: основные популяции и стадии дифференцировки. *Российский иммунологический журнал.* 2014; 8 (17): 947–64.
13. Dong C. Cytokine Regulation and Function in T Cells. *Annu Rev Immunol.* 2021; 39: 51–76. DOI: 10.1146/annurev-immunol-061020-053702.
14. Goronzy JJ, Lee WW, Weyand CM. Aging and T-cell diversity. *Exp Gerontol.* 2007; 42 (5): 400–6. DOI: 10.1016/j.exger.2006.11.016.
15. Lefebvre JS, Lorenzo EC, Masters AR, et al. Vaccine efficacy and T helper cell differentiation change with aging. *Oncotarget.* 2016; 7 (23): 33581–94. DOI: 10.18632/oncotarget.9254.
16. Haynes L, Lefebvre JS. Age-related Deficiencies in Antigen-Specific CD4 T cell Responses: Lessons from Mouse Models. *Aging Dis.* 2011; 2 (5): 374–81.
17. Huang J, Xu X, Yang J. miRNAs Alter T Helper 17 Cell Fate in the Pathogenesis of Autoimmune Diseases. *Front Immunol.* 2021; 12: 593473. DOI: 10.3389/fimmu.2021.593473.
18. Takeuchi Y, Hirota K, Sakaguchi S. Impaired T cell receptor signaling and development of T cell-mediated autoimmune arthritis. *Immunol Rev.* 2020; 294 (1): 164–76. DOI: 10.1111/imr.12841.
19. Shao F, Zheng P, Yu D, Zhou Z, Jia L. Follicular helper T cells in type 1 diabetes. *FASEB J.* 2020; 34 (1): 30–40. DOI: 10.1096/fj.201901637R.
20. Chang SH. T helper 17 (Th17) cells and interleukin-17 (IL17) in cancer. *Arch Pharm Res.* 2019; 42 (7): 549–59. DOI: 10.1007/s12272-019-01146-9.
21. Wu X, Fajardo-Despaigne JE, Zhang C, et al. Altered T Follicular Helper Cell Subsets and Function in Chronic Lymphocytic Leukemia. *Front Oncol.* 2021; 11: 674492. DOI: 10.3389/fonc.2021.674492.
22. Dahal LN. The dichotomy of T helper 17 cells in cancer. *Nat Rev Immunol.* 2017; 17 (9): 592. DOI: 10.1038/nri.2017.93.
23. Marshall EA, Ng KW, Kung SH, et al. Emerging roles of T helper 17 and regulatory T cells in lung cancer progression and metastasis. *Mol Cancer.* 2016; 15 (1): 67. DOI: 10.1186/s12943-016-0551-1.
24. Mazzarella G, Bianco A, Catena E, De Palma R, Abbate GF. Th1/Th2 lymphocyte polarization in asthma. *Allergy.* 2000; 55 (Suppl 61): 6–9. DOI: 10.1034/j.1398-9995.2000.00511.x.
25. Chen R, Wang YW, Fornace AJ Jr, Li HH. Impairment of the Intrinsic Capability of Th1 Polarization in Irradiated Mice: A Close Look at the Imbalanced Th1/Th2 Response after Irradiation. *Radiat Res.* 2016; 186 (6): 559–67. DOI: 10.1667/RR14401.1.
26. Zhang X-L, Komada Y, Chipeta J, Li Q-S, Inaba H, Azuma E, Yamamoto H, Sakurai M. Intracellular cytokine profile of T cells from children with acute lymphoblastic leukemia. *Cancer Immunol Immunother.* 2000; 49: 165–72.
27. Yatnda P, Mintz P, Grigoriadou K, Lemonnier F, Vilmer E, Langlade-Demoyen P. Analysis of T-cell defects in the specific immune response against acute lymphoblastic leukemia cells. *Exp Hematol.* 1999; 27: 1375–83.

28. De Toter D, Reato G, Mauro F, et al. IL-4 production and increased CD30 expression by a unique CD8 — T-cell subset in B-cell chronic lymphocytic leukaemia. *Br J Haematol.* 1999; 104: 589–99.
29. Pan B, Zeng L, Cheng H, et al. Altered balance between Th1 and Th17 cells in circulation is an indicator for the severity of murine acute GVHD. *Immunol Lett.* 2012; 142 (1–2): 48–54. DOI: 10.1016/j.imlet.2011.12.005.
30. Bazzazi H, Aghaei M, Memarian A, Asgarian-Omran H., Behnampour N, Yazdani Y. Th1–Th17 ratio as a new insight in rheumatoid arthritis disease. *Iran J Allergy Asthma Immunol.* 2018; 17 (1): 68–77.
31. Kusunoki Y, Yamaoka M, Kasagi F, Hayashi T, MacPhee DG, Kyoizumi S. Long-lasting changes in the T-cell receptor V beta repertoires of CD4 memory T-cell populations in the peripheral blood of radiation-exposed people. *Br J Haematol.* 2003; 122: 975–84. DOI: 10.1046/j.1365-2141.2003.04520.x.
32. Yoshida K, Misumi M, Kubo Y, Yamaoka M, Kyoizumi S, Ohishi W, et al. Long-term effects of radiation exposure and metabolic status on telomere length of peripheral blood T cells in atomic bomb survivors. *Radiat Res.* 2016; 186: 367–76. DOI: 10.1667/RR14389.1.
33. Kiselev SM, Sokolnikov ME, Lyss LV, Ilyina NI. Immunological monitoring of the personnel at radiation hazardous facilities. *Radiation Protection Dosimetry.* 2016; 173 (1–3): 124–30. DOI: 10.1093/rpd/ncw346.
34. Rybkina VL, Azizova TV, Scherthan H, Meineke V, Doerr H, Adamova GV, et al. Expression of blood serum proteins and lymphocyte differentiation clusters after chronic occupational exposure to ionizing radiation. *Radiat Environ Biophys.* 2014; 53 (4): 659–70. DOI: 10.1007/s00411-014-0556-3.
35. Zhang H, Weyand CM, Goronzy JJ. Hallmarks of the aging T-cell system. *FEBS J.* 2021; 288 (24): 7123–142. DOI: 10.1111/febs.15770.
36. Bentebibel SE, Lopez S, Obermoser G, et al. Induction of ICOS+CXCR3+CXCR5+ TH cells correlates with antibody responses to influenza vaccination. *Sci Transl Med.* 2013; 5 (176): 176ra32. DOI: 10.1126/scitranslmed.3005191.
37. Brenna E, Davydov AN, Ladell K, et al. CD4+ T Follicular Helper Cells in Human Tonsils and Blood Are Clonally Convergent but Divergent from Non-Tfh CD4+ Cells. *Cell Rep.* 2020; 30 (1): 137–52. DOI: 10.1016/j.celrep.2019.12.016.
38. Olatunde AC, Hale JS, Lamb TJ. Cytokine-skewed Tfh cells: functional consequences for B cell help. *Trends Immunol.* 2021; 42 (6): 536–50. DOI: 10.1016/j.it.2021.04.006.

EVALUATION OF THE IMPACT OF COVID-19 PANDEMIC ON OVERALL MORTALITY IN OZYORSK URBAN DISTRICT

Osipov MV¹✉, Sokolova VA², Kushnir AS²

¹ Southern Urals Biophysics Institute of the Federal Medical Biological Agency, Ozyorsk, Russia

² Clinical Hospital "RZhD-Medicine", Chelyabinsk, Russia

COVID-19 pandemic announced by World Health Organization in March 2020 raised concern on potential demographic losses. This retrospective study was aimed to analyze the pandemic-related changes in the demographic status of the Ozyorsk urban district located close to the nuclear industry facility — the "Mayak" Production Association. Population changes in the Ozyorsk urban district over the last decade were analyzed based on the open-access demographic data. The impact of the COVID-19 pandemic on the demographic status of the Ozyorsk urban district was assessed using the crude overall mortality rates. Comparison of the overall mortality rates has been performed between 2020 and each previous year to assess the deviation of mortality from the forecasted value. The overall mortality rate in 2020 has been found increased significantly by 19%. Excess mortality attributed to the impact of the pandemic was 13.4%. The expected absolute number of excess deaths from COVID-19 being the main cause of death was 60 (4.2%). The COVID-19 pandemic had a significant negative impact on the demographic status of the Ozyorsk urban district; however, the role of COVID-19-associated deaths in overall mortality was not predominant.

Keywords: pandemic, coronavirus infection, COVID-19, SARS-CoV-2, population changes, mortality rate, Ozyorsk

Acknowledgements: the authors would like to express their appreciation to Yulia V. Tzareva, PhD, research fellow at the Department of Epidemiology, Southern Urals Biophysics Institute, for discussing the study results.

Author contribution: Osipov MV — concept, design, research coordination, statistical analysis and data interpretation, drawing conclusions, manuscript writing, and translation; Sokolova VA — analysis, study planning, data interpretation, discussion; Kushnir AS — literature analysis, data interpretation, manuscript writing.

✉ **Correspondence should be addressed:** Mikhail V. Osipov
Ozyorskoe shosse 19/1, k. 108, Ozyorsk, 456780, Russia; osipov@subi.su

Received: 10.03.2022 **Accepted:** 02.04.2022 **Published online:** 21.04.2022

DOI: 10.47183/mes.2022.011

ОЦЕНКА ВЛИЯНИЯ ПАНДЕМИИ COVID-19 НА ОБЩИЙ КОЭФФИЦИЕНТ СМЕРТНОСТИ НАСЕЛЕНИЯ ОЗЕРСКОГО ГОРОДСКОГО ОКРУГА

М. В. Осипов¹✉, В. А. Соколова², А. С. Кушнир²

¹ Южно-Уральский институт биофизики Федерального медико-биологического агентства, Озёрск, Россия

² Клиническая больница «РЖД-Медицина», Челябинск, Россия

Пандемия COVID-19, объявленная Всемирной организацией здравоохранения в марте 2020 г., обусловила необходимость оценки потенциального демографического ущерба для населения. Целью работы было провести ретроспективный анализ изменения демографической ситуации в Озерском городском округе, расположенном вблизи предприятия атомной промышленности ПО «Маяк». На основе опубликованных в открытом доступе демографических данных было ретроспективно проанализировано изменение численности населения за десятилетний период. Уровень общей смертности в 2020 г. сравнивался с каждым предыдущим годом в течение исследуемого периода для оценки величины отклонения уровня смертности от его прогнозируемого значения. Оценка влияния пандемии COVID-19 на демографический статус Озерского городского округа выполнялась с использованием грубого показателя общей смертности. Показано статистически значимое повышение уровня общей смертности в 2020 г. по сравнению с его ожидаемой оценкой на 19%. Абсолютный избыток общей смертности, отнесенный к влиянию пандемии, составил 13,4%. Ожидаемое число избыточных случаев смерти в результате заболевания COVID-19 как основной причины смерти составило 60 (4,2%). Пандемия COVID-19 оказала статистически значимое негативное влияние на демографический статус Озерского городского округа, однако ее влияние на общую смертность не было преобладающим.

Ключевые слова: пандемия, коронавирусная инфекция, COVID-19, SARS-CoV-2, показатели общей смертности, Озёрск

Благодарность: авторы выражают благодарность научному сотруднику отдела эпидемиологии Южно-Уральского института биофизики, к. м. н. Ю. В. Царевой за помощь в обсуждении результатов исследования.

Вклад авторов: М. В. Осипов — идея, дизайн, координация исследования, статистический анализ и интерпретация результатов, формулирование выводов, подготовка рукописи; В. А. Соколова — анализ, планирование исследования, интерпретация данных, обсуждение результатов; А. С. Кушнир — работа с литературой, анализ и интерпретация данных, подготовка рукописи.

✉ **Для корреспонденции:** Михаил Викторович Осипов
Озерское шоссе, д. 19/1, к. 108, г. Озёрск, 456780, Россия; osipov@subi.su

Статья получена: 10.03.2022 **Статья принята к печати:** 02.04.2022 **Опубликована онлайн:** 21.04.2022

DOI: 10.47183/mes.2022.011

On March 11, 2020 the World Health Organization (WHO) announced a new global threat, the outbreak of COVID-19 caused by the novel coronavirus infection SARS-CoV-2, the spread of which had become a pandemic. The COVID-19 associated atypical severe acute respiratory syndrome (SARS) [1], prone to progression towards severe forms in 20% of infected [2] and characterized by high probability of lethal outcome [3], has become a subject of concern for clinicians and epidemiologists all over the world. As of December 31,

2020, the total number of diseased due to infection of novel coronavirus SARS-CoV-2 in the world was about 83,200,000 [4], with over 1,815,000 deaths from various causes among them. Case fatality rate among patients with confirmed cases of COVID-19 varied greatly from country to country within a range of 0.3–5.8% [5].

The global spread of the novel coronavirus infection associated with increased morbidity and mortality is a risk factor potentially affecting the population changes. This could

be particularly important for the sparsely populated areas and small urban districts, such as the closed administrative territory Ozyorsk, located close to the “Mayak” nuclear complex [6]. The sanitary and epidemiologic wellbeing of the Ozyorsk urban district population is an important task of the Federal Target Program “Nuclear and Radiation Safety in 2016–2020, and until 2030” [7], that is why evaluation of possible sanitary losses due to impact of the pandemic becomes especially important.

Since the announcement of the pandemic, a number of research studies has been conducted by Russian and foreign scientists, including those aimed to assess the COVID-19-associated demographic losses [3–5, 8–12]. Specific mortality rates such as *infection fatality ratio* (IFR) and *case fatality ratio* (CFR) based on the number of deaths among infected has been widely used by the epidemiologists to characterize the impact of the pandemic to population. However, these specific indicators used to characterize the prevalence of infection depend on certain demographic and economic conditions which may vary from country to country. According to WHO, the true level of transmission is frequently underestimated because a substantial proportion of people with the infection are undetected either because they are asymptomatic or have only mild symptoms [13]. Therefore, the use of specific fatality rates (IFR and CFR) to assess true level of the pandemic spread could be compromised by underestimation [11, 12].

On the other hand, an in-patient specific mortality indicator used to monitor the infection spread [14] which is calculated for patients seeking medical care, would be obviously higher than among the rest of the population. Thus, the consequences of the SARS-CoV-2 spreading in the population estimated using specific indicators are likely to be overestimated [15]. The fatality rates calculated in different periods of the epidemic process may vary greatly, which could result in erroneous interpretation of the comparison results in various populations at different time [8] and make it difficult to predict the expected sequelae [16]. The use of different methods for fatality rates calculation implemented in different countries serves as a source of bias that led to wide variability (0.1–25% and more) [13], which could mislead researchers when comparing the data reported.

The one of the possible ways to minimize the impact of these uncertainties is the use of the non-specific crude overall mortality rate indicator, which, unlike specific indicators, is insensitive to the use of different calculation methods, since it is a proportion of deaths from all causes in the population. According to that, in this study the pandemic-associated excess mortality in the population of the Ozyorsk urban district has been evaluated using the comparison of the crude overall mortality rates.

METHODS

A retrospective cohort study has been conducted among the population of the Ozyorsk urban district during the period from 2010 to 2020. The statistical analysis has been performed using the data from official statistics [17]. The number of deaths from all causes (M_t) and the population size (P_t) given by the end of the year (t) were used to calculate the overall crude mortality rate (μ_t) per 1000 using equation:

$$\mu_t = \frac{M_t}{P_t} \times 1000. \quad (1)$$

The annual increase in the crude mortality rate was calculated using equation:

$$\Delta\mu = \frac{\mu_t - \mu_{t-1}}{\mu_{t-1}} \times 100\%, \quad (2)$$

where μ_t — crude overall mortality rate in the current year, μ_{t-1} — crude overall mortality rate in the previous year. Excess mortality was calculated as the difference between the 2020 crude mortality rate and the average mortality rate during the decade before the COVID-19 pandemic announcement, assuming the static demographic trend over the years. Trend estimation was performed using the linear correlation coefficient (r) and approximation coefficient R^2 [18].

To characterize the mortality rate per 1000 (‰), a conventional scale was used [19]. According to that scale, the mortality rate in the Ozyorsk urban district was ranged:

$$\begin{aligned} (\mu_t) < 10\text{‰} & \text{— low,} \\ 10\text{‰} \leq (\mu_t) < 15\text{‰} & \text{— medium,} \\ 15\text{‰} \leq (\mu_t) < 25\text{‰} & \text{— high.} \end{aligned} \quad (3)$$

The statistical hypothesis on the existing impact of the COVID-19 pandemic on the mortality rate in the Ozyorsk urban district population was tested against the null hypothesis using the comparison of the overall crude mortality rates given by previous decade. Statistical significance of the differences between the annual mortality rates was assessed by frequency analysis of binary outcomes (presence or absence) in 2×2 contingency tables using Pearson Chi-square test implemented in the “WinPepi” statistical software package [20]. The results were considered significant at $p < 0.01$. The probability of replication of the results (P -rep) [21] was considered sufficient reaching 80% with the significance level $\alpha = 0.05$.

RESULTS

The dynamics of population changes in the Ozyorsk urban district during the study period is shown in Fig. 1.

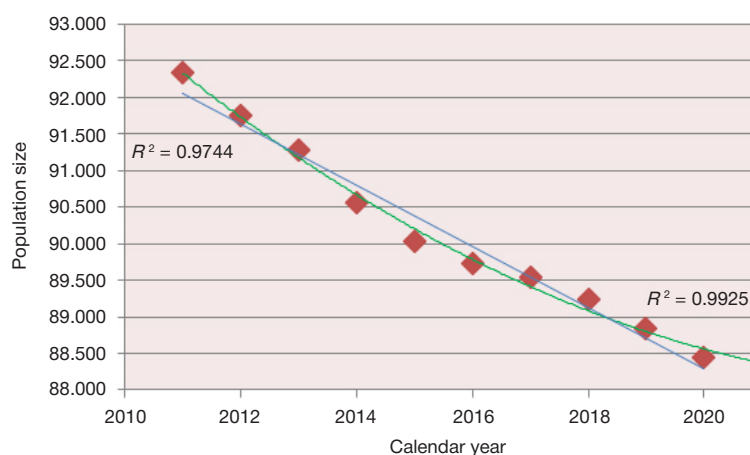


Fig. 1. Dynamics of population changes in the Ozyorsk urban district, 2010–2020

Table 1. Population size and mortality in the Ozyorsk urban district, 2010–2020

Year	Population	Deaths	Deaths increase	Mortality rate (μ)	$\Delta \mu$, %
2010	97,832	1309	–	13.38	–
2011	92,335	1243	–66	13.46	0.6
2012	91,744	1226	–17	13.36	–0.74
2013	91,285	1181	–45	12.94	–3.14
2014	90,567	1240	59	13.69	5.8
2015	90,029	1237	–3	13.74	0.37
2016	89,724	1279	42	14.25	3.71
2017	89,545	1227	–52	13.7	–3.86
2018	89,230	1241	14	13.91	1.53
2019	88,835	1197	–44	13.47	–3.16
2020	88,399	1430	233	16.18	20.12

The dynamics of population changes in the Ozyorsk urban district over a 10-year period show a clear downward trend which can be approximated using linear quadratic model ($R^2 = 0.99$). The linear correlation coefficient is 0.84 ($p < 0.05$). The linearity of the trend was within $0.7 < r < 0.9$ ($R^2 = 0.97$), which points to the distinct linear component.

Annual overall crude mortality rates (μ), as well as annual absolute and relative mortality rate increase ($\Delta \mu$, %) during 2010–2020 are shown in Table 1.

The increase in the absolute number of deaths by 2020 in Ozyorsk urban district population was 233, compared to the previous year, or 192 deaths, compared to the average number of deaths for the previous decade (2010–2019). The expected number of excess deaths that could be related to the first year of the pandemic was 2.17 per 1000, or 13.4% of the overall mortality.

The increase in the overall mortality rate ($\Delta \mu$) in the Ozyorsk urban district in 2020 was 20.12%, compared to the 2019. The overall mortality ratio, $\mu_{2020} / \mu_{2010-2019}$ compared to the previous decade was 1.19 (95% CI: 1.1–1.28; $p = 6.0 \times 10^{-6}$) which corresponds to 19% average excess mortality.

According to the mortality range scale (3), the mortality level observed in the Ozyorsk urban district remained “medium” until 2019, and increased to a “high” level since 2020. The changes in the overall mortality rates in the Ozyorsk urban district compared to similar indicators for Chelyabinsk region in the recent decade (2010–2020) are shown in Fig.2.

During the recent decade, a linear downward trend of the overall mortality rate ($R^2 = 0.9$) in Chelyabinsk region has

persisted, compared to the same in the Ozyorsk urban district which fluctuates between 12.5 and 14.5 showing a weak upward trend (linear correlation 0.69). It is noteworthy that in recent years mortality rates in the Ozyorsk urban district exceed that of the region.

According to the official demographic data, the mortality rate in Chelyabinsk region in 2020 reached 15.9, compared to the Ozyorsk urban district (16.2) [22], which showed a substantial deviation from the predicted value calculated based on linear extrapolation. Pairwise comparisons of the annual 2020 mortality with the previous decade were performed in order to test the null hypothesis, using the 2019 mortality as a reference value.

Comparisons of the 2020 overall mortality within the decade, significance testing and reproducibility of the results are shown in Table 2.

Pairwise comparisons of the 2020 mortality with the each mortality rate for the non-pandemic years revealed significant differences in all pairs ($p < 0.05$) with the high level of reproducibility (> 80%). At the same time, comparison with the reference value (2019) revealed no significant differences in any of the pairs ($p > 0.05$), except for the 2020.

DISCUSSION

Our findings show a significant increase of crude mortality rate by 20.1% in the Ozyorsk urban district compared to the 2019, and by 19.0% compared to the average estimate for the non-

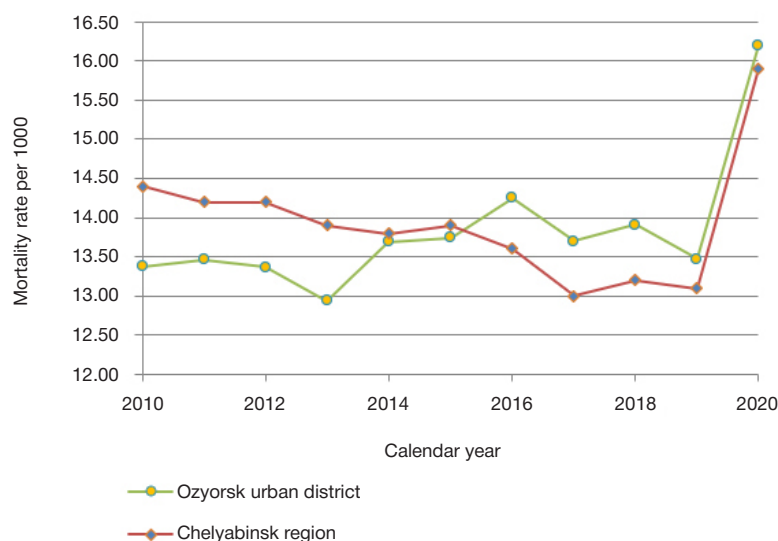


Fig. 2. Annual changes in the crude overall mortality rate per 1000 in the Ozyorsk urban district and Chelyabinsk region, years 2010–2020

Table 2. Comparison of the overall mortality rates in the Ozyorsk urban district within the decade

Year	Pearson χ^2 <i>p</i> -value	<i>P</i> -rep, %	Year	Pearson χ^2 <i>p</i> -value	<i>P</i> -rep, %
2010	5.8×10^{-7}	93	2010	0.86	–
2011	1.8×10^{-6}	92	2011	0.98	–
2012	7.6×10^{-7}	93	2012	0.84	–
2013	1.0×10^{-8}	94	2013	0.32	67
2014	1.4×10^{-5}	92	2014	0.69	–
2015	2.3×10^{-5}	91	2015	0.63	–
2016	9.3×10^{-4}	89	2016	0.16	28
2017	1.7×10^{-5}	92	2017	0.68	–
2018	8.7×10^{-5}	91	2018	0.43	89
2019	2.6×10^{-6}	92	2019	–	–
2020	–	–	2020	2.6×10^{-6}	92

pandemic decade (2010–2019). This suggests that in 2020 a new negative factor appeared in the study population which has significantly affected the mortality.

These results are consistent with the national statistics data. According to the Russian Government Statistical Service (“Rosstat”) [23], 288,000 more people died in 2020 in the Russian Federation compared to the average number of deaths over the previous 5-year period, and the excess mortality was 18.9% compared to the previous year (2019), which was confirmed by recent studies [10–12]. The estimated proportion of deaths caused by the COVID-19 as the main cause of death in the 2020 in the Russian Federation (excess mortality) was 31%.

In this study we have limited access to the information on the number of fatal cases among infected with SARS-CoV-2 in the Ozyorsk urban district. However, the COVID-19 specific mortality for the Ozyorsk population can be estimated using the “Rosstat” excess mortality coefficient, in the assumption that there are no substantial differences in age and gender structure between the populations of the Ozyorsk urban district and the Russian Federation, and the changes in mortality rate with time at risk, as well. Assuming the aetiological fraction of 31%, the expected number of deaths due to COVID-19 in the Ozyorsk urban district would be 59.5, and the expected annual specific mortality rate per 100,000 would be 67.3.

In comparison with the crude mortality from cardiovascular diseases (CVD) and cancer, as the most socially significant disorders, ranked as the leading causes of death in the Russian Federation, the role of COVID-19 in the overall mortality was not predominant. In case of main cause of death, COVID-19 mortality would be 8.5 lower compared with the CVD-associated mortality rate for 2019 (573.2 deaths per 100,000 population) [24], and 3.0 times lower (203.5 deaths per 100,000 compared to cancer-induced deaths.

According to that, the expected number of related to the pandemic but not induced by the COVID-19 excess deaths in the Ozyorsk urban district in 2020 would be about 132. These excess fatal cases may be associated both with SARS-Cov-2 infection, and the other causes that are not related to COVID-19 itself, but significantly related to the pandemic.

Due to the rapid spread of the pandemic in early 2020, according to WHO recommendations governments of the

majority of the countries, including Russia, imposed certain restriction measures aimed to reduce the number of SARS-CoV-2 infected individuals and improve medical care to COVID-19 patients. Despite these mandatory measures, the healthcare system forced real difficulties because the number of in-patient beds for patients with non-communicable diseases in the Chelyabinsk region decreased rapidly in favour of COVID-19 beds (Table 3).

Repurposing of many hospital departments and clinics into the infectious in 2020 has led to insufficiency of healthcare providing to patients with chronic non-communicable diseases, e. g. cardiovascular pathology and cancer, which has the highest prevalence in the population [24]. Such healthcare interventions are particularly sensitive for people older than 60 [12, 25] who shared 29% of the Ozyorsk urban district population at the end of 2020, due to severe chronic diseases and comorbidities [26] which can result in excess mortality. The situation was further complicated by the quarantine measures implemented in many medical hospitals, along with the shortage of specialists engaged in fighting against COVID-19. All this showed that healthcare system experienced serious difficulties when working in a pandemic mode [27] that could result in the increased mortality from non-infectious diseases.

Thus, in the context of the pandemic, along with the specific COVID-19-associated mortality, it is necessary to distinguish the excess mortality not directly related to the SARS-CoV-2 infection, but resulted from the impact of socio-economic factors and preventive measures, the effectiveness of which in reducing the COVID-19 related mortality is widely discussed [28]. Based on the above considerations, planning sanitary anti-epidemic measures during the pandemic requires the assessment complex character of potential sanitary losses.

CONCLUSIONS

Announcement of the global COVID-19 pandemic in 2020 had a distinct negative impact on the demographic status of the Ozyorsk urban district. A significant increase in the overall mortality rate of population has been found compared to the previous non-pandemic decade. The overall mortality rate increase observed during the first pandemic year was

Table 3. Number of in-patient beds in medical hospitals of the Chelyabinsk region, 2016–2020

Hospital bed profile	Number of beds per year					Difference
	2016	2017	2018	2019	2020	2019–2020
Non-infectious	20,064	19,525	19,124	19,035	15,846	–3189
Infectious	1230	1209	1180	1134	6355	5221

19%. Excess overall mortality attributed to the impact of the pandemic was 13.4%, and the expected COVID-19-associated specific mortality rate was 4.2%. The significant impact of COVID-19, however, doesn't play a predominant role in the total demographic losses of the Ozyorsk urban district. Taking

into account the prolonged nature of the COVID-19 pandemic, the control of the demographic losses must be implemented pay attention to complex nature of the relationship between the mortality and both direct impact of the COVID-19, and the other pandemic-related socio-economic factors.

References

- Lotfi M, Hamblin MR, Rezaei N. COVID-19: Transmission, prevention, and potential therapeutic opportunities. *Clin Chim Acta*. 2020; 508: 254–66. DOI: 10.1016/j.cca.2020.05.044.
- Müller O, Neuhann F, Razum O. Epidemiologie und Kontrollmaßnahmen bei COVID-19 [Epidemiology and control of COVID-19]. *Dtsch Med Wochenschr*. 2020; 145 (10): 670–74. DOI: 10.1055/a-1162-1987.
- Modig K, Ahlbom A, Matthews A. COVID-19 — deaths and analysis. *Lakartidningen*. 2020; 117: F3XL. PMID: 32365212.
- Lai CC, Shih TP, Ko WC. Severe acute respiratory syndrome coronavirus 2 (SARS-CoV-2) and coronavirus disease-2019 (COVID-19): The epidemic and the challenges. *Int J Antimicrob Agents*. 2020; 55 (3): 105924. DOI: 10.1016/j.ijantimicag.2020.105924.
- Ensheng D, Hongru D, Lauren G. An interactive web-based dashboard to track COVID-19 in real time. *The Lancet Infectious Diseases*. 2020; 20 (5): 533–34. DOI: 10.1016/S1473-3099(20)30120-1.
- Novoselov VN, Nosach YuF, Entyakov BN. Atomnoe serdce Rossii. Chelyabinsk: Izd-vo «Avtograf», 2014; 528 s. Russian.
- Federal'naya celevaya programma «Obespechenie yadernoj i radiacionnoj bezopasnosti na 2016–2020 gody i na period do 2030 goda». Dostupno po ssylke (data obrashheniya 22.02.2022): <http://fcp-yarb2030.rf/about/overview/>. Russian.
- Drapkina OM, Samorodskaya IV, Sivceva MG, Kakorina EP, Briko NI, Cherkasov SN, i dr. Metodicheskie aspekty ocenki zaboлеваemosti, rasprostranennosti, letal'nosti i smertnosti pri COVID-19. *Kardiovaskulyarnaya terapiya i profilaktika*. 2020; 19 (3): 302–09. DOI: 10.15829/1728-8800-2020-2585. Russian.
- Weiss P, Murdoch DR. Clinical course and mortality risk of severe COVID-19. *The Lancet*. 2020; 395: 1014–5.
- Druzhinin PV, Molchanova EV. Smertnost' naseleniya rossijskix regionov v usloviyax pandemii COVID-19. *Regionologiya*. 2021; 29 (3): 666–85. DOI: 10.15507/24131407.116.029.202103.666-685. Russian.
- Lifshits ML, Neklyudova NP. COVID-19 mortality rate in Russian regions: forecasts and reality. *R-economy*. 2020; 6 (3): 171–82. DOI: 10.15826/recon.2020.6.3.015.
- Druzhinin PV, Molchanova EV, Podlevskikh YuL. Vliyaniye pandemii Covid-19 na smertnost' naseleniya rossijskix regionov. *Trudy Karel'skogo nauchnogo centra RAN*. 2021; 7: 116–128. DOI: 10.17076/them1421. Russian.
- Vsemirnaya organizaciya zdorov'ya (VOZ). Ocenka pokazatelej smertnosti ot Covid-19. Dostupno po ssylke (data obrashheniya 22.02.2022): <https://www.who.int/news-room/commentaries/detail/estimating-mortality-from-covid-19>. Russian.
- Richardson S, Hirsch JS, Narasimhan M, Crawford JM, McGinn T, Davidson KW, et al. Presenting characteristics, comorbidities, and outcomes among 5700 patients hospitalized with COVID-19 in the New York City Area. *JAMA*. 2020; 323 (20): 2052–9. DOI: 10.1001/jama.2020.6775.
- Grasselli G, Zangrillo A, Zanella A, Antonelli M, Cabrini L, Castelli A, et al. COVID-19 Lombardy ICU Network. Baseline Characteristics and Outcomes of 1591 Patients Infected With SARS-CoV-2 Admitted to ICUs of the Lombardy Region, Italy. *JAMA*. 2020; 323 (16): 1574–81. DOI: 10.1001/jama.2020.5394.
- Obesnyuk VF. Group health risk parameters in a heterogeneous cohort. Indirect assessment as per events taken in dynamics. *Health Risk Analysis*. 2021; 2: 17–32. DOI: 10.21668/health.risk/2021.2.02.eng.
- Pasport Ozyorskogo gorodskogo okruga. Dostupno po ssylke (data obrashheniya 22.02.2022): <http://ozerskadm.ru/regulatory/passport/>. Russian.
- Fletcher R, Fletcher S, Vagner Eh. *Klinicheskaya ehpidemiologiya. Osnovy dokazatel'noj mediciny*. M.: Izd-vo «Media Sfera», 1998; 352 s. Russian.
- Merkov AM, Suxarebskij LM. *Statistika na sluzhbe narodnogo zdorov'ya*. M.: Izd-vo «Statistika», 1968; 48 s. Russian.
- Abramson, JH. WINPEPI updated: computer programs for epidemiologists, and their teaching potential. *Epidemiologic Perspectives & Innovations*. 2011; 8 (1). DOI: 10.1186/1742-5573-8-1.
- Reality check on reproducibility. *Nature*. 2016; 533 (7604): 437. DOI: 10.1038/533437a.
- Regiony Rossii. Social'no-ehkonomicheskie pokazateli. *Statisticheskij sbornik*. 2020. Dostupno po ssylke (data obrashheniya 22.02.2022): https://gks.ru/bgd/regl/b20_14p/Main.htm. Russian.
- Federal'naya sluzhba gosudarstvennoj statistiki «Rosstat». Dostupno po ssylke (data obrashheniya 22.02.2022): <https://rosstat.gov.ru/storage/mediabank/TwbjciZH/edn12-2020.html>. Russian.
- Zdravooxranenie v Rossii. *Stat. sb. M.: Izd-vo «Rosstat», 2021; 171 s. Russian.*
- Blagosklonny MV. From causes of aging to death from COVID-19. *Aging (Albany NY)*. 2020; 12 (11): 10004–21. DOI: 10.18632/aging.103493.
- Guan WJ, Liang WH, Zhao Y, Liang HR, Chen ZS, Li YM, et al. China Medical Treatment Expert Group for COVID-19. Comorbidity and its impact on 1590 patients with COVID-19 in China: a nationwide analysis. *Eur Respir J*. 2020; 55 (5): 2000547. DOI: 10.1183/13993003.00547-2020.
- Bong CL, Brasher C, Chikumba E, McDougall R, Mellin-Olsen J, Enright A. The COVID-19 Pandemic: Effects on Low- and Middle-Income Countries. *Anesth Analg*. 2020; 131 (1): 86–92. DOI: 10.1213/ANE.00000000000004846.
- Herby J, Joung L, Hanke S. A Literature Review and Meta-Analysis of the Effects of Lockdowns on COVID-19 Mortality. *Studies in Applied Economics*. 2022; 200: 1–61.

Литература

- Lotfi M, Hamblin MR, Rezaei N. COVID-19: Transmission, prevention, and potential therapeutic opportunities. *Clin Chim Acta*. 2020; 508: 254–66. DOI: 10.1016/j.cca.2020.05.044.
- Müller O, Neuhann F, Razum O. Epidemiologie und Kontrollmaßnahmen bei COVID-19 [Epidemiology and control of COVID-19]. *Dtsch Med Wochenschr*. 2020; 145 (10): 670–74. DOI: 10.1055/a-1162-1987.
- Modig K, Ahlbom A, Matthews A. COVID-19 — deaths and analysis. *Lakartidningen*. 2020; 117: F3XL. PMID: 32365212.
- Lai CC, Shih TP, Ko WC. Severe acute respiratory syndrome coronavirus 2 (SARS-CoV-2) and coronavirus disease-2019 (COVID-19): The epidemic and the challenges. *Int J Antimicrob Agents*. 2020; 55 (3): 105924. DOI: 10.1016/j.ijantimicag.2020.105924.
- Ensheng D, Hongru D, Lauren G. An interactive web-based dashboard to track COVID-19 in real time. *The Lancet Infectious*

- Diseases. 2020; 20 (5): 533–34. DOI: 10.1016/S1473-3099(20)30120-1.
6. Новосёлов В. Н., Носач Ю. Ф., Ентяков Б. Н. Атомное сердце России. Челябинск: Изд-во «Автограф», 2014; 528 с.
 7. Федеральная целевая программа «Обеспечение ядерной и радиационной безопасности на 2016–2020 годы и на период до 2030 года». Доступно по ссылке (дата обращения 22.02.2022): <http://фцп-яр62030.рф/about/overview/>.
 8. Драпкина О. М., Самородская И. В., Сивцева М. Г., Какорина Е. П., Брико Н. И., Черкасов С. Н. и др. Методические аспекты оценки заболеваемости, распространенности, летальности и смертности при COVID-19. Кардиоваскулярная терапия и профилактика. 2020; 19 (3): 302–09. DOI:10.15829/1728-8800-2020-2585.
 9. Weiss P, Murdoch DR. Clinical course and mortality risk of severe COVID-19. *The Lancet*. 2020; 395: 1014–5.
 10. Дружинин П. В., Молчанова Е. В. Смертность населения российских регионов в условиях пандемии COVID-19. *Регионология*. 2021; 29 (3): 666–85. DOI: 10.15507/24131407.116.029.202103.666-685.
 11. Lifshits ML, Neklyudova NP. COVID-19 mortality rate in Russian regions: forecasts and reality. *R-economy*. 2020; 6 (3): 171–82. DOI: 10.15826/recon.2020.6.3.015.
 12. Дружинин П. В., Молчанова Е. В., Подлевских Ю. Л. Влияние пандемии Covid-19 на смертность населения российских регионов. *Труды Карельского научного центра РАН*. 2021; 7: 116–128. DOI: 10.17076/them1421.
 13. Всемирная организация здравоохранения (ВОЗ). Оценка показателей смертности от Covid-19. Доступно по ссылке (дата обращения 22.02.2022): <https://www.who.int/news-room/commentaries/detail/estimating-mortality-from-covid-19>.
 14. Richardson S, Hirsch JS, Narasimhan M, Crawford JM, McGinn T, Davidson KW, et al. Presenting characteristics, comorbidities, and outcomes among 5700 patients hospitalized with COVID-19 in the New York City Area. *JAMA*. 2020; 323 (20): 2052–9. DOI: 10.1001/jama.2020.6775.
 15. Grasselli G, Zangrillo A, Zanella A, Antonelli M, Cabrini L, Castelli A, et al. COVID-19 Lombardy ICU Network. Baseline Characteristics and Outcomes of 1591 Patients Infected With SARS-CoV-2 Admitted to ICUs of the Lombardy Region, Italy. *JAMA*. 2020; 323 (16): 1574–81. DOI: 10.1001/jama.2020.5394.
 16. Obesnyuk VF. Group health risk parameters in a heterogeneous cohort. Indirect assessment as per events taken in dynamics. *Health Risk Analysis*. 2021; 2: 17–32. DOI: 10.21668/health.risk/2021.2.02.eng.
 17. Паспорт Озёрского городского округа. Доступно по ссылке (дата обращения 22.02.2022): <http://ozerskadm.ru/regulatory/passport/>.
 18. Флетчер Р., Флетчер С., Вагнер Э. Клиническая эпидемиология. Основы доказательной медицины. М.: Изд-во «Медиа Сфера», 1998; 352 с.
 19. Мерков А. М., Сухаребский Л. М. Статистика на службе народного здоровья. М.: Изд-во «Статистика», 1968; 48 с.
 20. Abramson, JH. WINPEPI updated: computer programs for epidemiologists, and their teaching potential. *Epidemiologic Perspectives & Innovations*. 2011; 8 (1). DOI: 10.1186/1742-5573-8-1.
 21. Reality check on reproducibility. *Nature*. 2016; 533 (7604): 437. DOI: 10.1038/533437a.
 22. Регионы России. Социально-экономические показатели. Статистический сборник. 2020. Доступно по ссылке (дата обращения 22.02.2022): https://gks.ru/bgd/regl/b20_14p/Main.htm.
 23. Федеральная служба государственной статистики «Росстат». Доступно по ссылке (дата обращения 22.02.2022): <https://rosstat.gov.ru/storage/mediabank/TwbjciZH/edn12-2020.html>.
 24. Здравоохранение в России. Стат. сб. М.: Изд-во «Росстат», 2021; 171 с.
 25. Blagosklonny MV. From causes of aging to death from COVID-19. *Aging (Albany NY)*. 2020; 12 (11): 10004–21. DOI: 10.18632/aging.103493.
 26. Guan WJ, Liang WH, Zhao Y, Liang HR, Chen ZS, Li YM, et al. China Medical Treatment Expert Group for COVID-19. Comorbidity and its impact on 1590 patients with COVID-19 in China: a nationwide analysis. *Eur Respir J*. 2020; 55 (5): 2000547. DOI: 10.1183/13993003.00547-2020.
 27. Bong CL, Brasher C, Chikumba E, McDougall R, Mellin-Olsen J, Enright A. The COVID-19 Pandemic: Effects on Low- and Middle-Income Countries. *Anesth Analg*. 2020; 131 (1): 86–92. DOI: 10.1213/ANE0000000000004846.
 28. Herby J, Joung L, Hanke S. A Literature Review and Meta-Analysis of the Effects of Lockdowns on COVID-19 Mortality. *Studies in Applied Economics*. 2022; 200: 1–61.

SCREENING THE ACTIVITY OF INCORPORATED RADIONUCLIDES IN THE RESEARCH ORGANIZATION EMPLOYEES

Turlakov YuS, Grabsky YuV, Arefeva DV[✉], Shayakhmetova AA, Firsanov VB, Petushok AV

Scientific Research Institute of Marine and Industrial Medicine of the Federal Medical and Biological Agency, St. Petersburg, Russia

Studying the features of radiological situation in the workplace and assessing the individual effective doses in employees of research organizations working with open radiation sources (RS) are an urgent scientific task due to additional risks resulting from variability in the conditions and regimes of the technological operations. The study was aimed to assess the working conditions and intake of radionuclides by the employees of the V. G. Khlopin Radium Institute working with open RS. The data on exposure to work-related radiation factors were obtained by dosimetry, radiometry, and spectrometry. It was found that radiological situation in the employees' workplaces was characterized by the broad range of the gamma ambient dose equivalent rate values (0.10–122 μ Sv/h), alpha and beta working surface contamination, radioactive pollution of air in the working areas. In some individuals, spectrometry revealed the following: 125 I in the thyroid gland (up to 9,850 Bq), 90 Sr in the skeleton (up to 16,500 Bq), 137 Cs in the whole body (up to 1,100 Bq), etc. The findings can provide the basis for developing the measures to improve the quality of individual internal dose control and the efficiency of medical care provision to the research organization employees dealing with open RS.

Keywords: internal exposure, personnel, radiation factor, working conditions

Funding: state contract dated July 15, 2019 № 35.102.19.2 on implementation of the applied research project Justification of Directions for Improving the Internal Exposure Monitoring System for Employees of Research Institutes Served by the Federal Medical and Biological Agency (on the example of V. G. Khlopin Radium Institute) (code: SICH-19).

Author contributions: Turlakov YuS, Grabsky YuV — overall study management, final version of the article; Arefeva DV — planning, arrangement, analysis of the research results, manuscript writing; Shayakhmetova AA — radiometric survey, data processing and analysis; Firsanov VB — spectrometry, dosimetry, and radiometric survey, data processing; Petushok AV — dosimetry and radiometric survey, data processing.

✉ **Correspondence should be addressed:** Daria V. Arefeva
Yuri Gagarin prospect, 65, liter A, St. Petersburg, 196128, Russia; niipmm.210@gmail.com

Received: 24.03.2022 **Accepted:** 04.05.2022 **Published online:** 18.05.2022

DOI: 10.47183/mes.2022.014

СКРИНИНГ АКТИВНОСТИ ИНКОРПОРИРОВАННЫХ РАДИОНУКЛИДОВ У ПЕРСОНАЛА НАУЧНО-ИССЛЕДОВАТЕЛЬСКОЙ ОРГАНИЗАЦИИ

Ю. С. Турлаков, Ю. В. Грабский, Д. В. Арефьева[✉], А. А. Шаяхметова, В. Б. Фирсанов, А. В. Петушок

Научно-исследовательский институт промышленной и морской медицины Федерального медико-биологического агентства, Санкт-Петербург, Россия

Исследование особенностей формирования радиационной обстановки на рабочих местах и оценка индивидуальных эффективных доз облучения персонала научно-исследовательских организаций при выполнении работ с открытыми источниками ионизирующих излучений (ИИИ) является актуальной научной задачей в связи с наличием дополнительных рисков из-за вариативности условий и режимов выполнения технологических операций. Целью работы было оценить условия труда и поступление радионуклидов в организм персонала АО «Радиовый институт им. В. Г. Хлопина», работающего с открытыми ИИИ. Данные об уровне воздействия производственных факторов радиационной природы на персонал получены в ходе дозиметрических, радиометрических и спектрометрических измерений. Установлено, что радиационная обстановка на рабочих местах персонала характеризуется широким диапазоном уровней мощности амбиентного эквивалента дозы гамма-излучения (0,10–122 мкЗв/ч), наличием поверхностного загрязнения рабочих поверхностей альфа- и бета-частицами, наличием загрязнения радиоактивными веществами воздуха рабочих помещений. В результате спектрометрических исследований обнаружено наличие у отдельных лиц из персонала 125 I в щитовидной железе (до 9850 Бк), 90 Sr — в скелете (до 16 500 Бк), 137 Cs — во всем теле (до 1100 Бк) и др. Результаты исследований могут быть основой для разработки мероприятий по повышению качества контроля индивидуальных доз внутреннего облучения и эффективности медицинского обеспечения персонала научно-исследовательских организаций, имеющего контакт с открытыми ИИИ.

Ключевые слова: внутреннее облучение, персонал, радиационный фактор, условия труда

Финансирование: Государственный контракт от 15.07.2019 № 35.102.19.2 на выполнение прикладной научно-исследовательской работы «Обоснование направлений совершенствования системы контроля внутреннего облучения персонала научно-исследовательских институтов, обслуживаемых Федеральным медико-биологическим агентством (на примере АО «Радиовый институт им. В. Г. Хлопина»)» (шифр «СИЧ-19»).

Вклад авторов: Ю. С. Турлаков, Ю. В. Грабский — общее руководство исследованием, финальная редакция статьи; Д. В. Арефьева — планирование, организация и анализ результатов исследования, подготовка статьи; А. А. Шаяхметова — проведение радиометрических исследований, обработка и анализ полученных данных; В. Б. Фирсанов — проведение спектрометрических, дозиметрических и радиометрических исследований, обработка полученных данных; А. В. Петушок — проведение дозиметрических и радиометрических исследований, обработка полученных данных.

✉ **Для корреспонденции:** Дарья Владимировна Арефьева
пр. Юрия Гагарина, д. 65, литер А, г. Санкт-Петербург, 196128, Россия; niipmm.210@gmail.com

Статья получена: 24.03.2022 **Статья принята к печати:** 04.05.2022 **Опубликована онлайн:** 18.05.2022

DOI: 10.47183/mes.2022.014

Active development of the nuclear industry and nuclear medicine results in the increase in the volume of work with radioactive substances, including open radioactive sources. When carrying out such work, employees are exposed to a combination of harmful and/or dangerous work-related radiation factors: gamma ambient dose equivalent rate, alpha and beta surface contamination, radioactive air pollution in the work areas,

which increase the risk of the radionuclide intake by workers. Objective assessment of internal exposure and forecasting its effects on the human health are an urgent scientific issue that remains poorly understood despite the progress made by experimental studies in this area and clinical trials [1, 2].

The use of open radioactive sources (RS) in scientific research poses additional risks due to variability in the

conditions and regimes of the technological operations depending on the tasks to be performed. According to the production control data, individual effective doses from internal exposure in employees of the companies and organizations, whose professional activities involve dealing with the sources of ionizing radiation, do not exceed maximum permissible levels. However, in certain cases, especially when performing some non-standard technological operations, or in emergency situations, the risk of intake and accumulation of radionuclides present in the working environment by workers increases. Depending on the route of intake and the radionuclide physical and chemical properties, the methods for assessment of the expected internal effective dose are distinguished that are currently based on the workplace dosimetric monitoring data or individual dosimetric control data (by direct and indirect measuring methods) [3].

During their professional activities, the employees are exposed to the so-called low doses, characterized by the risk of the stochastic effect emergence [4, 5]. Therefore, it is also necessary to take into account the type of radiation (alpha, beta, gamma, etc.), incorporated radionuclide half-lives, duration of the radionuclide retention in the body, and radionuclide localization in organs and tissues to predict the internal exposure effects on the human body.

The study was aimed to perform the radiation hygiene assessment of working conditions and intake of radionuclides by the employees of the V.G. Khlopin Radium Institute working with open radioactive sources.

METHODS

The system of individual dosimetric monitoring for internal exposure of the research organization personnel working with open radioactive sources (RS) was the object of the study.

The study was carried out in 2019–2021 in the V.G. Khlopin Radium Institute.

The following parameters were measured in order to obtain the baseline data on the characteristics of harmful and/or dangerous work-related radiation factors the surveyed personnel was exposed to:

- gamma ambient dose equivalent rate (ADER);
- spectral composition of the gamma-emitting radionuclides at workplaces (spectral measurements);
- removable radioactive working surface contamination;
- alpha and beta particles flux density;
- volumetric activity of radionuclides in the air of working premises.

Gamma ADER was measured using the DKS-AT1123 dosimeter (Atomtex; Republic of Belarus) in accordance with the operating manual and Methodological Guidelines MU 2.6.5.008-2016 “Monitoring of Radiation Environment. General Requirements”. To get a picture of the radiation field formation in the workplace, the measurements were performed in every point at the following height from the floor: 0.1 m, 1 m, 1.4 m and 1.7 m. The levels of alpha and beta working surface contamination were measured with the MKS-AT1117M dosimeter-radiometer (Atomtex; Republic of Belarus) in accordance with the operating manual. The expanded uncertainty ($k = 2$) of measurement was considered equal to the relative error of the measuring tool assuming a normal distribution of readings.

Removable radioactive surface contamination was measured by the indirect method involving taking smears with subsequent determination of their activity in accordance with the regulatory documents [6, 7], measurement uncertainty

was calculated in accordance with the measurement procedure [7].

To define volumetric activity of radionuclides, air samples were collected in the working premises using the PA-300M-1 aspirator (Ecotech-Ural; Russia) with the aerosol filters AFA RSP-20 (Electroforming Technologies; Russia) and iodine filter AFA SRF-20 (Electroforming Technologies; Russia) in accordance with the aspirator operating manual, with subsequent measurement using the MKGB-01 RADEK spectrometer-radiometer (STC RADEK; Russia). The expanded uncertainty of measurement was calculated taking into account the error of the spectrometer sensitivity coefficient (8%), error of the ambient air sample volume (10%), and procedural error resulting from inconsistency of the load composition (5%) that accounted for 16%.

Spectrometric study of employees engaged in working with open RS (45 people, of them 34 were assessed in 2019 and 21 were assessed in 2020) and the control group employees (10 people) was performed by the direct measurement of radionuclides in the human body or organ with the SEG-10P-02 (STC RADEK; Russia) and SICH-100 (Scientific Research Institute of Marine and Industrial Medicine of FMBA; Russia) whole body spectrometers. Inclusion criteria: working with open RS during the last year, prior to assessment. Control group inclusion criteria: no exposure to open RS when working. Measurements were performed by registration of the photon radiation emitted by human body. Measurements with the SICH-100 spectrometer were performed in the “linear longitudinal scan” measurement geometry, and SEG-10P-02 used the “lung” and “thyroid” measurement geometries. The content of the ^{90}Sr radionuclide in the bone tissue was defined based on the bremsstrahlung radiation spectrum with the energy range of 50–150 keV registered by two scintillation detectors with the CsI(Tl) single crystals sized $\varnothing 150 \times 3$ mm, installed in the SICH-100 unit. The measurement duration of 30 min was used in both spectrometers.

Calibration of the SICH-100 spectrometer was performed using the UP-02T unified solid phantom of the whole body and the ARDF-11-C anthropomorphic whole body phantom with ^{90}Sr radionuclide in the skeleton. The UP-02T phantom consists of a number of PET blocks with the set of rod sources assembled into models, the phantoms of human body with the specified radionuclide content, on site. The ARDF-11-C phantom is a prefabricated unit consisting of the anthropomorphic models of organs (thyroid gland, liver, lung, kidney, etc.), skeleton, and integument manufactured from materials that mimic biological tissues, equivalent to human tissues in terms of interaction with ionizing radiation.

Calibration of the SEG-10P-02 whole body spectrometer in the “lung” measurement geometry was performed by direct calibration with the use of the FLT-05 chest phantom in combination with the standard phantom of an adult man (body weight 70 kg, height 170 cm). There was a polyurethane lung simulator equipped with the large RSs containing ^{60}Co , ^{152}Eu , ^{241}Am radionuclides in the chest phantom. Calibration was performed serially for each of the listed above radionuclides.

To measure the activity of ^{125}I in the thyroid gland, thin NaI(Tl) detection unit previously calibrated based on the ^{133}Ba characteristic radiation using the phantom of thyroid PT-04T was used. The phantom was a model of human neck with two ^{133}Ba radionuclide sources in its cavity positioned similar to the thyroid lobes. Since the detection area of the unit included not only the thyroid gland, but also blood vessels of the neck, the energy spectrum of background radiation was measured in the forearm in order to take into account the contribution of these blood vessels.

Table 1. Gamma ADER, alpha and beta particles flux density measured at the employees' workplaces

Tasks performed at the workplace	Range of measured ADER values, $\mu\text{Sv/h}$	Maximum flux density, particles/($\text{cm}^2 \times \text{min}$)	
		alpha particles	beta particles
Analysis of highly radioactive solutions, X-ray absorptiometry, working with samples under the fume hood or in the box	4,0–53,0	30	1830
Technological operations with highly radioactive solutions, packing and distribution of the ^{90}Sr preparations	5,0–122,0	No data available	1100
Opening ampoules, dissolution, calibration of solutions and producing the sources	3,4–56,0	4,2	4000
Preparation of the simulant solution containing ^{90}Sr , ^{137}Cs , ^{241}Am , ^{152}Eu and other isotopes. Extraction of ^{90}Sr , ^{137}Cs from the simulant solution. Preparation of the ^{238}U and ^{239}Pu nitric acid solution. Preparation of the ^{238}U and ^{239}Pu oxide powders, sorption extraction of impurities, packing	0,5–4,3	0,8	15
Packing ^{125}I	0,9–18,2	< 0,1	1680
Extraction and chromatographic separation of products from the spent nuclear fuel and irradiated ^{226}Ra processing	0,4–4,6	29	32
Acceptance, chopping up, storage and transfer of the spent nuclear fuel and highly radioactive materials, nuclear waste repacking and discharge	0,1–0,6	0,4	30
Dissolution, precipitation, evaporation, clarification of the spent nuclear fuel components	0,1–0,2	< 0,1	200
Extraction, evaporation, solidification of nuclear waste	0,1–0,3	< 0,1	20
Technological equipment decontamination and repair, nuclear waste sorting, packing and preparation for removal	11,0–54,5	78	1680

Note: the values were calculated taking into account the expanded uncertainty of measurement ($k = 2$).

The expanded uncertainty for the confidence level of $P = 0.95$ and coverage factor of $k = 2$ for the SEG-10P-02 and SICH-100 spectrometers was calculated taking into account the errors of the spectrometer sensitivity coefficients defined based on the phantoms (8%), procedural error resulting from uneven distribution of activity in the human body or organs (10%), and procedural error resulting from incomplete equivalence of the phantoms and human body (20%), which accounted for 24%.

Statistical data processing was performed by standard methods used for analysis of the radiation hygiene and biomedical data. The mean, median, standard error of the mean, and significance of the differences were calculated for all parameters with the significance level set at $p = 0.95$. All the calculations were performed using the modern software products (Microsoft Excel, v. Professional Plus 2010; USA) designed for working with spreadsheets, as well as for data visualization and analysis.

The employees' working conditions were assessed in accordance with the regulations [8].

RESULTS

When performing the radiation hygiene assessment of the employees' workplaces in the research organization, a total of 17 production premises were assessed where the work with open RS was carried out. The results of the gamma ambient dose equivalent rate and the alpha and beta particles flux density measurement at the employees' workplaces are provided in Table 1.

The highest gamma ADER values were observed when working with highly radioactive solutions. The maximum values of the alpha and beta particles flux density were registered when opening ampoules, performing dissolution and calibration of solutions, producing the sources. Surface contamination by alpha particles in the amount not exceeding the reference

values in accordance with the requirements of RSS-99/2009 was also observed in the workplaces. In addition, removable surface activity and volumetric activity of radionuclides in the air of working areas were measured due to surface contamination of the employees' workplaces.

Based on the results of measuring the levels of the alpha and beta working surface contamination in the employees' workplaces, removable surface activity was detected not exceeding the permissible values defined by the RSS-99/2009 [9]. The highest levels of the beta removable surface contamination (^{90}Sr) were registered when opening ampoules, performing dissolution and calibration of solutions, producing the sources.

Based on the results of measuring the volumetric activity of radionuclides in the air of working areas, the highest values were registered when working with the ^{125}I and ^{137}Cs radionuclides (volumetric activity of ^{125}I was 240 Bq/m^3 , and volumetric activity of ^{137}Cs was 315 Bq/m^3).

Based on the radiation monitoring data, the potential upper effective dose limit for the personnel performing technological operations was calculated in accordance with legislative requirements [8]. It was found that the working conditions of personnel working with open RS were within the range from acceptable (class 2) to dangerous (class 4) based on the characteristics of exposure to harmful and/or dangerous work-related radiation factors.

According to the data obtained in 2016–2019, the average values of the employees' individual effective doses from external exposure were 3.4 mSv per year, which was well below the dose limit established for the group A personnel. The highest values were registered in the leading industrial engineers, and the average values for the four-year period were 7.5 mSv .

When performing the spectrometric study in some employees working with open RS, incorporated radionuclides were found in their bodies (Table 2). The table also presents

Table 2. Characteristics of the surveyed employees' internal exposure

Radionuclide	Radionuclide activity, Bq	Expected equivalent dose from internal exposure, mSv per year
¹³⁷ Cs	120–1100	0.001–0.004 (whole body)
⁹⁰ Sr	5200–16500	0.3; 0.9 (bone tissue)
²²⁶ Ra	360–770	0.47–1.00 (bone tissue)
²²³ Ra	550–2800	0.9; 4.8 (bone tissue)
¹²⁵ I	2930–9850	0.18–2.1 (thyroid gland)
⁶⁰ Co	840	0.03 (lungs)

the values of the expected equivalent dose from internal exposure of the employees resulting from the radionuclide intake. Calculations were performed taking into account the spectrometry data of reference dose coefficients [10, 11].

In addition to radionuclides presented in Table 2, incorporated ²⁴¹Am was found in three employees. Due to the lack of calibration of the used measuring equipment, it was impossible to accurately measure activity of this radionuclide in the skeleton.

DISCUSSION

According to the results of the radiometric survey, radiological situation in the workplaces of the research organization employees working with open RS could be characterized as follows:

- broad range of the gamma ADER levels (0.10–122 µSv/h);
- alpha and beta working surface contamination (the following radionuclides were detected in smears from working surfaces: ¹³⁷Cs, ¹²⁵I, ²⁴¹Am, ¹⁵⁴Eu, ²⁴³Am with the ²³⁹Np decay product, and ²²³Ra with the ²¹¹Bi decay product);
- radioactive pollution of air in the working areas (including such radionuclides as ¹²⁵I and ¹³⁷Cs).

In some individuals the following were found: ¹²⁵I in the thyroid gland (up to 9,850 Bq), ⁹⁰Sr in the skeleton (up to 16,500 Bq), ¹³⁷Cs in the whole body (up to 1,100 Bq). The finding of the ²²³Ra intake in employees stands out, since the ²²³Ra half life period is 11 days, and the ²²³Ra contribution to the internal exposure dose is much higher compared to other radionuclides.

The fact of radionuclide incorporation was confirmed by periodic spectrometry-based assessment of the same employees performed in 2019 and 2020. These employees should be considered a group at high risk of occupational, work-related and chronic diseases.

Currently, in the research organization under consideration, the expected effective doses from internal exposure in employees are monitored by computation (based on the dosimetry in workplaces), which is not fully effective when working with the large number of radionuclides, including the short-lived ones. That is why developing the programme of screening with the use of portable spectrometers is one of the ways to improve the efficiency of the internal dosimetry monitoring system in employees working with open RS. The studies are aimed to confirm the fact of the radionuclide intake and determine the radionuclide composition. In case

of radionuclide intake detection in the employee, assessment should be performed in the specialized institution using the high precision whole body radiation spectrometer. Such approach would provide the radiation safety service employees with the main instruments for effective implementation of the internal exposure monitoring programme [12–14].

The database was developed and registered in order to perform accumulation and processing of data on the levels of the employees' external and internal exposure in the planned exposure situations together with the results of the periodic medical examinations [15]. Introduction of the database in practice would make it possible to assess the general trends in occupational exposure of the staff and analyze the research results in order to reveal the correlation between the incidence of occupational, work-related, and chronic somatic disorders, as well as the emergence of medical contraindications for work, and the levels and duration of exposure to the harmful and/or dangerous work-related radiation factors and other factors (length of employment, age, gender, etc.).

CONCLUSIONS

(1) Working conditions of the research organization personnel working with open RS are within the range from acceptable (class 2) to dangerous (class 4) based on the characteristics of exposure to harmful and/or dangerous work-related radiation factors. Compliance with the established norms and radiation safety regulations does not exclude radionuclide intake and incorporation in employees. (2) Regular spectrometry-based assessment of the V. G. Khlopin Radium Institute employees and the development of screening programmes (with the use of portable spectrometers), aimed at assessing radionuclide intake and, in case of confirming incorporation, performing in-depth spectrometry-based assessment with the high precision whole body radiation spectrometer, are required for analysis of the dynamic changes in the individual effective doses from internal exposure. This will make it possible to improve the quality of the individual internal dose control and the efficiency of the radiation protection of workers. (3) Further studies are necessary aimed at assessing the trends and defining the correlation between the incidence of occupational and chronic somatic disorders, as well as the emergence of medical contraindications for work in the research organization employees working with open RS, and the levels and duration of exposure to harmful and/or dangerous work-related radiation factors and other factors.

References

1. Tang F, Loganovsky K. Low dose or low dose rate ionizing radiation-induced health effect in the human, *Journal of Environmental Radioactivity*. 2018; 192: 32–47.
2. Muirhead CR, O'hagan JA, Haylock RGE, Phillipson MA, Willcock T, Berridge GLC, et al. Mortality and cancer incidence following occupational radiation exposure: third analysis of the National Registry for Radiation Workers. *British journal of cancer*. 2009; 100 (1): 206–12.
3. Metodicheskie ukazaniya MU 2.6.1.065-2014 «Dozimetriceskij kontrol' professional'nogo vnutrennego obluchenija. Obshhie trebovaniya». Moskva, 2014; 46 s. Dostupno po ssylke: https://fmba.gov.ru/upload/iblock/dc0/mu_2.6.1.065-2014.pdf. Russian.
4. Akleev AV, Aladova EE, Anciferov AN, i dr. *Jadernaja medicina: spravochnik dlja personala otdelenij, laboratorij i centrov mediciny*. M.: FGBU GNC FMBC im. A.I. Burnazjana FMBA Rossii, 2020; 388 s. Russian.
5. Ljaginskaja AM, Shandala NK, Kiselev SM, Ermalickij AP, Petojan IM, Kupcov VV, i dr. Sostojanie zdorov'ja personala predprijatija po obrashheniju s radioaktivnymi otdodami utiliziruemogo atomnogo flota SSSR. Radiacija i risk (Bjulleten' Bjulleten' Nacional'nogo radiacionno-jepidemiologičeskogo registra). 2019; 28 (4): 73–87. Russian.
6. Metodicheskie ukazaniya MU 2.6.5.032-2017 «Kontrol' radioaktivnogo zagraznenija poverhnostej». M., 2017. Dostupno po ssylke: <https://docs.cntd.ru/document/456087187>. Russian.
7. Metodika izmerenija snimaemoj poverhnostnoj aktivnosti al'fa- i beta- izluchajushhijh radionuklidov s ispol'zovaniem nosimogo ili stacionarnogo radiometra, ustrojstva dlja otbora mazkov UOM-01T i prispособlenija dlja izmerenija aktivnosti radionuklidov v fiksirovannoj geometrii UIM-01T, FGUP NII PMM, nomer v Federal'nom reestre metodik izmerenij: FR.1.40.2015.19924, svidetel'stvo ob attestacii metodiki izmerenij # 451/210-(01.00250-2008)-2013. Dostupno po ssylke: <https://docs.cntd.ru/document/437126129>. Russian.
8. Rukovodstvo R 2.2.2006-05 Gигиена труда. Rukovodstvo po gигиенической oценке faktorov rabochej sredy i trudovogo processa. Kriterii i klassifikacija uslovij truda. Bjulleten' normativnyh i metodičeskijh dokumentov Gossan'jepidnadzora. 2005; 3 (21). Russian.
9. Sanitarnye pravila i normativy SanPiN 2.6.1.2523-09 «Normy radiacionnoj bezopasnosti NRB 99/2009». Dostupno po ssylke (data obrashhenija 25.01.2022): <http://docs.cntd.ru/document/902170553/>. Russian.
10. ICRP, Dose Coefficients for Intakes of Radionuclides by Workers, ICRP Publication № 68, Ann. ICRP 24 4. Oxford: Elsevier Science, 1994.
11. ICRP, Age-Dependent Doses to Members of the Public from Intake of Radionuclides, Part 5, Compilation of Ingestion and Inhalation Dose Coefficients, ICRP Publication № 72, Ann. ICRP 26. Oxford: Elsevier Science, 1996.
12. Medici S, Carbonez P, Damet J, Bochud F, Bailat C, Pitzschke A, Detecting intake of radionuclides: In vivo screening measurements with conventional radiation protection instruments. *Radiation Measurements*. 2019; 122: 126–32.
13. Medici S, Carbonez P, Damet J, Bochud F, Pitzschke A, Use of portable gamma spectrometers for triage monitoring following the intake of conventional and novel radionuclides. *Radiation Measurements*. 2020; 136: 106426. Available from: <https://doi.org/10.1016/j.radmeas.2020.106426>.
14. Galeev R, Butterweck G, Boschung M, Hofstetter-Boillat B, Hohmann E, Mayer S. Suitability of portable radionuclide identifiers for emergency incorporation monitoring. *Radiation Protection Dosimetry*. 2017; 173 (1–3): 145–50. Available from: <https://doi.org/10.1093/rpd/ncw330>.
15. Arefeva DV, Petushok AV, Shajahmetova AA, avtory; Federal'noe gosudarstvennoe unitarnoe predpriyatie nauchno-issledovatel'skij institut promyshlennoj i morskoy mediciny Federal'nogo mediko-biologičeskogo agentstva, Mediko-dozimetriceskij registr personala gruppy A Akcionernogo obshhestva «Radievj institut im. V.G. Hlopina», rabotajushhego s otkrytymi istochnikami ionizirujushhijh izluchenij: Svidetel'stvo o gosudarstvennoj registracii bazy dannyh # 2021620928 Rossijskaja Federacija, 05.05.2021. Russian.

Литература

1. Tang F, Loganovsky K. Low dose or low dose rate ionizing radiation-induced health effect in the human, *Journal of Environmental Radioactivity*. 2018; 192: 32–47.
2. Muirhead CR, O'hagan JA, Haylock RGE, Phillipson MA, Willcock T, Berridge GLC, et al. Mortality and cancer incidence following occupational radiation exposure: third analysis of the National Registry for Radiation Workers. *British journal of cancer*. 2009; 100 (1): 206–12.
3. Методические указания МУ 2.6.1.065-2014 «Дозиметрический контроль профессионального внутреннего облучения. Общие требования». Москва, 2014; 46 с. Dostupno po ssylke: https://fmba.gov.ru/upload/iblock/dc0/mu_2.6.1.065-2014.pdf.
4. Аклеев А. В., Аладова Е. Е., Анциферов А. Н., и др. *Ядерная медицина: справочник для персонала отделений, лабораторий и центров медицины*. М.: ФГБУ ГНЦ ФМБЦ им. А.И. Бурназяна ФМБА России, 2020; 388 с.
5. Лягинская А. М., Шандала Н. К., Киселев С. М., Ермалицкий А. П., Петоян И. М., Купцов В. В., и др. Состояние здоровья персонала предприятия по обращению с радиоактивными отходами утилизируемого атомного флота СССР. Радиация и риск (Бюллетень Бюллетень Национального радиационно-эпидемиологического регистра). 2019; 28 (4): 73–87.
6. Методические указания МУ 2.6.5.032-2017 «Контроль радиоактивного загрязнения поверхностей». М., 2017. Dostupno po ssylke: <https://docs.cntd.ru/document/456087187>.
7. Методика измерения снимаемой поверхностной активности альфа- и бета- излучающих радионуклидов с использованием носимого или стационарного радиометра, устройства для отбора мазков UOM-01T и приспособления для измерения активности радионуклидов в фиксированной геометрии UIM-01T, ФГУП НИИ PMM, номер в Федеральном реестре методик измерений: ФР.1.40.2015.19924, свидетельство об аттестации методики измерений № 451/210-(01.00250-2008)-2013, Dostupno po ssylke: <https://docs.cntd.ru/document/437126129>.
8. Руководство Р 2.2.2006-05 Гигиена труда. Руководство по гигиенической оценке факторов рабочей среды и трудового процесса. Критерии и классификация условий труда. Бюллетень нормативных и методических документов Госсанэпиднадзора. 2005; 3 (21).
9. Санитарные правила и нормативы СанПиН 2.6.1.2523-09 «Нормы радиационной безопасности НРБ 99/2009». Dostupno po ssylke (data obrashhenija 25.01.2022): <http://docs.cntd.ru/document/902170553/>.
10. ICRP, Dose Coefficients for Intakes of Radionuclides by Workers, ICRP Publication № 68, Ann. ICRP 24 4. Oxford: Elsevier Science, 1994.
11. ICRP, Age-Dependent Doses to Members of the Public from Intake of Radionuclides, Part 5, Compilation of Ingestion and Inhalation Dose Coefficients, ICRP Publication № 72, Ann. ICRP 26. Oxford: Elsevier Science, 1996.
12. Medici S, Carbonez P, Damet J, Bochud F, Bailat C, Pitzschke A, Detecting intake of radionuclides: In vivo screening measurements with conventional radiation protection instruments. *Radiation Measurements*. 2019; 122: 126–32.
13. Medici S, Carbonez P, Damet J, Bochud F, Pitzschke A, Use of portable gamma spectrometers for triage monitoring following

- the intake of conventional and novel radionuclides. *Radiation Measurements*. 2020; 136: 106426. Available from: <https://doi.org/10.1016/j.radmeas.2020.106426>.
14. Galeev R, Butterweck G, Boschung M, Hofstetter-Boillat B, Hohmann E, Mayer S. Suitability of portable radionuclide identifiers for emergency incorporation monitoring. *Radiation Protection Dosimetry*. 2017; 173 (1–3): 145–50. Available from: <https://doi.org/10.1093/rpd/ncw330>.
15. Арефьева Д. В., Петушок А. В., Шаяхметова А. А., авторы;

Федеральное государственное унитарное предприятие научно-исследовательский институт промышленной и морской медицины Федерального медико-биологического агентства, Медико-дозиметрический регистр персонала группы А Акционерного общества «Радиовый институт им. В. Г. Хлопина», работающего с открытыми источниками ионизирующих излучений: Свидетельство о государственной регистрации базы данных № 2021620928 Российская Федерация, 05.05.2021.

PSYCHOLOGICAL WELL-BEING OF THE DEPARTMENT HEADS AT HEALTHCARE ORGANIZATIONS

Kochubey AV¹ ✉, Yarotsky SYu¹, Kochubey VV²¹ Federal Scientific and Clinical Center of Specialized Types of Medical Care of the Federal Medical and Biological Agency, Moscow, Russia² A.I. Yevdokimov Moscow State University of Medicine and Dentistry, Moscow, Russia

Increased workloads among heads of clinical departments that result from working as both clinicians and managers may lead to the significant decline in their psychological well-being. The study was aimed to assess psychological well-being of the clinical department heads. The online survey of 216 department heads aged 32–70 having a 8–51-year experience in healthcare was conducted using the Ryff's scales of psychological well-being adopted by Shevelenkova–Fesenko, sent by e-mail or posted on the distance learning portal. The survey involved 123 men (56.9%) and 93 women (43.1%); among them 117 people (54.2%) worked in inpatient settings, 114 people (52.8%) worked in the red zone, 138 people (63.89%) were assigned a qualification category, 63 people (29.1%) had an academic degree. Mean values, percentage, Pearson correlation coefficient, Student's t-test were calculated with the IBM SPSS Statistics 23 software. Correlations and mean differences were considered significant at $p < 0.05$. The average psychological well-being score was 378.67 ± 78.33 ; in 26 men (26%) and 28 women (43.1%) aged 36–55, the score was below standard values. Psychological well-being correlated with age ($r = 0.2$; $p = 0.019$) and years of service ($r = 0.2$; $p = 0.008$). No correlations were revealed between psychological well-being and gender ($p = 0.798$), type of organization ($p = 0.642$), the fact of having second higher education ($p = 0.854$), qualification category ($p = 0.645$), academic degree ($p = 0.204$), and the experience of working in the red zone ($p = 0.926$). Thus, more than a third of individuals aged 36–55 have psychological well-being scores below standard values. Psychological well-being of women is lower than that of men. Psychological well-being of men over the age of 35 decreases to a greater extent than standard values.

Keywords: psychological well-being, personal growth, heads of departments**Author contribution:** Kochubey AV — concept, design, research coordination, statistical analysis and data interpretation, manuscript writing; Yarotsky SYu — analysis, research planning, data interpretation, discussion; Kochubey VV — literature review, data analysis and interpretation, manuscript writing.**Compliance with ethical standards:** the study was conducted in accordance with the ethical principles stipulated by the Declaration of Helsinki of the World Medical Association.✉ **Correspondence should be addressed:** Adelina V. Kochubey
Volokolamskoye shosse, 91, Moscow, 125371, Russia; kochoubeya@gmail.com**Received:** 08.05.2022 **Accepted:** 08.06.2022 **Published online:** 19.06.2022**DOI:** 10.47183/mes.2022.021

ПСИХОЛОГИЧЕСКОЕ БЛАГОПОЛУЧИЕ ЗАВЕДУЮЩИХ ОТДЕЛЕНИЯМИ МЕДИЦИНСКИХ ОРГАНИЗАЦИЙ

A. В. Кочубей¹ ✉, С. Ю. Яроцкий¹, В. В. Кочубей²¹ Федеральный научно-клинический центр специализированных видов медицинской помощи Федерального медико-биологического агентства, Москва, Россия² Московский государственный медико-стоматологический университет имени А. И. Евдокимова, Москва, Россия

Повышенная нагрузка заведующих клиническими отделениями в связи с реализацией трудовых функций врача-клинициста и менеджера может привести к значимому ухудшению психологического благополучия. Целью работы было изучить психологическое благополучие заведующих клиническими отделениями. Используя версию Шевеленковой–Фесенко опросника Риффа, с помощью электронной почты и портала дистанционного обучения проводили заочное анкетирование 216 заведующих отделениями в возрасте 32–70 лет со стажем работы в сфере здравоохранения 8–51 лет. В опросе участвовали 123 мужчины (56,9%) и 93 женщины (43,1%), из них работали в стационаре 117 человек (54,2%), в «красной зоне» — 114 (52,8%), имеют квалификационную категорию 138 человек (63,89%), ученую степень — 63 (29,1%). Расчеты средних значений, процентов, коэффициента корреляции Пирсона, критерия Стьюдента проводили в программе IBM SPSS Statistics 23. Корреляцию и разницу средних значений считали значимой при $p < 0,05$. Средний балл психологического благополучия — $378,67 \pm 78,33$, ниже нормативных значений — у 26 (26%) мужчин, 28 (43,1%) женщин 36–55 лет. Выявлена корреляция психологического благополучия с возрастом ($r = 0,2$; $p = 0,019$) и стажем ($r = 0,2$; $p = 0,008$). Не обнаружена зависимость психологического благополучия от пола ($p = 0,798$), типа организации ($p = 0,642$), наличия второго образования ($p = 0,854$), категории ($p = 0,645$), ученой степени ($p = 0,204$), работы в «красной зоне» ($p = 0,926$). Таким образом, более трети лиц 36–55 лет имеют баллы психологического благополучия ниже нормативных значений. Женщины имеют худшее психологическое благополучие, чем мужчины. Психологическое благополучие мужчин после 35 лет снижается в большей степени, чем нормативные значения.

Ключевые слова: психологическое благополучие, личностный рост, заведующий отделением**Вклад авторов:** А. В. Кочубей — идея, дизайн, координация исследования, статистический анализ и интерпретация результатов, подготовка рукописи; С. Ю. Яроцкий — анализ, планирование исследования, интерпретация данных, обсуждение результатов; В. В. Кочубей — работа с литературой, анализ и интерпретация данных, подготовка рукописи.**Соблюдение этических стандартов:** исследование проведено в соответствии с этическими принципами Хельсинкской декларации Всемирной медицинской ассоциации.✉ **Для корреспонденции:** Аделина Владимировна Кочубей
Волоколамское шоссе, д. 91, г. Москва, 125371, Россия; kochoubeya@gmail.com**Статья получена:** 08.05.2022 **Статья принята к печати:** 08.06.2022 **Опубликована онлайн:** 19.06.2022**DOI:** 10.47183/mes.2022.021

In 1989, the World Health Organization announced that facilitating innovations by encouraging professional curiosity in healthcare professionals was one of the objectives for healthcare quality assurance [1]. Such strategy of the WHO results from the fact that the impact on human resources is a highly

effective method for quality assurance in medical care [2–4]. The health service staff professionalism provides extraordinary basis for improving the processes and results [5]. For its part, professional curiosity of the staff depends on psychological well-being, including the desire for personal growth [6].

Unfortunately, healthcare providers are a professional group at risk of psychological problems [7] due to high levels of stress and psychological disorders [8, 9]. Occupational well-being was studied in physicians [10–12] and nursing staff [13, 14] of various medical specialties. It was found that depression, being the worst manifestation of psychological ill-being, formed the basis for medical malpractice [13].

Heads of clinical departments are the key figures in healthcare quality assurance [15], that is why their psychological well-being is extremely important. Heads of clinical departments work as both clinical specialists and healthcare managers [15], i.e., increased workloads are coupled with the responsibility for directing the work of the entire department. These factors together with the requirements for mastering a wider range of competencies and professional development in both medical specialty and management can adversely affect the psychological well-being of this cohort of healthcare professionals.

The study was aimed to assess psychological well-being of the department heads at healthcare organizations.

METHODS

The study involved an online survey of residents who received the continuing professional education training at the Academy of Postgraduate Education of the Federal Scientific and Clinical Center of Specialized Types of Medical Care of FMBA in 2019–2021. Inclusion criteria: respondents holding a position of the head of clinical department. Exclusion criteria: unfinished questionnaires. The survey was conducted using the standardized Russian version of the Ryff's scales of psychological well-being adopted by Shevelenkova–Fesenko [16]. Such choice is explained by the fact that standard values of psychological well-being for four gender and age groups are provided in relation to this version. The questionnaires were sent to respondents by e-mail or incorporated in the training courses and posted on the distance learning platform.

The questionnaire includes 84 items with six scales: Positive Relations with Others, Autonomy, Environmental Mastery, Personal Growth, Purpose in Life, Self-Acceptance, and three integral categories, Affect Balance, Meaningful Life, Human Being as an Open System, which were scored separately. A 6-point Likert scale (1 — Strongly disagree, 6 — Strongly agree) was used to assess psychological well-being. Higher scores indicated better subjective well-being. This principle was applicable to all scales of the questionnaire and two integral categories (Meaningful Life, Human Being as an Open System). Lower scores in the Affect Balance category indicated better condition of the respondent.

Characteristics of respondents

The survey involved 216 respondents (Table 1). Owing to the unavailability of data on the sampled population size, deterministic sampling method was used that was based on the expert judgement provided by the group of experts [17].

Characteristics were selected based on the third party research data on the impact of gender, age, increased workloads, better education and professional development on psychological well-being. It was thus suggested that increased workloads, experienced by the respondents working in inpatient settings and in the red zones, adversely affected their psychological well-being. We also assumed that the fact of having second higher education, qualification category, academic degree, that could be regarded as an indirect

confirmation of the desire for personal growth, had a beneficial effect on psychological well-being.

The differences in years of service between men and women were significant: $t = 7.44$; $p < 0.001$. There were significant differences in age and years of service between the respondents working in inpatient and outpatient settings: $t = 6.87$; $p < 0.001$. At the time of the survey, more than half of the respondents worked in the departments that provided care to patients with coronavirus infection, where enhanced hygiene and infection prevention and control regime together with specific zoning (hereinafter, “the red zone”) were used. The differences in the average age and years of service between those who had an experience or no experience of working in the red zone were significant: $t = 6.62$; $p < 0.001$. There were no significant differences in age ($t = 0.648$; $p = 0.197$) and years of service ($t = 0.457$; $p = 0.095$) between individuals assigned and not assigned a qualification category. The differences in age ($t = 2.536$; $p = 0.012$) and years of service ($t = 1.987$; $p = 0.048$) between the respondents having and not having an academic degree were significant. The differences in age ($t = 0.123$; $p = 0.902$) and years of service ($t = 0.186$; $p = 0.853$) between the respondents having and not having second higher education were non-significant.

Comparative analysis of scores was performed for three gender and age groups, men aged 20–35 and 36–55, women aged 36–55, where the standard values of psychological well-being were available. There were no women aged 20–35 among the respondents. The average psychological well-being scores were provided for the general group and five gender and age groups: men aged 20–35, 36–55, and over 56; women aged 36–55 and over 56.

IBM SPSS Statistics 23 software (IBM Company; USA) was used to calculate the mean, median, mode, standard deviation, percentage, Student's t -test, Pearson correlation coefficient. Correlations and mean differences for independent samples were considered significant at $p < 0.05$.

RESULTS

The mean score of psychological well-being on the Ryff's scales was 378.67 ± 78.33 , median was 398.5, mode was 438.00; in 54 respondents (25%), the psychological well-being score was below 342.25, and in 54 people (25%) it exceeded 442.75. In 86 respondents (39.8%) the scores of psychological well-being were below average. The average levels of psychological well-being in women aged 36–55, men aged 20–35 and 36–55 exceeded standard values (Table 2). However, in 26 men (26%) and 28 women (43.1%) aged 36–55, the levels of psychological well-being were below standard values.

The correlation of psychological well-being with age ($r = 0.2$; $p = 0.019$) and years of service ($r = 0.2$; $p = 0.008$) was revealed. There were no significant differences in the mean scores of psychological well-being between men (377.47 ± 81.13) and women (380.25 ± 74.87 ; $t = 0.257$, $p = 0.798$); heads of departments working in inpatient settings (376.38 ± 82.38) and primary health care institutions (381.37 ± 73.58 ; $t = 0.466$, $p = 0.642$); respondents having (379.63 ± 81.23) and not having second higher education (377.66 ± 75.51 ; $t = 0.185$, $p = 0.854$); those assigned (380.52 ± 78.06) and not assigned a qualification category (375.39 ± 79.21 ; $t = 0.461$, $p = 0.645$); those having (389.24 ± 68.48) and not having an academic degree (374.32 ± 81.86 ; $t = 1.274$, $p = 0.204$); those having an experience (378.20 ± 81.26) or no experience of working in the red zone (379.19 ± 75.32 ; $t = 0.093$; $p = 0.926$).

The mean scores for the categories and scales of the Ryff's questionnaire by gender and age groups are provided in Table 2.

Table 1. Characteristics of respondents

Characteristics	Number, abs. (%)	Average age, years	Average years of service
All respondents	216	47.9 ± 8.08	23.18 ± 8.60
Women	93 (43.1)	52.15 ± 6.653	27.06 ± 7.079.
Men	123 (56.9)	44.77 ± 7.621	20.06 ± 8.435
Worked in inpatient settings	117 (54.2)	44.79 ± 7.715	20.10 ± 8.569
Worked in outpatient settings	99 (45.8)	51.68 ± 6.848	26.59 ± 7.229
Worked in the red zones	114 (52.8)	44.81 ± 7.803	20.14 ± 8.669
Never worked in the red zones	102 (57.2)	51.46 ± 6.878	26.35 ± 7.259
Were assigned a qualification category	138 (63.9)		
– board certification	83 (38.4)	47.7 ± 7.19	22.5 ± 7.51
– second category	22 (10.2)	48.1 ± 9.66	23.4 ± 10.06
– first category	33 (15.3)	49.7 ± 8.22	25.2 ± 8.78
No qualification category	78 (36.1)	47.5 ± 8.49	22.7 ± 9.18
Had an academic degree	63 (29.2)		
– doctoral degree	48 (22.2)	49.5 ± 8.26	24.2 ± 8.79
– post-doctoral degree	15 (6.9)	51.9 ± 8.72	27.0 ± 10.27
No academic degree	153 (70.8)	47.1 ± 7.82	22.3 ± 8.28
Had second higher education	111 (51.4)	47.9 ± 8.25	23.2 ± 8.92
– specialization in management	105 (48.6)		
No second higher education	105 (48.6)	48.0 ± 7.94	22.9 ± 8.29

The mean scores in the categories Affect Balance and Meaningful Life were below standard values in all the surveyed gender and age groups. In 20 men (20%) and 17 women (26.2%) aged 36–55, the Affect Balance scores exceeded standard values.

The Meaningful Life scores were below standard values in 11 men (54.5%) aged 25–35, 60 men (60%) and 46 women (70.8%) aged 36–55. The mean scores in the category Human Being as an Open System were below standard values in women and men aged 35–55, but exceeded standard values in men aged 25–35. The scores in this category were below standard values in 2 men (18.2%) aged 25–35, as well as in 53 men (53.0%) and 41 women (63.1%) aged 36–55.

In the general group of respondents, the Affect Balance scores were above average in 88 people (40.7%), the Meaningful Life scores were below average in 88 people (40.7%), and the scores in the category Human Being as an Open System were below average in 95 people (44.0%).

The mean scores on the Ryff's scales Personal Growth, Positive Relations with Others, Autonomy, Environmental Mastery, Purpose in Life, Self-Acceptance exceeded standard values in all the gender and age groups. The Personal Growth scores were below standard values in 3 men (27.3%) aged 25–35, 47 men (47%) and 15 women (23.1%) aged 36–55. The scores on the scale Positive Relations with Others were below standard values in 22 men (22%) and 23 women (35.4%) aged 36–55. The Autonomy scores were below standard values in 25 men (25%) and 16 women (24.6%) aged 36–55. The Environmental Mastery scores were below standard values in 25 men (25%) and 18 women (27.7%) aged 36–55. The scores on the scale Purpose in Life were below standard values in 28 men (28%) and 23 women (35.4%) aged 36–55. The Self-Acceptance scores were below standard values in 23 men (23%) and 24 (36.9%) women aged 36–55.

In the general group of respondents, the scores on the following scales were below average: Personal Growth in 93 people (43.1%), Positive Relations with Others in 103 people (47.7%), Autonomy in 77 people (35.6%), Environmental

Mastery in 79 people (36.6%), Purpose in Life in 90 people (41.7%), Self-Acceptance in 99 surveyed department heads (45.8%).

There was a correlation of age and years of service with the scores in all categories and scales of the questionnaire ($p \leq 0.05$), except the Self-Acceptance scale ($p > 0.05$). Age and years of service negatively correlated with the Affect Balance, and positively correlated with other categories and scales.

All the categories and scales of the questionnaire were intercorrelated ($p \leq 0.05$), there was a negative correlation with the Affect Balance category. Based on some categories and scales of psychological well-being, there were no correlations between scores and gender, the fact of having second higher education, qualification category, or academic degree, the type of organization where the respondent worked, and the experience of working in the red zone ($p > 0.05$).

DISCUSSION

Psychological well-being of almost 40% of respondents scored below average. Since standard values of psychological well-being for all gender and age groups are not available, let us focus on the respondents aged 36–55, whose share in the age structure of department heads is the largest. Thus, 43.1% women and 26% men in this age group have psychological well-being scores below standard values. The results of survey that targeted this age group from the prospective of categories and scales reveals the variants of psychological ill-being.

Based on the Affect Balance category, almost a third of women and 20% of men aged 36–55 show life dissatisfaction, low assessment of their capabilities of learning and overcoming life's problems, poor skills of maintaining healthy relationships with others. Based on the scale Positive Relations with Others, more than a third of women and more than 20% of men have a propensity for privacy and distrust in relationships; based on the Personal Growth scale, more than 20% of women and almost half of men of this age group show no desire for self-realization, cognition, behavioral changes.

Table 2. Mean scores and standard values for scales and integral categories of the Ryff's scales by gender and age groups ($M \pm \sigma$)

Gender	Age groups	Psychological well-being	Affect Balance	Meaningful Life	Openness	Personal Growth	Positive Relations	Autonomy	Environmental Mastery	Purpose in Life	Self-Acceptance	
Female	25-35 years, $n = 0$	–	–	–	–	–	–	–	–	–	–	
	Standard values	370 ± 34.68	84 ± 15.61	97 ± 12.61	65 ± 6.07	65 ± 6.04	65 ± 8.28	58 ± 7.31	58 ± 7.35	64 ± 8.19	61 ± 9.08	
	36–55 years, $n = 65$	358.8 ± 79.27	81.0 ± 25.52	83.36 ± 17.26	61.12 ± 12.44	58.94 ± 13.53	62.25 ± 14.88	58.75 ± 13.79	60.54 ± 12.60	61.75 ± 13.18	60.95 ± 14.80	
	Standard values	351 ± 23.93	93 ± 9.58	95 ± 10.06	64 ± 3.95	63 ± 7.90	58 ± 7.59	57 ± 5.61	59 ± 8.32	59 ± 6.99	57 ± 6.14	
	56 years and older, $n = 28$	430.04 ± 22.93	60.03 ± 7.11	100.64 ± 5.65	73.82 ± 4.94	73.75 ± 2.96	75.96 ± 7.16	69.43 ± 3.80	69.82 ± 3.85	74.71 ± 3.76	71.43 ± 6.40	
	Standard values	No										
	Total $n = 93$	380.25 ± 74.87	74.68 ± 23.69	88.56 ± 16.74	64.95 ± 12.21	63.40 ± 13.29	66.38 ± 14.46	61.97 ± 12.68	63.33 ± 11.54	65.66 ± 12.68	64.11 ± 13.70	
Male	25–35 years, $n = 11$	422.36 ± 24.17	62.45 ± 6.15	97.45 ± 6.12	72.27 ± 5.55	70.36 ± 7.51	73.91 ± 4.61	67.45 ± 2.07	69.55 ± 3.78	73.73 ± 4.41	73.00 ± 5.98	
	Standard values	363 ± 24.20	91 ± 17.09	99 ± 7.64	65 ± 5.62	65 ± 4.94	63 ± 7.12	56 ± 6.86	57 ± 6.27	63 ± 5.16	59 ± 6.99	
	36–55 years, $n = 100$	364.52 ± 84.30	80.07 ± 27.59	84.04 ± 18.37	62.43 ± 13.22	59.90 ± 15.20	63.41 ± 15.49	59.41 ± 13.98	61.23 ± 13.45	62.98 ± 14.56	62.08 ± 15.28	
	Standard values	336 ± 33.94	105 ± 13.66	95 ± 12.74	63 ± 5.58	58 ± 7.80	54 ± 6.52	57 ± 7.73	56 ± 8.27	58 ± 8.51	52 ± 5.31	
	56 years and older, $n = 12$	444.33 ± 9.73	55.83 ± 3.58	103.41 ± 1.67	76.33 ± 1.87	74.67 ± 1.37	80.42 ± 2.81	71.75 ± 3.33	72.00 ± 1.21	76.75 ± 1.14	75.50 ± 3.50	
	Standard values	No										
	Total $n = 123$	377.48 ± 81.13	76.13 ± 26.31	87.13 ± 17.91	64.67 ± 12.94	62.28 ± 14.76	66.01 ± 15.12	61.33 ± 13.30	63.02 ± 12.74	65.28 ± 14.05	64.37 ± 14.72	
Total	25–35 years, $n = 11$	422.36 ± 24.17	62.45 ± 6.15	97.45 ± 6.12	72.27 ± 5.55	70.36 ± 7.51	73.91 ± 4.61	67.45 ± 2.07	69.55 ± 3.78	73.73 ± 4.41	73.00 ± 5.98	
	36–55 years, $n = 165$	362.27 ± 82.16	80.43 ± 26.72	83.77 ± 17.89	61.92 ± 12.90	59.52 ± 14.53	62.95 ± 15.22	59.15 ± 13.87	60.96 ± 13.09	62.50 ± 14.00	61.64 ± 15.06	
	56 years and older, $n = 40$	434.33 ± 20.85	58.77 ± 6.55	101.47 ± 4.95	74.58 ± 4.38	74.03 ± 2.61	77.30 ± 6.48	70.13 ± 3.78	70.48 ± 3.42	75.33 ± 3.32	72.65 ± 5.95	
	Total $n = 216$	378.67 ± 78.33	75.50 ± 25.17	87.75 ± 17.39	64.79 ± 12.60	62.76 ± 14.12	66.17 ± 14.81	61.61 ± 13.01	63.16 ± 12.21	65.44 ± 13.45	64.25 ± 14.26	

Based on the Self-Acceptance scale, almost 40% of women and 20% of men aged 36–55 are concerned about poor personal characteristics, but are dissatisfied with their status in society in the perception of the surrounding world. That explains why 70.8% of women and 60% of men in this age group tend to perceive their life as meaningless and pointless based on the Meaningful Life category; more than a third of women and almost a third of men have no sense of purpose together with limited or no goals and aspirations based on the scale Purpose in Life.

Based on the category Human Being as an Open System, 63.1% of women and 53% of men aged 36–55 show a lack of willingness to make use of the experience gained and are reluctant to perceive adequately the realities of life. In addition, based on the Environmental Mastery scale, more than a quarter of women and a quarter of men are unable not only to control things, but also to take advantage of emerging opportunities to implement changes; based on the Autonomy scale, a quarter of women and men show dependence on people around them and are prone to submissive behavior.

It should be noted that the findings are correlated with the data on poor professional competencies in the field of management in heads of medical organizations [18].

A survey of women deserves special attention. The groups of men and women showed similar levels of psychological well-being in general, and in certain psychological well-being categories and scales ($p > 0.05$). However, we would like to remind that psychological well-being scores in the age group 36–55 were below standard values in 26% of men and 43.1% of women. It should be noted that there were no women below the age of 35 among the respondents, while men of this age

accounted for 8.9% of male respondents. On the contrary, there were 30.1% of women over 56 among the respondents of this gender, and men of this age accounted only for 9.6%. The number of women among the respondents over the age of 56 was more than two times higher than the number of men: 28 and 12, respectively, while in the population of the country the number of females per 1000 males increases from 1,067 between the ages of 35–55 to 1,233 between the ages of 56–60 (Rosstat, <https://rosstat.gov.ru/folder/12781>). That is, women become heads of departments later and less frequently (the average age of female respondents is significantly higher compared to male respondents; $t = 7.44$, $p \leq 0.001$). We believe that there is discrimination against women concerning career progression. Our assumptions, that career inhibition and inefficient struggle against it result in lower psychological well-being among women, are in line with other studies [19–21].

The decline in indicators of psychological well-being as a whole and in all the categories and scales in men over the age of 35 is one more interesting aspect of the study. It should be noted that the components of psychological well-being change with age: well-being decreases until midlife and increases in late life [22]. Detrimental changes in standard values are also observed in men over the age of 35, but to a lesser degree. However, Autonomy scores become even higher (Table 2). In male respondents over the age of 35, mean levels of psychological well-being decrease to 58 points ($\approx 14.0\%$ of the level of 25–35 years). The most significant reduction in scores in terms of category is observed in the Affect Balance category: the score is reduced by 18 points (29.0% of the level of 25–35 years). The Autonomy and Environmental Mastery categories are the least affected: the score is reduced by

8 points ($\approx 11\%$ of the level of 25–35 years). The Meaningful Life score has decreased by 13 points ($\approx 14.0\%$ of the level of 25–35 years); the scores on the scales Personal Growth, Purpose in Life, Self-Acceptance have decreased by 11 points ($\approx 15\%$ of the level of 25–35 years), and the Openness and Positive Relations scores have decreased by 10 points ($\approx 14.0\%$ of the level of 25–35 years).

We have found no effects of the other studied respondents' characteristics on their psychological well-being. We expected that increased workloads experienced by employees working in the res zones would have a negative impact on their psychological well-being. It can be assumed that the effects of increased workloads are alleviated by satisfaction from the growing sense of accomplishment, direct personal involvement in addressing a global health problem, realization of altruistic behavior, markedly positive attitude of the society [7, 8]. We also expected to find a positive correlation between psychological well-being and formal characteristics of professional development: second higher education, qualification category, academic degree. However, formal characteristics of professional development had no effect, even on the respondents' personal growth (qualification category, $p = 0.990$; academic degree, $p = 0.430$; second higher education, $p = 0.686$). At the same time, the fact that more than 40% of respondents have Personal Growth scores below average is a particular cause for concern, as the requirements

for intense professional development of physicians and healthcare managers grow.

CONCLUSIONS

Although the average levels of the respondents' psychological well-being exceed standard values, the findings reveal several problematic aspects. First, high proportion of individuals with the scores of psychological well-being and its components below standard values was found in the group aged 36–55. Second, lower psychological well-being of women was noted in the studied group. Third, there was a significant decline in psychological well-being among men over the age of 35. The findings expand understanding of psychological well-being of the department heads and healthcare professionals. However, the features of psychological well-being discovered entail identification of the underlying cause. Furthermore, it is necessary to confirm no correlation of psychological well-being, especially personal growth, with formal characteristics of professional development and workloads. In this regard, further research in this area could be recommended, involving the expansion of certain gender and age groups included in the sample population and the use of a larger number of the respondents' characteristics, to develop fully fledged recommendations regarding personnel management of medical organizations.

References

1. The principles of quality assurance. WHO Working Group. *Qual Assur Health Care*. 1989; 1 (2–3):79–95. DOI: 10.1093/intqhc/1.2-3.79.
2. Donabedian A. Evaluating the quality of medical care. 1966. *Milbank Q*. 2005; 83 (4): 691–729. DOI: 10.1111/j.1468-0009.2005.00397.x.
3. Brynza NS, Kicha DI, Zaxarchenko NM. Efficektivnost' podxodov obespecheniya kachestva medicinskoj pomoshhi i nepreryvnogo medicinskogo obrazovaniya v kontekste polozhitel'nyx trendov zabolevaemosti Vyatskij medicinskij vestnik. 2017; 1 (53). 60–63. Russian.
4. Manturova NE, Kochubey VV, Kochubey AV. The competence of plastic surgeons. *Bulletin of RSMU*. 2018; 2: 63–7. DOI: 10.24075/brsmu.2018.023.
5. Donabedian A. Methods for deriving criteria for assessing the quality of medical care. *Med Care Rev*. 1980; 37 (7): 653–98.
6. Chmielewska M, Stokwizewski J, Filip J, Hermanowski T. Motivation factors affecting the job attitude of medical doctors and the organizational performance of public hospitals in Warsaw, Poland. *BMC Health Serv Res*. 2020; 20 (1): 701. DOI: 10.1186/s12913-020-05573-z.
7. Yates SW. Physician stress and burnout. *Am J Med*. 2020; 133 (2): 160–4. DOI: 10.1016/j.amjmed.2019.08.034.
8. Azam K, Khan A, Alam MT. Causes and adverse impact of physician burnout: A systematic review. *J Coll Physicians Surg Pak*. 2017; 27: 495–501.
9. Sibeoni J, Bellon-Champel L, Mousty A, Manolios E, Verneuil L, Revah-Levy A. physicians' perspectives about burnout: a systematic review and metanalysis. *J Gen Intern Med*. 2019; 34 (8): 1578–90.
10. Rotenstein LS, Torre M, Ramos MA, Rosales RC, Guille C, Sen S, et al. Prevalence of burnout among physicians: a systematic review. *JAMA*. 2018; 320 (11): 1131–50. DOI: 10.1001/jama.2018.12777. PMID: 30326495; PMCID: PMC6233645.
11. Shawahna R, Maqboul I, Ahmad O, Al-Issawy A, Abed B. Prevalence of burnout syndrome among unmatched trainees and residents in surgical and nonsurgical specialties: a cross-sectional study from different training centers in Palestine. *BMC Med Educ*. 2022; 22 (1): 322. DOI: 10.1186/s12909-022-03386-8. PMID: 35473599; PMCID: PMC9041277.
12. Clough BA, March S, Leane S, Ireland MJ. What prevents doctors from seeking help for stress and burnout? A mixed-methods investigation among metropolitan and regional-based Australian doctors. *J Clin Psychol*. 2019; 75 (3): 418–32. DOI: 10.1002/jclp.22707.
13. Melnyk BM, Kelly SA, Stephens J, Dhakal K, McGovern C, Tucker S, et al. Interventions to improve mental health, well-being, physical health, and lifestyle behaviors in physicians and nurses: a systematic review. *Am J Health Promot*. 2020; 34 (8): 929–41. DOI: 10.1177/0890117120920451. PMID: 32338522; PMCID: PMC8982669.
14. Collin V, Toon M, O'Selmo E, Reynolds L, Whitehead P. A survey of stress, burnout and well-being in UK dentists. *Br Dent J*. 2019; 226 (1): 40–49. DOI: 10.1038/sj.bdj.2019.6. PMID: 30631165.
15. Prikaz Ministerstva truda i social'noj zashhity RF ot 7 noyabrya 2017 g. # 768n «Ob utverzhdenii professional'nogo standarta «Specialist v oblasti organizacii zdravooxraneniya i obshhestvennogo zdorov'ya». Russian.
16. Shevelenkova TD, Fesenko TP. Psixologicheskoe blagopoluchie lichnosti. *Psixologicheskaya diagnostika*. 2005; 3: 95–121. Russian.
17. Otdelnova KA. Opreделение neobxodimogo chisla nablyudenij v social'no-gigienicheskix issledovaniyax. *Sbornik trudov 2-go MMI*. 1980; 150 (6): 18–22. Russian.
18. Konanyxina AK. Ocenka kompetencij kak osnova formirovaniya individual'noj traektorii nepreryvnogo obrazovaniya rukovoditelej medicinskoj organizacii. *Sbornik nauchnyx trudov Akademii postdiplomnogo obrazovaniya FGBU FNKC FMBA Rossii*. 2022; 1: 3–16. Russian.
19. Lucia-Casademunt AM, Salinas-Pérez JA. Gender differences in psychological well-being and health problems among European health professionals: analysis of psychological basic needs and job satisfaction. *Int J Environ Res Public Health*. 2018; 15 (7): 1474. Available from: <https://doi.org/10.3390/ijerph15071474>.
20. Moreau E, Mageau GA. The importance of perceived autonomy support for the psychological health and work satisfaction of health professionals: Not only supervisors count, colleagues too! *Motiv Emot*. 2012; 36: 268–86.

21. Koropec OA. Social'no-psixologicheskoe blagopoluchii rabotnikov raznykh kategorij. Vestnik Altajskoj akademii ehkonomiki i prava. 2020; 11 (3): 499–506. DOI: 10.17513/vaael.1454. Russian.
22. Blanchflower DG, Oswald AJ. Do humans suffer a psychological

low in midlife? Two approaches (with and without controls) in seven data sets. Bonn: Institute of Labor Economics (IZA). 2017; Available from: <https://www.econstor.eu/bitstream/10419/170942/1/dp10958.pdf>.

Литература

1. The principles of quality assurance. WHO Working Group. Qual Assur Health Care. 1989; 1 (2–3):79–95. DOI: 10.1093/intqhc/1.2-3.79.
2. Donabedian A. Evaluating the quality of medical care. 1966. Milbank Q. 2005; 83 (4): 691–729. DOI: 10.1111/j.1468-0009.2005.00397.x.
3. Брынза Н. С., Кича Д. И., Захарченко Н. М. Эффективность подходов обеспечения качества медицинской помощи и непрерывного медицинского образования в контексте положительных трендов заболеваемости Вятский медицинский вестник. 2017; 1 (53). 60–63.
4. Мантурова Н. Е., Кочубей В. В., Кочубей А. В. Компетентность пластических хирургов. Вестник Российского государственного медицинского университета. 2018; 2: 67–71. DOI: 10.24075/vrgmu.2018.023.
5. Donabedian A. Methods for deriving criteria for assessing the quality of medical care. Med Care Rev. 1980; 37 (7): 653–98.
6. Chmielewska M, Stokwizewski J, Filip J, Hermanowski T. Motivation factors affecting the job attitude of medical doctors and the organizational performance of public hospitals in Warsaw, Poland. BMC Health Serv Res. 2020; 20 (1): 701. DOI: 10.1186/s12913-020-05573-z.
7. Yates SW. Physician stress and burnout. Am J Med. 2020; 133 (2): 160–4. DOI: 10.1016/j.amjmed.2019.08.034.
8. Azam K, Khan A, Alam MT. Causes and adverse impact of physician burnout: A systematic review. J Coll Physicians Surg Pak. 2017; 27: 495–501.
9. Sibeoni J, Bellon-Champel L, Mousty A, Manolios E, Verneuil L, Revah-Levy A. physicians' perspectives about burnout: a systematic review and metanalysis. J Gen Intern Med. 2019; 34 (8): 1578–90.
10. Rotenstein LS, Torre M, Ramos MA, Rosales RC, Guille C, Sen S, et al. Prevalence of burnout among physicians: a systematic review. JAMA. 2018; 320 (11): 1131–50. DOI: 10.1001/jama.2018.12777. PMID: 30326495; PMCID: PMC6233645.
11. Shawahna R, Maqboul I, Ahmad O, Al-Issawy A, Abed B. Prevalence of burnout syndrome among unmatched trainees and residents in surgical and nonsurgical specialties: a cross-sectional study from different training centers in Palestine. BMC Med Educ. 2022; 22 (1): 322. DOI: 10.1186/s12909-022-03386-8. PMID: 35473599; PMCID: PMC9041277.
12. Clough BA, March S, Leane S, Ireland MJ. What prevents doctors from seeking help for stress and burnout? A mixed-methods investigation among metropolitan and regional-based Australian doctors. J Clin Psychol. 2019; 75 (3): 418–32. DOI: 10.1002/jclp.22707.
13. Melnyk BM, Kelly SA, Stephens J, Dhakal K, McGovern C, Tucker S, et al. Interventions to improve mental health, well-being, physical health, and lifestyle behaviors in physicians and nurses: a systematic review. Am J Health Promot. 2020; 34 (8): 929–41. DOI: 10.1177/0890117120920451. PMID: 32338522; PMCID: PMC8982669.
14. Collin V, Toon M, O'Selmo E, Reynolds L, Whitehead P. A survey of stress, burnout and well-being in UK dentists. Br Dent J. 2019; 226 (1): 40–49. DOI: 10.1038/sj.bdj.2019.6. PMID: 30631165.
15. Приказ Министерства труда и социальной защиты РФ от 7 ноября 2017 г. № 768н «Об утверждении профессионального стандарта «Специалист в области организации здравоохранения и общественного здоровья».
16. Швеленкова Т. Д., Фесенко Т. П. Психологическое благополучие личности. Психологическая диагностика. 2005; 3: 95–121.
17. Отдельнова К. А. Определение необходимого числа наблюдений в социально-гигиенических исследованиях. Сборник трудов 2-го ММИ. 1980; 150 (6): 18–22.
18. Конаныхина А. К. Оценка компетенций как основа формирования индивидуальной траектории непрерывного образования руководителей медицинской организации. Сборник научных трудов Академии постдипломного образования ФГБУ ФНКЦ ФМБА России. 2022; 1: 3–16.
19. Lucia-Casademunt AM, Salinas-Pérez JA. Gender differences in psychological well-being and health problems among European health professionals: analysis of psychological basic needs and job satisfaction. Int J Environ Res Public Health. 2018; 15 (7): 1474. Available from: <https://doi.org/10.3390/ijerph15071474>.
20. Moreau E, Mageau GA. The importance of perceived autonomy support for the psychological health and work satisfaction of health professionals: Not only supervisors count, colleagues too! Motiv Emot. 2012; 36: 268–86.
21. Кoropec O. A. Социально-психологическое благополучии работников разных категорий. Вестник Алтайской академии экономики и права. 2020; 11 (3): 499–506. DOI: 10.17513/vaael.1454.
22. Blanchflower DG, Oswald AJ. Do humans suffer a psychological low in midlife? Two approaches (with and without controls) in seven data sets. Bonn: Institute of Labor Economics (IZA). 2017; Available from: <https://www.econstor.eu/bitstream/10419/170942/1/dp10958.pdf>.

MEDICAL REHABILITATION OF HIGH PERFORMANCE ATHLETES AFTER RECONSTRUCTION OF ANTERIOR CRUCIATE LIGAMENT OF THE KNEE

Boichenko RA, Gornov SV ✉

Federal Research and Clinical Center for Sports Medicine and Rehabilitation of the Federal Medical Biological Agency, Moscow, Russia

The professional activity of high performance, or elite sportsmen involves loads approaching extreme exertion, which often leads to injuries of the lower limbs. Anterior cruciate ligament (ACL) injury is one of the most common types of knee injuries. This study aimed to evaluate the effectiveness of a comprehensive rehabilitation program for athletes that underwent arthroscopic ACL reconstruction. The study involved 64 athletes aged from 17 to 31 years. Treatment group participants were offered a comprehensive medical rehabilitation program that included isokinetic training sessions on the TECNOBODY IsoMove biomechanical exercising machine; the sessions followed a purpose-designed method. The results of medical rehabilitation of the athletes were assessed through gait analysis done with a DIERS Motion 4D complex. The assessments took place 8 and 15 weeks after the reconstruction. At 8 weeks after the surgery, gait analysis parameters revealed no significant differences between the groups. Fifteen weeks after the reconstruction, when treatment group (TG) members were through all the isokinetic training sessions, the results were as follows: for the Stand Time parameter, the operated limb (OL) support deficit was 0.04% compared to the healthy limb (HL) support, and for the Single Limb Support parameter it was 3.71%, while in the control group (CG) that had no isokinetic training sessions the values were 12.44% and 18.55%, respectively. As for the Swing Time parameter, TG participants showed the deficit of HL transfer symmetry (relative to OL) of 3.99%, while the value of this parameter in the CG was 20.54%. The difference is significant, which proves the effectiveness of the developed isokinetic training method as part of the comprehensive medical rehabilitation program, the application of which resulted in faster recovery of muscle strength and compromised walking-associated support and locomotor functions in TG athletes.

Keywords: ACL, arthroscopy, rehabilitation, isokinetic training, gait analysis, highly trained athletes

Author contribution: R.A. Boichenko — literature review, data collection, data analysis, text authoring, determination of gait comparison parameters, statistical data processing; S.V. Gornov — study design development, editing and approval of the final version of the article.

Compliance with ethical standards: the study was approved by the Ethics Committee of the Federal Research and Clinical Center for Sports Medicine and Rehabilitation of the Federal Medical Biological Agency (Minutes of Meeting #01-09 of September 15, 2018). All athletes signed a voluntary consent to participate in the study.

✉ **Correspondence should be addressed:** Sergey Valeryevich Gornov
B. Dorogomilovskaya, 5, Moscow, 121059, Russia; gornovsv@gmail.com

Received: 11.04.2022 **Accepted:** 30.05.2022 **Published online:** 23.06.2022

DOI: 10.47183/mes.2022.022

МЕДИЦИНСКАЯ РЕАБИЛИТАЦИЯ В СПОРТЕ ВЫСШИХ ДОСТИЖЕНИЙ ПОСЛЕ РЕКОНСТРУКЦИИ ПЕРЕДНЕЙ КРЕСТООБРАЗНОЙ СВЯЗКИ КОЛЕННОГО СУСТАВА

Р. А. Бойченко, С. В. Горнов ✉

Федеральный научно-клинический центр спортивной медицины и реабилитации Федерального медико-биологического агентства, Москва, Россия

Профессиональная деятельность спортсменов спорта высших достижений в условиях нагрузок, близких к экстремальным, часто приводит к травмам нижней конечности. Повреждение передней крестообразной связки (ПКС) — один из наиболее распространенных видов травм коленного сустава. Целью исследования было оценить эффективность комплексной программы реабилитации спортсменов после артроскопической реконструкции ПКС. В исследовании участвовали 64 спортсмена (от 17 до 31 года). Участникам основной группы, проходившим комплексную программу медицинской реабилитации, проводили изокINETические тренировки на биомеханическом комплексе TECNOBODY IsoMove по разработанной методике. Результаты медицинской реабилитации спортсменов оценивали путем анализа походки на аппаратном комплексе DIERS Motion 4D через 8 и 15 недель после операции. Через 8 недель после операции не наблюдалось статистически значимых различий в группах по параметрам анализа походки. Через 15 недель после операции по завершении изокINETических тренировок у спортсменов основной группы (ОГ) по параметру Stand time дефицит в опоре на оперированную конечность (ОК) относительно здоровой конечности (ЗК) составил 0,04%, по параметру «одиночная поддержка» — 3,71%, в сравнении со спортсменами группы клинического сравнения (ГС), у которых по параметру Stand time дефицит в опоре на ОК относительно ЗК составил 12,44%, по параметру «одиночная поддержка» — 18,55%. По параметру Swing-time у спортсменов ОГ дефицит в симметрии переноса ЗК относительно ОК составил 3,99%, а у спортсменов ГС — 20,54%, что статистически значимо и доказывает эффективность разработанной методики изокINETических тренировок в комплексной программе медицинской реабилитации, что привело к более быстрому восстановлению мышечной силы, нарушений опорной и локомоторной функции ходьбы у спортсменов ОГ.

Ключевые слова: ПКС, артроскопия, реабилитация, изокINETические тренировки, анализ походки, высококвалифицированные спортсмены

Вклад авторов: Р. А. Бойченко — обзор литературы, сбор материала, анализ полученных данных, написание текста, определение параметров сравнения походки, статистическая обработка данных; С. В. Горнов — разработка дизайна исследования, редактирование и утверждение финального варианта статьи.

Соблюдение этических стандартов: исследование одобрено этическим комитетом ФГБУ ФНКЦСМ ФМБА России (протокол заседания № 01-09 от 15 сентября 2018 г.). Все спортсмены подписали добровольное информированное согласие на участие в исследовании.

✉ **Для корреспонденции:** Сергей Валерьевич Горнов
ул. Б. Дорогомилловская, д. 5, г. Москва, 121059, Россия; gornovsv@gmail.com

Статья получена: 11.04.2022 **Статья принята к печати:** 30.05.2022 **Опубликована онлайн:** 23.06.2022

DOI: 10.47183/mes.2022.022

Anterior cruciate ligament (ACL) reconstruction is the main method of treatment of ruptured ACL in elite athletes. Non-contact ACL injuries are most common in athletes aged 15–40 years that practice sports involving sharp changes of the movement biomechanics: football, handball, rugby, volleyball,

alpine skiing, etc. [1, 2]. Every year, about 3% of amateur athletes suffer ACL injuries. In the high performance sports realm, this figure can go up to 15% [2]. Women are two to eight times more likely to damage the ACL, a probable reason thereof being the differences in neuromuscular patterns in

men and women during and after puberty [3, 4]. Studies have shown that 35% of elite athletes fail to achieve their previous level of performance within two years after injury [5]. In 2015, Federal clinical guidelines "Rehabilitation of Knee Capsular Ligaments Injuries (Surgical Treatment)" were published [6]. The rehabilitation includes four stages. Duration of the first (early postoperative) and second (late postoperative) stages is up to three to four months, that of the third stage (pre-training) is up to six months, fourth stage (training) — up to a year. Some authors have identified the following timeframes in the four main stages of rehabilitation of patients with ACL injury: early postoperative (1 week); late postoperative (2–4 weeks); functional (5–8 weeks); training and recovery (9–24 weeks) [7]. The program of post-ACL reconstruction rehabilitation [8] allows strength training in the training and recovery period (9–32 weeks) from the ninth week; such training involves use of cable (pulley) machines to load knee and hip joint during flexion and extension exercises. High-class athletes need more advanced exercises to restore muscle strength of quadriceps and hamstring muscles, and these exercises should not put the ACL autograft in danger. Currently, biomechanical exercising machines capable of providing biofeedback meet these requirements better than any other option.

Athletes need accelerated rehabilitation programs, since a long path back to loads common to competitions can translate into deterioration or loss of their professional skills. There are some general post-ACL reconstruction care trends adopted by the orthopedic community, but there is neither a standardized protocol nor an established timeframe for returning to the competition level training loads [9]. Therefore, the rehabilitation of athletes after ACL reconstruction is an urgent topic today.

This study aimed to design a comprehensive rehabilitation program for athletes after arthroscopic ACL reconstruction, develop the isokinetic exercising technique that relies on the TECNOBODY IsoMove biomechanical exercising machine and evaluate the effectiveness thereof.

Table 1. Federal Clinical Guidelines (Recommendations) Program

Period	Timeframe	Treatment plan
I, early post-surgery	up to 3–4 months	General developmental exercises for the contralateral limb. Dynamic exercises for non-immobilized joints of the ipsilateral limb. Knee brace allowing leg bending at an angle of 160–150°, which is gradually brought to 100–90°. Isometric muscle tension. Full extension within 2–3 weeks. Passive movements of the patella. Electromyostimulation. Training to use a functional splint and walk with crutches
II, late post-surgery		Removal of immobilizing bracing. Self-assisted dynamic exercises. Relaxation exercises, active-passive exercises. Isometric muscle contractions in limited amounts. Postural exercises (postural treatment techniques). Mechanotherapy with cable (pulley) machines. Hydrokinesitherapy. Massage
III, pre-training	up to 6 months	Therapeutic gymnastics (walking training, running, complexly coordinated exercises with additional weights and resistance). Hydrokinesitherapy (swimming). Mechanotherapy (pendulum type and isokinetic devices for muscle training), exercise machines (bicycle ergometer, stapler, etc.). Massage. Dynamic electrical stimulation. Training sessions adjusted to factor in the phase of postoperative restructuring of connective tissue structures and the functional state of the periarticular muscles
IV, training	up to 1 year	Training of special locomotor capabilities, with the set compiled by a sports coach to factor in specifics of the practiced sport Recovery of special locomotor skills

METHODS

By design, this study was a prospective controlled non-randomized study; it involved 64 athletes aged 17–31 years, all practicing sports that imply extreme locomotor activity; all had their ACL reconstructed. Gender-wise, we recruited 38 (59.4%) women (mean age 22 ± 4.2 years) and 26 (40.6%) men (mean age 26 ± 4.8 years). In all cases, the surgery took place less than a week after the athletes were diagnosed with ACL rupture. The ligament reconstruction materials were autografts of tendons of the semitendinosus and tender muscles, tendons of the long peroneal muscle.

The inclusion criteria were: age 16–40 years; first ever arthroscopic ACL reconstruction with/without partial resection of the meniscus, with/without arthroscopic meniscus suture.

The exclusion criteria were: age below 16 and over 40 years; arthroscopic interventions on adjacent and contralateral joints of the lower limbs; history of knee osteoarthritis; refusal to participate at any stage of rehabilitation.

The total duration of the study was 38 months (from October 2018 to November 2021).

We compared effectiveness of the designed comprehensive rehabilitation program and the one suggested by the Federal clinical guidelines "Rehabilitation of Knee Capsular Ligaments Injuries (Surgical Treatment)" (hereinafter referred to as the Recommendations) in the context of rehabilitation of athletes. The comparison necessitated division of the participants into two groups: treatment group (TG) of 30 individuals that were rehabilitated following the purpose-designed program, and control group (CG) of 34 athletes whose rehabilitation followed the Recommendations.

The rehabilitation of all participating athletes was organized at the Federal Research and Clinical Center for Sports Medicine and Rehabilitation of the Federal Medical Biological Agency. The programs started 3–4 weeks post surgery, which is the

Table 2. Comprehensive program of medical rehabilitation of athletes after surgery on the knee joint

Phase	Timeframe	Treatment plan	Criteria for transition to the next phase and completion of rehabilitation
I	up to 2 weeks	<p>Extension exercises with a towel roll under the heel, hanging the lower leg out while lying on the stomach on a couch.</p> <p>Motor retraining of the quadriceps femoris muscle (electromyostimulation).</p> <p>Knee brace locked in the full extension position (1st week), then a 30° bend (2nd week).</p> <p>Crutches-assisted limited loading of the limb (1st week — 25%, 2nd week — 50% of body weight) [11].</p> <p>Arbitrary tension of the anterior and posterior thigh muscle groups, gluteal muscles.</p> <p>Mobilization of the patella.</p> <p>Active flexion/passive extension of the knee joint while sitting on a couch; the range is 0–60°, repetitions assisted with the healthy leg.</p> <p>Straight leg raises (in all planes).</p> <p>For leg raises from supine position the knee brace should be locked at 0°.</p> <p>Exercising on a bicycle ergometer with a short pedal crank.</p> <p>Resistance exercises for thigh muscles.</p> <p>Cardio training and training for the upper shoulder girdle (as tolerated).</p> <p>Local cryotherapy</p>	<p>Ability to raise the operated leg when it is straightened. Absence of flexion-related contracture manifestations.</p> <p>Knee joint motion range from 0 to 60° (assisted).</p> <p>Absence of pain the operated limb when loaded</p>
II	Weeks 3–6	<p>Knee brace bending limits: up to 60° (3rd week), up to 90° (4th week), up to 120° (5th week), up to 140° and more (from the 6th week) [11].</p> <p>Increased reliance on the operated limb for support (monitor severity of the pain), in the absence of antalgic elements in the gait - refusal of crutches.</p> <p>Exercising on a standard bicycle ergometer (when the knee starts to bend for over 115°).</p> <p>Active and assisted exercises aimed at extending the range of motion.</p> <p>Mini squats/shifting body weight from side to side.</p> <p>Proprioceptive training on unstable platforms, on simulators like a gymnastic spin, with elastic bands on the opposite limb.</p> <p>Beginning of step-up training (step platform height — 10, 15, 20 cm).</p> <p>Training on the stair climber.</p> <p>Straight leg raises with progressive resistance</p> <p>Hamstring and posterior chain muscles training with progressive resistance.</p> <p>Improvement of elasticity of the musculoskeletal system of back of thigh and lower leg.</p> <p>Hardware arthrometry of the knee joint 6 weeks after surgery; no manual examination with application of maximum traction force to the lower leg should be done.</p> <p>Lymphatic drainage massage, electrical stimulation, magnetotherapy, US therapy</p>	<p>Knee joint motion range from 0 to 140°.</p> <p>Normal gait type.</p> <p>Ability to step up to a platform 20 cm high.</p> <p>Restoration of mobility of the patella.</p> <p>Improvement of functional indicators, as registered with arthrometry and motor tests</p>
III	Weeks 7–14	<p>Squats.</p> <p>Beginning of step-down training.</p> <p>Leg presses.</p> <p>Lunges.</p> <p>Knee joint extensions in isotonic mode, range 90 to 40° (preference should be given to exercises in a closed kinematic chain).</p> <p>Advanced proprioceptive training (active unbalancing).</p> <p>Training on the TECNOBODY IsoMove biomechanical exercising machine.</p> <p>Agility development exercises (with stretch cords).</p> <p>Reverse ladder training.</p> <p>Backward walking/running.</p> <p>Thigh and calf muscles stretching.</p> <p>Arthrometry 3 months after surgery.</p> <p>Adjustment of the home training program based on the results of dynamic observation</p>	<p>Unlimited knee joint movement.</p> <p>Ability to descend stairs with a step height of 20 cm without pain, with good control of the leg.</p> <p>Improvement of functional indicators, as registered with arthrometry and motor tests</p>
IV	Weeks 15–21	<p>Running, if the patient descends from a 20 cm step platform successfully.</p> <p>More advanced/difficult strength and flexibility exercises.</p> <p>Advanced sport-specific agility exercises.</p> <p>Plyometric training, if the adequate muscle strength level has been achieved.</p> <p>Knee joint extensions in isotonic mode, full movement range, no pain neither crepitus (preference should be given to exercises in a closed kinematic chain).</p> <p>Home rehabilitation program based on the results of dynamic monitoring of the patient</p>	<p>Symmetric painless running.</p> <p>Minimum symmetry between limbs in the jump test — 75%.</p> <p>Progress in functional training.</p> <p>Successful passing of the functional</p>
V	from week 22	<p>Strength training for the lower limbs with sport-specific elements.</p> <p>Advanced program of plyometric exercises.</p> <p>Use of the knee brace when practicing sports.</p> <p>Dynamic monitoring of the patient's condition and assessment of his/her complaints (pain, swelling).</p> <p>Adjustment of the rehabilitation program, if necessary.</p> <p>Persuading the patient to work out at home on a regular basis.</p> <p>Arthrometry 6 months after surgery</p>	<p>Muscle strength deficit less than 15%, as registered with isokinetic testing.</p> <p>Symmetry over 85%, as registered with a single leg jump test. No pain nor instability during all sport-specific movements.</p> <p>Flexibility as required for the particular sport</p>

II phase in the timeframe of the purpose-designed program. All participants attended the sessions 3 times a week.

The Recommendations program [6] is divided into four periods (Table 1).

The comprehensive rehabilitation program designed in the context of this study has five phases (Table 2).

The comprehensive program of medical rehabilitation included isokinetic training on a machine providing

biofeedback. Isokinetic training of muscles in the concentric mode delivered a significant improvement of the quadriceps and hamstring muscle strength (average and maximum torque at angular velocities of 30 and 60° per second) [10]. Biodex 3 System (Model 333–250; Biodex Medical Systems, Shirley; USA) was employed with the following parameters: angular velocity of 180° per second, three sets of 20 repetitions twice a week.

We have proposed a technique involving the TECNOBODY IsoMove biomechanical complex (Figure 1). Isokinetic exercises had the knee flexors and extensors loaded in the concentric mode, with the range of motion from 20 to 110° and angular velocity of 30° per second. The sessions took place twice a week; for the first two weeks, the number of repetitions was 10, then the routine changed to three sets of repetitions for the first two weeks, then twice a week, three sets of 15 repetitions for the next 2 weeks, then three sets of 20 reps for two weeks and then a week with three sets of 20 repetitions. The total number of sessions was 15. The movements started with extension of the knee joint. First, the healthy limb was trained, then the operated one. These training sessions began eight weeks post surgery.

Eight weeks post surgery, during the III phase of the rehabilitation, both groups had the following parameters/indicators assessed: impairments in the support and locomotor functions; lower limbs load distribution symmetry (enabled by DIERS Motion 4D, Figure 2) in the gait analysis mode (pedogait) at the speed of 3 km/h. The repeated control examinations took place 15 weeks post surgery at the end of the isokinetic training program.

The stride cycle (SC) for each limb consists of two main phases, support phase and transfer phase. The duration of the support phase is 58–61% of the SC, that of the transfer phase is 42–39%. The distinction is made between right and left SC, with the two constituting the act of walking [12, 13]. We evaluated CS phases of OL and HL and compared the respective results registered in the TG and the CG. The evaluated parameters were Stand time (%), which is the time the limb supports from the moment the toe is off the ground to the moment heel of the contralateral limb accepts the load; Swing-time (%), which is the time of transfer of the non-supporting limb; Single limb support (%); Load sensitivity (%); Pre-swing (%), which is the time from resting on the toe to bouncing off (Fig. 3). The first three parameters were statistically significant for the comparison.

Statistical processing of the results was done manually in Microsoft Excel and Statistica for Windows v. 5.1. To establish significance of the differences we used Student's t-test. The differences (t) were considered statistically significant at $p < 0.05$.

RESULTS

The following criteria were chosen for an objective assessment of effectiveness of the programs compared: pain assessment on a visual analogue scale (VAS), range of motion, zigzag jump test, stride parameters in gait analysis.

The participants took the jump test 15 weeks after surgery. In the TG, less than 75% symmetry between limbs during the jump was seen in two athletes (6.7%), while in the CG it was registered in nine athletes (26.5%).

In the TG group, four athletes (13.3%) reported pain of 4 VAS points and one (3.3%) — 5 VAS points; in the CG, seven participants (20.6%) put the pain sensation at 4 VAS points and two (5.9%) at 3 VAS points. Three months later, only one athlete (3.3%) reported pain of 2 VAS points in the TG, and in the CG the respective number of participants was 3 (8.8%).

A month later, the recorded active flexion radius in both groups was 100–110°, and passive flexion ranged up to 115–130°. One athlete from the TG had active extension limited to 7° and passive extension to 3°. After months later, no contractures were registered in any of the groups.

Stability tests (Lachman drawer test, pivot shift test) performed 15 weeks later revealed no positive symptoms in any of the TG athletes. In the CG, these tests allowed registering a



Fig. 1. TECNOBODY IsoMove biomechanical exercising machine



Fig. 2. DIERS Motion 4D complex

slight anterior translation of the lower leg with a clear final point.

Table 3 shows the results of assessment of violations of the support and locomotor functions, lower limbs load distribution as registered with the DIERS Motion 4D complex.

Eight weeks after surgery, there were no significant differences found between groups in the parameters of support and locomotor functions violations as registered and analyzed with the DIERS Motion 4D complex. However, fifteen weeks after the reconstruction, when the TG members were through all the isokinetic training sessions, the results were as follows: for the Stand Time parameter, the OL support deficit was 0.04% compared to the HL support, and for the Single limb support parameter it was 3.71%, while in the CG the values were 12.44% and 18.55%, respectively. As for the Swing Time parameter, TG participants showed the deficit of HL transfer symmetry (relative to OL) of 3.99%, while the value of this parameter in the CG was 20.54%.

DISCUSSION

The results of the gait parameter analysis for the TG participants indicate a more effective recovery of muscle strength of the knee joint stabilizers, healing of disorders of the support and locomotor functions in the postoperative period that included isokinetic training, which implies resistance when a certain angular velocity is reached, translating into load for exercised muscles. These findings are consistent with those reported by other authors earlier [9, 10]. Therefore, the resistance that the athlete has to overcome is adaptable, it changes constantly

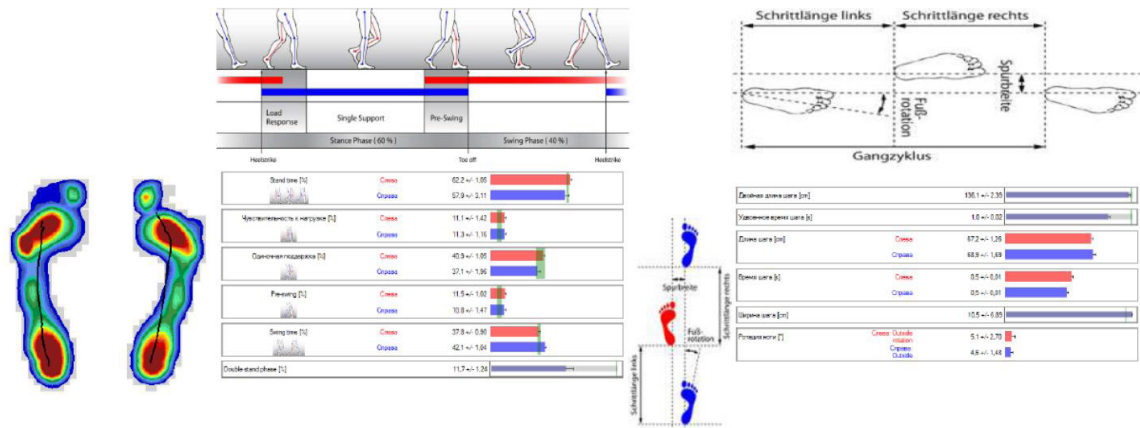


Fig. 3. Gait parameters on the DIERS Motion 4D complex

Table 3. Comparison of the results of examinations of participating athletes

Gait parameters	TG (n = 30) Me/Q ₁ /Q ₃		CG (n = 34) Me/Q ₁ /Q ₃	
	HL	OL	HL	OL
	After 8 weeks			
Stand time, %	68,6/68,03/ 69,75	57,6/55,23/ 59,78	69,15/ 67,05/ 50,45	55,70/ 50,45/ 56,9
Single limb support, %	42,9/37,65/45,23	31,9/31,4/32,6	44,1/ 43,48/ 48,43	31,35/ 30,13/ 32,73
Swing-time, %	31,4/30,3/32	42,4/40,2/44,8	30,85/29,43/ 34,73	44,3/43,1/49,55
Sensitivity to load, %	12,35/11,23/15,4	13,4/11,33/15,58	11,85/10,9/12,3	12,25/11,9/14,18
Pre-swing, %	15,1/12,5/16,7	11,95/11,6/14	12,05/11,6/13,65	11,65/ 11,33/ 13,08
	After 15 weeks			
Stand time, %	65,8/64,4/69,2	63,7/63/65,5	67,5/65,3/68,7	59,1/58,7/60,3
Single limb support, %	36,4/31,1/37,1	35,05/31,2/35,8	41,5/40,2/42,7	33,8/31,6/34,7
Swing-time, %	34,85/31,55/35,58	36,3/33,65/36,98	32,5/31,3/34,68	40,9/39,73/41,28
Sensitivity to load, %	15,2/14,3/18,5	14,7/18,1/18,1	13,4/12,7/14,8	13,5/12,7/14,1
Pre-swing, %	15/14/18,7	15,25/14,2/18,4	13,3/12,7/14,6	13,4/12,9/14,5

Note: Me — (median); Q₁ is the 25% quartile; Q₃ is the 75% quartile; differences between TG and CG at p < 0.05.

in proportion to the effort exerted. As a result, the process of muscle strength recovery gain in effectiveness.

CONCLUSIONS

1. The designed comprehensive post-ACL reconstruction medical rehabilitation program for elite athletes has proven to be effective in restoring the knee joint stabilizer strength,

healing of the support and locomotor function disorders, poor symmetry in the distribution of load on lower limbs. 2. The use of equipment providing biofeedback for rehabilitation of athletes allows speeding this process up and thus have the athletes recover their competition level capabilities sooner. 3. It is necessary to continue the search for the most effective isokinetic training technique relying on the TECNOBODY IsoMove biomechanical complex.

References

1. Prodromos CC, Han Y, Rogowski J, et al. A meta-analysis of the incidence of anterior cruciate ligament tears as a function of gender, sport, and a knee injury-reduction regimen. *Arthroscopy*. 2007; 23: 1320–5.
2. Moses B, Orchard J, Orchard J. Systematic review: annual incidence of ACL injury and surgery in various populations. *Res Sports Med*. 2012; 20: 157–79.
3. Yoo JH, Lim BO, Ha M, et al. A meta-analysis on the effect of neuromuscular training on the prevention of the anterior cruciate ligament injury in female athletes. *Knee Surg Sports Traumatol Arthrosc*. 2010; 18: 824–30.
4. Myer GD, Sugimoto D, Thomas S, et al. The influence of age on the effectiveness of neuromuscular training to reduce anterior cruciate ligament injury in female athletes: a meta-analysis. *Am J Sports Med*. 2013; 41: 203–15.
5. Van Melick N, et al. Evidence-based clinical practice update: practice guidelines for anterior cruciate ligament rehabilitation based on a systematic review and multidisciplinary consensus. *Br J Sports Med*. 2016; 0: 1–13. DOI:10.1136/bjsports-2015-095898.
6. Reabilitaciya pri povrezhdenii kapsul'no-svyazochnogo apparata kolennogo sustava (operativnoe lechenie). *Klinicheskie rekomendacii Obshherossijskoj obshhestvennoj organizacii sodejstvija razvitiyu medicinskoj reabilitologii "Soyuz reabilitologov Rossii"*, 2015 g. Russian.
7. Fedulova DV, Yamaletdinova GA. Sravnitel'nyj analiz programm lechebnoj gimnastiki posle artroskopicheskoj rekonstrukcii perednej krestoobraznoj svyazki. *Rossiya mezhdru modernizaciej i arxaizaciej: 1917–2017 gg. Materialy XX Vserossijskoj nauchno-prakticheskoj konferencii Gumanitarnogo universiteta*. 2017; 2: 459–64. Russian.

8. Ajdarov VI, Xasanov EhR, Axtyamov IF. Programma reabilitacii pacientov, perenesshix plastiku perednej krestoobraznoj svyazki kolennogo sustava. Voprosy kurortologii, fizioterapii i lechebnoj fizicheskoj kul'tury. 2020; 97 (2): 29–35. Russian.
9. Marshall NE, et al. Current practice: postoperative and return to play trends after ACL reconstruction by fellowship-trained sports surgeons. *Musculoskeletal surgery*. 2019; 103 (1): 55–61. DOI: 10.1007/s12306-018-0574-4.
10. Cheng-Pu Hsieh, Ta-Sen Wei, Chia-Chieh Wu. The early effects of isokinetic muscle training on knee joint muscle strength after modified double-bundle anterior cruciate ligament reconstruction. *Int J Clin Exp Med*. 2016; 9 (7): 14461–70.
11. Tixilov RM, Trachuk AP, Bogopolskij OE, Serebryak TV. Vosstanovitel'noe lechenie posle artroskopii kolennogo sustava (ruководство dlya pacientov). Sankt-Peterburg: Rossijskij nauchno-issledovatel'skij institut travmatologii i ortopedii im. R. R. Vredena, 2006. Russian.
12. Ob'ektivnaya ocenka funkcii xod'by. Klinicheskie rekomendacii Nacional'noj associacii po bor'be s insult'om, Soyuza reabilitologov Rossii, Rossijskoj associacii po sportivnoj medicine i reabilitacii bol'nyx i invalidov, Mezhhregional'noj obshhestvennoj organizacii «Ob'edinenie nejroanesteziologov i nejroreanimatologov», 2016. Russian.
13. Skvorcov DV. Klinicheskij analiz dvizhenij. Analiz poxodki. Moskva: Stimul, 1996; 375 s. Russian.

Литература

1. Prodromos CC, Han Y, Rogowski J, et al. A meta-analysis of the incidence of anterior cruciate ligament tears as a function of gender, sport, and a knee injury-reduction regimen. *Arthroscopy*. 2007; 23: 1320–5.
2. Moses B, Orchard J, Orchard J. Systematic review: annual incidence of ACL injury and surgery in various populations. *Res Sports Med*. 2012; 20: 157–79.
3. Yoo JH, Lim BO, Ha M, et al. A meta-analysis on the effect of neuromuscular training on the prevention of the anterior cruciate ligament injury in female athletes. *Knee Surg Sports Traumatol Arthrosc*. 2010; 18: 824–30.
4. Myer GD, Sugimoto D, Thomas S, et al. The influence of age on the effectiveness of neuromuscular training to reduce anterior cruciate ligament injury in female athletes: a meta-analysis. *Am J Sports Med*. 2013; 41: 203–15.
5. Van Melick N, et al. Evidence-based clinical practice update: practice guidelines for anterior cruciate ligament rehabilitation based on a systematic review and multidisciplinary consensus. *Br J Sports Med*. 2016; 0: 1–13. DOI:10.1136/bjsports-2015-095898.
6. Реабилитация при повреждении капсульно-связочного аппарата коленного сустава (оперативное лечение). Клинические рекомендации Общероссийской общественной организации содействия развитию медицинской реабилитации "Союз реабилитологов России", 2015 г.
7. Федулова Д. В., Ямалетдинова Г. А. Сравнительный анализ программ лечебной гимнастики после артроскопической реконструкции передней крестообразной связки. Россия между модернизацией и архаизацией: 1917–2017 гг. Материалы XX Всероссийской научно-практической конференции Гуманитарного университета. 2017; 2: 459–64.
8. Айдаров В. И., Хасанов Э. Р., Ахтямов И. Ф. Программа реабилитации пациентов, перенесших пластику передней крестообразной связки коленного сустава. Вопросы курортологии, физиотерапии и лечебной физической культуры. 2020; 97 (2): 29–35.
9. Marshall NE, et al. Current practice: postoperative and return to play trends after ACL reconstruction by fellowship-trained sports surgeons. *Musculoskeletal surgery*. 2019; 103 (1): 55–61. DOI: 10.1007/s12306-018-0574-4.
10. Cheng-Pu Hsieh, Ta-Sen Wei, Chia-Chieh Wu. The early effects of isokinetic muscle training on knee joint muscle strength after modified double-bundle anterior cruciate ligament reconstruction. *Int J Clin Exp Med*. 2016; 9 (7): 14461–70.
11. Тихилов Р. М., Трачук А. П., Богопольский О. Е., Серебряк Т. В. Восстановительное лечение после артроскопии коленного сустава (руководство для пациентов). Санкт-Петербург: Российский научно-исследовательский институт травматологии и ортопедии им. Р. Р. Вредена, 2006.
12. Объективная оценка функции ходьбы. Клинические рекомендации Национальной ассоциации по борьбе с инсультом, Союза реабилитологов России, Российской ассоциации по спортивной медицине и реабилитации больных и инвалидов, Межрегиональной общественной организации «Объединение нейроанестезиологов и нейрореаниматологов», 2016.
13. Скворцов Д. В. Клинический анализ движений. Анализ походки. Москва: Стимул, 1996; 375 с.

EARLY COMPREHENSIVE REHABILITATION OF PATIENT WITH POSTOPERATIVE DYSPHAGIA

Orlova OS^{1,2,3}, Magomed-Eminov MSh⁴, Uklonskaya DV⁵ ✉, Zborovskaya YuM⁴¹ Federal Center of Brain and Neurotechnologies of Federal Medical Biological Agency, Moscow, Russia² National Medical Research Center for Otorlaryngology of Federal Medical Biological Agency, Moscow, Russia³ Moscow Pedagogical State University, Moscow, Russia⁴ Lomonosov Moscow State University, Moscow, Russia⁵ Central Clinical Hospital RZD-Medicine, Moscow, Russia

Postoperative paresis and paralysis of the larynx, associated with breathing, voice and swallowing disorders, are actual problem of surgical treatment of the thyroid and mediastinal diseases. Traditionally, more attention is paid to phonation disorders treatment. Swallowing recovery methods are not described sufficiently. The paper reports a clinical case of early speech therapy intervention aimed at alleviating postoperative dysphagia caused by the limited flexibility of the larynx. Detailed swallowing disorder diagnosis in patient was carried out before and after the logopaedic correction of dysphagia. The main directions and results of the correctional and pedagogical work with psychological support within comprehensive rehabilitation are described. The findings confirm the need for correctional impact during the early stages of rehabilitation in case of dysphagia in surgical patients with the paresis or paralysis of the larynx.

Keywords: paresis and paralysis of the larynx, dysphagia, logopaedic impact, early rehabilitation, psychological support

Author contribution: Orlova OS, Magomed-Eminov MSh, Uklonskaya DV — study concept; Uklonskaya DV, Zborovskaya YuM — literature review; Uklonskaya DV, Zborovskaya YuM — research procedure; Uklonskaya DV, Zborovskaya YuM — manuscript writing; Orlova OS, Magomed-Eminov MSh — editing.

Compliance with ethical standards: the study was approved by the Ethics Committee of the Federal Center of Brain and Neurotechnologies of FMBA of Russia (protocol № 01/28-03-22 dated March 28, 2022), and conducted in accordance with the Declaration of Helsinki of the World Medical Association; the patient submitted the informed consent to participation and release of data.

✉ **Correspondence should be addressed:** Daria V. Uklonskaya
Budayskaya, 2, Moscow, 129128, Russia; d_uklonskaya@mail.ru

Received: 31.03.2022 **Accepted:** 05.05.2022 **Published online:** 01.06.2022

DOI: 10.47183/mes.2022.017

РАННЯЯ КОМПЛЕКСНАЯ РЕАБИЛИТАЦИЯ ПАЦИЕНТА С ПОСТОПЕРАЦИОННОЙ ДИСФАГИЕЙ

О. С. Орлова^{1,2,3}, М. Ш. Магомед-Эминов⁴, Д. В. Уклонская⁵ ✉, Ю. М. Зборовская⁴¹ Федеральный центр мозга и нейротехнологий Федерального медико-биологического агентства, Москва, Россия² Национальный медицинский исследовательский центр оториноларингологии Федерального медико-биологического агентства, Москва, Россия³ Московский педагогический государственный университет, Москва, Россия⁴ Московский государственный университет имени М. В. Ломоносова, Москва, Россия⁵ Центральная клиническая больница «РЖД-Медицина», Москва, Россия

Хирургическое лечение заболеваний щитовидной железы и органов средостения может привести к послеоперационным парезам и параличам гортани, сопровождающимся расстройствами функций дыхания, голоса и глотания. Традиционно большое внимание уделяется коррекции нарушений фонации. Методы нормализации глотания описаны недостаточно. В статье представлен клинический случай раннего логопедического воздействия в целях нивелирования послеоперационной дисфагии, обусловленной ограничением подвижности гортани. Проведена подробная диагностика расстройства глотания у пациентки до начала логопедической коррекции дисфагии и по ее завершении. Описаны основные направления и результаты коррекционно-педагогической работы с психологическим сопровождением в рамках комплексной реабилитации. Полученные результаты подтверждают необходимость коррекционного воздействия на ранних этапах реабилитации в случае возникновения дисфагии при парезах и параличах гортани у пациентов хирургического профиля.

Ключевые слова: парезы и параличи гортани, дисфагия, логопедическое воздействие, ранняя реабилитация, психологическое сопровождение

Вклад авторов: О. С. Орлова, М. Ш. Магомед-Эминов, Д. В. Уклонская — разработка исследования; Д. В. Уклонская, Ю. М. Зборовская — литературный обзор; Д. В. Уклонская, Ю. М. Зборовская — проведение исследования; Д. В. Уклонская, Ю. М. Зборовская — подготовка текста; О. С. Орлова, М. Ш. Магомед-Эминов — редактирование.

Соблюдение этических стандартов: исследование одобрено этическим комитетом ФЦМН ФМБА России (протокол № 01/28-03-22 от 28 марта 2022 г.), проведено в соответствии с Хельсинкской декларацией Всемирной медицинской ассоциации; пациентом подписано информированное согласие на участие в исследовании и публикацию данных.

✉ **Для корреспонденции:** Дарья Викторовна Уклонская
ул. Будайская, д. 2, г. Москва, 129128, Россия; d_uklonskaya@mail.ru

Статья получена: 31.03.2022 **Статья принята к печати:** 05.05.2022 **Опубликована онлайн:** 01.06.2022

DOI: 10.47183/mes.2022.017

Paresis and paralysis of the larynx caused by recurrent laryngeal nerve impairment are among the most common complications of the thyroid, parathyroid, and thoracic surgery [1, 2]. Successful surgery does not always have the expected functional result and sometimes leads to postoperative complications associated with the breathing and voice function disorders, thus leading to communication difficulties and reduced working capacity. Phonatory and breathing

disorders persist for a long time and become a problem during comprehensive rehabilitation measures aimed at resocialization and improving the quality of life [3, 4].

The larynx not only enables breathing and voice functions, but is also involved in swallowing. According to our observations, there are specific swallowing disorders in postoperative period. In the literature, when discussing clinical picture of the peripheral neurogenic laryngeal paresis and

paralysis, the authors focus on the breathing and voice function disorders; when correcting functional disorders no attention is paid to leveling of specific swallowing disorders, caused by the limited flexibility of the larynx. The majority of well-known effective methods for elimination of swallowing disorders have been proposed by foreign and domestic experts to improve meal process in patients with acute cerebrovascular disease, traumatic brain injury and brain tumors [3, 5–7].

The methods of sequential rehabilitation could not be considered reasonable in cases of vital function disorders. The risk of food and liquid aspiration in airways developing within a few hours after surgery calls for early rehabilitation impact. Traditionally, speech pathologists are responsible for correctional measures for elimination of swallowing disorders [8–10]. Specific manifestations of the peripheral neurogenic swallowing disorders in surgical patients, including cancer patients, present certain difficulties for specialists and demand specific approaches to rehabilitation. Malignant tumor diagnosis limits in application of a number of methods for overcoming dysphagia (logopaedic massage, hardware techniques stimulation), widely used in the rehabilitation system for patients with cerebrovascular disease and post-stroke patients [6, 7].

According to the Ministry of Health of the Russian Federation regulations, rehabilitation process should be carried out by the interdisciplinary rehabilitation team in accordance with the clinical guidelines. It is recommended to carry out the first stage of rehabilitation in the structural units of medical organization, including the oncology profile. There will be specialists of the psychological and pedagogical field (a speech pathologist/medical speech pathologist and a psychologist/medical psychologist) as a link of the team necessary for achieving the most possible effect of rehabilitation [11].

The study was aimed to discuss the clinical case in order to identify the features of the swallowing disorder manifestation and to find effective ways for early rehabilitation of swallowing function in patients with postoperative dysphagia, provide a personalized early rehabilitation program for patients with swallowing disorders after the surgical treatment of the head and neck tumors within interdisciplinary interaction [12], and the optimal and effective logopaedic techniques for the postoperative swallowing disorders leveling, taking into account the features of the underlying disease.

Clinical case

A patient K-ko GS was under our observation after readmission for surgical treatment after thyroidectomy due to thyroid cancer (T1N1M0).

Preoperative indirect laryngoscopy showed that all parts of the larynx were well defined, vocal folds were even, mobility was fully preserved. Voice and speech respiration were normal. No meal disorders were noted.

The patient was interviewed before surgery in order to initiate contact, provide psychological support, form motivation for rehabilitation, and provide information about the mechanisms underlying voice production and speech respiration. The patient was informed about the main principles of speech respiration as physiological function and trained in basic diaphragmatic breathing skills.

The surgical procedure included the right-sided fascial compartment neck excision, anterior neck lymph node dissection. During the postoperative period, the patient complained about discomfort in the operated area and the larynx, impaired voice and speech respiration, trouble

in swallowing liquids (cough and choking). The right-sided laryngeal paresis was diagnosed by indirect laryngoscopy.

To assess the swallowing disorder severity, the condition of oral cavity and dentition along with difficulties when chewing and swallowing liquid or solid food, and preferred food textures were defined through a questionnaire; the feeling of having food stuck in the throat, pain when mealing were recorded. Special attention was paid to emotions associated with meals, as well as to body weight changes. When filling out the questionnaire for subjective assessment of swallowing problems, the woman noted trouble in swallowing liquids (tea, coffee, water, juice), that she identified as very threatening.

Psychological support included the meaning-narrative analysis of interviews with the patient within the meaning-activity approach during the rehabilitation course and was focused on assessing her psychological condition dynamics at various stages of speech therapy [13]. It was found that such categories as anxiety, fear, worry, introversion, and difficulty of interacting with the specialists prevailed at the stage of diagnosis. Motivational combination included evenly the achieving tendency and failure tendency, the affiliative tendency and sensitivity to rejection, that created difficulties in forming motivation for rehabilitation.

To clarify the character and severity of swallowing disorders in the early postoperative period (on day 2), speech pathology assessment was performed, which included assessing respiration and phonatory breathing, maximum vowel phonation time (MPT), and auditory assessment of voice using the Union of the European Phoniaticians (UEP) scale [3]. When performing auditory evaluation, opinions of three auditors among the members of the interdisciplinary rehabilitation team were taken into account. In the reported case, auditory voice evaluation was assigned UEP score 3 (moderate dysphonia), and MPT was 5.3 s.

Preliminary assessment of the swallowing disorders was carried out using the 3-sip test (the patient was asked to take three sips of water from a spoon. After the patient coped with the task, she was asked to drink half a glass of water; at this stage choking was detected, the patient started to cough). Furthermore, endoscopist, in the presence of operating surgeon and speech pathologist, performed videolaryngoscopy with the real-time swallowing evaluation using the Patent Blue V Food Color (Zeelandia; Netherlands), water and the Resource ThickenUp Clear thickening agent (Nestle; Switzerland). Swallowing was assessed by sequential swallowing of three different liquid consistencies with subsequent assessment of the larynx condition with patented method [14].

Videolaryngoscopy with swallowing evaluation showed that epiglottis was symmetrically arranged and mobile. The right half of the larynx had limited flexibility. The vocal fold was in paramedian position. The glottis was sufficient for respiration, a linear slot under 2 mm persisted during phonation. Subglottic space and pyriform sinuses were free. When swallowing liquid, all components of the larynx up to and including the vocal folds were stained with the contrast agent; the dye solution entered the lower respiratory tract reaching the infraglottic space, caused cough, which was considered as aspiration into the airways with an adequate protection reflex. The dye test was positive.

Conclusion: right-sided laryngeal paresis. Moderate pharyngeal dysphagia.

Exercises for further speech rehabilitation were chosen based on the laryngoscopic condition and the swallowing process condition [4, 10].

On day 3 after surgery, the speech therapy course with psychological support was started. The main tasks were to

increase pharyngeal muscle activity and the pharynx–larynx interaction recovery in the swallowing process.

The patient was recommended to continue practicing breathing exercises in order to recover phonatory expiration and develop physiological respiration, she was also recommended to do the Effortful Swallow exercise (three repetitions up to 10 times a day) [15].

To alleviate physical and psychological discomfort during meals, the patient was provided advice on nutrition based on the character and severity of the swallowing disorders (posture: the Chin Thuck maneuver), food consistencies (thickening liquids to a thick syrup) [4].

It is worth mentioning that the need for intense activity in the postoperative period had a positive influence on the patient's emotional sphere, that facilitated specific meaning work in the new non-everyday life situation. It is important to emphasize postoperative asthenia, which could worsen as dysphagia became more severe, among features of conducting speech therapy during the early postoperative period. This fact required training in a sparing mode, in a fractional manner, with the progressively increasing load and training session duration, as well as the increasing complexity of the proposed material when changing the stages of the rehabilitation impact.

In a week the patient was able to do breathing exercises, that made it possible to move to the stage of active training using the methods of “direct” therapy (exercises on strengthening pharyngeal muscles, muscles of the soft palate and larynx). The methods of “indirect” therapy were also used: functional training using small amounts of food or liquid. The patient continued repeating the Effortful Swallow exercise with increasing load (5 repetitions 10–12 times a day).

After 14 days further improvements were noted: the number of choking episodes during meals decreased, the voice sonority and phonatory expiration time increased. It was recommended to keep the diet and increase the number of repetitions of the Effortful Swallow exercise to 7 times per session. After 21 days, the stage of the “safe” swallowing skill automatization started: exercises for practicing vowel sounds and their combinations, as well as for differentiation of the swallowing, respiration and phonation processes.

Clinical case discussion

After the four-week course of speech therapy, videolaryngoscopy with swallowing evaluation was performed again [14]. It showed that epiglottis was symmetrically arranged and mobile. The right half of the larynx had limited flexibility. The vocal fold was in paramedian position. The glottis was sufficient for respiration; the tendency for vocal fold closing on the injured side due to

the increased activity of the left vocal fold was observed during phonation. Subglottic space and pyriform sinuses were free. When swallowing liquids of three proposed consistencies, all components of the larynx up to and including the vocal folds showed no signs of staining. No aspiration in airways was revealed. The dye test was negative.

Conclusion: right-sided postoperative laryngeal paresis. No dysphagia.

When re-filling in the questionnaire, the patient denied difficulties when drinking liquids and had no feeling of having food stuck in the throat when swallowing. She noted that she could take meals of any consistencies and experienced no negative emotions when drinking liquids. Speech therapy sessions aimed at improving phonatory expiration and acoustic characteristics of voice were resumed during the final stages of rehabilitation and had a positive effect [3].

Thus, speech therapy sessions, which were conducted from early postoperative period within the comprehensive rehabilitation program, aimed not only at phonatory respiration and voice. Logopaedic impact started with adaptation to the new conditions of taking liquids and elimination of dysphagia on day 3 after surgery. The measures for dysphagia correction during the early postoperative period had a positive influence on the rehabilitation effectiveness and smoothed out the meal difficulties in a short time. Immediate alleviation of swallowing disorders made it possible to reduce significantly physical and psychological discomfort in the patient. Comparative analysis of narratives provided by the patient before and after the completion of measures to level dysphagia revealed motivational shift towards achieving tendency and affiliative tendency. The number of patient's statements related to the categories of anxiety and fear decreased with the increasing number of statements related to confidence in achieving good rehabilitation result. All of the above provided the necessary conditions for further successful speech rehabilitation.

CONCLUSION

The findings show that the timely speech therapy impact aimed at swallowing process recovery, discussed in the case study, may be considered the necessary and urgent type of rehabilitation impact used during the early stages of rehabilitation in case of the postoperative dysphagia occurrence. Early correctional-pedagogical sessions with psychological support within comprehensive rehabilitation facilitated the lasting positive effect, improved the patient's psychological condition, had a favorable influence on the quality of life, facilitating leveling up of rehabilitation potential and specific meaning work of the person in the new non-everyday situation of being.

References

1. Reshetov IV, Polunin GV, Ananichuk AV, Ippolitov LI, Kovalenko AA. Vozmozhnosti vosstanovleniya funktsii gortani: sovremennyy podhod. Vestnik otorinolaringologii. 2017; 82 (6): 18–23. Russian.
2. Klinicheskie rekomendatsii. Differentsirovannyj rak shchitovidnoj zhelezy. M.: Ministerstvo zdravoohraneniya RF, 2020; 47 s. Russian.
3. Lavrova EV. Logopediya. Osnovy fonopedii. M.: V. Sekachev, 2016; 182 s. Russian.
4. Orlova OS, Uklonskaya DV. Optimizatsiya metodov korrektsionno pedagogicheskogo vozdejstviya pri narusheniyah rechi i glotaniya u lits posle hirurgicheskogo lecheniya opuholej golovy i shei. Spetsialnoe obrazovanie. 2017; 3 (47): 122–30. Russian.
5. Ikenshtejn, Guntram V. i dr. Diagnostika i lechenie nejrogennoj disfagii. Bremen-London-Boston: UNI-MED Verlag AG; 96 s. Russian.
6. Balashova IN, Belkin AA, Zueva DN. Diagnostika i lechenie disfagii pri zabelevaniyah tsentralnoj nervnoj sistemy. Klinicheskie rekomendatsii. M., 2013; 38 s. Russian.
7. Orlova OS, Uklonskaya DV, Pokrovskaya YuA, Polyakova TA, Berdnikovich ES, Minaeva OD i dr. Disfagiya u detej i vzroslyh. Logopedicheskie tekhnologii. M.: LOGOMAG, 2020; 116 s. Russian.
8. Uklonskaya D, Agaeva V, Pokrovskaya Yu. Professionalism of speech pathologist as a member of multidisciplinary team:

- competence in dysphagia correction. SHS Web of Conferences. 2020; (87): Art.№00066.
9. Magomed Eminov MSh, Orlova OS, Uklonskaya DV, Zborovskaya YuM. Logopedicheskaya rabota kak znachimyj aspekt rannej kompleksnoj reabilitatsii patsientov posle hirurgicheskogo lecheniya opuholej golovy i shei. *Sovremennyy uchyonyj*. 2020; (4): 35–40. Russian.
 10. Wing-Hei Viola Yu, Che-Wei Wu. Speech therapy after thyroidectomy. *Gland Surg*. 2017; 6 (5): 501–9.
 11. Prikaz Ministerstva zdravooohraneniya RF ot 31 iyulya 2020 g. N788n «Ob utverzhdenii Poryadka organizacii medicinskoj reabilitacii vzroslyh». Russian.
 12. Dajhes NA. Mezhdisciplinarnyj podhod i novye tekhnologii v nauchno-klinicheskom razvitii otorinolaringologii. *Vestnik Rossijskoj Akademii Nauk*. 2021; 91 (7): 58–65. Russian.
 13. Magomed-Eminov MSh. Deyatel'nostno-smyslovoj podhod k psihologicheskoy transformacii lichnosti [dissertaciya]. M., 2009. Russian.
 14. Lelyuk SA, Uklonskaya DV, Reshetov DN, Sokolova OB, Timchenko IV, Hohlov IA, Matveeva SP, avtory; Lelyuk SA, Uklonskaya DV, patentoobladateli. Sposob diagnostiki nejrogennoj perifericheskoj disfagii pri ogranicheniyah podvizhnosti gortani pod kontrolem transnazal'noj endoskopicheskoy laringoskopii. Patent RF № RU 2748545 C1. 26.05.2021. Russian.
 15. Malagelada J, Bazzoli F, Boeckxstaens G, De Looze D, Fried M, Kahrilas P i dr. Disfagiya. *Global'nye prakticheskie rekomendacii i Kaskady. Obnovlenie Sentyabr' 2014*. Vsemirnaya gastroenterologicheskaya organizaciya, 2014; 25 s. Russian.

Литература

1. Решетов И. В., Полунин Г. В., Ананичук А. В., Ипполитов Л. И., Коваленко А. А. Возможности восстановления функции гортани: современный подход. *Вестник оториноларингологии*. 2017; 82 (6): 18–23.
2. Клинические рекомендации. Дифференцированный рак щитовидной железы. М.: Министерство здравоохранения РФ, 2020; 47 с.
3. Лаврова Е. В. Логопедия. Основы фонopedии. М.: В. Секачев, 2016; 182 с.
4. Орлова О. С., Уклонская Д. В. Оптимизация методов коррекционно-педагогического воздействия при нарушениях речи и глотания у лиц после хирургического лечения опухолей головы и шеи. *Специальное образование*. 2017; 3 (47): 122–30.
5. Икенштейн, Гунтрам В. и др. Диагностика и лечение нейрогенной дисфагии. Бремен-Лондон-Бостон: UNI-MED Verlag AG; 96 с.
6. Балашова И. Н., Белкин А. А., Зуева Д. Н. Диагностика и лечение дисфагии при заболеваниях центральной нервной системы. *Клинические рекомендации*. М., 2013; 38 с.
7. Орлова О. С., Уклонская Д. В., Покровская Ю. А., Полякова Т. А., Бердникович Е. С., Минаева О. Д. и др. Дисфагия у детей и взрослых. *Логопедические технологии*. М.: ЛОГОМАГ, 2020; 116 с.
8. Uklonskaya D, Agaeva V, Pokrovskaya Yu. Professionalism of speech pathologist as a member of multidisciplinary team: competence in dysphagia correction. SHS Web of Conferences. 2020; (87): Art.№00066.
9. Магомед-Эминов М. Ш., Орлова О. С., Уклонская Д. В., Зборовская Ю. М. Логопедическая работа как значимый аспект ранней комплексной реабилитации пациентов после хирургического лечения опухолей головы и шеи. *Современный ученый*. 2020; (4): 35–40.
10. Wing-Hei Viola Yu, Che-Wei Wu. Speech therapy after thyroidectomy. *Gland Surg*. 2017; 6 (5): 501–9.
11. Приказ Министерства здравоохранения РФ от 31 июля 2020 г. N788n «Об утверждении Порядка организации медицинской реабилитации взрослых».
12. Дайхес Н. А. Междисциплинарный подход и новые технологии в научно-клиническом развитии оториноларингологии. *Вестник Российской Академии Наук*. 2021; 91 (7): 58–65.
13. Магомед-Эминов М. Ш. Деятельностно-смысловой подход к психологической трансформации личности [диссертация]. М., 2009.
14. Лелюк С. А., Уклонская Д. В., Решетов Д. Н., Соколова О. Б., Тимченко И. В., Хохлов И. А., Матвеева С. П., авторы; Лелюк С. А., Уклонская Д. В., патентообладатели. Спосob диагностики нейрогенной периферической дисфагии при ограничениях подвижности гортани под контролем трансназальной эндоскопической ларингоскопии. Патент РФ № RU 2748545 C1. 26.05.2021.
15. Malagelada J, Bazzoli F, Boeckxstaens G, De Looze D, Fried M, Kahrilas P. и др. Дисфагия. Глобальные практические рекомендации и Каскады. Обновление Сентябрь 2014. *Всемирная гастроэнтерологическая организация*, 2014; 25 с.